Diss. ETH No. 13940

About Physical – Chemical Factors, their Changes during Manufacturing and Influence on the Rheological and Structural Properties of Chocolate Like Model Systems

A dissertation submitted to the
Swiss Federal Institute of Technology Zurich
(ETH Zurich)
for the degree of
Doctor of Technical Sciences

presented by
Peter Braun
Dipl.-Ing. (T.H. Karlsruhe, Germany)
born on December 15, 1964 in Freiburg, Germany

accepted on the recommendation of
Prof. Dr.-Ing. E. J. Windhab, examiner
Dr. M. Lindblom, co-examiner

Zurich 2000

About Physical – Chemical Factors, their Changes during Manufacturing and Influence on the Rheological and Structural Properties of Chocolate Like Model Systems

Acknowledgement

Table of contents

List of Symbols

Latin	Description	Units
A	Area	m^2
A	Hamaker constant	J
B	Offset factor	-
c	Concentration	-
c_p	Heat capacity at const. pressure	J/(kg K)
c_v	Heat capacity at const. volume	J/(kg K)
c_v	Solid volume concentration	-
$c_{v,max}$	Maximum packing density	-
C	Constant	-
d	Diameter	m
De	Deborah number	-
De*	Modified Deborah number	-
e	Electrical charge of a single proton	C
E_v	Volume specific energy input	J/m^3
F	Force	N
G	Gibbs free enthalpy	J
G	Rigidity modulus	Pa
h	Height, thickness, distance	m
h	Plank´s constant	W/s^2
H	Gap width	m
H	Enthalpy	J
k	Shape factor	-
k	Boltzmann´s constant	J/K
L_D	Debye length	m
m	Mass	kg
M	Torque	N m
n	Refractive index	-
n	Number of layers	-
n	Number of revolutions	1/min
n	Number of surrounding particles	-
n_i	Concentration of ionic species i	-
N	Number of particles	-
Ne	Newton number	-
p	Pressure	Pa
P	Power	W
Pe	Peclet number	-
$q(x)_{3,log}$	Density distribution, logarithmic	-
r	Radius	m
R	Radius	m
Re	Reynolds number	-
Re_{crit}	Critical Reynolds number	-

S	Entropy	J/K
S	Degree of saturation	-
S	Surface Area	m^2
S_v	Volume specific surface area	1/m
t	Time	s
T	Temperature	K
T_g	Glass transiton temperature	K
v	Velocity	m/s
V	Volume	m^3
w	Displacement	m
W	Work	N m
W_g	Water content that determines glass transition temperature	-
w(h)	Interparticle pair potential	J
x	Distance, measured size	m
z	Valency of ion	-

Greek	**Description**	**Units**
γ	Deformation under shear	-
$\dot{\gamma}$	Rate of deformation, shear rate	1/s
δ	Differential distance	-
ε	Relative dielectric constant	-
ε_0	Dielectric constant	$C^2/(J\ m)$
η	Dynamic viscosity (of the suspension)	Pa s
η_{app}	Apparent viscosity measured with stirrer type geometry	N m s
η_S	Dynamic viscosity of the suspending liquid	Pa s
θ	Surface coverage	-
λ	Wavelength	m
μ_i	Chemical potential of component i	J/mol
ν	Frequency	1/s
ρ	Density	kg/m^3
σ	Normal stress	Pa
τ	Shear stress	Pa
τ_0	Yield value	Pa
ψ	Degree of deagglomeration	-
Ψ	Electrical potential	V
ω	Angular velocity	rad/s

Summary

Chocolate is a multiphase system composed of cocoa butter and milk fat being the solidified and continuous fat phase and sugar, milk powder and cocoa being the disperse phase in this system. At room temperature, 80% to 90% w/w of the fat continuous phase are solidified and present in the crystalline state. Increase of temperature leads to melting of the fat phase. Once chocolate is liquefied, it can be described as a highly concentrated suspension. For processing, both the liquid state and its transition to the solidified state are of interest.

During manufacturing the product is treated in a way such as flow and deformation processes take place. The behavior during deformation is governed through the rheological properties of the product. To execute manufacturing processes at a constant level of quality, an understanding of and control over the factors affecting product's quality is required. The rheological properties are thereby a measure of product's structure and quality.

The key processes in chocolate manufacture are refining and conching. Refining is necessary to reduce the size of the particulate ingredients to their final particle size (below 25µm to avoid a gritty perception). Conching is the process where structural transitions and aroma development take place. In this process step the refined product (present in the powdered state) is transferred through application of mechanical and thermal energy input and by addition of further liquid phase and surfactant into a concentrated suspension. Refining and conching are the processes where the rheological properties of the final product (for a given composition) are established.

This work was focussed on the identification of factors influencing the rheological properties of chocolate. Therefore variables were separated and experiments were performed such as the complex system was first disassembled into model units and reassembled step wise with increasing complexity. The structural changes occurring during conching were studied using different model systems. Suspensions of limestone and silicon oil were prepared to study the pure effect of deagglomeration on suspension's rheology. Replacing limestone with sugar revealed the influence of physical state transitions (amorphous to crystalline) on the rheological properties of the suspensions. Recrystallization took place in the presence of water. Water adsorption altered the interfacial properties of these suspensions and thus effected the rheological properties. The influence of water sorption was investigated further, using sugar-cocoa butter-lecithin samples. It was found that water sorption causes a significant increase in viscosity caused by the increased difference of polarity within the system. Recrystallization of amorphous sugar took place during water sorption and led to formation of stable agglomerates. The formation of such agglomerates can be avoided if deagglomeration is performed in a way such as humidification and recrystallization takes place after the agglomerates had been disrupted and particles are kept in the dispersed state.

Humidity was found to have a significant influence on the structural and rheological properties of chocolate and chocolate like modelsystems. Consequently the water sorption behavior of the ingredients and the thereof prepared suspensions was assessed. For cocoa liquor and milk powder it was seen that they adsorb considerable amounts of water and therefore act as a carrier and as an internal source for water.

In case of milk powder amorphous phases are present. Water sorption affects the glass transition temperature of these amorphous structures and thus alters the mechanical properties of the milk powder. Variations in mechanical properties have an impact on the structural changes that take place during grinding. For milk powder that had been ground in different

type of mills, different microstructures were obtained. The structure present after grinding is thereby of major importance for the rheological properties of chocolate and of the corresponding model systems.

In course of this work the physical-chemical processes taking place on the product side had been identified and were assessed. Their influence on the structural properties of sugar oil suspensions was shown and put into relation to chocolate. Models explaining the effects and also describing the mechanisms behind were proposed and their impact on processing was outlined. Based on these findings new ways to produce chocolate were suggested.

In order to fully exploit the influence of process parameters and to be able to relate the process to the specific product properties a special Ring Shear Apparatus was designed and built. Performing investigations in such an apparatus enables to apply controlled mechanical and thermal energy to the sample. Simultaneously structural and chemical changes can be tracked. With that apparatus chocolate can be produced in quantities sufficient for sensory testing under well defined conditions (controlled shear and normal forces, controlled thermal energy input, controlled mass transfer) and effects on textural and sensorial attributes can be assessed.

Zusammenfassung

Schokolade ist ein Multiphasensystem, in dem sich die kontinuierliche und verfestigte Phase aus Kakaobutter und Milchfett und die partikuläre, disperse Phase aus Zucker, Milchpulver und Kakaofeststoff zusammensetzt. Hierbei liegen bei Raumtemperatur 80% bis 90% der kontinuierlichen Fettphase im festen, kristallisierten Zustand vor. Eine Erhöhung der Temperatur führt zu einem Aufschmelzen der Fettphase und zu einer Verflüssigung der Schokolade. Im flüssigen Zustand kann die Schokolade als eine hochkonzentrierte Suspension beschrieben werden. Sowohl das Fliessvererhalten der Schokolade im flüssigen Zustand als auch die Kristallisation während des Überganges in den festen Zustand sind dabei von technologischem Interesse.

Im Laufe der Herstellung wird das Produkt verschiedenen Prozessen unterzogen, für deren optimale Funktionsweise entsprechende, rheologische Eigenschaften notwendig sind. Um die Produktqualität dabei sicherzustellen, ist es notwendig diese rheologischen Eigenschaften in einem engen Band zu erzielen. Die rheologischen Eigenschaften sind damit ein Maß für die Qualität und Struktur des Produktes. Um diese Qualität sicherzustellen, ist es notwendig zu verstehen, welche Prozesse und Faktoren Einfluss auf die Fliesseigenschaften, und damit auf die Qualität, nehmen.

Die Hauptprozesse in der Schokoladenmasseherstellung sind das Zerkleinern und das Conchieren. Ausgehend von den grob dispersen Rohstoffen ist es notwendig, diese derart zu zerkleinern, dass ein "sandiges" Mundgefühl nicht mehr wahrgenommen werden kann. Hierzu sollte die Grenzkorngrösse weniger als 25μm betragen. Die Zerkleinerung wird vorzugsweise auf Walzenstühlen durchgeführt. Infolge dieser Art der Zerkleinerung kommt es zur Bildung von Pressagglomeraten. Diese Agglomerate gilt es im nachfolgenden Conchierprozess, durch Aufprägung mechanischer Energie zu zerteilen. Durch Zugabe von weiterer fluider Phase und grenzflächenaktiven Substanzen wird eine fliessfähige, hochkonzentrierte Suspension erhalten. Neben diesen strukturellen Änderungen ist die weitere Aufgabe des Conchierens die Aromabildung, welche durch entsprechende thermische Behandlung realisiert wird. Zerkleinern und Conchieren sind dabei die Prozesse, die für eine gegebene Rezeptur im entscheidenden Masse die rheologischen Eigenschaften der Schokolade bestimmen.

Diese Arbeit befasst sich mit der Identifizierung von Faktoren, die die Fliesseigenschaften von Schokolade im aufgeschmolzenen Zustand beeinflussen. Hierzu war es zunächst notwendig, die Einflussgrössen zu identifizieren und zu separieren. Ihr Einflusspotential wurde dann sowohl an Hand von geeigneten Modellsystemen als auch am realen System untersucht und dargestellt. Die ablaufenden strukturellen Veränderungen während der Conchierens wurden dabei an verschiedenen Modellsystemen untersucht. Hierzu erfolgte die Herstellung der verwendeten Systeme entsprechend den Prozessen der Schokoladeproduktion (Mischen, Walzen, Conchieren). Die Verwendung von Kalkstein und Silikonöl, erlaubte zunächst die Untersuchung des reinen Desagglomerationseffektes. Im nächsten Schritt wurden Untersuchungen am System Zucker-Silikonöl vorgenommen. Im Vergleich zu Kalkstein, zeigt Zucker bei der Zerkleinerung eine ausgeprägte Bildung von amorphen Grenzflächen, die ihrerseits hygroskopisch und zeitlich instabil sind. Durch die Aufnahme von Wasser aus der Umgebung, gehen die amorphen Phasen in den kristallinen Zustand über und die Grenzfläche Zucker-Öl erfährt damit eine zeitliche Veränderung. Damit konnte für das System Zucker Silikonöl der kombinierte Einfluss von Deagglomeration und Grenzflächenveränderung auf das Fliessverhalten und damit auf die strukturellen Eigenschaften gezeigt

werden. Der rheologische und strukturelle Einfluss der Wasseranlagerung an die Zucker-Öl Grenzfläche infolge Wassersorption, wurde dabei speziell für das System Zucker-Kakaobutter-Lezithin untersucht. Es konnte dabei festgestellt werden, dass die Wasseradsorption zu einer sehr starken Zunahme der Viskosität (in Abhängigkeit von der Schergeschwindigkeit) führt, was sich mit der Zunahme der Polaritätsdifferenz (hydrophil-lipophil) durch Wassersorption erklären lässt. Die Adsorption von Wasser an die amorphen Zuckergrenzflächen führt zur Rekristallisation dieser. Im Falle, dass eine Rekristallisation stattfindet bevor die aus dem Walzprozess stammenden Agglomerate zerteilt werden konnten, kommt es zur Bildung von sehr stabilen Sekundäragglomeraten. Die Bildung dieser kann vermieden werden, sofern die Rekristallisation im vollständig dispergierten Zustand durchgeführt wird.

Es konnte gezeigt werden, dass die Adsorption von Wasser einen starken Einfluss auf die strukturellen und rheologischen Eigenschaften von Schokolade und schokoladeähnlichen Modellsystemen hat. Es wurde deshalb das Wassersorptionsverhalten der einzelnen Komponenten untersucht. Kakaomasse und Milchpulver (Magermilch- und Vollmilchpulver) zeigen dabei eine starke Wasseraufnahme und können als interne Quelle für Wasser verstanden werden. Im Falle von Milchpulver ist zu beachten, dass dieses amorphe Phasen beinhaltet, die bei Raumtemperatur meist im Glaszustand vorliegen. Die Aufnahme von Wasser führt dabei zu einer Verringerung der Glasumwandlungstemperatur und bewirkt damit eine Veränderung der mechanischen Eigenschaften bei gegebener Bearbeitungstemperatur. Dies beeinflusst das Zerkleinerungsverhalten und damit die sich durch die Zerkleinerung verändernde und nach Zerkleinerung vorliegende Mikrostruktur.

In Abhängigkeit von dem Zerkleinerungsprozess (Walzenvermahlung und Trockenvermahlung) konnten für verschiedene Milchpulver unterschiedliche Mikrostrukturen festgestellt werden. Hierbei ist zu beachten, dass die nach der Zerkleinerung vorliegende Mikrostruktur der Partikel eine wesentlichen Einfluss auf das Fliessverhalten nimmt.

Im Rahmen der vorliegenden Arbeit, konnten die produktseitig stattfindenden physikalisch-chemischen Veränderungen aufgeklärt werden. Ihr Einfluss auf die strukturellen Eigenschaften von Zucker-Öl Suspensionen konnte gezeigt und in Beziehung zur Schokolade gesetzt werden. Es wurden Modelle erarbeitet, die die zugrundeliegenden Effekte und Mechanismen beschreiben und deren Bedeutung für die Prozessgestaltung und -führung darstellen.

Zur vollständigen Beschreibung des Einflusses von Prozessparametern wurde ein spezieller Ring-Scher Apparat entwickelt und gebaut. Mit Hilfe dieser Apparatur ist es möglich, einer Probe kontrollierte mechanische (Druck/Schub) und thermische Beanspruchungen aufzuprägen und zeitgleich, die strukturellen und rheologischen Eigenschaften zu messen. Die Verwendung von On-Line und Off-Line Analytik erlaubt es ferner, Aussagen zu den physikalischen und chemischen Veränderungen zu treffen. Darüberhinaus ist es möglich, Produkt in für sensorische Bewertung ausreichenden Mengen herzustellen und damit sensorische Evaluationen vorzunehmen.

1 Objectives

Chocolate is a confectionery product which has its roots in South America. It is reported that the Aztecs of Mexico had been one of the first cultures who used roasted and ground cocoa beans for the preparation of drinks which were called "kakauatl" which means cocoa and water. Whereas the word chocolate is derived from the word "xocoatl" which stands for a sacred brew made from cocoa beans. Although the Aztecs become always associated with cocoa it is worth mentioning that even before they appeared in Mexico cocoa already had been planted in that area. In 1520 then cocoa was brought to Europe by the Spaniards. Milk chocolate in its solid form was invented by the Swiss Daniel Peter in 1875. Four years later it was Rodolph Lindt (1879) who discovered (by chance) that a several days lasting mechanical treatment of the chocolate gives a much better quality (*Finke, H. (1965)*, *Beckett, S.T. (1994b)*). This discovery gave birth to the process step of "conching". Since then processes had been modified but chocolate manufacturing always remained a traditional process. As a consequence of these traditions quality of the product could be maintained during the years but conversion costs (cost of converting ingredients into a finished product) also remained on a rather high level. This offers the opportunity for process improvement and productivity increase whilst maintaining or improving product's quality.

As the process is handled in a traditional manner, many things are made because of "best practise" under these circumstances but not because they are basically understood and optimized. One example would be the process step of conching. Conching is considered to be the core process in chocolate manufacturing. In this rather complex process the mixed and refined chocolate ingredients are treated up to 72 h (usually 6h to 24h) to convert the ingredient mixture into chocolate (*Sommer, K., Palke, E. (1974)*, *Ley, D. (1983)*, *Kleinert-Zollinger, J. (1991)*, *Beckett, S.T. (1994b)*, *Süsswaren (1994)*). This process still offers a great potential for improvement. Therefor a project with the following objectives was started.

Objectives of the Project:

- increase the basic knowledge on the core process, i.e. conching

- meet the needs resulting from industrial application (improve ratio of output (volume) to costs whilst maintaining the current product quality)

- improve process through applicable solutions and thus ensure conversion cost reduction through process optimization supported by increased knowledge of processing

These tasks were tackled through an approach that allowed to identify and to separate the variables followed by an intense study of their influence.

Chocolate Process - Background

Chocolate is a product that is composed of cocoa, cocoa butter, sugar, milk powder, milk fat and most often lecithin used as an emulsifier. Chocolate is commercially available in different shapes (tablets, countlines etc.) and is present in the solidified state at room temperature.

The crystallized fat thereby gives the product its solid appearance. When eating chocolate the crystallized fat melts and the chocolate liquefies *(Finke, H. (1965), Beckett, S.T. (1994b))*. In the liquefied state chocolate can be considered a suspension where the solids (sugar, milk powder, cocoa) are embedded in the liquid fat matrix. To ensure that the solids can not be perceived, hence the chocolate is smooth rather then gritty in texture, the particles' size (usually 90% w/w of all particles) should be below 25μm *(Rostagno, W. (1969), Niediek, E.A. (1978), Beckett, S.T. (1994a))*. In order to obtain the special characteristics (smoothness, mouthfeel, taste etc.) of the final product, chocolate processing involves many unit operations. Thereby chocolate manufacturing most often *(Bouzas, J., Brown, B.D. (1995)* shows the following pattern (see Figure 1-1).

Dosing

```
┌─────────────────────────┐
│         Mixing          │
└─────────────────────────┘

┌─────────────────────────┐
│         Refining        │
└─────────────────────────┘

┌─────────────────────────┐
│         Conching        │
└─────────────────────────┘

┌─────────────────────────┐
│         Moulding        │
└─────────────────────────┘
```
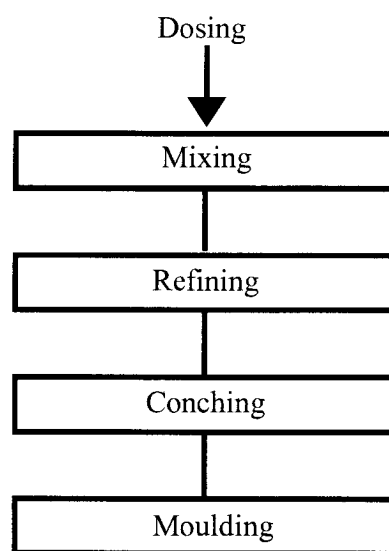
Figure 1-1 *Principle processes applied for manufacturing of chocolate*

Mixing and Refining

First the individual ingredients are weighed into a mixing vessel, mixed and are then transferred to the grinding unit. Grinding usually takes place in two stages, pre refining and refining. For pre refining a 2 roll refiner is used whereas refining is performed with a so called 5 roll refiner. In the 5 roll refiner 5 rolls are placed above each other. The speed of the rolls is increased from roll 1 to 5 and the rotating direction is altered from roll to roll. Between rolls 1 to 5, 4 gaps are formed through which the product passes and thus is ground. At the 5th roll a knife is mounted which scrapes off the refined product. The mass fed into the refiner is of a pasty, dough like structure, whereas the product obtained after refining exhibits a powder like structure. In the roll refiner large compression forces act on the particles.

When the particle fracture the fractured pieces of the particles can not "disappear" because they are surrounded by other particles and thus are pressed together. This causes the formation of so called press agglomerates. At the surface of the particles and in the voids of the agglomerates liquid is entrapped and immobilized. Immobilization of fluid causes the powder like appearance and structure of the refined product. Figure 1-2 gives a particle of limestone that was compressed between two plates. Like sugar limestone is also a crystalline

and brittle material. It can be seen that many cracks are formed but the fractured pieces are still bound together. The cracks form cavities in which liquid can be entrapped.
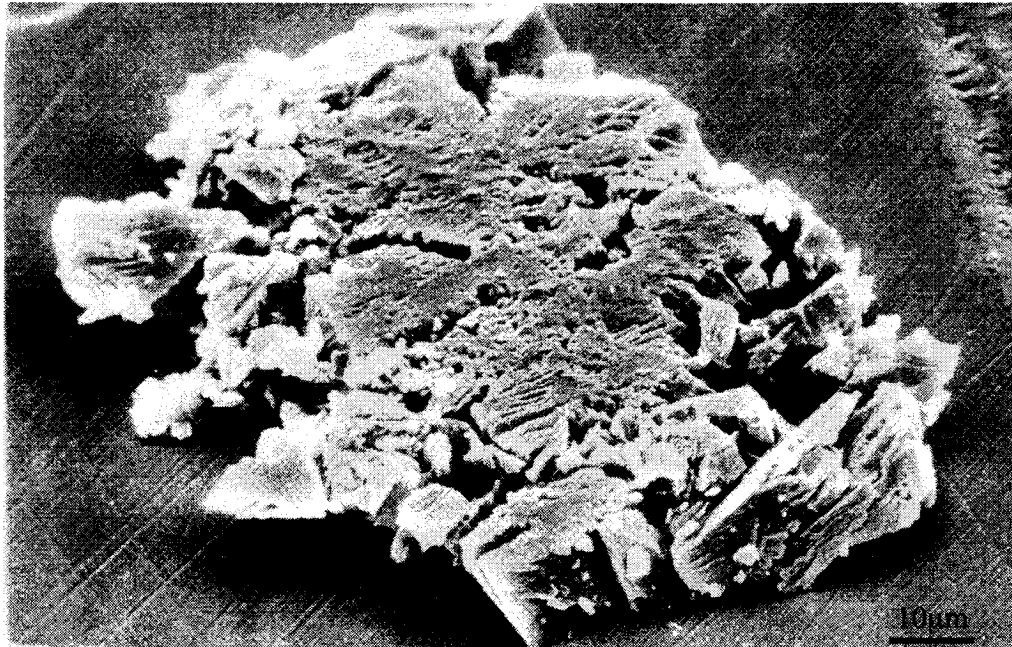
Figure 1-2 Compressed lime stone particle (Hess, W. (1980))

Figure 1-3 (*Braun, P., Windhab, E.J., Attaie, H. (1997)*) shows a mixture of unground sugar and oil in a concentration like it is used in chocolate production (22% w/w to 30% w/w of fat in the mixture prepared prior to grinding). The sugar is embedded in the liquid matrix and the structure can be described as wet sand like. Figure 1-4 gives the structure of the same product after refining. The refined sugar oil mixture exhibits a powder like structure.
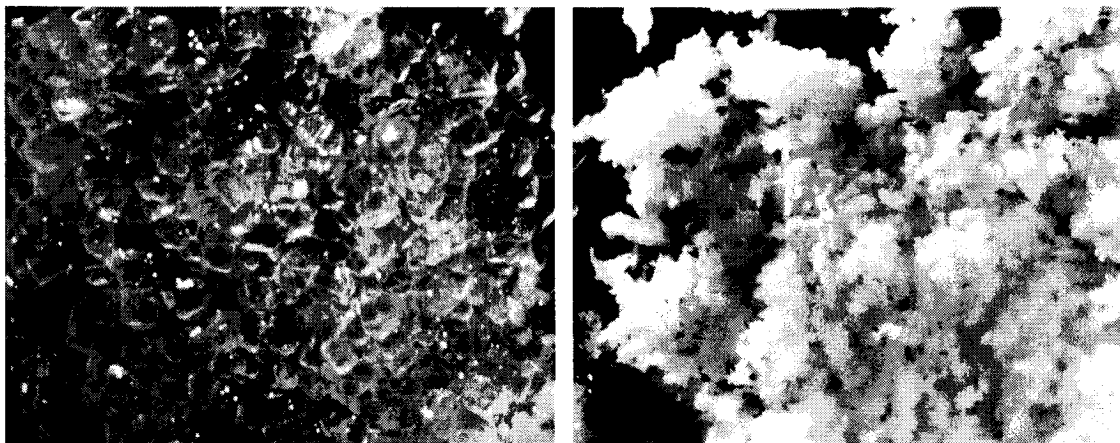
Figure 1-3 Sugar oil mixture before refining   Figure 1-4 Sugar oil mixture after refining

Taking the microstructure of the fractured limestone particle into account it can be easily imagined that the liquid is now entrapped between the fractured pieces of the solid, i.e. the "solid in liquid" mixture has transformed into a "liquid in solid mixture"(*Braun, P., Windhab, E.J. (1995)*).

Figure 1-5 gives the microstructure of a refined milk chocolate mix (*Braun, P., Windhab, E.J. (1995)*). The picture was derived from cold stage scanning electron microscopy. The porous and agglomerated structure of this product is evident and some pieces of sugar particles that are attached to other particles can be detected. From Figure 1-2 to Figure 1-5 it is clearly seen that during refining not only particles are fractured but also large agglomerates were formed. These agglomerates immobilize fluid phase which has to be released in the conching step.
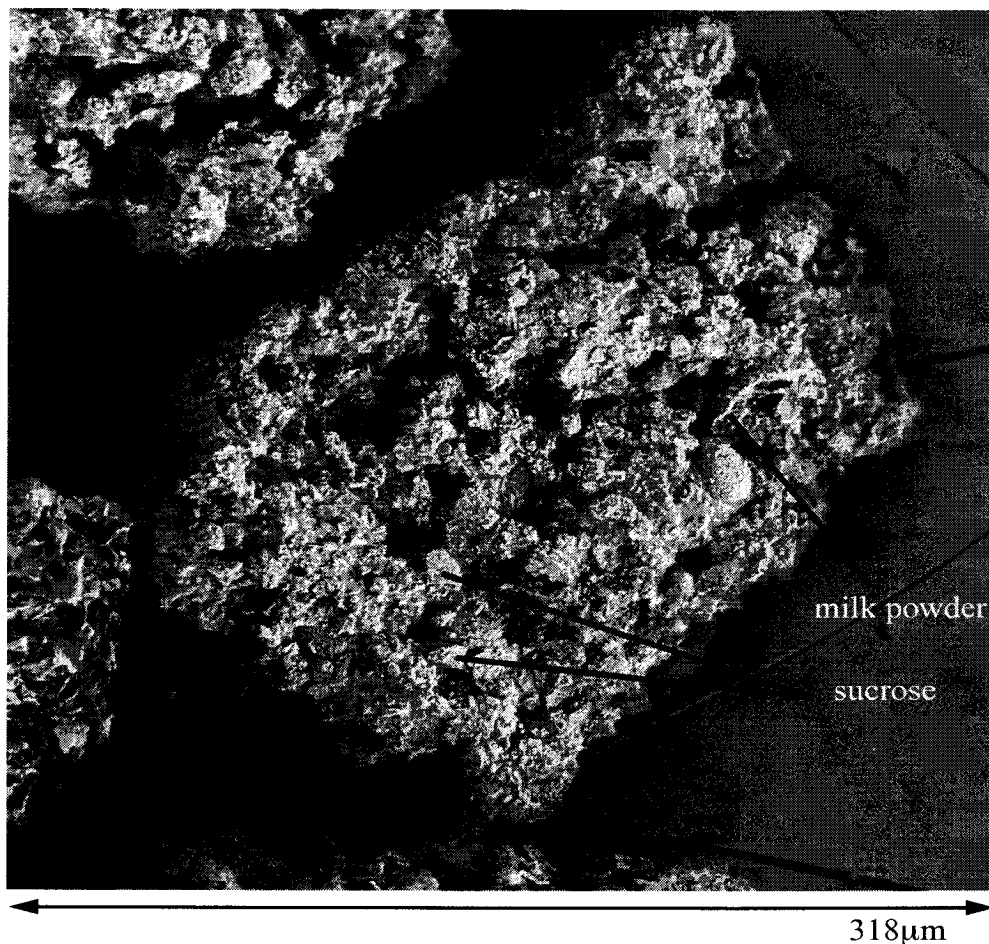
Figure 1-5 Micrograph of milk chocolate flakes, cryo- scanning electron microscopy

Conching

In the conching process the mixed and refined ingredients are treated further. Similar to refining also in this process a transition of structure is taking place (*Sommer, K. (1974), Hoskin, J., Dimick, P. (1980), Hausmann, A., Tscheuschner, H.-D. (1992)*). The powder-like chocolate flakes obtained from refining are transformed into a liquid suspensions, where the solids are suspended in the liquid phase. This is achieved through an intense kneading process, most often carried out batch-wise in so-called conches. During conching mechanical energy is applied. The agglomerates, resulting from the grinding process, are destroyed and entrapped fluid is liberated. Furthermore thermal energy is applied causing aroma reactions and removal of unpleasant and volatile compounds (*Bouzas, J., Brown, B.D. (1995)*). To

obtain the final fat content (commonly between 26%w/w to 32%w/w for milk chocolate) further fat is added which yields a high viscous fluid. Addition of emulsifier dramatically reduces viscosity and the chocolate shows its final flow properties.

Figure 1-6 Powder like state of the chocolate flakes in the beginning of conching, 24% w/w of fat, T=25°C
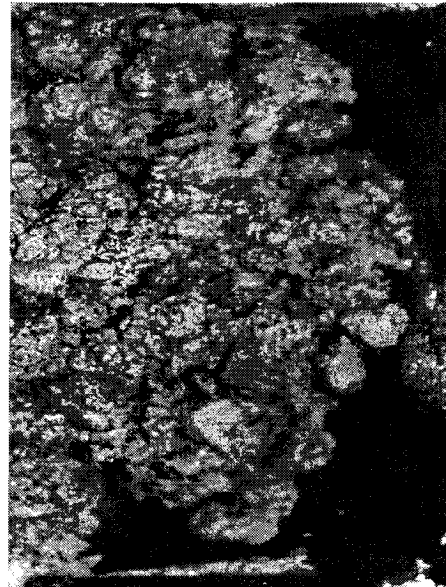
Figure 1-7 Crumbly like structure after some kneading and temperature increase had taken place, 24% w/w of fat, T=60°C

Figure 1-8 Paste like structure after addition of cocoa butter and further kneading, 31% w/w of fat, T=70°C

Figure 1-9 Liquid like structure after addition of 0.5% w/w of emulsifier (lecithin), 31% w/w of fat, T= 70°C

Figure 1-6 to Figure 1-9 give the different structures obtained during various stages of conching (*Braun, P., Windhab, E.J. (1995)*). Figure 1-6 shows the flakes at the beginning of conching. The powder like structure is well visible. Figure 1-7 illustrates the sample after thermal and mechanical energy had been applied to the sample but before addition of fat or emulsifier. The flaky structure has changed to a crumbly, ball like structure.

In this phase higher mechanical power can be applied because the sample is viscous enough to build up high resistance forces when passing the kneading zone. This was not the case in the powdery phase (Figure 1-6). Figure 1-8 gives the sample after cocoa butter was added to it. The structure has changed to paste-like. Increased temperature and continuous kneading further liquefies the mass. Figure 1-9 shows the mass after emulsifier was added to it. The structure is now homogenous and of liquid appearance. This demonstrates the enormous effect emulsifiers have in this system.

After conching the chocolate is finished and has its final attributes that define its quality for further processing and consumption. Following to conching moulding, cooling and wrapping takes place. There the liquid chocolate is put in its final shape such as tablets, countlines, pralines etc. Although the shape of the product is different now, the sensorial attributes like texture, aroma and thus taste are already formed in the conching process. Therefore conching is considered to be of utmost importance for the product quality.

Like illustrated before, conching is a quite complex process through which many transitions and reactions occur (*Sommer, K., Palke, E. (1974), Bouzas, J., Brown, B.D. (1995), Schmitt, A., Baumberg, R., Küpers, G. (1997)*). To be able to understand this process better the governing factors need to be identified.

One factor is the change of structure. Applying mechanical and thermal energy to the chocolate flakes, causes a structural transition from powder-like to crumbly to pasty. Mechanical treatment leads to a breakdown of the agglomerates and to liberation of entrapped fluid. Release of entrapped fluid yields liquefaction and thus structure of the mass changes.

Another factor is temperature and its relevance to aroma reactions. During conching temperature rises from 35°C up to 80-90°C (depending on product & recipe). Exposing the variety of aroma precursor, already present in the ingredients, to these temperatures yields a wide band of aroma compounds that are typical for chocolate (*Ziegleder, G. (1997)*)

To be able to have control over these different aspects it is necessary to have an apparatus available for which

- Mechanical power and energy input can be controlled throughout all the structural transitions

- Mechanical stresses are applied homogenously throughout the volume

- Thermal energy input is controlled

- Small temperature gradients exist throughout the volume

- Mass exchange takes place in a controlled manner - possibility of applying ventilation

- Head space analytic can be performed to assess progress in aroma reactions

- Volume is big enough to produce product in amounts sufficient for sensory testing.

Designing and building such an apparatus is key for gaining a better understanding of the conching process and thus provides a basis to meet the objectives of the project.

Looking at chocolate manufacturing, the most obvious transition observed is the change of structure from a flake-like to a liquid-like product during conching. Knowledge of the processes taking place and being involved in this transition, is a prerequisite for understanding structure formation and development of rheological properties. Disassembling the complex system into model systems and reassembling it with step-wise increased complexity allows to identify the processes involved at each level.

During the course of this work experiments with chocolate like model systems were carried out. Key influence factors in respect to rheology and microstructure were identified and their effects on the rheological and structural properties of chocolate like model systems and chocolate was described.

In a second step an apparatus was designed and built which allows to perform investigations in a way that the different requirements mentioned before are met. This offers the opportunity to transfer the knowledge gained from the experiments with the chocolate like model systems to the "real" chocolate system. Experiments can then be conducted under mechanically and thermally well defined and well controlled conditions.

2 Background

2.1 Rheology

Rheology is *the study of the deformation and flow of matter* (*Barnes, H.A., Hutton, J.F. (1989)*). It therefore investigates how materials exhibit / deform under application of external forces. Deformation expresses the relative movement of the "particles" (atoms, molecules, solid particles...) that make up the material. Consequently the way a material deforms depends upon the structure of the material. The degree of deformation is thereby a function of the external forces applied, the properties of the material and of time. External force, time and the responding deformation are values that can be measured and provide a macroscopically derived information on the material's properties and structure. Structure is the sum of the effects that take place on a molecular level. Therefore rheology can be understood as a tool to relate macroscopically derived data to the molecular / microstructure of a material. To do so a setup needs to be chosen which allows to apply external forces to the sample of interest and to measure the responding deformation.

In Figure 2-1 a set up is shown that allows to analyze how the material of interest behaves under shear.
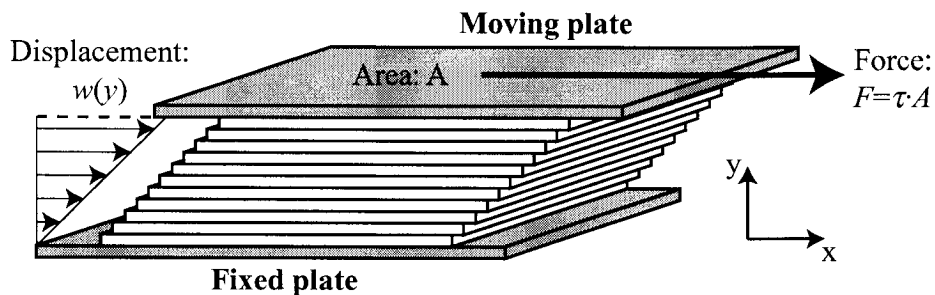
Figure 2-1 Shear stress and related deformation

The material is sandwiched between two parallel planes, each of area A. Applying a force F to the upper plane and keeping the lower plane fixed yields a shear deformation of the material. In absence of slip the deformation γ can then be written as displacement dw at a position y related to dy.

$$\gamma = \frac{dw(y)}{dy} \tag{2.1}$$

The rate of deformation $\dot{\gamma}$ is thereby obtained from rate of displacement dw/dt related to dy. The rate of displacement equals the velocity v at a position y. It can also be written

$$\dot{\gamma} = \frac{d\gamma}{dt} = \frac{(dw(y))/(dt)}{dy} = \frac{dv}{dy} \qquad (2.2)$$

The force F applied to a plane of area A expresses a shear stress τ.

In case of a Hookean solid an applied stress will be followed by an instantaneous deformation. The relationship between applied stress and the deformation observed is given by Eq. (2.3) where G is the rigidity modulus. G expresses the rigidity of the material and thus the resistance to deformation which is governed by the internal structure and stability.

$$\tau = G \cdot \gamma \qquad (2.3)$$

In case of a Newtonian liquid a stress applied will lead to a flow of the upper plane and the material continuously deforms with time, hence the value of interest is the rate of deformation. The relationship between applied stress and rate of deformation is given by Eq. (2.4) where η is the viscosity.

$$\tau = \eta \cdot \dot{\gamma} \qquad (2.4)$$

η expresses the resistance to flow and therefore is a measure of the "internal friction".

With Eq. (2.2), Eq. (2.4) can also be written as

$$\tau = \eta \cdot \dot{\gamma} = \eta \cdot \frac{(dw)/(dt)}{dy} = \eta \cdot \frac{dv}{dy} \qquad (2.5)$$

In this equation η is the factor of proportionality. Plotting shear stress versus velocity gradient or shear rate (see Figure 2-2) yields in case of Newtonian fluid a straight line (*Barnes, H.A., Hutton, J.F. (1989)*).
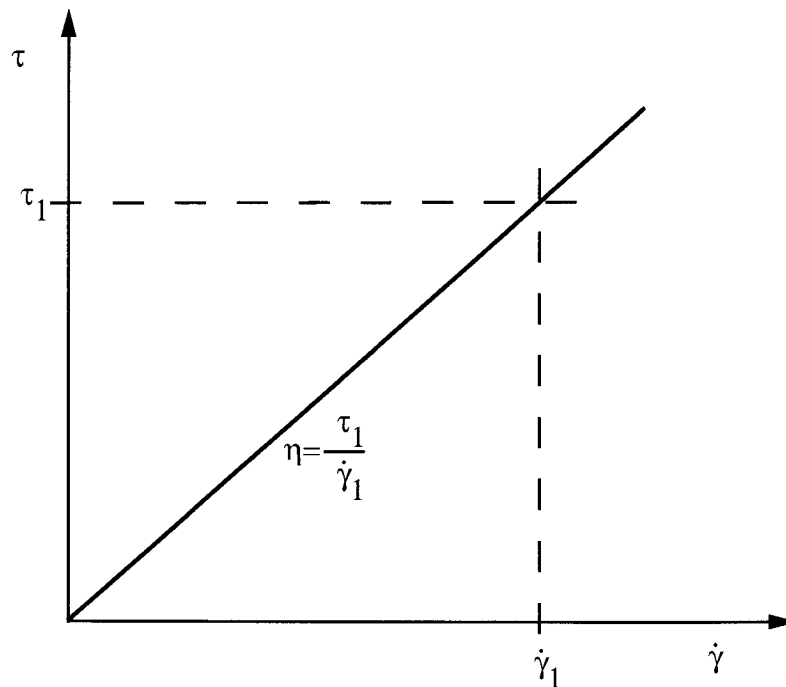
Figure 2-2 Relationship between shear stress and shear rate for a Newtonian liquid

Rewriting Eq. (2.5), viscosity can be calculated as

$$\eta = \frac{\tau}{\dot{\gamma}} \qquad (2.6)$$

which is only in case of a Newtonian liquid equal to the slope of the straight line and is only for Newtonian liquids independent from the shear rate. Eq. (2.6) is thereby the general definition of viscosity.

Another way of how to interpret Eq. (2.5) is shown in the following.

Multiplying both sides of Eq. (2.5) with dv/dy yields

$$\frac{F}{A} \cdot \frac{dv}{dy} = \left(\frac{F \cdot dw}{A \cdot dy}\right) / (dt) = \eta \cdot \left(\frac{dv}{dy}\right)^2 \qquad (2.7)$$

A force times an increment of distance Fdw equals an increment of energy dE. An area times an increment of distance Ady equals an increment of volume dV. Since the force under consideration measures viscous resistance to flow, the quantity dE/dV measures the energy dissipated per unit volume dE_v and thus Eq. (2.7) can be rewritten as

$$\frac{dE_v}{dt} = \eta \cdot \left(\frac{dv}{dy}\right)^2 \qquad (2.8)$$

which gives the rate of energy dissipation per unit volume. It is seen that the rate of energy dissipation is proportional to the square of the velocity gradient and proportional to the viscosity.

Rewriting Eq. (2.8) into shows that

$$\eta = \frac{dE_v/(dt)}{\dot{\gamma}^2} \qquad (2.9)$$

viscosity is thereby a measure for the energy dissipation at a given shear rate (*Hiemenz, P.C., Rajagopalan, R. (1997)*). Materials with high internal friction will dissipate more energy than materials showing less internal friction. The amount of internal friction is thereby given by the materials structure and thus shows that viscosity can be understood as a measure for structure.

Food is a material which often exhibits a complex structure. The structure itself often changes under application of external stresses (which is well observed when eating food). If structure changes and viscosity is regarded as a measure of structure it will change as well. In this case viscosity is no longer independent from the forces applied but becomes a function of the external stresses and also of time. The principle types of flow behavior are shown in Figure 2-3. In Figure 2-3 a) shear rate is plotted as a function of shear stress. In that case shear stress is considered the input and shear rate the response. More common is to plot shear stress as a function of shear rate (Figure 2-3 b) which is often more suitable to discuss the various effects.

In order to illustrate the relationship between viscosity and shear rate or viscosity and shear stress the so called flow function is used. In Figure 2-4 a) the flow function is plotted with shear stress as the x-axis whereas Figure 2-4 b) gives the viscosity as a function of shear rate. In case of a Newtonian fluid viscosity is independent from shear stress or shear rate and remains constant. Shear thinning and shear thickening fluids are also easy to detect. Looking

at a Bingham fluid it is seen that a yield value is in case of Figure 2-4 a) shown as the intercept with the x-axis whereas in case of Figure 2-4 b) a yield value is expressed by an asymptotic curve. This results from the definition of viscosity (Eq. (2.6)). For a fluid exhibiting a yield value a minimum stress needs to be overcome before flow is observed. This means that for shear rate approaching unity a finite value for the stress exists and thus viscosity approaches infinity (*Barnes, H.A., Hutton, J.F. (1989)*).
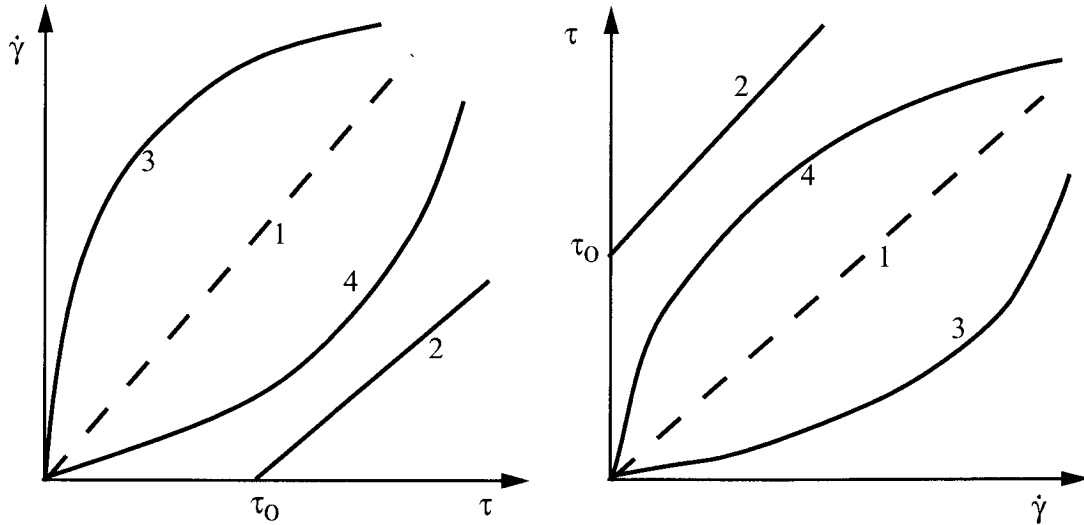
Figure 2-3 *a) Type of flow behavior*
shear rate vs. shear stress
1 Newtonian, 2 Bingham,
3 shear thickening, 4 shear thinning

b) *Type of flow behavior*
shear stress vs. shear rate
1 Newtonian, 2 Bingham,
3 shear thickening, 4 shear thinning
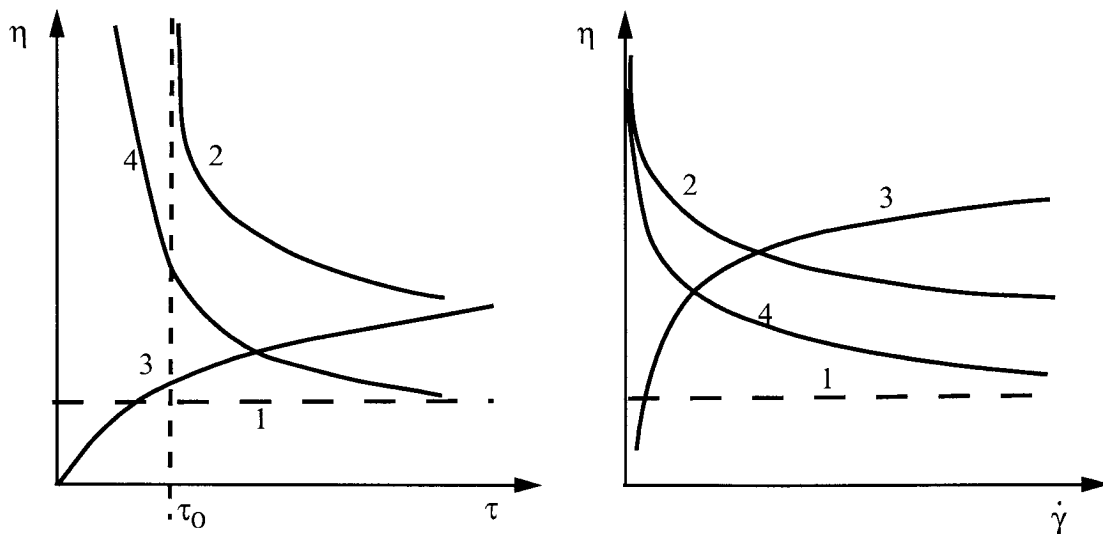
Figure 2-4 *a) Viscosity vs. shear stress*
1 Newtonian, 2 Bingham,
3 shear thickening, 4 shear thinning

b)*Viscosity as a function of shear rate*
1 Newtonian, 2 Bingham,
3 shear thickening, 4 shear thinning

2.2 Rheology of Concentrated Suspensions

Concentrated suspensions belong to those type of fluids that exhibit complex flow behavior. The viscosity function of suspensions thereby follows a certain pattern which is qualitatively shown in Figure 2-5. At very low shear rates and depending on the type of suspension it can either exhibit a Newtonian plateau or a yield value. Increasing shear rate will lead to a shear thinning region which levels off to a upper Newtonian plateau. At some point in the upper Newtonian region there can be an increase in viscosity which is based on instability effects. The structures that can be related to each segment of the flow curve will be considered (*Barnes, H.A., Hutton, J.F. (1989), Windhab, E.J. (1995), Windhab, E.J. (1997), Windhab, E.J. (2000)*).
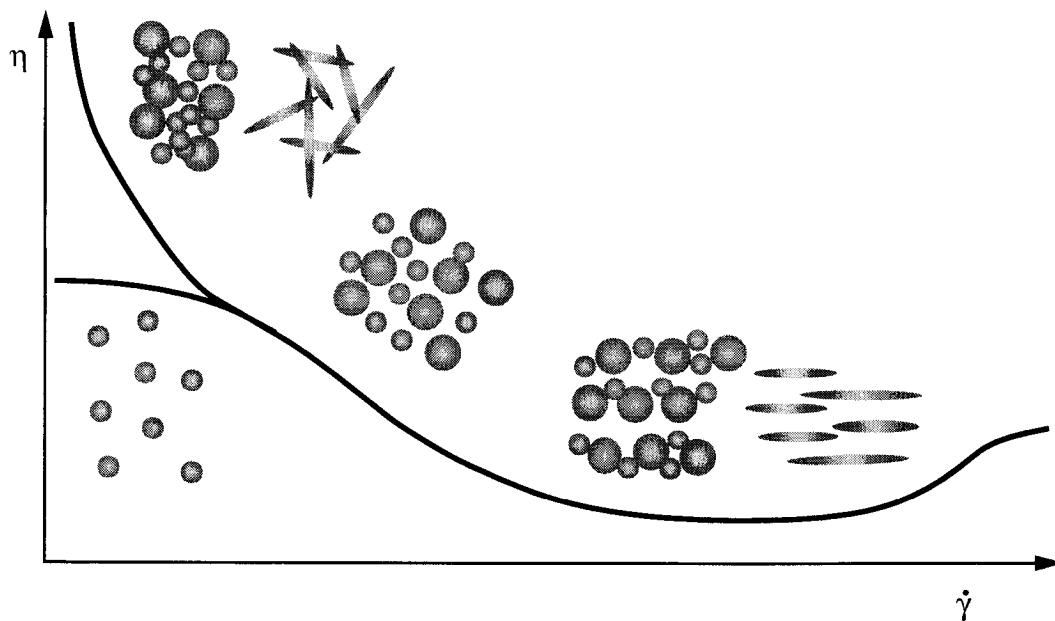
Figure 2-5 *Schematic representation of the flow curve of a concentrated suspension - Interplay between structure and rheology*

The structure of the fluid changes for increasing shear rates. The driving force is the balance between structure preserving (inner) forces and destructive (outer) forces. Two major domains can be identified.

- The structural domain present at very low shear rates is the region where hydrodynamic forces can be neglected and flow behavior is dominated by structural forces.

- The hydrodynamic domain present at increased shear rates is the region where the hydrodynamic forces get the same and higher magnitude as the structural forces.

These two domains can also be described in terms of the Peclet Pe number. The Pe-number compares the effect of imposed shear (convective effect) with the effect of diffusion or Brownian motion of particles. The Pe-number is expressed as the ratio of time required for diffusion (t_{Diff}) to the time scale of shear (t_{Shear}) (*Hiemenz, P.C., Rajagopalan, R. (1997)*).

$$Pe = \frac{t_{Diff}}{t_{Shear}} \tag{2.10}$$

In case the time of diffusion is shorter than the time of shear then Pe <1. For Pe < 1, the time required to restore, after a disturbance caused is very short. The distribution of the particles is only slightly altered by the flow and the behavior is dominated by the diffusional relaxation time.

When Pe>1, convective (hydrodynamic) effects dominate the behavior. The time scale on which the system restores is longer than the time of shear and thus structure is altered. In that case shear thinning behavior is expected.

Figure 2-5 will now be discussed for suspension composed of a Newtonian continuos phase and a disperse phase.

Considering first a colloidal systems with negligible interactions, Brownian motion preserves an isotropic structure and Newtonian flow is observed at low shear rates (small Pe-numbers). This is expressed by the lower Newtonian plateau shown at low shear rates in Figure 2-5.

For a system with strong attractive interactions particles flocculate. For diluted suspensions the flocks are far enough apart to not interact with each other. In this case also a Newtonian plateau is observed.

For high concentrations distance between the individual flocks decreases and continuos networks are formed. Such a system exhibits a "yield" value. Examples of continuos networks are concentrated fibre suspensions, gels (macromolecules), agglomerated particles (ceramics) and particle gels.

In all agglomerated systems liquid phase is immobilized within the agglomerates and thus the freely available liquid phase is less than the total amount of liquid phase. For increasing shear the forces acting on the particles increase and the structures are altered. The agglomerates will brake up, release the entrapped liquid phase and dilute the system. This decreases the resistance to flow and hence viscosity. In case of fibres, orientation will take place and the sterical hindrance is decreased which decreases viscosity. In both cases shear thinning behavior is observed.

For higher shear forces and shear rates the flocks will be completely disrupted and layered structures of the disperse phase are formed. In that case flow properties are only dependent on the shearing of the continuos phase and will show a Newtonian type of behavior.

Further increase of shear rate will lead to instability effects and cause a shear thickening. Such instabilities can be due to sterical effects (crowding of particles) or the break up of droplets. The underlaying effects are subject of ongoing research (*Ouriev, B. (2000)*).

It is seen that the flow behavior of suspensions mirrors the structure of the system. This can be further extended by applying oscillatory methods and thus look into the small deformation domain.

The structure and thus the rheological properties of suspensions depend on the properties of the disperse phase, of the continuos phase and the interactions between both. More general it can be stated that the rheological properties are influenced by

• Physical-mechanical properties

• Physical chemical properties

of its constituents.

2.2.1 Physical - Mechanical Influence Factors

The physical-mechanical factors that influence the flow properties of suspensions are the physical and mechanical properties of the disperse and the continuous phase.

These are

- Solid volume concentration
  - Free and immobilized liquid phase concentration
  - Maximum packing density

- Morphology of particles
  - Particle size
  - Particle shape
  - Particle microstructure (porous-compact)
  - Surface roughness and surface area

- Viscosity of continuos phase

The way those factors influence the flow properties is discussed in the following.

2.2.1.1 Solid Volume Concentration

The presence of particles in the liquid increases the resistance against flow. The flow is disturbed by the particles and the liquid has to flow around those. The velocity gradient across the particle causes also rotation of the particles which requires also more energy. As more energy is dissipated viscosity of the system is increased compared to a particle free system. In order to quantify the effect of solid concentration the following is considered. Shearing a pure liquid in between two parallel plates generates a linear velocity profile with a certain velocity gradient. Insertion of particles which by hypothesis do not rotate slow down the fluid so that the layers on opposite sides of the particle have the same velocity, that of the particle itself. Furthermore the free volume for the liquid to flow is reduced by the particle volume. This means that the free cross-sectional area was reduced. This is illustrated in Figure 2-6.
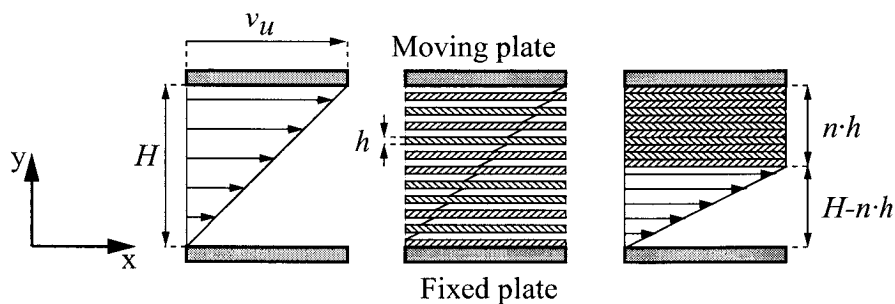
Figure 2-6 Concept of inner shear rate

The effect of particle concentration can be quantified as follows. In both cases the upper plate is moving with the same velocity v_u and the lower plate is fixed. The velocity of the fluid is on opposite sides of the particles the same. This leads to an overall increase of the inner shear rate although the externally applied velocity is the same in both cases.

In case of pure liquid the shear rate is given as the ratio between v_u and the gap width H.

$$\dot{\gamma} = \frac{v_u}{H} \qquad\qquad (2.11)$$

Whereas for the situation where particles are present the free gap width is reduced by the particles and the inner shear rate ($\dot{\gamma}_i$)is calculated on basis of the reduced free gap width

$$\dot{\gamma}_i = \frac{v_u}{H-(n\cdot h)} = \frac{v_u}{H\cdot(1-c_v)} \qquad\qquad (2.12)$$

The relative increase of the shear rate within the suspending liquid is expressed by the offset factor B which is the ratio between inner shear rate and the macroscopically observed shear rate (*Gleissle, W., Baloch, M.K. (1983), Windhab, E.W. (1986)*).

$$B = \frac{\dot{\gamma}_i}{\dot{\gamma}} = \frac{H}{H-(n\cdot h)} = \frac{1}{1-c_v} \qquad\qquad (2.13)$$

Consequently the viscosity of the suspension with particles is also increased by B compared to the viscosity of the pure liquid.

$$\eta = \eta_S \cdot \frac{H}{H-(n\cdot h)} = \eta_S \cdot B \qquad\qquad (2.14)$$

This model of internal shear rate or also called layering model is only valid if interactions between solids and liquid (fluid phase immobilization at particle surface, slip between solids and liquid phase) are neglected.

The influence of concentration of particles was first considered by Einstein. He derived an equation that quantifies the impact of particle concentration (c_v) and viscosity of the continuos phase (suspending liquid η_S) on the viscosity of dispersion (η).

$$\eta = \eta_S \cdot (1+2.5 \cdot c_v) \qquad\qquad (2.15)$$

This equation is only valid for diluted dispersions composed of non interacting rigid spheres which show Newtonian flow behavior. Experimentally it was found that the equation holds up to a concentration of 10% v/v of solids (*Hiemenz, P.C., Rajagopalan, R. (1997)*).

For increasing particle concentration packing density ($c_{v,max}$) and particle shape become important which is reflected by the equation from Krieger-Dougherty

$$\frac{\eta}{\eta_S} = \left(1-\frac{c_v}{c_{v,max}}\right)^{-k \cdot c_{v,max}} \qquad\qquad (2.16)$$

In that equation the solid volume concentration c_v is related to the maximum packing fraction $c_{v,max}$ that can be reached. The maximum packing fraction depends on the shape of the particle which is expressed by the shape factor k (*Barnes, H.A., Hutton, J.F. (1989), Hiemenz, P.C., Rajagopalan, R. (1997)*). Furthermore $c_{v,max}$ is also dependent on the particle size distribution which is discussed in the next section.

2.2.1.2 Particle Morphology

Particle morphology covers all the physical attributes of the particles like

- Particle size and size distribution

- Particle shape

- Particle microstructure

- Surface roughness and area

In the previous chapter it was shown that the viscosity of concentrated suspensions is significantly influenced by the solid volume concentration and maximum packing density. The maximum packing density of non interacting particles is thereby a function of the particle's size and shape (*Kamal, M.R., Mutel, A. (1985)*). Furthermore packing density can depend upon orientating effects caused by shear flow, which is the case for fibres (*Eischen, J.C. (1999)*) and plates (card house structures) and particle interactions (flocculation) (*Barnes, H.A., Hutton, J.F. (1989)*). In case of spheres, maximum packing fractions can be calculated. If particles of different size are used rather than monodisperse particles the small ones fit between the bigger ones and thus reduce the void volume. Usage of bi-, or multimodal size distributions allows to significantly increase the maximum packing density and to lower viscosity (*Farris, R.J. (1968), Chong, J.S., Christiansen, E.B., Baer, A.D. (1971), Cheng, D. et al. (1990), Sadler, L.Y., Kian, G.S. (1991)*).

Beside the shape of the size distribution (monodisperse, mono-, bi-, or multimodal) also the average particle size is of interest. For non interacting glass spheres of narrow size distribution it was found that particle size has no influence on viscosity (*Chong, J.S., Christiansen, E.B., Baer, A.D. (1971),Metzner, A.B. (1985)*).

In case of interacting particles it was found that in the low shear rate domain (structural forces dominant) viscosity is affected by particles size (*Windhab, E.W. (1986)*). The smaller the size the higher viscosity. This can be explained by two effects. Smaller particles have a larger surface than big particles of the same solid volume concentration. The particles can immobilize liquid at there surface and thus increase the effective solid volume concentration or reduce the free liquid concentration. As smaller particles have a larger surface area more liquid is immobilized and thus viscosity is increased compared to coarse particles. Another effect are the number of interacting particles. For the same volume concentration there is a higher number of particles and thus more points of interaction for smaller particles than for big particles. In case of attractive particle interaction also flocculation. Flocculation again immobilizes liquid phase and thus increases the effective solid volume concentration which increases viscosity (*Lewis, T.B., Nielsen, L.E. (1968), Windhab, E.J. (2000)*).

2.2.1.3 Continuous Phase

The viscosity of the continuous phase is the lowest possible viscosity a suspension can reach (see also Eq. (2.16)). Consequently it defines the lower viscosity limit. Besides this purely physical effect, the continuous phase also influences the particle interactions. Those are determined by the particle's and the surrounding liquid's physical chemical properties.The physical chemical properties are therefore crucial for effects like flocculation which is subject of the following section.

2.2.2 Physical - Chemical Influence Factors

Beside the purely physical mechanical factors also the physical-chemical properties of the disperse and continuous phase influence the flow properties of suspensions.

The following factors are considered as the physical-chemical properties

- Particle interactions

- Surface active components

- Physical state of the interacting surfaces

The physical chemical properties of the continuous and disperse phase play an important role in understanding the flow properties of suspensions (*Becker, U. (1984), Kao, S. et al. (1975), Tsai, S., Zammouri, K. (1988)*). The deviation from Newtonian flow behavior is often attributed to physical chemical effects taking place at the interfaces between disperse and continuos phase.

2.2.2.1 Particle Interactions

Consider two isolated spherical particles of a medium 2 separated by the distance h in a medium 1, the interactions between two isolated particles can be described in terms of an interparticle pair potential. The interparticle pair potential, w(h) is the energy required to bring two particles from an infinite distance apart to a surface-to-surface separation of h (see Figure 2-7).
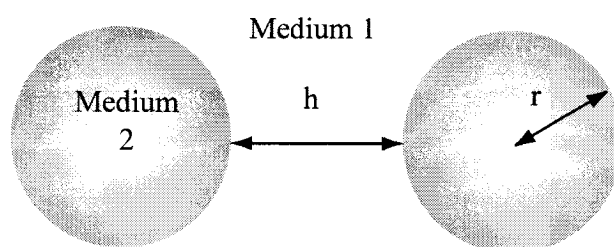
Figure 2-7 *Particles of radius r and medium 2 separated by a surface-to-surface separation h in a medium 1*

Between the particles there can be attractive ($w_{attractive}(h)$) and repulsive ($w_{repulsive}(h)$) interactions which are dependant from the distance h. The overall interaction between the droplet depends on the relative magnitude and range of repulsive and attractive interactions (*Israelachvili, J.N. (1985), McClements, D.J. (1999)*). The pair interaction potential also depends on the size of the "particles" looked at. In case of molecules and atoms the interactions are of importance for very short distances (h<1nm) and steeply decrease with increasing distance (Lenard-Jones potential, $w_{attractive} \sim -1/h^6$, $w_{repulsive} \sim 1/h^{12}$). For increasing "particle" size this dependence changes. In case of large condensed bodies the attractive interaction decays much more slowly with distance (1/h for spheres) and is also proportional

the particles size. The interactions are now more long range compared to the interactions between molecules (*Israelachvili, J.N. (1985)*). The total pair interaction potential is the sum of all attractive and repulsive contributions, and depending on the size of the "particles" looked at (molecular or macroscopic level) the overall potential at the same distance h can be attractive or repulsive (*Israelachvili, J.N. (1985)*).

In general the overall pair interaction potential thereby depends on the various types of attractive and repulsive contributions (Eq. (2.17)). Not all of these interactions act independently from another but some are coupled which has to be taken into account for calculation (*McClements, D.J. (1999)*).

$$w_{total}(h) = w_{vdWaals}(h) + w_{electrostatic}(h) + w_{steric}(h) + w_{depletion}(h) \qquad (2.17)$$
$$+ w_{hydrophobic}(h) + w_{hydration}(h) + w_{thermal}(h)$$

Not all of these interactions play an important role in every type of system, and it is often possible to identify two or three interactions which dominate the overall interaction.

In the following the van der Waals and the electrostatic interactions will be discussed.

Van der Waals Interactions

Intermolecular van der Waals interactions arise because of the attraction between atoms and molecules that have been electronically or orientationally polarized (*Israelachvili, J.N. (1985), Hiemenz, P.C., Rajagopalan, R. (1997), McClements, D.J. (1999)*). In addition to acting between individual molecules, van der Waals interactions also act between macroscopic bodies (particles) that contain a large number of molecules.

The van der Waals interactions between two macroscopic bodies (medium 1, spheres of radius r_1 and r_2, separated by surface-to-surface distance h) in a liquid (medium 2) can be calculated according to:

$$w_{vdWaals} = -\frac{A_{121}}{6}\left[\frac{2 \cdot r_1 \cdot r_2}{h^2 + 2r_1h + 2r_2h} + \frac{2 \cdot r_1 \cdot r_2}{h^2 + 2r_1h + 2r_2h + 4r_1r_2} + \ln\left(\frac{h^2 + 2r_1h + 2r_2h}{h^2 + 2r_1h + 2r_2h + 4r_1r_2}\right)\right] \qquad (2.18)$$

where A_{121} is the Hamaker function.

At close separation and for spheres of equal size the above equation can be simplified to:

$$w_{vdWaals} = -\frac{A_{121} \cdot r}{12 \cdot h} \qquad (2.19)$$

The Hamaker function is thereby the parameter that incorporates all of the physical-chemical properties of the media 1 and 2. Based on Lifshitz theory, where the atomic structure is ignored and the forces acting between large bodies are derived in terms of such bulk properties as their dielectric constants and refractive indices, the Hamaker constant can be approximated according to Israelachvili (*Israelachvili, J.N. (1985)*):

$$A_{121} = A_{v=0} + A_{v>0} \qquad (2.20)$$

where

$$A_{v=0} = \frac{3}{4}kT \sum_{s=1}^{\infty} \frac{1}{s^3}\left(\frac{\varepsilon_1-\varepsilon_2}{\varepsilon_1+\varepsilon_2}\right)^{2s} \qquad\qquad A_{v>0} = \frac{3hv_e}{16\sqrt{2}} \frac{\left(n_1^2-n_2^2\right)^2}{\left(n_1^2+n_2^2\right)^{3/2}} \qquad (2.21)$$

The zero frequency term $A_{v=0}$ is due to orientation and induction contribution (Keesom and Debye) whereas the frequency dependant part $A_{v>0}$ is related to dispersion contribution (London). Here ε is the static dielectric constant, n the refractive index, v_e is the major electronic absorption frequency in the ultraviolet region of the electromagnetic spectrum, h is Plank's constant.

It is also possible to derive approximate Hamaker constants using combining relations. The Hamaker constant for bodies of media 2 interacting through media 1 is given by (*Koglin, B. (1974), Koglin, B. (1978), Israelachvili, J.N. (1985)*):

$$A_{121} = \left(\sqrt{A_{11}}-\sqrt{A_{22}}\right)^2 \qquad (2.22)$$

Combining relations are applicable only when dispersion forces dominate the interactions, but break down when they are applied to media with high dielectric constants such as water and whenever the zero frequency contribution $A_{v=0}$ is large.

Electrostatic Interactions between Particles

A solid surface can become charged when it is in contact with another media. The type of media govers the mechanism of charging.

For solids in a gas atmosphere or vacuum charging occurs due to differences in contact potential between solids that are in contact (*Krupp, H. (1967)*).

For solids that are immersed in a liquids charging takes place due to:

- Polarization and orientation of liquid molecules at the solids liquid interface due to van der Waals forces or hydrogen bonds

- Dissolved substance in the liquid that adsorb to the solids

- Chemical reactions at the solid surface, pH based dissociation

Solids immersed in an aqueous media always exhibit surface charges and thus have a surface potential. The surface charge will be compensated by molecules of the surrounding liquid. For a negatively charged solid surface immersed in an aqueous electrolyte the situation can be described as follows.

The negative charge of the particle attracts opposite charged ions (counterions), whereas ions of similar charge are repelled. In a certain distance the charge then is reduced to the potential of the liquid and the whole system remains electrically neutral. In Figure 2-8 two regions can be identified, the inner and outer region.

In the inner region, the attraction between the counterions and charged surface is strong and therefore they are relatively immobile, whereas in the outer region, the attraction is much less and therefore the counterions are more mobile. The inner region is referred to as the Stern layer, while the boundary between the inner and outer regions is referred to as the Stern plane. The potential at the surface is the Nernst potential (Ψ_0), whereas the potential at the Stern plane is the Stern potential (Ψ_δ) which is different to Ψ_0 because of the presence of counterions in the Stern layer. At the boundary between inner and outer region mobility of
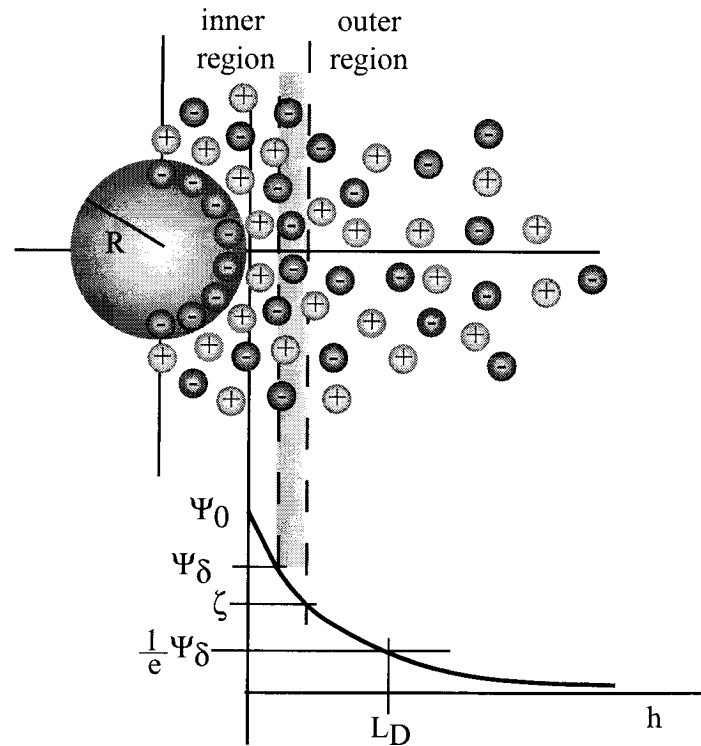
Figure 2-8 *Electrostatic interactions in an electrolyte - diffusive double layer*

the ions change. When a liquid flows past a charged surface, it "pulls" those counterions which are only weakly attached to the surface along with it, but leaves those ions that are strongly attached in place (i.e. those ions in the Stern plane). The shear plane is defined as the distance from the charged surface below which the counterions remain strongly attached and is referred to as zeta potential (ζ). The zeta potential can be measured by electrokinetic techniques and is a good approximation of the Stern potential, which can not be directly measured. In the outer region, the electrostatic interaction between the surface and counterions is usually weak because the ions in the Stern layer partially screen the surface charge.

The electrical potential (Ψ) as a function of the distance (h) to the surface can then be described as:

$$\Psi(h) = \Psi_\delta \cdot \frac{R}{h} \cdot \exp\left(\frac{-(h-R)}{L_D}\right)$$

(2.23)

where R is the radius of the particle and L_D is the Debye screening length. The Debye screening length is a measure of the thickness of the electrical double layer. It is related to the properties of the electrolyte solution by the following equation:

$$L_D = \sqrt{\frac{\varepsilon_0 \varepsilon_r kT}{e^2 \sum n_{i,0} z_i^2}}$$

(2.24)

where $n_{i,0}$ is the concentration of ionic species of type i in the bulk electrolyte solution, z_i is their valency, e is the electrical charge of a single proton, ε_0 is the dielectric constant of vacuum and ε_r is the relative dielectric constant of the solution (*McClements, D.J. (1999)*).

The Debye screening length determines how rapidly the electrical potential decreases with distance from the surface. The higher the concentration of ions and the higher their valency the shorter the distance at which surface charges are neutralized.

For systems with a low Stern potential ($\Psi_\delta < 25\text{mV}$) and under the condition that the Debye screening length and the surface to surface separation between two particles is much less than the particles size then the electrostatic interparticle pair potential for two similar sized particles can be derived at constant surface potential as (*McClements, D.J. (1999)*):

$$w_{electrostatic}^{\Psi}(h) = 2\pi\varepsilon_0\varepsilon_r r\Psi_\delta^2 \ln\left[1 + \exp\left(-\frac{h}{L_D}\right)\right] \qquad (2.25)$$

In order to see the total interaction potential the contribution of all interactions need to be taken into account. The DLVO theory assumes that the overall interaction between a pair of particles is the result of van der Waals attractive and electrostatic repulsive interactions.

In Figure 2-9 the interaction potential for van der Waals and electrostatic interactions as well as the resulting total potential are shown. The total potential thereby has a typical shape. Depending on the distance between the particles the interaction potential can be negative or positive. For separated particles approaching one another first attractive interactions are present which yield a secondary minimum. For decreasing distance repulsive interactions are dominant and a energy barrier has to be overcome. Having passed that barrier the interactions become attractive again and the particles reach the primary minimum.
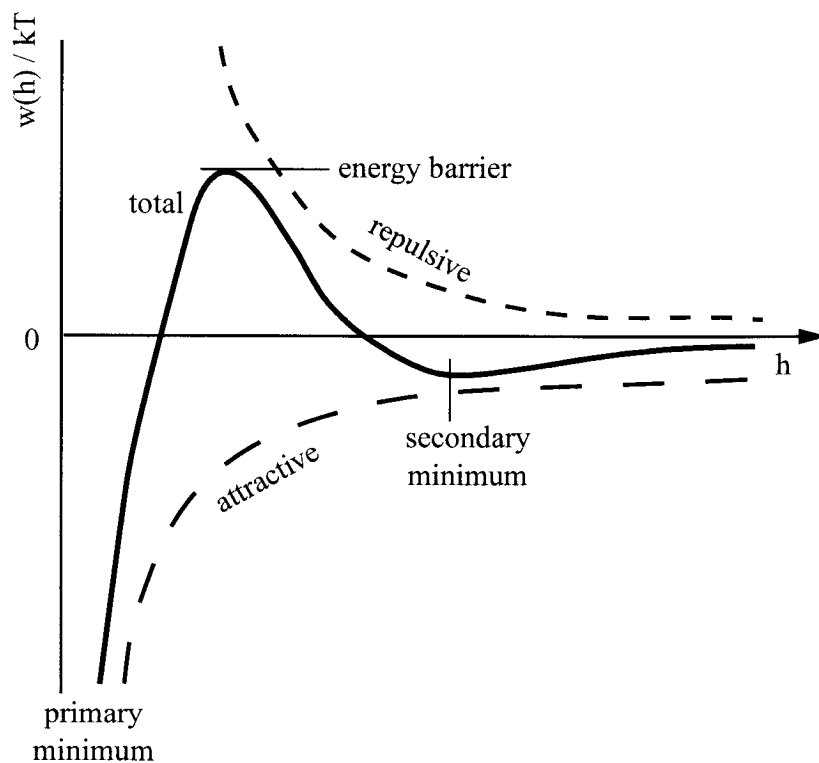
Figure 2-9 Overlay of attractive and repulsive Interactions, DLVO Theory

Depending on the contribution of each interaction different shapes for the total potential are obtained. The energy barrier can be high or low and the total interaction can be repulsive for large distances. Taking into account other effects like sterical hindrance or strong repulsion for adsorbed emulsifiers even a primary minimum can not be observed (*McClements, D.J. (1999)*).

2.2.2.2 Surface Active Components

In the previous section it was shown that the overall potential of interaction depends on the sum of the various types of attractive and repulsive interactions. Adsorption of surfactants can modify the Hamaker function and mask the characteristics of the underlying surface. Consequently the van der Waals Forces are affected. It is also possible to change the electrical double layer properties by adsorption of emulsifiers which act as an ionic species. Also the size of the emulsifier is of importance. Large polyvalent ions bind simultaneously to the surface of two particles which is observed for polysacharides and proteins. Sterical effects have then to be considered as well (*Hiemenz, P.C., Rajagopalan, R. (1997), McClements, D.J. (1999)*).

2.2.2.3 Physical State of Interacting Surfaces

The physical state of the surfaces affects the way the surface can interact with the media. An amorphous sucrose surface for example is highly hygroscopic and easily takes up water, whereas crystalline sucrose is much less hygroscopic. The uptaken water alters the properties of the surface and thus affects the interparticle potential (*Becker, U. (1984)*). In the amorphous state not all hydrogen bonds are "saturated" by surrounding sucrose molecules and therefore water can easily attach to the amorphous sucrose which lowers the energy of the system. In the crystalline state all hydrogen bonds are "saturated" in an optimum way and therefore the affinity to water is reduced compared to the amorphous state.

2.2.2.4 Deagglomeration and its Effect on Flow Properties

In the previous sections effects taking place between particles were described. In a suspension the flow properties are thereby affected by particle interactions as well as by the physical mechanical attributes of the disperse and continuos phase. Due to particle interactions agglomeration can take place in suspensions and thus generate a certain structure. Disruption of the so formed agglomerates can thereby influence the flow behavior in different ways which is discussed in the following.

In a first step a suspension that contains agglomerates that were formed in a roll refining process is considered. The agglomerates present are called primary agglomerates. The agglomerates are composed of non porous particles and fluid that is entrapped between the agglomerate forming, primary particles. Due to compression that takes place during refining the particles within the agglomerates exhibit a certain surface-to-surface distance which governs the strength and porosity of the agglomerates. The solid volume concentration of the suspension is given by the volume of the solids whereas the effective solid volume concentration is determined by the volume of the agglomerates which is bigger than the volume of the pure solids (*Windhab, E.J. (2000)*). In a second step the so prepared suspension is mechanically treated in order to destroy the agglomerates which yields suspensions with different amount of primary agglomerates. Thereby the effect of deagglomeration on the flow properties of the suspension can be studied. In Figure 2-10 schematic flow curves for different situations are given.The suspension that contains the primary agglomerates exhibits a
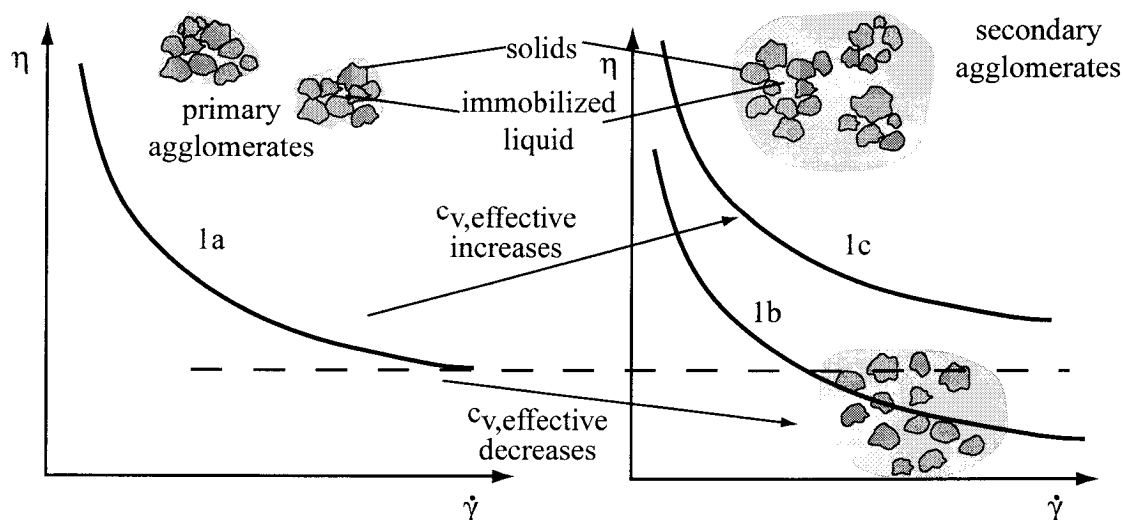
Figure 2-10 Potential effects of deagglomeration on flow behavior

certain flow behavior which is represented by curve 1a. Break down of the agglomerates releases immobilized fluid phase and thus decreases effective solid volume concentration which lowers viscosity. This is seen for comparison of curve 1a to 1b in Figure 2-10. On the other hand deagglomeration frees up particles which can reagglomerate due to particle interactions and thus form secondary agglomerates. Those secondary agglomerates most probably have larger surface-to-surface distance than the primary agglomerates that were formed by a roller compacting process. Consequently the porosity of the secondary agglomerate is higher and more liquid is immobilized within these "loose" agglomerates. This causes an increase of effective solid volume concentration and thus increases viscosity (curves 1a-1c). The particle interactions might also become a function of time if the solids' surfaces alter their composition and state with time. This is the case for amorphous sugar surfaces that adsorb water from the surrounding atmosphere or media and thus alter their surface composition with time. Furthermore water sorption also affects the physical state of the amorphous phases and allows them to transfer from the glassy into the rubbery state which is subject of the next section.

2.3 Phase and State Transition Phenomena

From a molecular-kinetic point of view all substances can exist in three different states, as gases, liquids and solids. These three states are distinguishable with respect to the degree of interaction of the smallest units of the corresponding substances (atoms, molecules), and consequently, with respect to the structure and mobility of the system. From a thermodynamic point of view the different states are defined as thermodynamic phases and the transitions between these states are particular cases of phase transformations (*Gutzow, I., Schmelzer, J. (1995)*).

Thermodynamics distinguish between 1st order and 2nd order phase transformation. 1st order phase transformation are related to transitions from solid <-> liquid, solid <-> gas, liquid <-> gas, whereas 2nd order transformations refer to transitions like glass to rubbery state. In order to separate between the different transitions, "phase transition" will be attributed to all transitions where the state of aggregation is changed (solid-liquid, solid-gas,

liquid-gas) whereas "state transition" essentially refers to non equilibrium transformations where the physical state is changed but not the state of aggregation, like amorphous-crystalline and glassy-rubbery transitions which typically take part in the solid state (*Roos, Y.H. (1995-1)*).

2.3.1 Thermodynamics

According to the Gibbs fundamental equation, the change of energy of a system (dU) is determined by the temperature (T), the change of entropy (dS), the pressure (p) and the change in volume (dV), the chemical potentials (μ_i) and the mole number (n_i) of the independent molecular species (components, i)

$$dU = TdS - pdV + \sum \mu_i dn_i \qquad (2.26)$$

where U and S are functions of T, V and n. Consider a closed system with constant volume V and a constant number of molecules n, Eq. (2.26) reduces to:

$$dU = TdS \qquad (2.27)$$

Where the influence of temperature for constant V and n is obtained from

$$\left(\frac{\partial U}{\partial T}\right)_{V,n} = T\frac{\partial S}{\partial T} \qquad (2.28)$$

which expresses how the change of entropy with temperature is related to the change of energy with temperature in an adiabatic system. This function thereby corresponds to the heat capacity at constant volume c_V.

$$c_V = T\left(\frac{dS}{dT}\right)_V \qquad (2.29)$$

The heat capacity at constant volume thus is a measure for the entropy increase with temperature in an adiabatic system at constant volume. More often systems are used that are kept at constant pressure. There the heat capacity at constant pressure is found to be:

$$c_p = T\left(\frac{dS}{dT}\right)_p \qquad (2.30)$$

which is derived in an analog way for constant p and n from Eq. (2.31)

$$dH = TdS + Vdp \qquad (2.31)$$

which is obtained from Eq. (2.26) using Eq. (2.32) for a system with constant n:

$$dH = dU + pdV + Vdp \qquad (2.32)$$

In addition to these equations the Gibbs free enthalpy G needs to be taken into account.

$$G = H - TS \qquad (2.33)$$

with

$$dG = -SdT + Vdp + \sum_i \mu_i dn_i \qquad (2.34)$$

For a system that consists of more than 1 phase the total free enthalpy can be written as the sum of the contributions of the individual (i) phases:

$$G = \sum_i G_i \qquad (2.35)$$

In equilibrium the phases coexist and T, P, and the chemical potential μ_i are the same in the coexisting phases and dG=0 (*Gutzow, I., Schmelzer, J. (1995)*).

2.3.2   1st Order Phase Transformation

For 1st order phase transformation the enthalpy and entropy changes (melting-crystallizing, evaporation-condensation, sublimation-desublimation) whereas dG=0 for phase equilibrium.

With $\Delta S = S_2 - S_1$ when going from state 1 into state 2 and taking into account that

$$\left(\frac{\partial G}{\partial T}\right)_p = -S \quad , \qquad \left(\frac{\partial G}{\partial p}\right)_T = V \qquad (2.36)$$

yields that

$$\left(\frac{\partial G^{(1)}}{\partial T}\right)_p \neq \left(\frac{\partial G^{(2)}}{\partial T}\right)_p \quad , \qquad \left(\frac{\partial G^{(1)}}{\partial p}\right)_T \neq \left(\frac{\partial G^{(2)}}{\partial p}\right)_T \qquad (2.37)$$

This means that the slope of the curve that gives the relationship between G and T is different for state 1 and state 2 (i.e. the first derivative of G(T)). Furthermore it shows that H, S and V are discontinuously changed when reaching the state transition temperature. When S changes discontinuously (step change) it is seen that c_p changes infinitely at the state transition temperature (*Gutzow, I., Schmelzer, J. (1995), Roos, Y.H. (1995-1)*).

$$\left(\frac{dS}{dT}\right)_p = \frac{c_p}{T} \quad \text{and} \quad \left(\frac{\partial^2 G}{\partial T^2}\right)_p = \frac{-c_p}{T} \text{ with Eq. (2.36)} \qquad (2.38)$$

This is illustrated in Figure 2-11.

2.3.3   2nd Order Phase Transformation

For a 2nd order phase transformation the second derivative of G as a function of T is discussed. In that case the second derivatives change when going from state 1 to state 2 (*Roos, Y.H. (1995-1), Gutzow, I., Schmelzer, J. (1995)*).

$$\left(\frac{\partial^2 G^{(1)}}{\partial p \partial T}\right) \neq \left(\frac{\partial^2 G^{(2)}}{\partial p \partial T}\right) \quad , \qquad \left(\frac{\partial^2 G^{(1)}}{\partial p^2}\right)_T \neq \left(\frac{\partial^2 G^{(2)}}{\partial p^2}\right)_T \quad , \qquad \left(\frac{\partial^2 G^{(1)}}{\partial T^2}\right)_p \neq \left(\frac{\partial^2 G^{(2)}}{\partial T^2}\right)_p \qquad (2.39)$$

This means that c_p, the thermal expansion coefficient α and the compressibility β change during state transition.

$$\Delta^{(1,2)}\left(\frac{\partial^2 G}{\partial p \partial T}\right) = \Delta V \alpha \quad , \qquad \Delta^{(1,2)}\left(\frac{\partial^2 G}{\partial p^2}\right)_T = -(\Delta V \beta) \quad , \qquad \Delta^{(1,2)}\left(\frac{\partial^2 G}{\partial T^2}\right)_p = \Delta \frac{-c_p}{T} \qquad (2.40)$$

Whereas the first derivatives are the same

$$\left(\frac{\partial G^{(1)}}{\partial T}\right)_p = \left(\frac{\partial G^{(2)}}{\partial T}\right)_p \quad , \qquad \left(\frac{\partial G^{(1)}}{\partial p}\right)_T = \left(\frac{\partial G^{(2)}}{\partial p}\right)_T \tag{2.41}$$

which means that H and S do not change at the transition temperature.

The changes taking place during 2nd order transitions are depicted in Figure 2-11 (*Gutzow, I., Schmelzer, J. (1995)*).
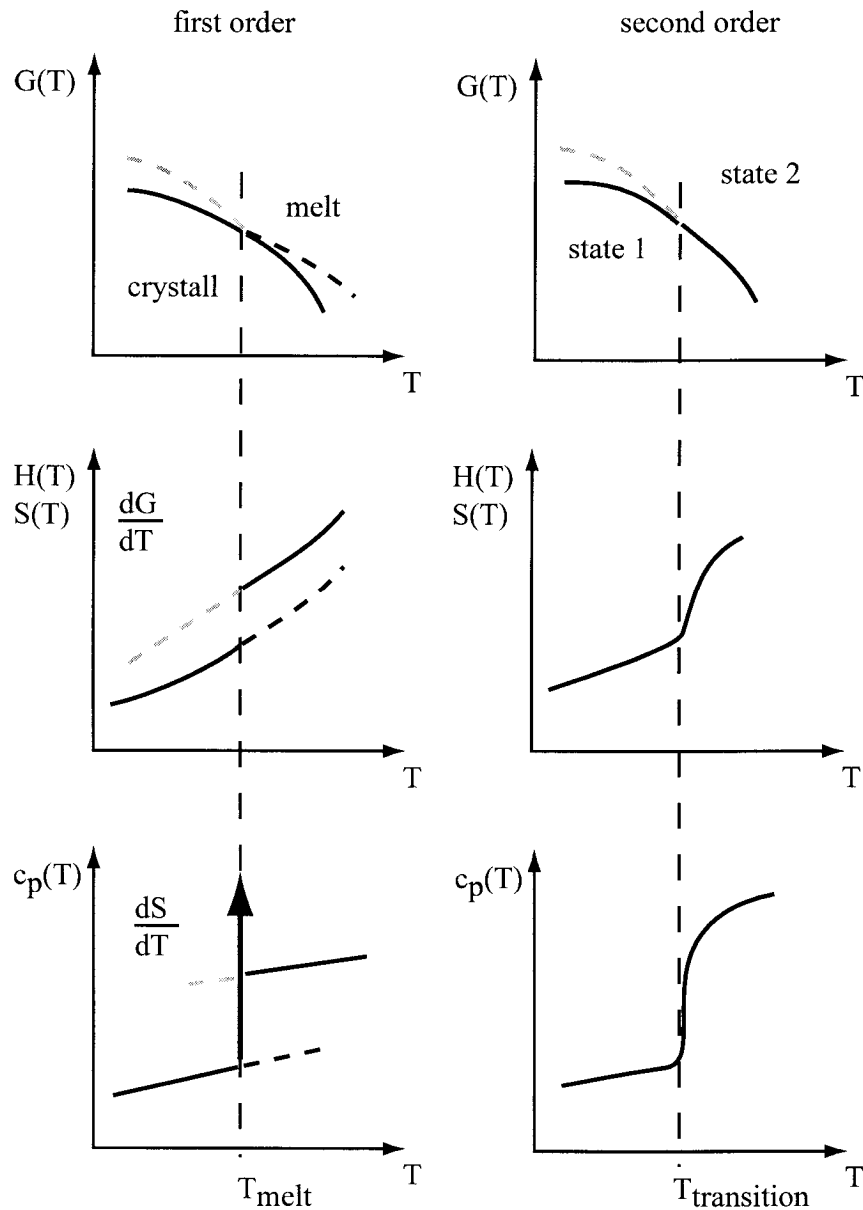
Figure 2-11 Overview on changes occurring during 1st and 2nd order phase transitions, redrawn from Gutzow, I., Schmelzer, J. (1995)

During the transformation from the glass like state to the rubbery state the molecules obtain a higher mobility. Accompanied with that, entropy is higher in the rubbery state than in the glass like state. This means that c_p is also higher in the rubbery state compared to the glassy state. The glass transition can therefore be detected by measuring the changes of c_p. Due to the increased molecular mobility also mechanical properties are affected. Increased molecular mobility reduces the resistance to flow and thus viscosity is decreased in the rubbery state compared to the glassy state (see Figure 2-12).
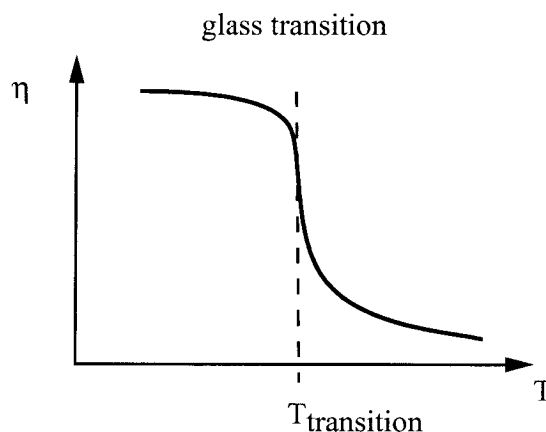
Figure 2-12 Change of viscosity during glass transition (Roos, Y.H. (1995-1))

The glassy state is comparable to the molecular arrangement a supercooled liquid has. The transition temperature is much lower than the phase transition temperature for melting. This means that in terms of G(T) the crystalline state would be favoured as there G is smaller than in the liquid state at that temperature (see Figure 2-11). Consequently the solidified system wants to get into the energetically more preferred crystalline state but the reduced molecular mobility prevents crystallization in the glassy state (Roos, Y., Karel, M. (1992), Roos, Y.H. (1995-1), Rao, M.A., Hartel, R.W. (1998)). Once temperature is increased and the rubbery regime is reached, molecular mobility is high enough to enable crystallization. The rubbery state is therefore a state which enables other type of transformations that can not take place in the glassy state which is due to the reduced molecular mobility.

3 Materials & Methods

3.1 Physical - Chemical Properties of Materials

3.1.1 Continuous / Liquid Phases

3.1.1.1 Silicon Oil

Silicon oils used here are polydimethylsiloxanes, where the backbone of the macromolecule is made up of a chain of alternating silicon and oxygen atoms and each silicon atom is bound to two methyl groups (*Rhône-Poulenc (1995)*). Mixing macromolecules of different chain length yields different viscosities such as viscosities ranging from 0.65mPas up to 1,000,000 mPas and higher can be achieved. A fluid exhibiting a viscosity of 10 mPas (25°C) corresponds to a molecular weight of 1200 g/mol and its molecular chains contain a calculated number of 16 siloxane units, whereas a viscosity of 1000 mPas (25°C) corresponds to 406 siloxane units per chain. Up to a viscosity of 1000 mPas silicon oils show Newtonian like flow behavior. For shear rates higher than 1000 1/s and for higher viscous oils shear thinning behavior is observed.

Silicon oil is a hydrophobic fluid that has a contact angle of 108° (silicon oil coated steel) which is similar to paraffin that shows an contact angle of 107° whereas uncoated steel yields a contact angle for water of 50° (*Wacker Chemie (1989)*). This illustrates its water repellent properties which is due to the orientation of the methyl groups towards the outside of the coating (*Rhône-Poulenc (1995)*). On the other hand silicon oil shows a high water vapor permeability and is therefore used as protective coating for clothes, shoes, or buildings for example.

Gas solubility at room temperature and normal atmosphere is about 0.024% w/w for air ($0.19cm^3$/g oil). The presence of water dramatically reduces the solubility of gases in silicon oil.

The silicon oil was obtained from Wacker Chemie, Germany. As oils the types AK2000 and AK 10 were used. Hereby AK2000 has a viscosity of 2000mPas at 20°C whereas AK10 has a viscosity of 10mPas at 20°C.

3.1.1.2 Cocoa Butter - Technical

Cocoa butter is a vegetable fat obtained from pressing milled and deshelled cocoa beans. It is mainly composed of palmitic, oleic and stearic acid and for temperatures higher than 40°C it is present in the liquid stage. Deodorized cocoa butter was sourced from a chocolate factory and different lots were used for the individual trial series, whereas within a series the same batch of cocoa butter was used.

3.1.1.3 Cocoa Butter - Purified

Commercial cocoa butter was purified using a purification method as described in literature (*Gaonkar, A.G. (1989)*). During purification surfactants (phospholipids, mono,-diglycerides) were removed and thus interfacial tension (vs. water) was increased.

3.1.1.4 Akomed

Akomed R was used as dispersant for particle size analysis. It is a special medium-chain-triglyceride produced from esterification of food grade fatty acids (deodorized caprylic and capric acids which are taken from Coconut and /or Palm kernel oil). It is liquid at room temperature and is miscible with cocoa butter. It has a refractive index of 1.450 at 20°C (*Karlshamns (1997)*) and was sourced from Karlshamns, Sweden.

3.1.1.5 Emulsifier - Lecithin

Lecithin stands for a mixture of phospholipids obtained from soy beans and is used in chocolate industry as an emulsifier. It can be obtained in different purities and phospholipid compositions. The lecithin used here was sourced from a chocolate factory and is a non standardized soy lecithin containing 40% soy oil and 60% w/w acetone insoluble components which are mainly composed of different types of phospholipids. Applying correct terminology, lecithin would stand for phosphatidylcholin only and not for a mixture of different phospholipids and soy bean oil.

3.1.2 Disperse Phases

3.1.2.1 Limestone - used for Refining

Limestone was used as a solid, crystalline and dense component. It was sourced from KSL Staubtechnik, Lauingen, Germany as a preground powder (different size classes are available) obtained from natural limestone. The size fraction of 0.5-1.0mm was used as raw material for production of mixtures of limestone and silicon oil that were refined in a 3 roll laboratory roll refiner. The purity of the limestone is about 99.1%, it is present in the crystalline state (calcite) and has a density of 2.7 g/ml.

3.1.2.2 Limestone - used as a Dry Ground Powder

For some trials fine, dry ground natural limestone was used. The material was obtained in the corresponding size range from KSL Staubtechnik, Lauingen, Germany.

The particle size of the used material is given in Figure 3-1.

It was measured by Laser diffraction (Malvern, Mastersizer 2000) dispersing the sample in a liquid media (Trichlorethan, TCE).
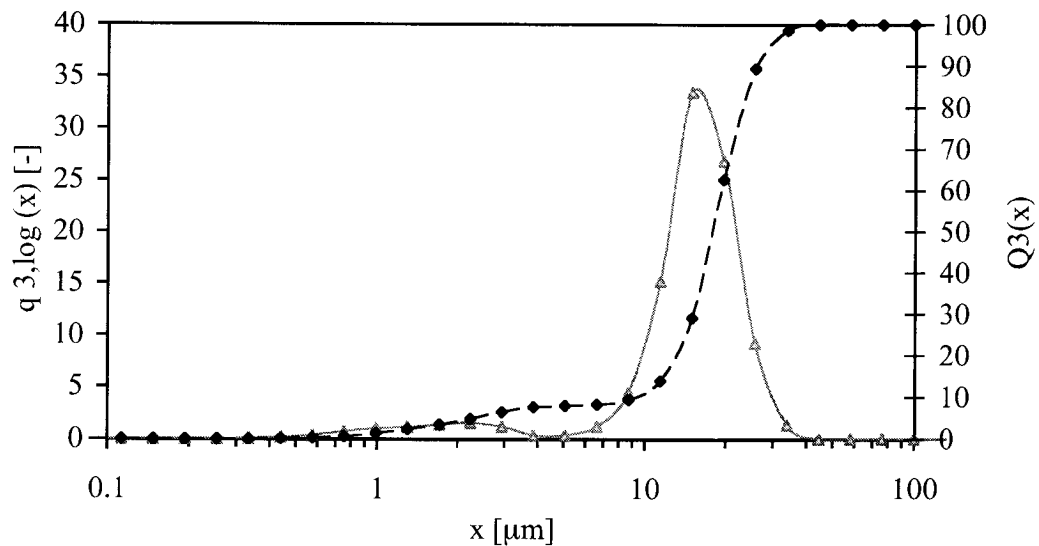
Figure 3-1 Particle size of dry ground, natural limestone, wet dispersion in TCE

3.1.2.3 Sugar

Sugar is the component which makes up 70% w/w of the solids in chocolate. Sugar was used as commercially available crystalline sucrose, of size below 1 mm. It was sourced from a chocolate factory.

3.1.2.4 Cocoa Liquor

Cocoa liquor used was obtained from industry. The average fat content was about 54.5%. The cocoa liquor was fine ground (<1%, 75μm sieve) and had an average water content of 1%.

3.1.2.5 Milk Powder

As milk powders, commercially available skim milk and whey powders were used. For the water sorption characteristics milk powders from different suppliers were used. For chocolate preparation milk powder from the same batch was used and commercially available milk fat was added in order to meet the legally required milk solids and fat content.

3.1.3   Mixtures - Make Up and Composition

In order to perform the various experiments mixtures and suspension were prepared. In the following, physical data of the components that were used are given. The physical data were obtained from measurements. In case of solids, density was measured on the basis of liquid volume displacement. For liquids density was measured with a commercial densimeter (see Section 3.2.3 on page 35). Viscosity was measured with a concentric cylinder system (see Section 3.2.1 on page 34).

3.1.3.1 Physical Data

The following table gives values for density and viscosity of the used components.

component	density [g/cm^3]	viscosity [mPas]
sugar (sucrose), 25°C	1.577[a]	
limestone, natural, 25°C	2.7[a]	
silicon oil, AK2000, 25°C	0.97[b]	1940[c]
cocoa butter, 45°C	0.97[b]	40.8[c]

Table 3-1 Physical data of the components used (measured values, a: volume displacement method; b: densimeter, see also Section 3.2.3; c: rheometry, conc. cylinder system, Bohlin)

In order to transfer mass based concentrations (c_m) into volume based ratios (c_V) the following equation was used. This equation can be applied if the particles itself are considered as nonporous and volume effects (volume dilation) can be excluded. The solid volume concentrations $c_{V,s}$ is then calculated as

$$c_{V,s} = \frac{V_{solids}}{V_{total}} = \frac{V_{solids}}{V_{solids} + V_{liquid}} = \frac{\dfrac{m_{solids}}{\rho_{solids}}}{\dfrac{m_{solids}}{\rho_{solids}} + \dfrac{m_{liquid}}{\rho_{liquid}}} \quad (3.1)$$

$$c_{V,s} = \frac{\rho_l}{\rho_l + \left(\dfrac{1 - c_{m,s}}{c_{m,s}}\right) \cdot \rho_s} \qquad \text{(divided by } m_{total}) \quad (3.2)$$

with the density of the liquid (l) and solid (s) phase (ρ_l, ρ_s) and $m_{total} = m_{solids} + m_{liquid}$.

In order to prepare suspensions, homogenous mixtures of the individual components were produced first. The mixtures which contained coarse particles were then ground in a laboratory 3 roll refiner (see 3.3.2 Mixing as Preparation for Refining and 3.3.3 Refining). The refined product was processed further in a labkneader. There kneading took place and through addition of further liquid, a suspension with the desired concentration was obtained. The following section gives the concentration of the mixtures used for refining as well as of the final suspensions. The concentrations are given as both, mass and volume based values.

3.1.3.2 Limestone - Silicon Oil

For the trials performed, two different concentrations of this system were used which are given in Table 3-2.

Table 3-2 Composition of limestone silicon oil systems

Component	mixture used for refining % w/w	mixture used for refining % v/v	suspension after kneading % w/w	suspension after kneading % v/v
Limestone	80	59.6	57.8	33.5
Silicon oil	20	40.4	42.2	66.5
Limestone	80	59.6	70	46
Silicon oil	20	40.4	30	54

3.1.3.3 Sugar - Silicon Oil

The trials were carried out with two different concentrations for this system which are given in Table 3-3.

Table 3-3 Composition of sugar silicon oil systems

Component	mixture used for refining % w/w	mixture used for refining % v/v	suspension after kneading % w/w	suspension after kneading % v/v
Sugar	70	58.9	45	33.5
Silicon oil	30	41.1	55	66.5
Sugar	75	65	58.3	46.2
Silicon oil	25	35	41.7	53.8

3.1.3.4 Sugar - Cocoa Butter - Lecithin

For the trials with sugar cocoa butter lecithin system the composition given in Table 3-4 was used.

Table 3-4 Composition of sugar - cocoa butter - lecithin systems

Component	mixture used for refining % w/w	mixture used for refining % v/v	suspension after kneading % w/w	suspension after kneading % v/v
Sugar	75	65	71.3	60
Cocoa butter	25	35	28	39
Lecithin	0	0	0.7	1

3.1.3.5 Milk Chocolate

The trials with milk chocolate were made with the following (Table 3-5) mixture. This mixture was only used for refining trials. The objective was to see the influence of different refining conditions on the stability of the resulting agglomerates. In trials referring to water sorption and rheology samples of commercially available quality milk chocolate were used.

Table 3-5 Composition of chocolate mix

Component	mixture %w/w
Sugar	46
Milk powder (skim milk & whey)	23
Cocoa liquor	15
Cocoa butter	12
Milk fat	4

3.2 Physical and Chemical Measurement Methods

3.2.1 Rheometry

Rheological measurements were performed using two different rheometers

- Rheometric Scientific, DSR, stress controlled rheometer

- Bohlin, CVO 120, high resolution, stress controlled rheometer

The rheological behavior of the pure liquids was determined by use of conventional type of geometries, like concentric cylinder system or cone and plate. The flow properties of the suspensions had been assessed most often with special, stirrer type geometries and in some individual cases with a concentric cylinder system (see also 4.2 Rheometry).

For analysis it was always waited for steady state conditions (gradient method applied, change in value reading less than 1%) and measurements were carried out in a step mode rather than in "continuous" mode (number of data points per measurement and steady state conditions). For time dependency tests, measurements were done at one distinct shear stress or in case of the Bohlin rheometer, at one distinct angular velocity (software routine allows to run also in a software controlled rate mode).

3.2.2 Sorption Balance - Detection of Amorphous Phases

The presence of amorphous sugar phases was detected by means of a water vapor sorption technique. Therefore a sorption balance from DVS, Type DVS 1000 was used. This device consists of a heatable sample chamber where different temperatures can be applied to the sample ranging from 10°C up to 80°C. The sample is placed in a sample cup which is connected to a Cahn balance. On the other side of the balance an empty cup is positioned and the difference in weight versus time is recorded with a precision of 0.1μg whilst different levels of humidity are applied. Water sorption takes place at defined humidity and temperature.

Amorphous phases that are present in the sample, take up water, recrystallize, and finally release the water. This can be detected as a peak in the weight signal. Depending on the type of material analyzed, different sorption temperatures were used. Powders and silicon oil containing suspensions were normally measured at a temperature of 25°C or 30°C, whereas cocoa butter containing suspensions were analyzed at 45°C.

Measurements were always performed in time mode where the sample was exposed to a distinct humidity for a given time before the next level of humidity was applied. Prior to any measurement the cups were checked for cleanliness through running vapor sorption measurements with the empty cups. Afterwards the balance was tared and the sample cup was filled with 20mg to 60 mg of the sample. After loading the balance normally an equilibration phase took place where the balance could equilibrate for 30 to 60 min. During this time a dry atmosphere was applied to the sample. After this equilibration period the measurement was started.

3.2.3   Density

Density measurement of the pure liquids were carried out using a DMA 35 densimeter (Anton Paar KG, Graz, Austria) where oscillatory measurements of a U-shaped glass tube revealed the density. Determination of solid's density was performed by a volume displacement method. Therefore a weighed amount of solids was placed in a degassed, non dissolving liquid and the displacement of liquid volume was measured.

3.2.4   Scanning Electron Microscopy

Scanning electron microscopy was performed using either a Hitachi S-700 or a cold stage unit Hitachi S-900. The samples were mounted on the sample holder using glycerin in case of cold stage observation or double sided tape for fixation. In some cases freeze etching was performed and some samples had been defatted in super critical CO_2 prior to sputtering.

3.3 Methods for Processing

3.3.1 Humidification Unit

In order to enforce recrystallization of the amorphous sugar or to be able to analyze the influence of water vapor uptake on the rheological properties of the systems assessed, a humidification unit was designed and built. The general set up of the unit is given in Figure 3-2.
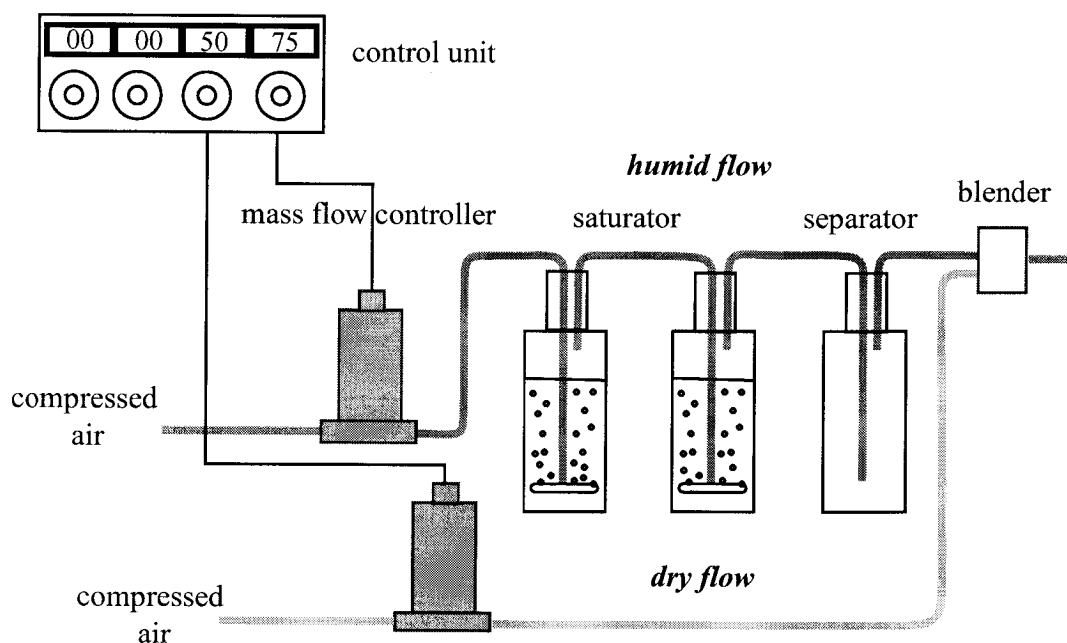
Figure 3-2 Humidification unit

Compressed air, which can be considered dry (2.5% r.h. 25°C) is fed into the system. The air flow is split into 2 streams each passing a mass flow controllers (MKS, München, Germany). Stream 1 is the dry flow, whereas stream 2 becomes the humid flow. Stream 2 passes a series of gas washing bottles where it becomes saturated with water. Both streams are then blended together and form again a mainstream. Measuring the humidity of the blended stream and controlling the flow rate of each stream allows to adjust any humidity between 2.5% and 100% r.h.

3.3.2 Mixing as Preparation for Refining

To prepare the different mixtures the ingredients were dosed into a bucket (volume 10 l) and intensively mixed (5-10min) using a helical ribbon type impeller attached to a drilling unit. The mixed mass was then refined in a lab 3 roll refiner. The concentrations used are given the tables in 3.1.3 Mixtures - Make Up and Composition.

3.3.3 Refining

Refining was performed with a laboratory 3 roll refiner (Bühler, Uzwil, Switzerland). In order to ensure that the amorphous phases generated during refining do not recrystallize, refining was executed in a special tent, which was flushed with compressed air. The refiner

was located in the tent and adjustment of the refiner was done through small manipulation openings in the tent. This ensured, that increase of humidity caused by transpiration of human body was negligible. Humidity and temperature in the tent was monitored through a sensor and was for all trials below 15% r.h. and 20°C.

The set up is illustrated in Figure 3-3.
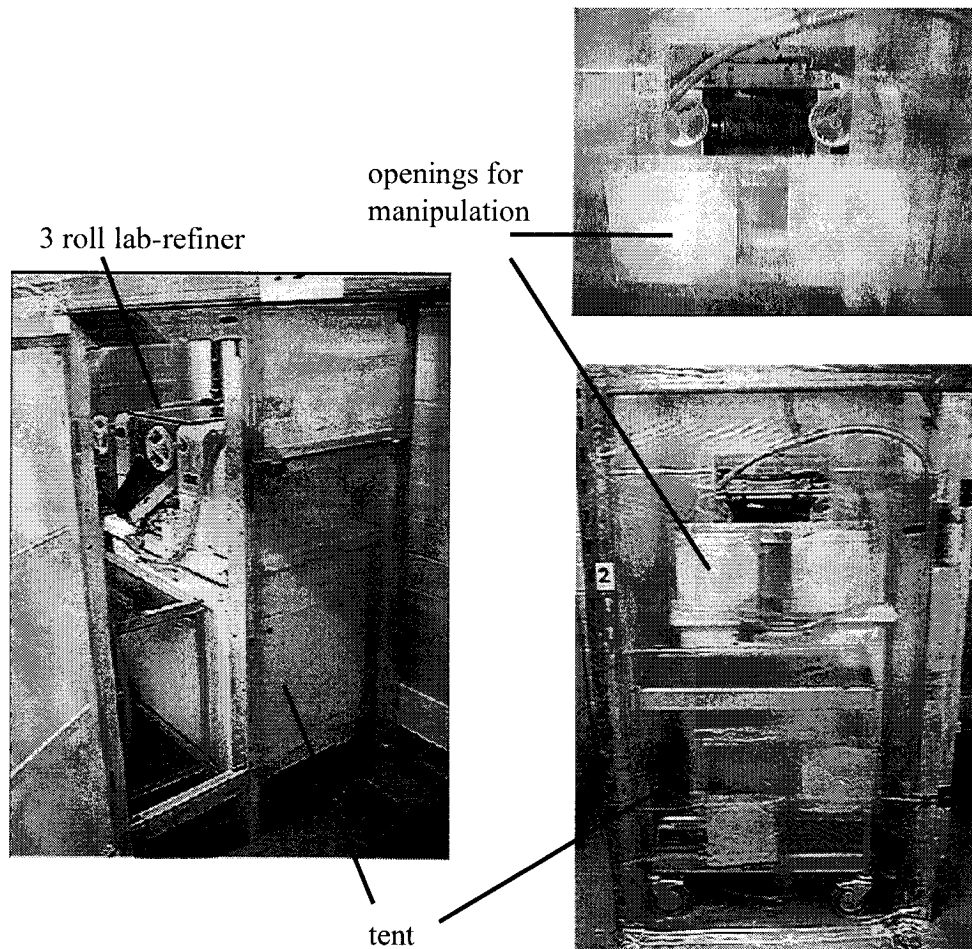
Figure 3-3 *Refiner set up*

3.3.4 Kneading

Kneading took place in a Brabender lab kneader. The kneading chamber had a volume of 500ml and was normally filled (in case of sugar oil mixtures) with 300g of product and was temperature controlled. The chamber was covered with a lid. In order to control and adjust the head space atmosphere, the head space of the kneading chamber was flushed with a flow of conditioned air. This airflow was provided by the humidification unit (see 3.3.1 Humidification Unit). The revolutions of the kneading arms were adjustable between 0 and 250rpm and the responding torque was measured. All signals (temperature of the chamber, head space conditions (humidity, temperature), number of revolutions, torque, time) were recorded on a data acquisition unit. The speed of the kneading arms as well as the amount of

liquid (not total amount) and time of addition was adjusted towards the special trial needs. In some cases it was desired to keep a crumbly texture for a long time in other cases rapid liquefaction had to be achieved. This could be managed through controlled addition of liquid phase.
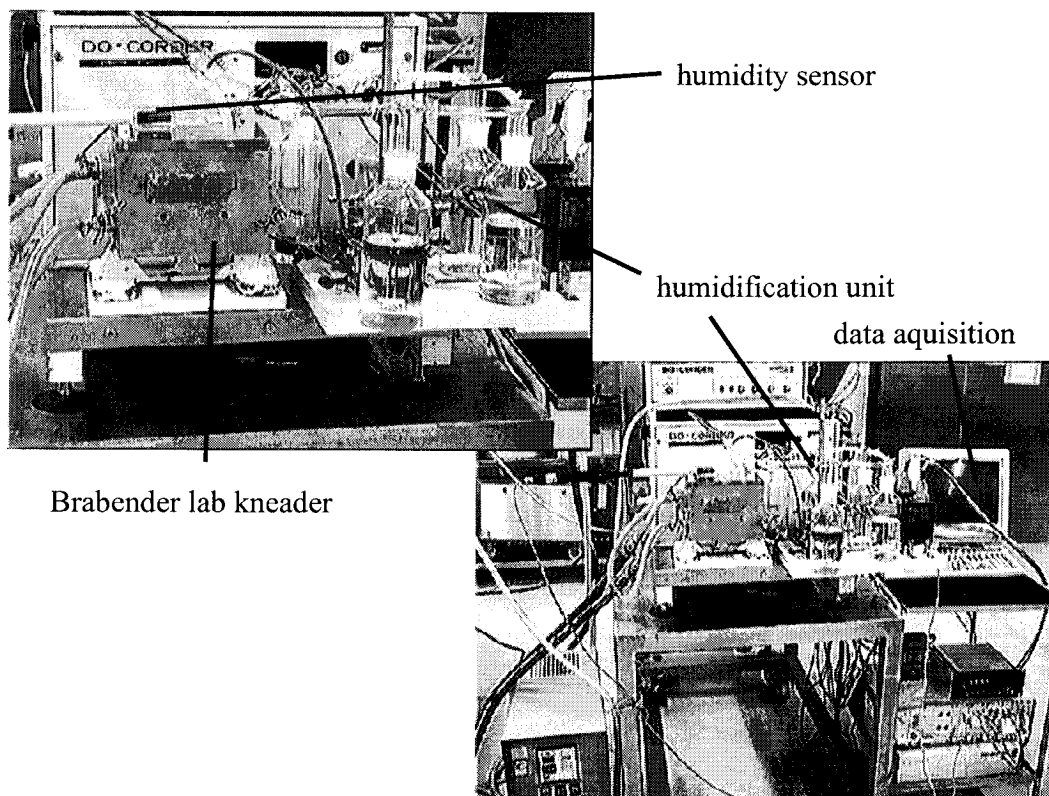
Figure 3-4 Setup used for kneading

4 Methods Developed

4.1 Agglomerate Analysis

Analysis of presence and size of agglomerates is essential for assessing progress of deagglomeration. Agglomerates can be identified by various methods. The two methods used here are based on light microscopy and visual identification of the agglomerates (single particle assessment) and on laser diffraction where bulks of particles are assessed simultaneously.

Both techniques require the dilution of the sample (concentration < 1% w/w) and thus do not allow for analysis of the sample in its original composition, i.e. in its original matrix. Dilution always requires mixing and homogenizing, hence mechanical energy is applied to the sample. Agglomerates are composed of individual, primary particles bound together with a certain strength. The agglomerates often show a stability distribution, i.e application of mechanical energy leads to partial or total disruption of the agglomerates. Consequently the way the sample is prepared and treated during analysis is of utmost importance for the results obtained.

4.1.1 Light Microscopy

To analyze the agglomerates' size distribution, it is necessary to identify the agglomerates in the mixture that consists of primary particles as well as of agglomerates. The easiest und most secure way doing this, is by visual observation. There agglomerates can be distinguished from primary particles. Therefor a method was developed that allowed to identify the agglomerates and to determine their amount and size distribution by means of light microscopy.

4.1.1.1 Sample Preparation

The aim of this method is to determine the size distribution of the agglomerates and to quantify their content, hence quantifiable figures must be available, i.e. dilution rates and sample composition need to be known.

The sample was weighed out and put into a 250ml glass beaker and diluted further with dispersant agent, (here sunflower oil or molten cocoa butter) to a final concentration of 0.7% w/w of solids. This mixture was then stirred gently on a heatable magnetic stirrer for 20 min. at temperatures of 25°C to 40°C (depending on type of dispersant used). From that sample a sub sample was taken, weighed out and poured onto a plastic petridish. On the plastic petridish a special sample area had been prepared. Therefore a circular ring with a diameter of 2cm was prepared with super glue on the petri dish. This ring acts as border for the sample and the diameter of it defines the area of the sample. When using plain petri dishes (without a ring) a cumulation of solids close to the walls was observed and thus leads to a separation of the sample. Knowing the sample area on the petri dish and the amount of sample put onto that area as well as the solid concentration of the sample, the total amount of solids on the

petri dish is known. This allows to relate the counted number of particles present in the individual size classes to the total mass of particles. The sample preparation is illustrated in Figure 4-1
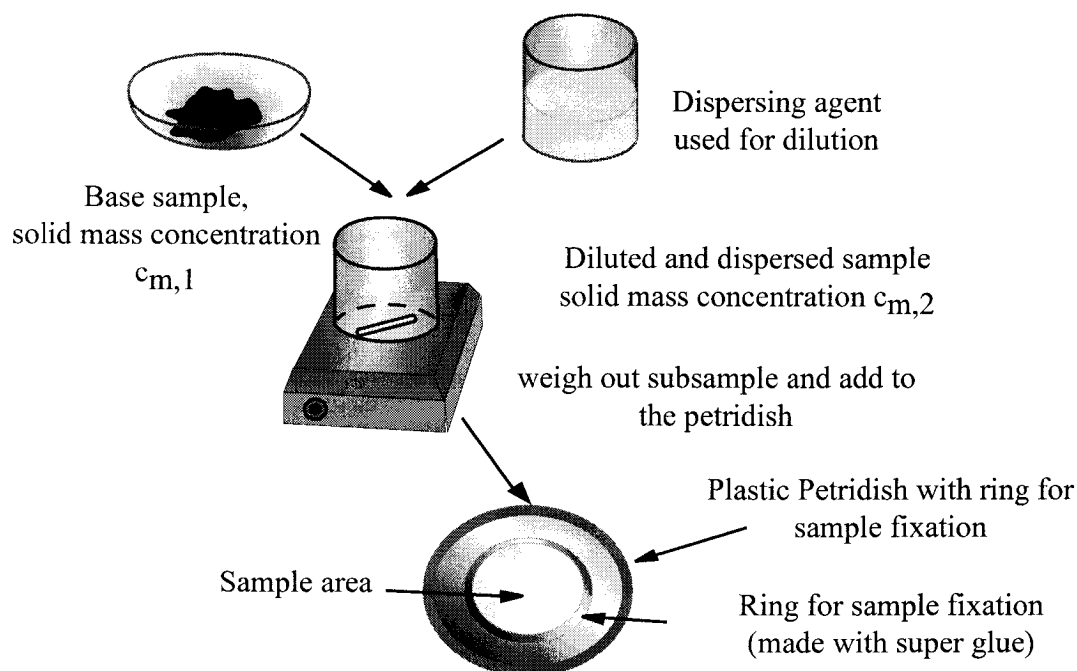
Figure 4-1 Sample preparation for microscopy

4.1.1.2 Set Up for Microscopy

For microscopy an inverse microscope, type Nikon Diaphot TMD was used. To the microscope a color video camera was attached (3 CCD, JVC, KY-F55BE) which was connected to a monitor and a video recorder. Taking the different magnifications of the video chip, video lenses used and of the objectives attached to the microscope the following total magnifications were reached. The magnification was calculated by use of a scaled glass slide.

Table 4-1 Magnification resulting from different combinations

Videolense	Objective	Total Magnification
0.45	4	100
1.00	10	470
1.00	20	900

4.1.1.3 Measurement Procedure

Accounting for the wide size range of the agglomerates different magnifications were used for analysis. For particles bigger than 70μm in diameter the whole plate was scanned and a picture of every position was taken and recorded on a video tape. Due to their lower concen-

tration agglomerates bigger than 70μm are in general no longer homogenously distributed across the sample area, thus a the whole area needs to be scanned.

Agglomerates belonging to size classes below 70μm were present in higher concentration and thus homogenously distributed. Consequently 50 pictures per sample were taken and repeats were performed for each sample, i.e. 100 pictures were used for analysis in that size class. Scanning of the sample was performed like illustrated in Figure 4-2.
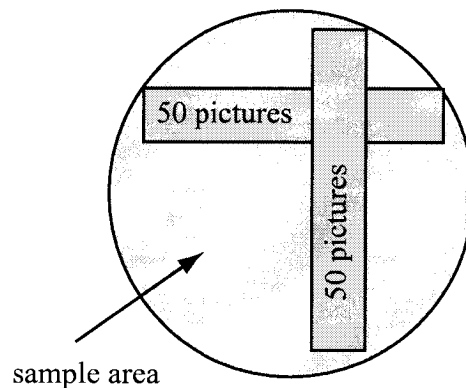
Figure 4-2 Scanning of sample area for size classes below 70μm

Table 4-2 shows the scanned area of the sample (petri dish) depending on the magnification, i.e. the analyzed size range.

Table 4-2 Number of pictures taken and area of sample scanned for analysis

Magnification	Size range	Number of pictures taken	Sampling area mm^2	percentage of total sample area
100 x	> 70μm	whole area	1256.64	100%
470 x	50μm-70 μm	2 x 50	12.98	1.03%
900 x	< 50μm	2 x 50	3.37	0.27%

The size was visually determined using a transparent foil with concentric circles of different diameter printed on (see Figure 4-3). It was placed on the monitor screen, whilst replaying the individual snap shot positions from the video tape. Depending on the magnification each circle corresponds to a certain diameter. The circle that circumscribes the particle defines its size.
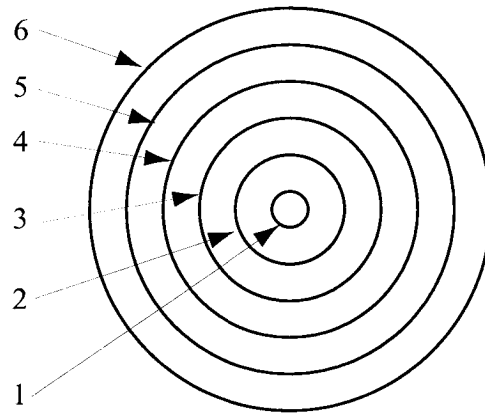
Figure 4-3 Sketch of foil used for size classification

With this set up the following classifications of size are obtained (see Table 4-3)

Table 4-3 Sizes classes used for size analysis

Magnification	100 x	470 x	900 x
Circle number	Size range μm	Size range μm	Size range μm
1	70-150		10-20
2	150-230		20-30
3	230-310	50-70	30-40
4	310-400		40-50
5	400-500		
6	> 500		

Counting the agglomerates for each magnification reveals the number of agglomerates per sample analyzed. Assuming a homogenous particle distribution and representative sampling as well as knowing the amount of sample and thus the amount of solids put on the petri dish, the total number of agglomerates per total mass of solids as well as the number of agglomerates being present in each size class per total mass of solids can be calculated (see also Figure 4-1).

4.1.2   Laser Diffraction Technique

Laser diffraction is based on degree of diffraction. When light of the wavelength λ hits particles of diameter x with x>> λ the light is diffracted (Fraunhofer diffraction). The degree of diffraction depends on the size of the particles. In general small particles cause large angle diffraction, big particles cause small angle diffraction. Simply by this crude diversification it is not possible to distinguish between primary particles and agglomerates. Any particle hit by light causes diffraction (λ<x) and scattering (λ >x).

To be able to use the laser diffraction method for agglomerate analysis the classification into primary particles and agglomerates has to be set in the sample preparation step.

Agglomerates are composed of the primary particles which are bound to each other. The strength of these bonds depend on their physical nature. The strongest bonds are present between particles that have built up solid bridges. The strength of those is of the same order as the strength of the primary particles. All other type of bonds (e.g. liquid bridges, electrostatic interactions, Van der Waals interactions) are weaker than those.

Applying different levels of mechanical stresses to the agglomerates will lead to a partial breakdown. Depending on the stress level, all agglomerates can be destroyed. The remaining particles are primary particles. The principle of the method builds on these steps. In course of sample preparation, different levels of mechanical stresses are applied to the sample. Finally all agglomerates, except for those that have built solid bridges and thus have formed a dense structure, are destroyed.

Laser diffraction measurements performed after such different treatments reveals size distributions that are shifted towards smaller sizes for increasing mechanical stress levels. From a certain point on, no further change in size distribution is observed although the mechanical stress applied had been increased. This indicates that the particles that are left, are stable enough to withstand the stresses applied, i.e. they are considered as being primary particles. As long as no agglomerates are present that are bound together by solid bridges, this is a valid assumption. For specially treated samples it could be proven that strong agglomerates (solid bridges) can withstand such stresses. This was verified by light microscopy.

4.1.2.1   Sample Preparation Method for Agglomerate Analysis

In order to achieve different states of deagglomeration, it is necessary to apply different levels of mechanical stress to the sample. This is done in a reproducible manner during a "five - level" treatment. The principle procedure of preparation is shown in Figure 4-4. The different levels and the associated procedures are described in the following paragraphs.

1st Level

Starting with the concentrated suspension, a small sample of that is taken and transferred into a glass beaker. This sample is then diluted with an appropriate dispersing agent (typical solids concentration 1% w/w) and gently stirred for a defined time on a magnetic stirrer at a constant stirrer speed. In this first step the lowest possible stresses should be applied. High enough to homogenize the mixture and dissolve lumps of solids in the sample (gentle dispersing) but low enough to maintain the agglomerates. The mechanical stresses applied here, already define which agglomerates are destroyed. The drawback of the method is, that only what is left can be seen, but never what was in before. Therefore all steps have to be carried out always with the same setup, otherwise mechanical power and energy input changes. In this first step the base sample for all other samples is prepared. The following conditions need to remain unchanged:

- Type of glass beaker (250ml, diameter 50mm)

- Type of magnetic stirrer (cylindrical, 35mm long, 6mm in diameter)

- Filling level of the beaker (100ml, volume specific power input)

- Stirrer speed (800 1/min., volume specific power input)

- Stirring time (20 min., volume specific energy input)

- Temperature (room temperature or 40°C when cocoa butter was used, viscosity of mixture - mechanical stresses)

With a plastic single use pipette, where the tip is cut off to have a big enough entry diameter of the remaining tip ensuring that also big particles can be sucked in, subsamples were taken from the base sample and treated further.
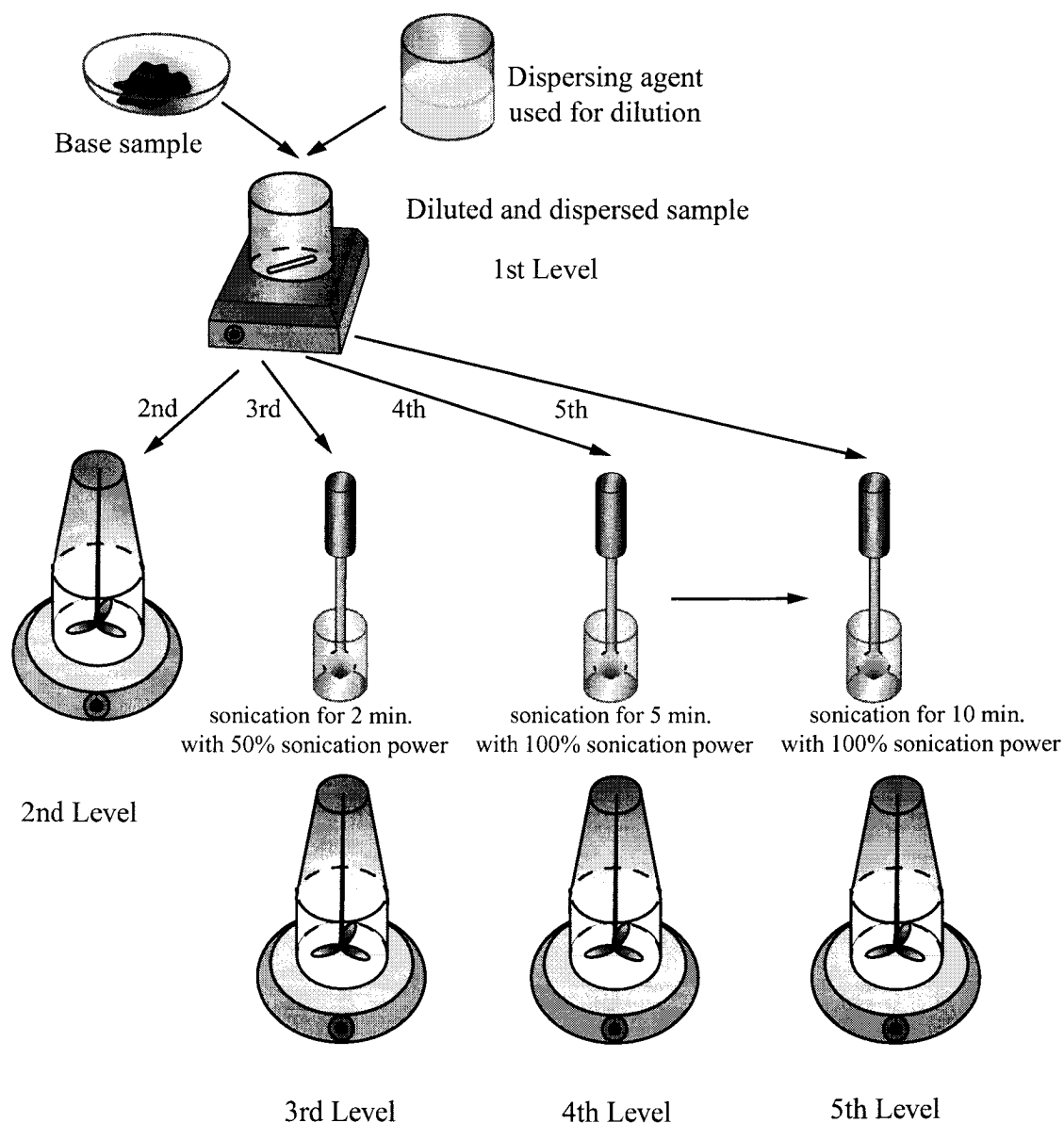
Figure 4-4 Sample preparation method for agglomerate analysis with laser diffraction

2nd Level

The second dispersing step takes place when the sample is transferred to the laser diffraction device. The system used here was a Malvern Mastersizer X and a Malvern 2000. Both systems were equipped with a MSX1 sample preparation unit. This is a small volume sample unit with a capacity of 200ml. The unit is equipped with a propeller type stirrer and a centrifugal pump. Both are speed adjustable. Connected to that unit is the measurement cell. The sample is circulated through this unit where it experiences different stress zones. The first zone is located around the stirrer. The second stress zone is present in the centrifugal pump, and the third when the sample flows through the tubes (circular cross section) and finally when it enters and flows through the measuring chamber (cross section changes from circular to rectangular and back to circular). In all these zones different stresses act on the sample. In order to keep those always the same, the parameters:

- Stirrer speed (sets pump speed hence flow rate)

- Viscosity function (determines together with flow rate the local velocity profiles - stress distributions)

- Circulation time (energy input)

have to be kept constant. At this level also agglomerate break down occurs. This can be seen for measurements performed after different times of circulation and after different stirrer speed levels had been applied (see Section 4.1.2.2). For the method used, circulation times of 1 min. were generally applied. The speed level of the stirrer speed was set to half of the maximum speed. In cases where stability investigations were performed, different circulation times and speed levels were used in order to apply different stress levels to the samples.

Ultrasound Treatment

Till level 2 treatment only "moderate" stress levels were applied to the sample (forces resulting from the flow field or from particle - rotor/stator/wall collisions (impact)). In order to further deagglomerate, the stresses need to be increased. Therefore ultrasound was applied to the sample. Using a power adjustable sonication unit the sample can be treated with different sonication power and energy. The general set up is illustrated in Figure 4-5 and is split into three different levels of treatment.

As sonication unit the following device was used: High intensity ultrasonic processor, Fiber Cell, Sonics (supplied by GMP, CH), 25/50 Watt power input (half /maximum level), 20kHz, 6mm microtip

3rd Level Treatment

The unit used here is an "ultrasound finger" with a high local power input at the tip of the finger. The finger is placed centrally in a 50ml glass beaker with a distance of 7mm between finger tip and beaker bottom. The glass beaker is filled with 20ml of the sample. The sample is then treated for 2 min. at half of the maximum power level.
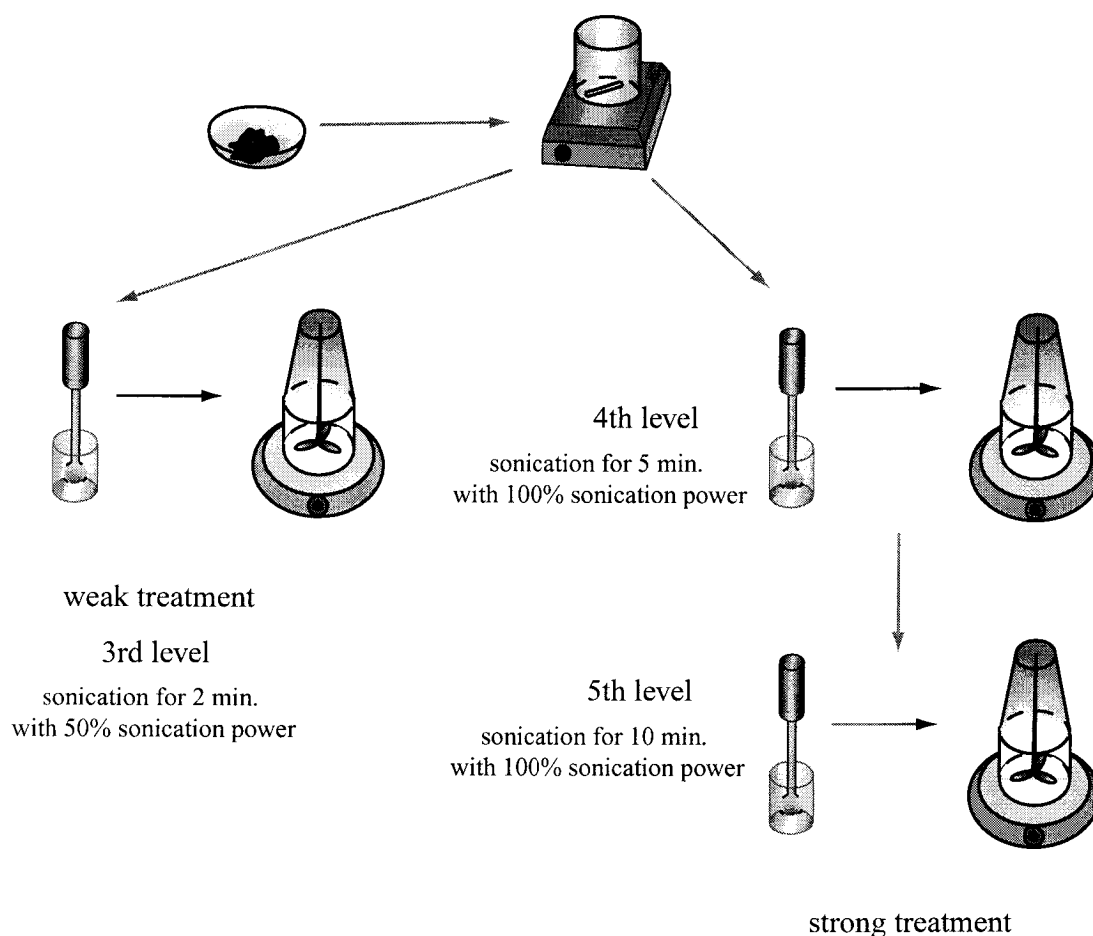
Figure 4-5 Setup for Ultrasound treatment

4th Level Treatment

The same set up like for the 3rd level treatment is used. Now the treatment takes place at maximum power level for a time of 5 min. Afterwards a subsample for size analysis is taken with a plastic pipette. The remaining part of the sample (15ml) that is left in the beaker is then used for the 5th level treatment.

5th Level treatment

This treatment is considered as maximum treatment after which all agglomerates, not bound by solid bridges to each other, should be destroyed. For this step the remaining sample (15ml) of the 4th level treatment is used. This sample is sonicated further for 5 min. at max. power level. As the sample volume was reduced (part of it was used for measurement after level 4 treatment), the volumetric power and energy input have increased.

Comment

The principle design of this method can be applied independent from the individual set up. The individual set up has to be adjusted towards the special needs. As stated earlier, this is

an invasive method and it is only capable of detecting what is left but does not detect what was present at the beginning. It also has to be taken into account that representative sampling of a system which is low viscous and thus exhibits a significant difference in density between solids (1.57 g/cm^3 to 2.7 g/cm^3) and liquid (0.9 g/cm^3) does need some experience. Stirring the sample in order to avoid sedimentation and rapid sampling has proven to be really advantageous. Furthermore it is necessary to cut off the tip of the plastic pipette. Otherwise the entry diameter of the pipette is too small and a size classification might occur. This is especially important when big agglomerates should be detected or when sub samples are taken from the base sample. Furthermore during preparation of the base sample, sometimes problems appear when a high viscous mass has to be mixed with a low viscous mass. This was the case for samples that had been prepared with silicon oil. The viscosity of the sample was 2000 to 5000 times higher than of the dispersing agent (AK10, 10 mPas at 25 °C). In this case a premix was prepared. The premix was then poured into the glass beaker and diluted further with the dispersing agent. For preparation of the premix, the required amount of the sample (1g) is mixed with 2 to 5 drops of the dispersing agent using a spatula. The texture changes from pasty to creamy to fluid. Once the texture is cream like it can be transferred to the beaker and treated further. During premixing also agglomerate break down might occur. This is a drawback especially for samples where only weak agglomerates are present. The influence of premixing can be controlled and reproducible measurements can be achieved if the preparation is done with care.

4.1.2.2 Repeatability of Method

To assess the quality of the method at the various levels (1 to 5) repeatability tests had been performed. These tests were made at different points in time with different equipment, i.e. each series is valid for itself and cannot be compared to others. Independent from the variation in equipment and time, good repeatability could be achieved and the robustness of the method was proven.

Repeatability for 1st, 2nd and 5th Level Treatment

Repeatability at the 1st and 2nd level treatment is most critical for the whole method. At that level particle size exhibits the widest range and representative sampling is most difficult. If good repeatability can be achieved on that level, all other levels will have a better repeatability (because of narrower size distribution and more homogeneous mixture - representative sampling is less critical).

In Figure 4-6 the measured size distributions after different times of circulation in the small volume sample presentation unit MSX1 are shown. For purpose of better illustration continuous lines instead of the correct histograms are plotted. Furthermore it has to be noted that the Y-axis gives the logarithmic value of the volume based density distribution and is therefore dimensionless. The model used here was the Fraunhofer diffraction model which is based on spherical, non transparent (black) particles. For reasons of relative comparison it is allowed to use these adjustments.

In Figure 4-6 the clear influence of the sample circulation time at constant pump speed can be seen. When increasing the pump speed a further break down occurs (curve:10 min. at max. stirrer speed). This illustrates, that pump speed and circulation time have to be controlled in order to obtain repeatable results. Furthermore, it shows that with this set up, agglomerates can be classified according to their stability. Classification thereby depends upon circulation time and pump speed.
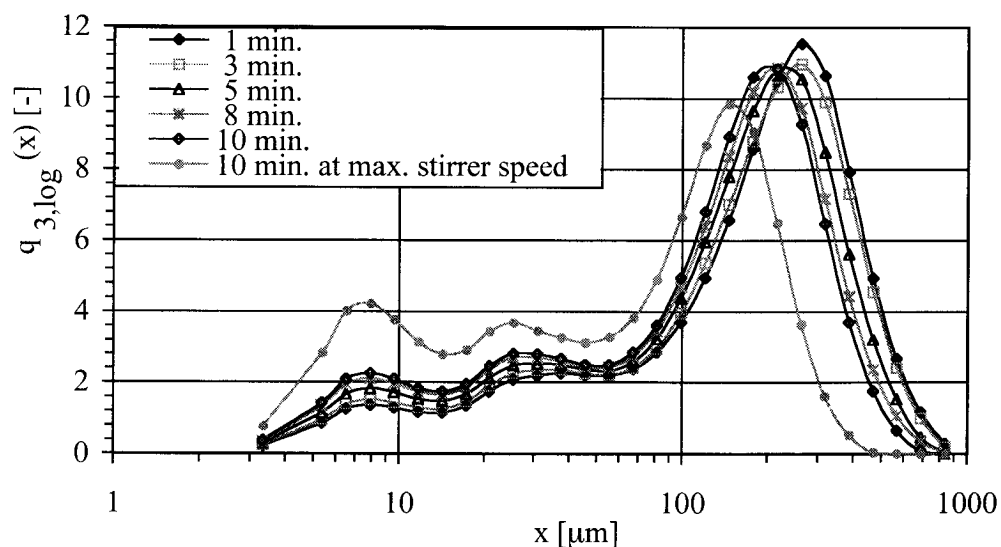
Figure 4-6 Repeatability for level 1, chocolate flakes measured after different times of circulation with Malvern Mastersizer X, 1000mm lens

For fixed pump speed and fixed circulation time repeatability tests were performed. Therefore 4 subsamples were taken from one base sample (chocolate flakes) and prepared according to the level 1& 2 treatment.
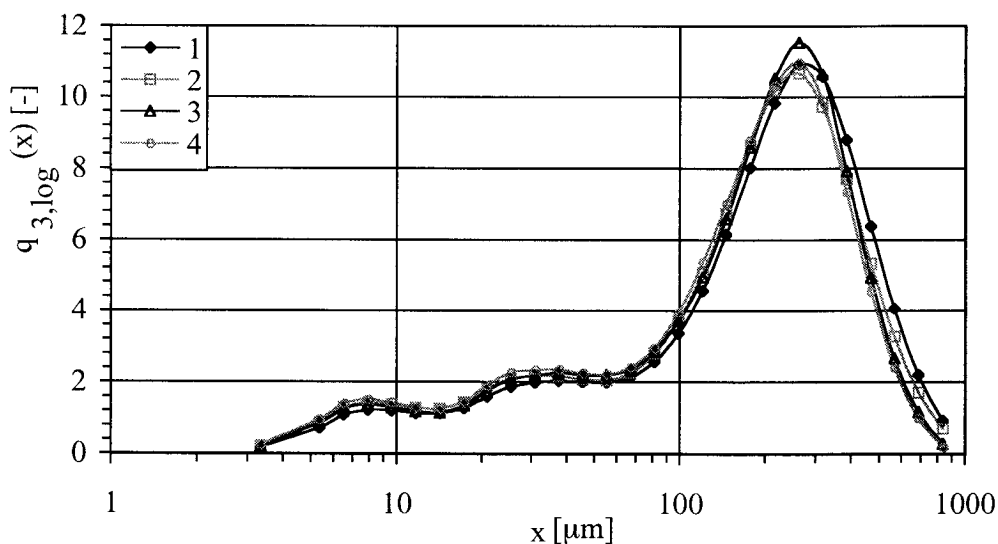
Figure 4-7 Repeatability of level 1 & 2 treatment, Malvern Mastersizer X, 1000mm lens, 20 min. stirring time with magnetic stirrer, 2 min. circulation time in the Malvern small volume presentation unit MSX 1

In Figure 4-7 the measured size distributions of the 4 repeat samples for level 1&2 treatment is shown. It is clearly demonstrated that on these levels representative sampling is guaranteed and repeatable results are obtained. This is expressed by the narrow band of variation in which the measurements fall together.

In Figure 4-8 the repeatability (5 repeats) for a fully deagglomerated sample (level 5 treatment) is shown. The same base sample as used for the measurements shown in Figure 4-7 was used. Here this sample was treated further which yields the corresponding size distribution of the primary particles. Accounting for the smaller particles a different lens had been used (300mm instead of 1000mm). Furthermore the sonication step was performed using a sonication bath rather than a sonication finger.
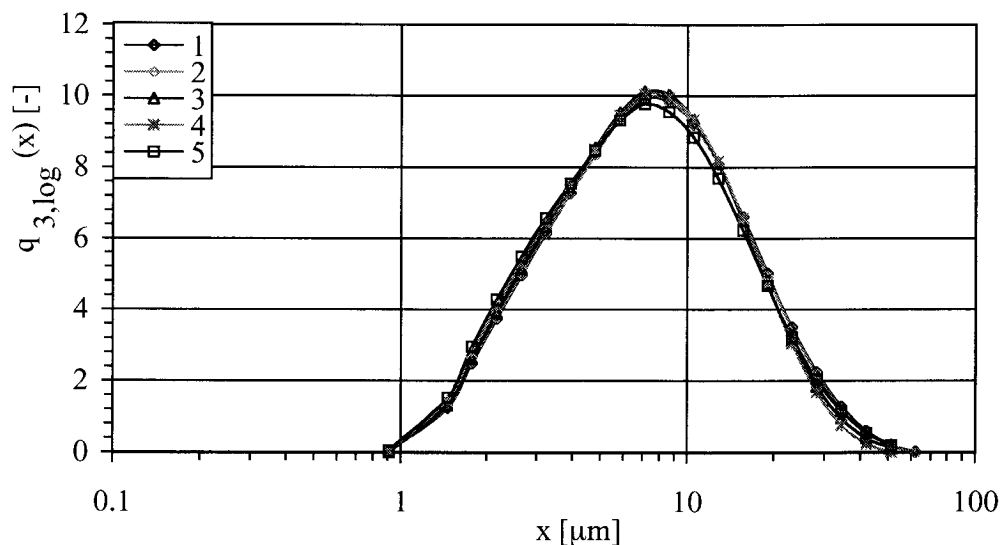
Figure 4-8 *Repeatability of level 5 treatment, Malvern Mastersizer X, 300mm lens, 20 min. stirring time with magnetic stirrer, 20 min. ultrasound (sonication bath), 2 min. circulation time in the Malvern small volume presentation unit (MSX 1)*

4.1.2.3 Laser Diffraction Devices and Models used

The Laser diffraction devices used for size analysis were

- a Malvern Mastersizer X, equipped with 300mm and 1000mm lens to analyze different size ranges

- a Malvern 2000, equipped with one lens ranging from $0.02\mu m$ to $2000\mu m$ and detectors for forward and back scattering

In cases where the Mastersizer X had been used, the Fraunhofer diffraction model was used for calculation of the size distributions.

In cases where the Malvern 2000 had been used, additionally the corresponding refractive indices for the particles and the dispersant were used for calculations applying Mie-theory. These values are (according to Malvern)

- 1.51 for sucrose, absorption coefficient: 0.1

- 1.572 for limestone, absorption coefficient: 0.1

- 1.403 for silicon oil

- 1.449 for Akomed

4.2 Rheometry

The suspensions that were prepared showed different physical characteristics which needed to be accounted for when rheological measurements were performed. Such characteristics are

- Wall slip

- Separation caused by sedimentation

- Coarse particles (size of agglomerates equal to gap width of conventional concentric cylinder systems)

- High viscosity, paste like structure

Depending on the sample some of these attributes were more others less pronounced, i.e. some samples could be measured using standard geometries (concentric cylinder systems or cone and plate) others required the use of special geometries.

4.2.1 Special Geometries

To be able to measure all samples with at least one geometry and thus obtain results that can be compared, it was decided to use stirrer type geometries. Therefore 4 types of stirrers had been used. Their principle design is illustrated in Figure 4-9 and Figure 4-10. Using stirrer type geometries for rheological measurements allows to obtain relative numbers that correlate with the rheological properties derived from uniaxial shear experiments (*Martinez-Padilla, L.P. et al. (1999)*). Consequently different samples can be compared on a relative rather than an absolute basis. Taking this into account the flow behavior can be characterized on a relative basis with such geometries (*Brito-De La Fuente, E. et al. (1996), Metzner, A.B., Otto, R.E. (1957)*).
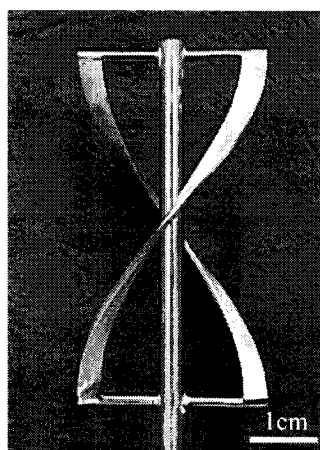
Figure 4-9 Helical ribbon type of stirrer
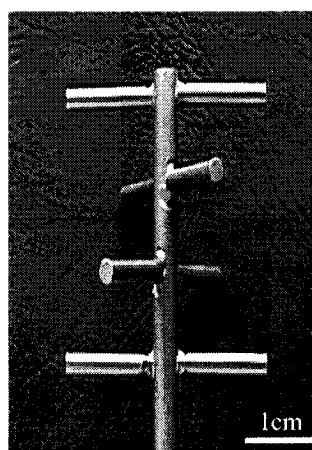
Figure 4-10   Cross bar type or thorn like stirrer (same scale like for left picture)

4.2.2   Power Characteristic of Individual Pairs of Stirrer & Cup

During the course of this work two different rheometers and 4 different stirrers had been used. Their design was either helical ribbon like or thorn like, the detailed geometry (diameter, length) of each is different which applies also to the geometry of the cups (see Figure 4-13, Figure 4-14).

Mixer viscosimetry can be performed if the power consumption of the stirrer is known and the measurements take place in the laminar flow regime (*Metzner, A.B., Otto, R.E. (1957)*). For each pair of stirrer - cup a power consumption characteristic was determined. The measurements always took place in the laminar flow regime at low stirrer speeds.

In the laminar regime the power consumption can be characterized as an inverse proportional relationship between the Power number *Ne* and the Reynolds number *Re*. Viscoelastic fluids were not taken into account, consequently the Weissenberg number *Wi* could be neglected. Applying only low stirrer speed levels the Froude number *Fr* was also not relevant. Furthermore the Weber number *We* was neglected (no or little power consumption for generation of new interfaces) (*Steffe, J.F. (1992)*).

The values obtained from the measurements were the torque applied (in case of stress controlled experiment) and the resulting angular velocity of the stirrer. For reasons of simplicity the ratio of torque (M) to angular velocity (ω) was calculated. This number describes the resistance against flow, hence is a measure of viscosity. Therefore it is called apparent viscosity $\eta_{apparent}$ with the dimension [Nms].

$$\eta_{apparent} = \frac{M}{\omega} \qquad [Nms] \qquad \qquad (4.1)$$

The parameters torque and angular velocity (or number of revolutions n) are also the parameters which are used for calculation of the Power (*Ne*, Eq. (4.2)) and the Reynolds (*Re*, Eq. (4.3)) number. Furthermore a characteristic diameter d of the stirrer, the density ρ_f and the viscosity η_f of the fluid have to be known.

$$Ne = \frac{2 \cdot \pi \cdot M}{n^2 \cdot d^5 \cdot \rho_f} \qquad \qquad (4.2)$$

$$Re = \frac{n \cdot d^2 \cdot \rho_f}{\eta_f} \qquad \qquad (4.3)$$

The power consumption as determined for each geometry is illustrated in Figure 4-12 and Figure 4-11.

For calculation of the *Ne* and *Re* number the diameter of the stirrer was used as characteristic length. Table 4-4 shows the geometrical dimensions of the individual stirrer and cup combinations. In Figure 4-13 and Figure 4-14 the detailed parameters for the different setups are given. As fluids, Newtonian silicon oils were used. The physical characteristics of those are summarized in Section 3.1.1.1 on page 29.
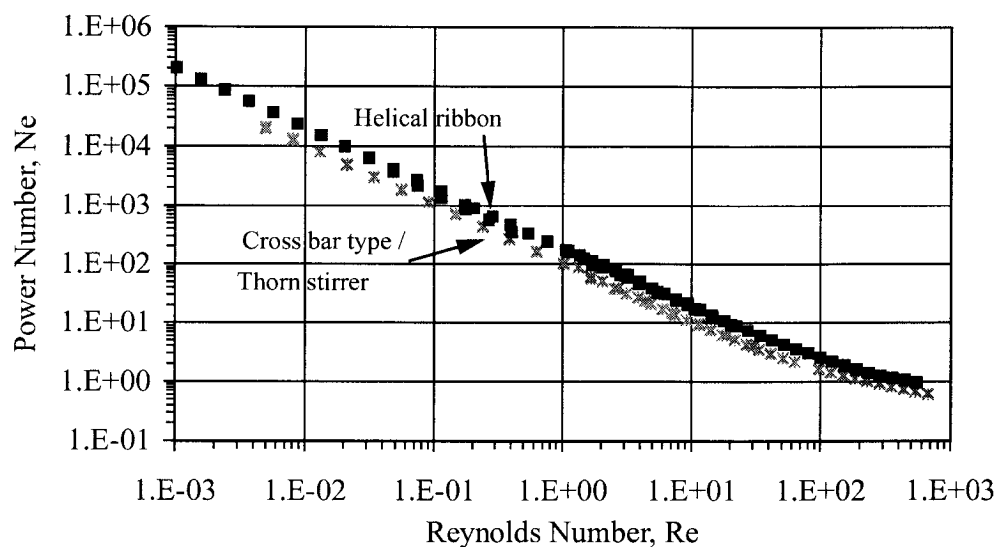
Figure 4-11 *Power consumption for helical ribbon and thorn like stirrer used with cup & stirrer for Bohlin CVO 120 HR rheometer*
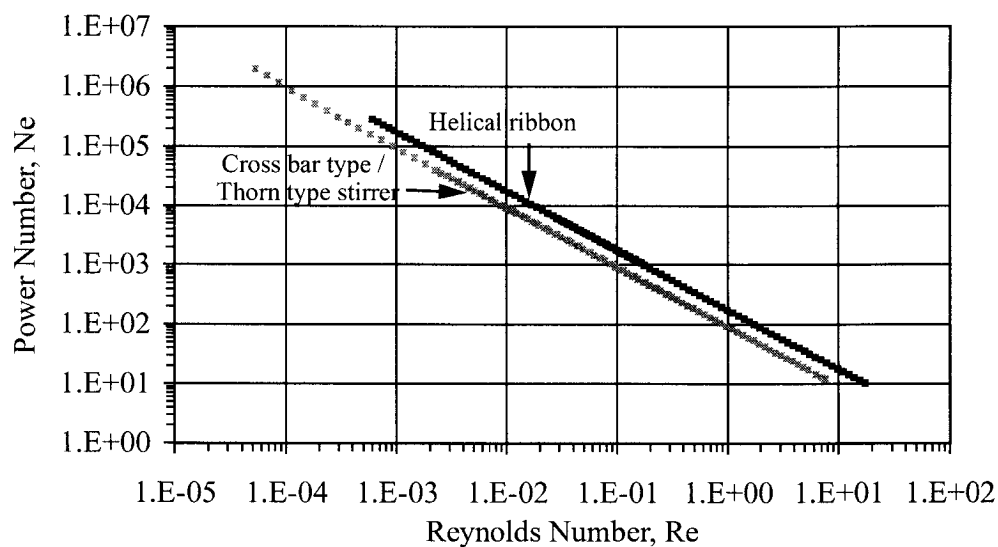
Figure 4-12 *Power consumption for helical ribbon and thorn like stirrer used with cup & stirrer for Rheometrics DSR rheometer*

Table 4-4 *Geometrical dimensions of stirrers and cups used in Rheometrics and Bohlin rheometer*

Cups of rheometer	Helical ribbon	Thorn like stirrer
d_{DSR}= 32 mm	d= 25.4 mm l= 30.0 mm	d= 25 mm l= 25 mm
d_{Bohlin}= 50 mm	d=40mm l= 75 mm	d= 44.7 mm l= 58 mm
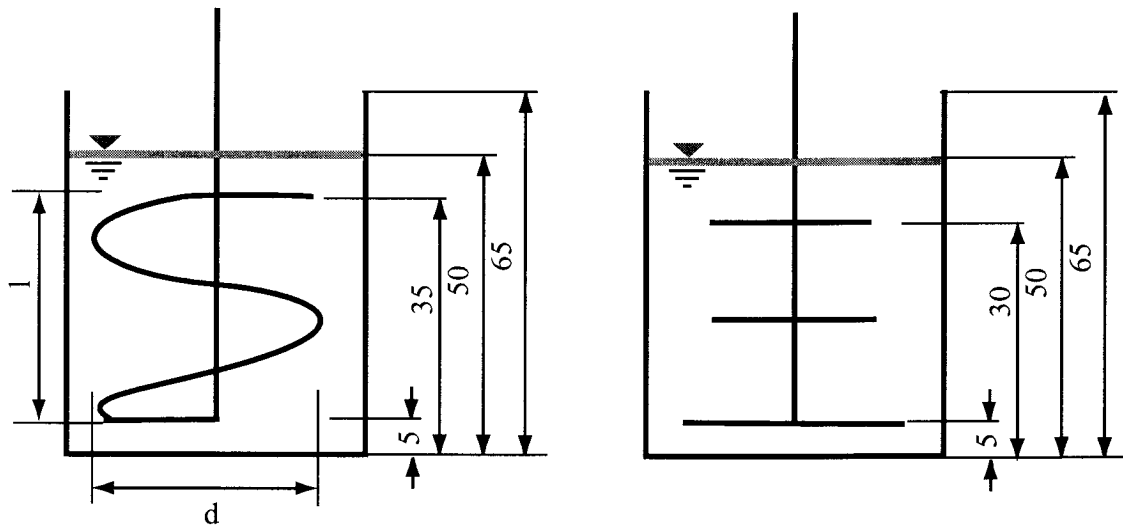
Figure 4-13 *System parameters used with Rheometrics rheometer, dimensions given for helical ribbon and thorn like stirrer*
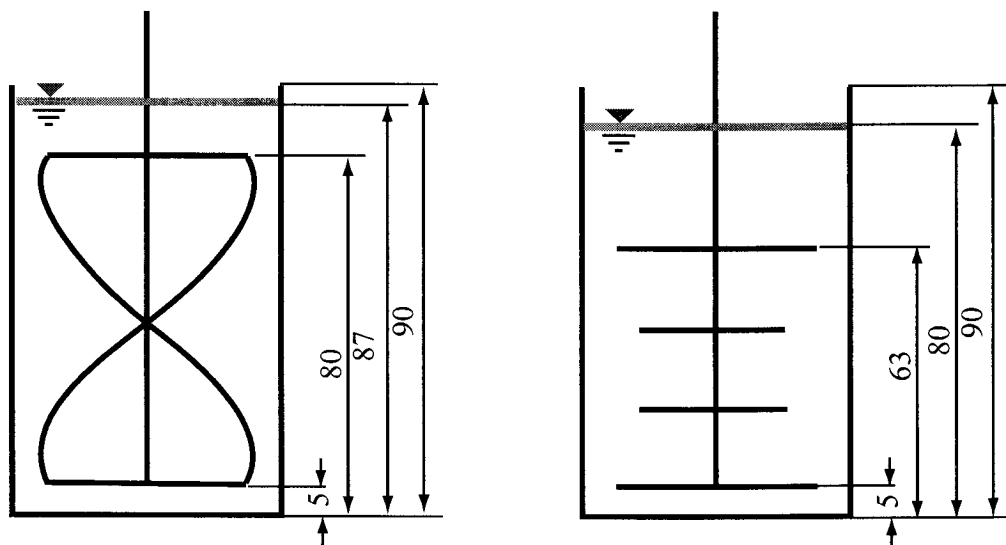
Figure 4-14 *Set up parameter for systems used with Bohlin rheometer, dimensions given for helical ribbon and thorn like stirrer*

4.2.2.1 Concept of Critical Values

The power consumption obtained for the assumption that the Ne number only depends on the Re number (Fr, Wi, We are neglected) exhibits different regimes (Figure 4-15). Within the so called laminar regime rheological measurements can be performed on a relative basis. This regime is characterized by the following relationship, where C is a so-called stirrer constant that depends upon geometry.

$$Ne = C \cdot \frac{1}{Re} \qquad (4.4)$$

The values for Ne and Re can be derived from the experiment carried out with Newtonian fluids. The value for C is calculated as

$$C = Ne \cdot Re \qquad (4.5)$$

Within the laminar regime C remains constant. For increasing Re numbers a critical value for Re exists for which C is no longer constant. This critical Re number (Re_{crit}) defines the end of the laminar regime. Plotting C as a function of Re easily reveals this value (Figure 4-16).
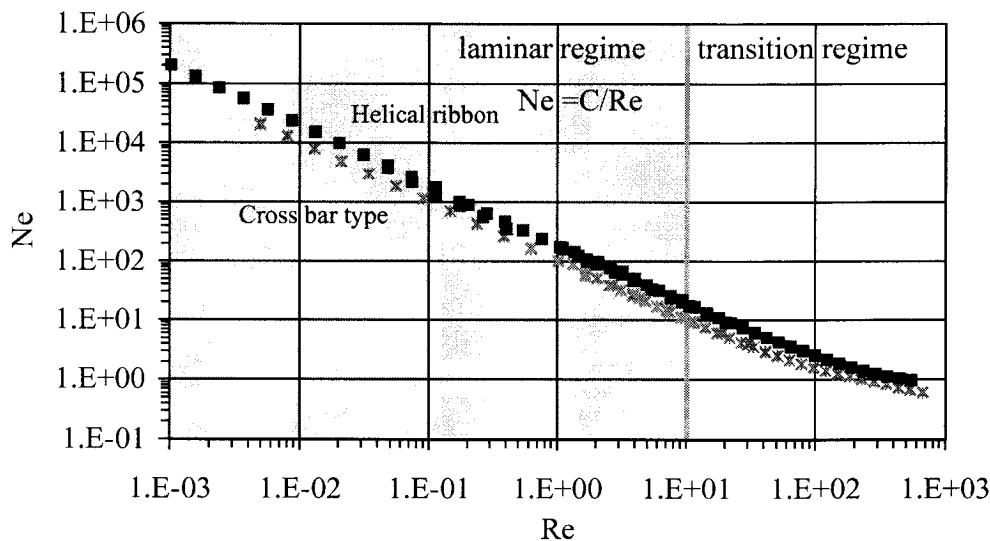
Figure 4-15 *Power consumption and different regimes*

If unknown substances are measured with a stirrer type geometry it is essential to stay within the laminar regime. As the substance is unknown it is not known in advance whether or not the condition of staying within the laminar regime is fulfilled. Depending on the type of sample it is also sometimes hardly possible to establish a power consumption for that type of sample, because the substance can not be assessed with conventional type of geometries (e.g. too big particles, i.e. gap blockage).

Building on the concept of matching viscosities allows to resolve this conflict. The phrase "matching viscosities" refers to the assumption that the representative shear rate for a non-Newtonian fluid is equal to the representative shear rate for a Newtonian fluid when the Newtonian viscosity equals the apparent viscosity of the non-Newtonian fluid (*Steffe, J.F. (1992)*). Performing measurements with a rheometer the two parameters angular velocity and torque are measured. Depending on the type of equipment either strain (angular displace-
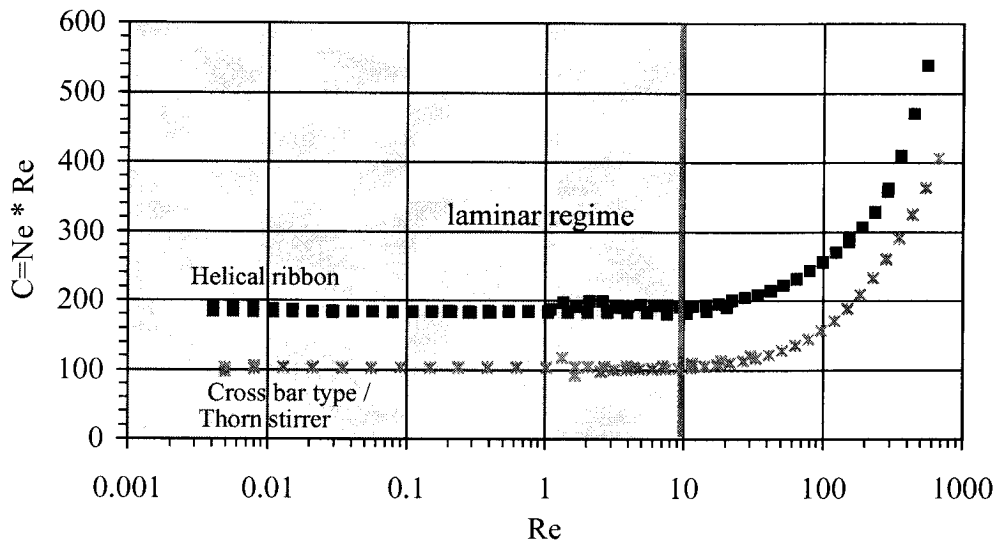
Figure 4-16 *C as function of Re*

ment, angular velocity) or stress (torque) is applied to the sample. The combination of both values determines in which regime (laminar or transition) the measurement takes place. From the power consumption curve a critical value for *Re* is obtained which defines the end of the laminar regime. From this critical *Re* number and for a given geometry critical values for torque and angular velocity can be derived which is demonstrated in the following.

The critical Re_{crit} number is reached when a fluid with a viscosity η_f and a density ρ_f is sheared at a critical shear rate $\dot{\gamma}_{crit}$ hence stirred with a critical number of revolutions n_{crit}. For different values of η_f and ρ_f the corresponding critical number of revolutions n_{crit} can be calculated (Eq. (4.6)).

$$n_{crit} = \frac{Re_{crit} \cdot \eta_f}{d^2 \cdot \rho_f} \tag{4.6}$$

The viscosity used here is the apparent viscosity of the non-Newtonian liquid which equals the viscosity of a Newtonian liquid at that representative shear rate hence number of revolutions.

Substituting Eq. (4.6) and Eq. (4.2) into Eq. (4.5),

$$C = Ne_{crit} \cdot Re_{crit} = \frac{2 \cdot \pi \cdot M_{crit}}{n_{crit} \cdot d^3 \cdot \eta_f} \tag{4.7}$$

hence for the critical torque M_{crit}

$$M_{crit} = \frac{1}{2 \cdot \pi} \cdot C \cdot n_{crit} \cdot \eta_f \cdot d^3 \tag{4.8}$$

With these equations the critical values for torque and number of revolutions can be calculated. Therefore any values for η_f are used in order to cover a wide range of torque and angular velocity. Thereby density can also be varied. The critical values obtained for torque and angular velocity are can be plotted in a diagram revealing a straight line that separates the

-55-

laminar regime from the transition regime. In Figure 4-17 critical border lines for torque and angular velocity for two stirrer-cup systems are plotted. For illustration, points for torque and angular velocity obtained from measurements are inserted as well. Every measurement performed was checked for compliance with this concept. Therefore it is ensured that all results reported were obtained from measurements performed in the laminar regime.
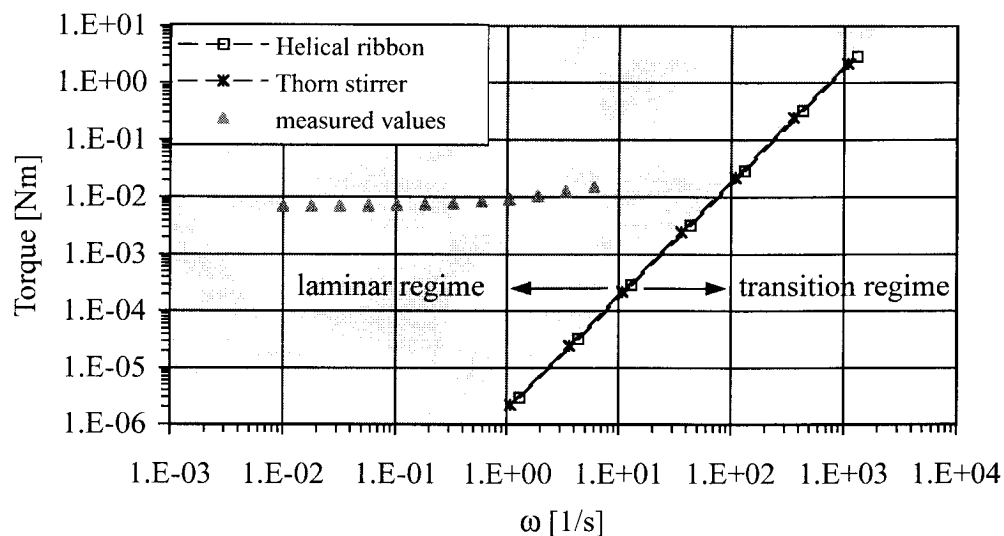
Figure 4-17 *Concept of critical values and laminar regime*

4.2.3   Head Space Controlled Rheometry

In order to be able to investigate the influence of water sorption on the rheological behavior of suspensions a special set up had been designed. The head space of the sample was covered with a hood and flushed with a conditioned air stream (humidification unit, see Section 3.3.1 on page 36). The humidity in the head space was analyzed with a humidity sensor (Type Rotronic Hygromer A2 and HP100A) and recorded. The principle set up is shown in Figure 4-18.
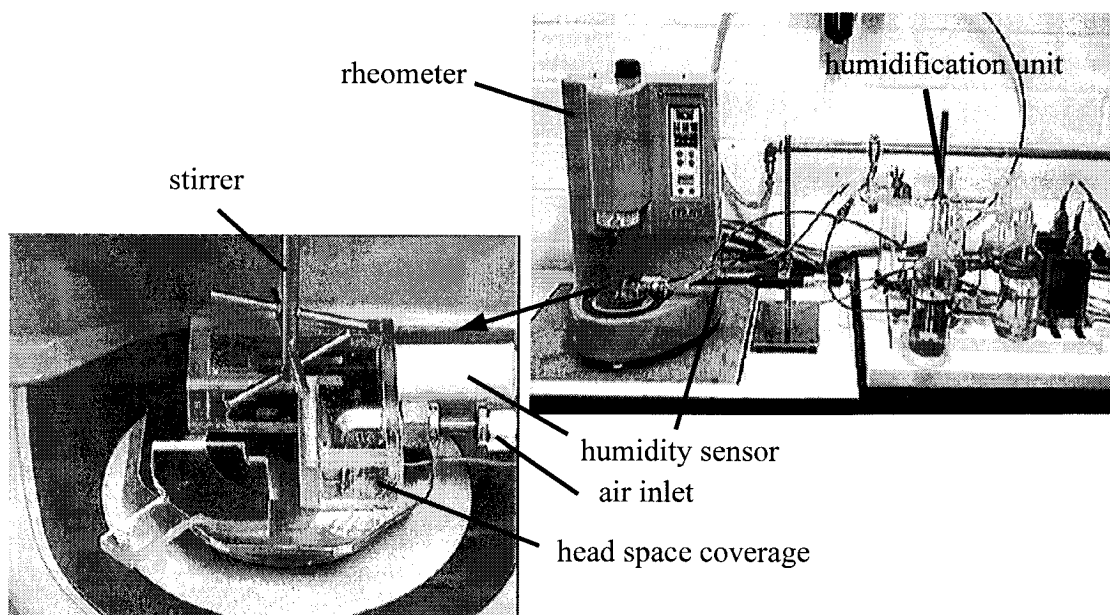
Figure 4-18 Set up used for head space controlled rheometry

5 Rheology: Deagglomeration and Interfacial properties

Many applications in industry deal with preparation of suspensions. Suspensions are processed in order to change the state and quality of a material. In foods, structure is a key quality parameter and the rheological properties of the related material are an indirect measure for its structure. It is of interest to understand the factors which alter and influence the structure and thus the rheological properties of a product. Therefore it is looked at a selected variety of factors that can have an impact on the flow properties of suspensions.

Generally it can be stated that the flow behavior of suspensions depends upon the "physical - mechanical" and "physical - chemical" properties of its components.

"Physical - mechanical" is here attributed to

- Particle size of disperse phase

- Morphology of disperse phase (e.g. porosity, surface roughness, surface area, shape)

- Packing density

- Free and immobilized liquid phase concentration

- Viscosity of continuous phase

whereas physical - chemical is donated to

- Particle interactions

- Surface active components

- Interfacial tension

- Physical state of components crystalline - amorphous.

Objective

The objective of this chapter is to illustrate how these different factors interact in the systems studied and to assess their potential to influence the rheological properties. In order to achieve this, different systems with increasing complexity were chosen and are described in the following sections.

5.1 Limestone - Silicon oil - System

Limestone silicon oil is a model system which is widely used in the field of rheology. It can be regarded as a model for systems that are dominated by physical mechanical factors and where physical chemical aspects are of minor importance.

5.1.1 Rheology - Influence of Deagglomeration

The Limestone - Silicon oil system (LS) is considered to represent a model system where Limestone being the disperse phase can be characterized as

- Dense, non porous

- Crystalline - calcite

- Irregular shaped after grinding

- Natural substance, 0.9% impurities (salts)

- Low water solubility

- High melting point

Low molecular weight silicon oil (AK 2000) being the continuous phase here, shows a Newtonian flow behavior and because of its chemical nature (Dimethylpolysiloxane), it exhibits hydrophobic properties.

Both components have been extensively investigated and are widely used as a model system for studying flow properties of concentrated suspensions (*Windhab, E.W. (1986)*).

To study the influence of deagglomeration on the flow properties first a mixture of natural limestone (size range 0.5-1mm) and silicon oil (AK2000) was prepared. This mixture, composed of 80% w/w limestone and 20% w/w AK2000 was then ground in a laboratory 3 roll refiner. The refined powder was then transferred into a lab kneader. Applying different processing conditions (time, power input) allowed to obtain batches of different degree of deagglomeration (see 3.3.4 "Kneading" on page 37).

The pictures given below illustrate the structure of two extreme samples obtained for different processing conditions. For qualitative comparison, the samples were placed on a spoon and left in the field of gravity and their structure is visualized. Figure 5-1 represents a highly agglomerated sample where the individual agglomerates can be seen. The structure is paste like and the material sticks to the spoon. Figure 5-2 shows the structure of a well deagglomerated sample. It is smooth in its appearance and it is free flowing in the field of gravity and thus is less "sticky".

To support these visual observations, rheological measurements had been performed. The different samples were analyzed in a stress controlled rheometer using a stirrer type geometry for measurements. Employing a stirrer type geometry allows to obtain viscosity analog values (apparent viscosity, see Eq. (4.1) on page 51) which are calculated as the ratio between the applied torque and the measured angular velocity.

Using the same geometry and the same experimental setup enables to compare the results obtained from the different measurements on a relative basis. All measurements were performed in the laminar regime given by the stirrer characteristic (See "Special Geometries" on page 50.).
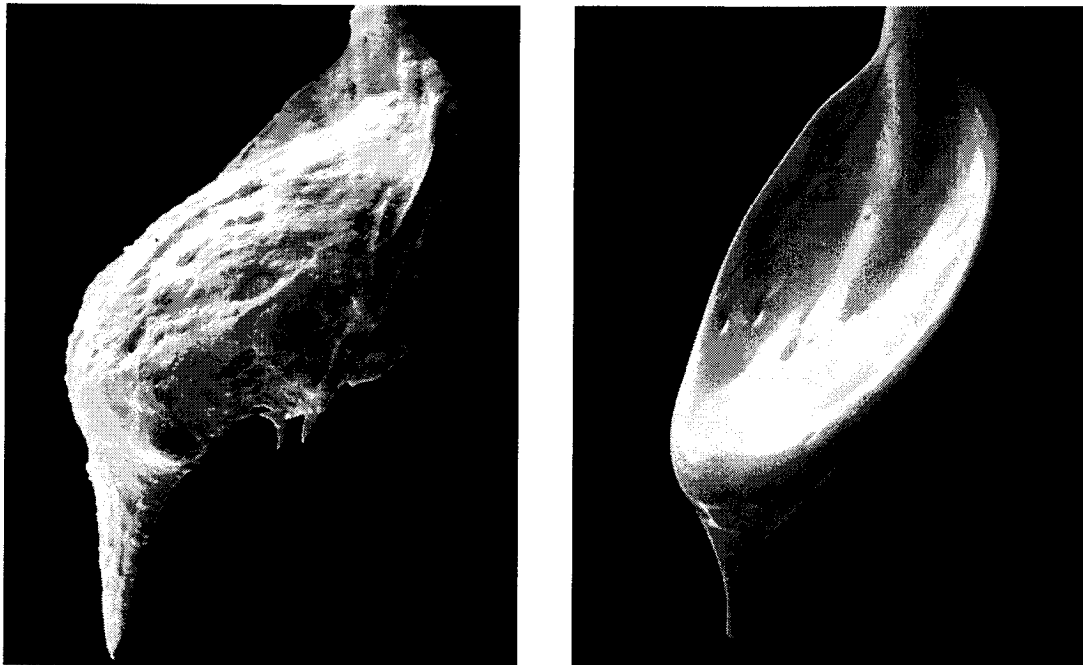
Figure 5-1 *Highly agglomerated sample of*
limestone silicon oil (c$_{v,s}$=33% v/v)

Figure 5-2 *Well deagglomerated sample of*
limestone silicon oil (c$_{v,s}$=33% v/v)

Figure 5-3 shows the development of the apparent viscosity (ratio of torque applied to angular velocity) in dependence on the degree of deagglomeration. The samples measured here, had been processed in a way such as the mechanical energy input was steadily increased and thus deagglomeration proceeded from sample 1 to 4.
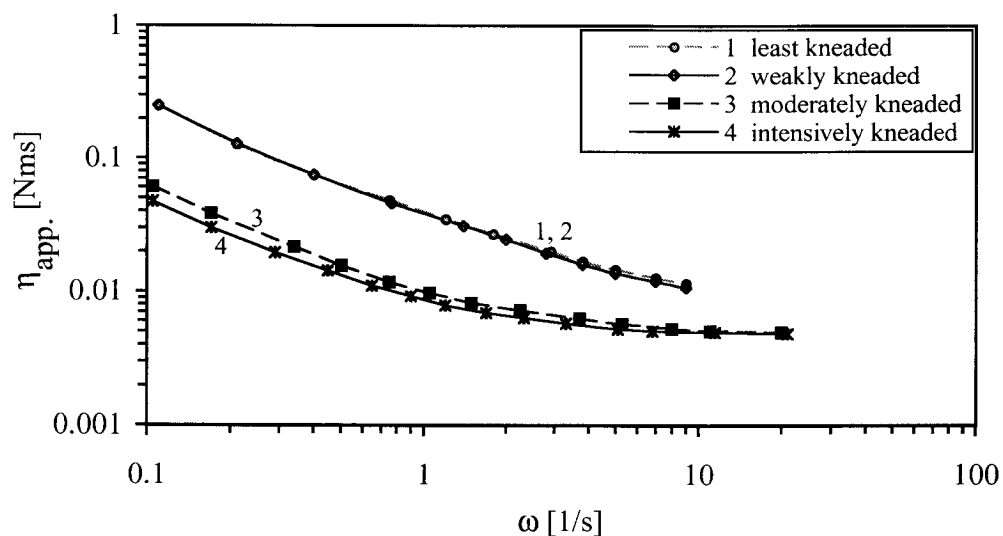
Figure 5-3 *Flow curves of differently kneaded and deagglomerated limestone silicon oil*
suspensions (1 to 4), Rheometrics DSR, helical ribbon impeller, T=30°C, c$_{v,s}$=33% v/v

For this set of measurements it can be clearly seen, that the higher the degree of deagglomeration the lower the resulting viscosities. This first trial series was carried out with a limestone silicon oil system having a solid mass concentration of 0.57 and a solid volume concentration $c_{v,s}$ of 0.33. For this trial the progress in deagglomeration was only followed by visual observation of the sample.

The same sample used for measurements with the helical ribbon impeller was measured with a concentric cylinder system. Also with the concentric cylinder system it is found that progressing deagglomeration decreases the viscosity, which is shown in Figure 5-4. Furthermore this shows that employing either conventional rheometric type or special type of geometries yields the same type of rheological behavior, i.e. can be used for rheometrical testing.
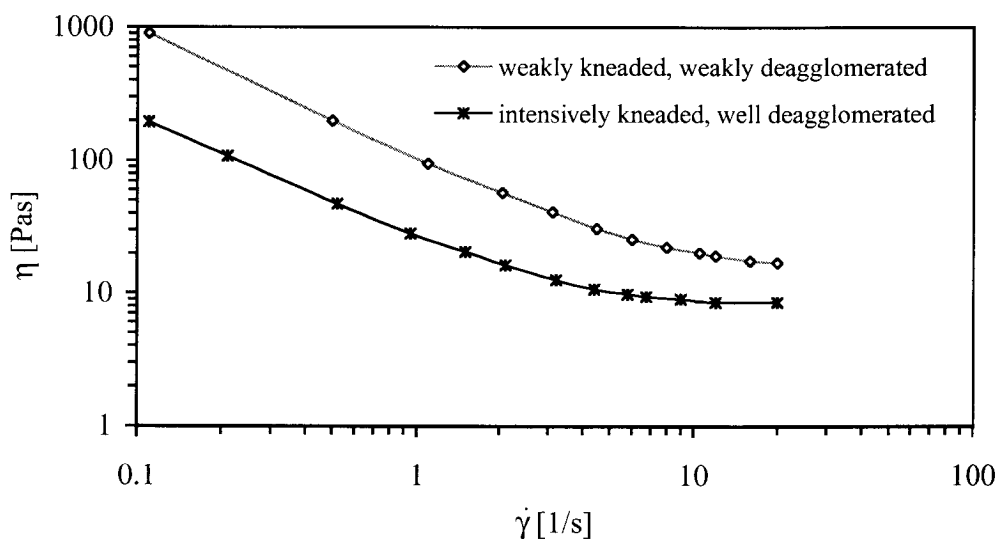
Figure 5-4 Flow curves of differently deagglomerated limestone silicon oil suspensions Rheometrics DSR, concentric cylinder system, $T=30°C$, $c_{v,s}=33\%$ v/v

In a second trial series a higher concentrated system was used and progress in deagglomeration was measured by means of agglomerate analysis employing a method described in "Agglomerate Analysis" on page 39.

The focus here was to concentrate on the influence of small changes in deagglomeration (which are not detectable by visual observation, i.e. non obvious and visual detection of agglomerates as shown in Figure 5-1) on the resulting flow properties of the suspension. It has to be noted, that the suspension analyzed here was higher concentrated ($c_{v,s}=0.45$ instead of 0.33) and that this trial series had been measured with a different rheometer and a different geometry (also thorn stirrer type but different stirrer and cup size) than the series plotted in Figure 5-3. Thus direct comparison of the two results is not possible.

The amount of agglomerates being present after having applied different kneading times and kneading intensities had been applied, was assessed first. Agglomerate analysis of the individual samples was performed according to "Sample Preparation Method for Agglomerate Analysis" on page 43.

In Figure 5-5 size distributions of the differently kneaded samples (samples 1 to 4) obtained after weakest pretreatment (level 2) are given. It can be seen that the samples show significant differences in size distributions. The amount of agglomerates becomes clear when looking at curve 5. Curve 5 represents the size distribution of the primary particles which was obtained after an intense ultrasound treatment (level 5). Sample 4 exhibits no difference between the weakest and the strongest pretreatment (gently stirred, level 2 <-> 10 min. ultrasound, level 5), hence this sample had been fully deagglomerated in the kneading step. All other samples are coarser, i.e. do contain agglomerates.
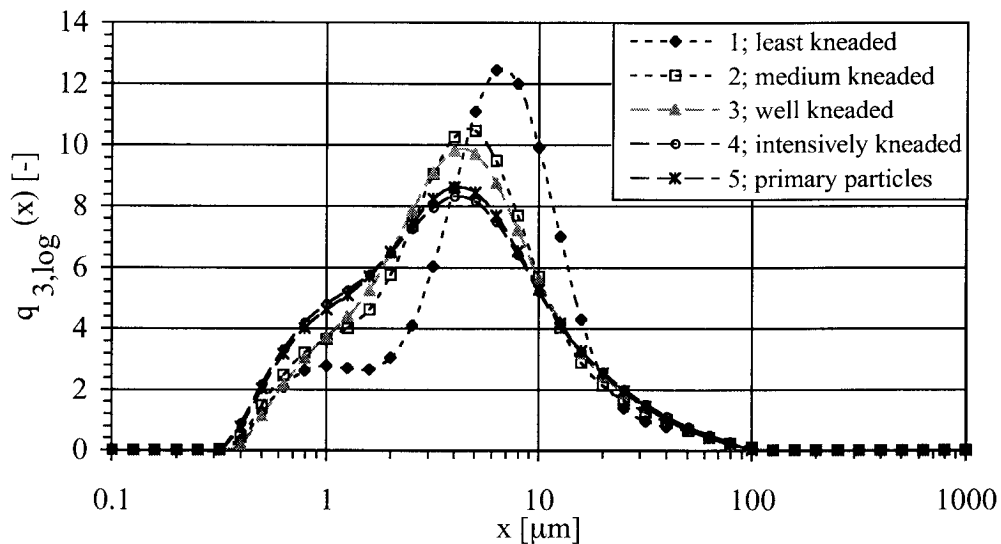
Figure 5-5 *Progress in deagglomeration for samples 1 to 4 (limestone silicon oil), lowest power input during analysis reveals presence of strong and weakest agglomerates; curve 5 gives sizes of primary particles obtained after intense ultrasound treatment*

Before looking at the rheological behavior of these samples, the aspect of agglomerate stability will be considered.

To illustrate the strength of the agglomerates different levels of mechanical power input were applied to the samples such as the stresses applied to the sample were increased from low to moderate to intense.

In the following sample 1 is considered which has experienced the lowest mechanical stresses during its preparation in the Brabender kneader and thus is the least deagglomerated one of that series.

Figure 5-6 gives the stability of the agglomerates (stress level applied during size analysis was increased from curve 1 to 5) analysed by laser diffraction, after kneading had taken place in the lab kneader. Curve 1 represents the lowest stress level, applied whilst mixing the sample in the glass beaker and circulating it for 1 min. in the dispersing unit of the Malvern at a speed level used during measurements (half of the maximum speed). Curve 2 was obtained from the same sample after a further circulation time of 1 min. at maximum speed. Curve 3 was obtained after circulation for 10 min. at maximum speed level. Curve 4 was obtained after ultrasound had been applied for 2 min. at half of the maximum sonication
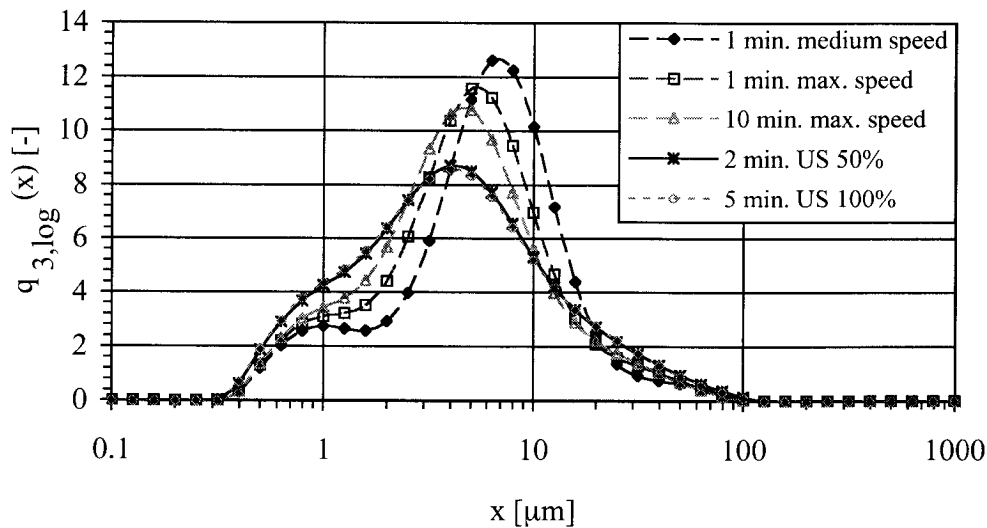
Figure 5-6 *Sample 1:Stability of agglomerates being present after the kneading step, limestone silicon oil*

power. Curve 5 was measured after 5 min. of ultrasound treatment during which maximum sonication power was applied to the sample.

It can be concluded that the agglomerates show a stability or strength distribution. Depending on the stress applied during sample preparation, partial or complete deagglomeration can be achieved. If higher stresses (ultrasound) are applied, agglomerates can be destroyed completely.

After discussion of the size and stability of the agglomerates, it will now be focused on the investigation of the influence of progressing deagglomeration on the flow properties of the limestone silicon oil samples. Figure 5-7 gives the flow curves of the differently deagglomerated samples (from curve 1 to 4). The corresponding size distributions were discussed before.

It can be concluded, that for progressing deagglomeration, hence increased energy and power input during the kneading step, viscosity of the suspension decreases. The reason therefore is the release of fluid which was immobilized in the agglomerates. Due to agglomerate break down, this liquid is set free and thus the effective solid volume concentration is decreased, hence the viscosity is decreased. Especially for suspensions with values for $c_{v,s}>$ 0.3 small changes in $c_{v,s}$ lead to an exponential change of the corresponding viscosities (*Barnes, H.A., Hutton, J.F. (1989)*).

To further support the effect of deagglomeration and thus the influence of the processing conditions applied during kneading of the suspension in the lab kneader, the power respectively the energy input applied during the kneading step will be considered. In the kneading process the speed of the kneading arms (n) can be varied and the torque (M) necessary to turn those is recorded. Keeping the filling weight constant throughout the different trials enables to calculate a mass based power and energy input. In that case it is also possible to directly compare the values obtained for power and energy input. The volume and thus density of the mass of course changes as structure collapses (powder like to liquid like) during kneading which has an effect on the volume based power and energy input.
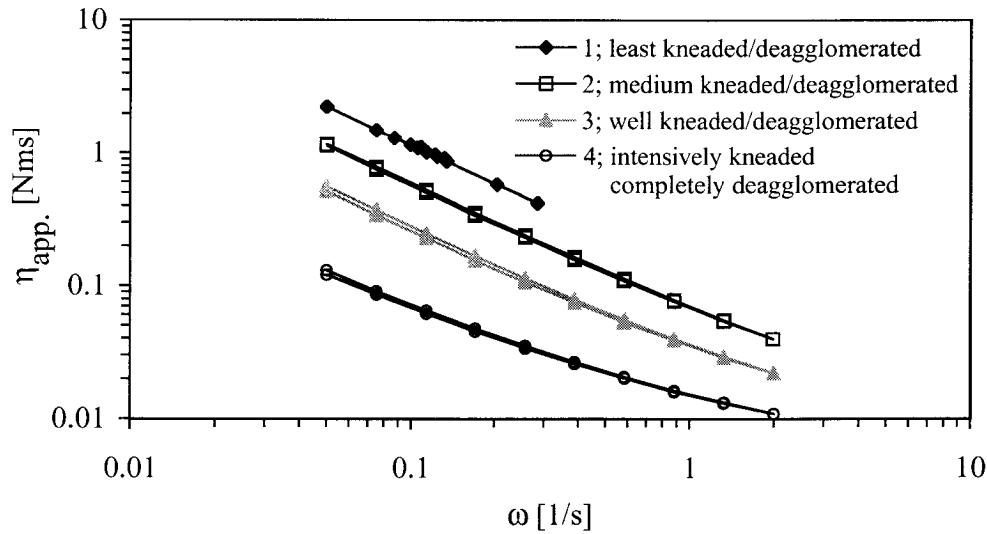
Figure 5-7 *Flow curves of differently deagglomerated limestone silicon oil suspensions ($c_{v,s}$=46% v/v, thorn like stirrer, Bohlin CVO, T=30°C)*

The power input is calculated as

$$P(t) = 2 \times \pi \times n(t) \times M(t) \tag{5.1}$$

and the energy or work W put into the system results from

$$W = \int_{(t = t_s)}^{(t = t_e)} P(t)dt \tag{5.2}$$

The samples discussed in Figure 5-7 had been deagglomerated differently by applying different power and energy input. The corresponding power and energy input applied to these samples during kneading is shown in Figure 5-8. The left y-axis represents the power input and the right y-axis the energy input. From sample 1 to 4 the energy input has increased. It has to be noted that sample 2 and 3 have experienced higher power inputs than sample 4, but sample 4 had been treated longer and thus higher energy was put into it. This indicates that for deagglomeration the energy is of importance.

Looking at the lab kneader, it is quite obvious that, depending on the structure of the sample, not every volume of the sample is passing the zones of highest stress. There is a stress distribution in the kneader and also a probability distribution for the sample to pass these stress zones. For deagglomeration the outer forces need to be higher than the inner, attractive, binding forces. Once the disruptive forces are high enough, it depends on the probability of passing the zones where these forces act. This time dependency is expressed through the effect that the process seems to be energy driven rather then power driven, which is only true when the disruptive forces are high enough.
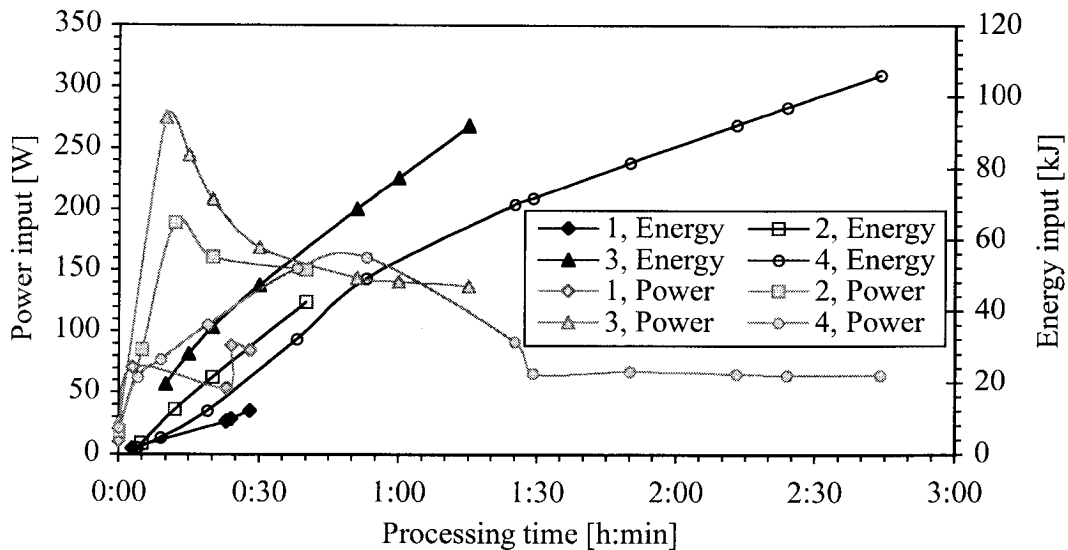
Figure 5-8 *Energy and power input applied during kneading, limestone silicon oil samples, corresponding flow curves discussed in Figure 5-7*

5.1.2 Rheology - Influence of Water Sorption

To assess the influence of water sorption on the resulting flow behavior of limestone silicon oil suspensions, well deagglomerated sample had been used for investigation. Whilst performing rheological measurements the samples had been exposed to different levels of head space humidity. To ensure good mixing and mass transfer the sample was analyzed with the helical ribbon impeller (See "Special Geometries" on page 50.). To allow for equilibration between head space humidity and water sorption of the sample, the samples were stirred in a first step at a constant angular velocity over time. After distinct times up and down flow curves were measured. Applying different levels of head space humidity and allowing the sample to adapt to those, revealed the influence of water sorption on the flow properties. The general set up is described in "Head Space Controlled Rheometry" on page 57.

In Figure 5-9 the change of apparent viscosity versus time for different levels of head space humidity is shown. The measurement was performed with a helical ribbon impeller at 30 °C at an angular velocity of 6 1/s. For increasing relative humidity the viscosity of the system increases. It is assumed that the incorporation of water increases the difference of polarity in this system which leads to higher particle - particle interactions, hence increases the viscosity.

Furthermore it has to be noted that in case up and down cycles (increasing - decreasing stress level) were carried out between two time tests, viscosity drops but recovers over time again. This leads to the conclusion, that structures are formed during the time test (carried out at constant angular velocity). From a certain point on, stresses (and thus shear rates) in the consecutively applied up down cycle are higher than during the time test. This means that the equilibrium structure formed over time is destroyed but reestablishes over time again. This

is seen in the second time test performed after the up and down cycle. Additionally it has to be noted that the sample used here was ground in 3 roll refiner and the fresh surface of the broken limestone particles had been surrounded by silicon oil i.e. protected against ambient atmosphere. This has also an impact on the state of the surfaces. In the following the aspect of ageing and protection of the fresh surfaces will be discussed.
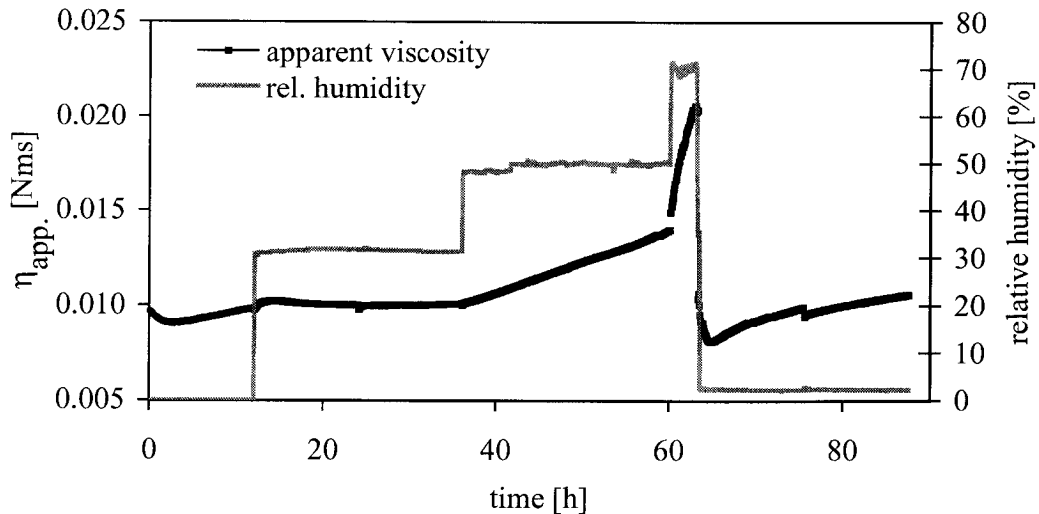
Figure 5-9 *Influence of water sorption on flow properties of a roll refined and well deagglomerated sample of limestone silicon oil (helical ribbon impeller, constant angular velocity 3 1/s, Bohlin CVO, $c_{v,s}=46\%$ v/v, T=30°C)*

5.1.3 Ageing of Surface

Fracturing of particles always lead to the generation of new, fresh surface. Such surfaces are not equilibrated to their surrounding media. Rumpf et. al. have shown (*Schönert, K. (1974)*, *Schwenk, W. (1971)*) that fresh surfaces alter their structure due to the adsorption of components from the surrounding media. In that case the surface is longer the pure material's surface but the material's surface with other components adsorbed to it. Consequently the interfacial properties have changed. The effect of different interfacial properties on the rheological behavior of limestone siliconoil suspensions is shown in the following. In the previous section limestone silicon oils suspensions were prepared through roll refining and kneading mixtures of limestone and silicon oil. It was found that water sorption has an effect on the rheological properties of the such prepared suspensions.

In another experiment dry ground limestone had been used for preparing a suspension of limestone and silicon oil. The limestone was obtained from dry grinding and had been stored for at least one year, i.e. could equilibrate to the surrounding atmosphere. In order to analyze what effect water sorption has on the rheological properties, the sample was exposed to different levels of humidity during the rheological measurement. From Figure 5-10 it can be seen that there is no influence of humidity (water sorption) on the flow properties. It has to be mentioned that this sample has a solid vol. conc. 33% v/v whereas the sample discussed in Figure 5-9 has a concentration of 46% v/v.
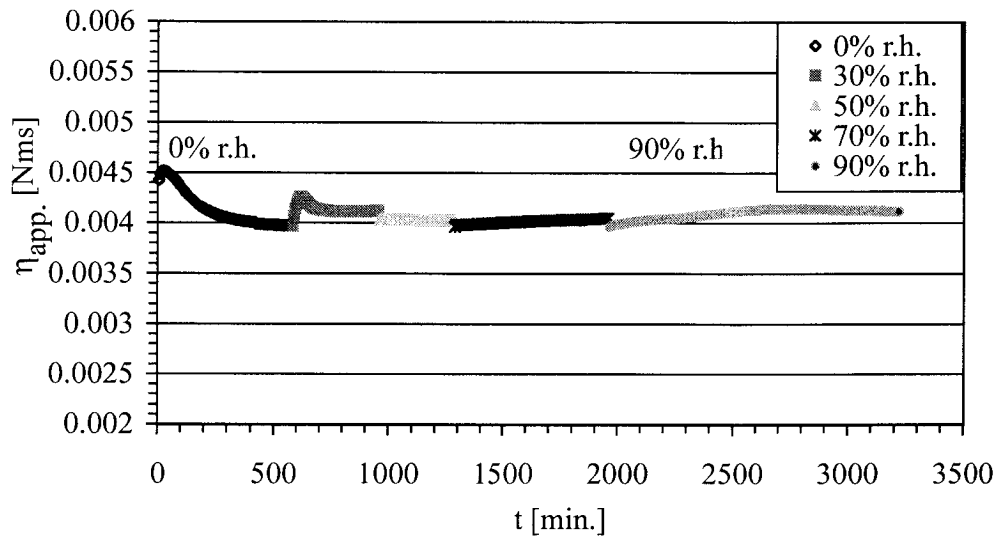
Figure 5-10 *Influence of water sorption on flow properties of a dry ground limestone-silicon oil sample (helical ribbon impeller, constant torque 15 mNm, corresponds to an angular velocity of 3.5 to 4 1/s, Bohlin CVO, $c_{v,s}$=33% v/v, T=30°C)*

The influence of water sorption is quite different to the sample shown before. It is believed that the reason therefore is the different treatment during and after refining. In case of dry ground limestone the limestone with its fresh surfaces had been exposed to the ambient air and equilibrated to this surrounding media. Furthermore it has to be noted that limestone is a natural material which contain also some impurities. When refining the limestone together with the silicon oil the fresh surfaces are covered with silicon oil hence can not equilibrate to the surrounding atmosphere. The whole system is in a non equilibrated state. Working with higher concentrated suspensions the interfacial properties are of greater importance. The unsaturated and non equilibrated interfaces react different to water than in case of the dry ground material. The molecular mechanisms behind could not be explained but the effects were observed. Whether or not electrostatic forces caused by intense friction in the roll refiner or purely non equilibrated surfaces and their special sorption behavior are the reason could not be clarified and might be subject of further investigations.

5.1.4 Summary

For the lime stone silicon oil system it was found that deagglomeration of the agglomerates formed during refining leads to an release of immobilized liquid phase. Release of immobilized liquid phase decreases the effective solid volume concentration and thus reduces viscoity. The effect of decreasing effective solid volume concentration is not compensated by the increased number of "free interaction points" (individual particles resulting from destroyed agglomerates), and thus by the increased particle interactions. This means that particle interactions present in this system are of minor importance. When working with unsaturated (roll refining, freshly ground limestone) surfaces, water sorption influences the rheological properties of such suspensions. For systems composed of dry ground limestone that had been stored after grinding ("old" surfaces) and silicon oil no influence of ambient air conditions on rheology could be observed.

5.2 Sugar - Silicon Oil -System

In the previous section a system was investigated, where the physical mechanical aspects are dominant. Replacing limestone by sugar introduces a component that exhibits an increased complexity. Comparing it to the limestone - silicon oil system it is expected to obtain different and more complex properties for the sugar silicon oil system. In confectionery sugar commonly stands for sucrose. If not mentioned differently also within this work sugar is used as a synonym for sucrose.

The characteristics of sugar, being the disperse phase can be described as

- Dense

- Non porous

- Irregularly shaped after grinding

- Pure substance

- Hydrophillic

- Good water solubility

- Amorphous - crystalline transition

- Medium high melting point (ca. 180°C)

Compared to the system limestone - silicon oil, the physical-chemical properties of this system are of increased importance and need to be taken into account when studying the flow behavior of the corresponding suspensions.

Sugar is the component that makes up 70% w/w of the solids in chocolate. Its physico-chemical properties have been widely investigated (*Roth, D. (1976), Blanshard, J.M.V., Lillford, P.J. (1993), Hartel, R.W. (1993), Saleki-Gerhardt, A., Zografi, G. (1994)*) and also the rheological behavior of sugar-oil systems had been analyzed extensively (*Niediek, E.A. (1968), Zielinski, M., Niediek, E.A, Sommer, K. (1974), Tscheuschner, H.D. (1993b), Winkler, T., Tscheuschner, H.-D. (1998a)*). But still the relationships and interactions between some special physical phenomena and their effect on the rheological properties of sugar oil systems have not been assessed till now. Sugar for its use in confectionery products is milled. During milling high energy dissipation takes place at the tip of the crack that moves through the breaking particle. This energy dissipation gives rise to local temperatures of about 2000°C. Partial melting and rapid solidification leads to the formation of amorphous surfaces (*Roth, D. (1976), Weichert, R. (1976)*). The fresh surfaces are now in the amorphous state. The amorphous surfaces are highly hygroscopic and pick up water from the ambient media (*Niediek, E.A. (1979), Niediek, E.A. (1982), Niediek, E.A. (1991a)*). The water gives rise to a higher mobility of the molecules which is necessary for crystallization. During crystallization there is no longer space for the water in the sugar crystal and thus it is expelled.

5.2.1 Influence of State Transitions (Amorphous - Crystalline)

In this study sugar was refined together with silicon oil under a dry atmosphere. This was to prevent water pick up and thus to avoid crystallization. The powder obtained after refining was then kneaded in a dry atmosphere and once deagglomerated and liquefied after addition of further liquid, transferred to the rheometer. The rheological measurements were performed under controlled headspace atmosphere. The controlled head space atmosphere was

necessary to apply a certain humidity which allowed the sugar to recrystallize. With this set up it was possible to investigate the influence of phase transition amorphous -.crystalline and the effect of water sorption on the rheological properties of sugar oil systems. The presence of amorphous phases was thereby detected with a sorption balance (See "Sorption Balance - Detection of Amorphous Phases" on page 34.).

Figure 5-11 shows the development of the apparent viscosity versus time when applying different head space humidities to the sample. The test was performed at a constant angular velocity (rate controlled) using a thorn type impeller.
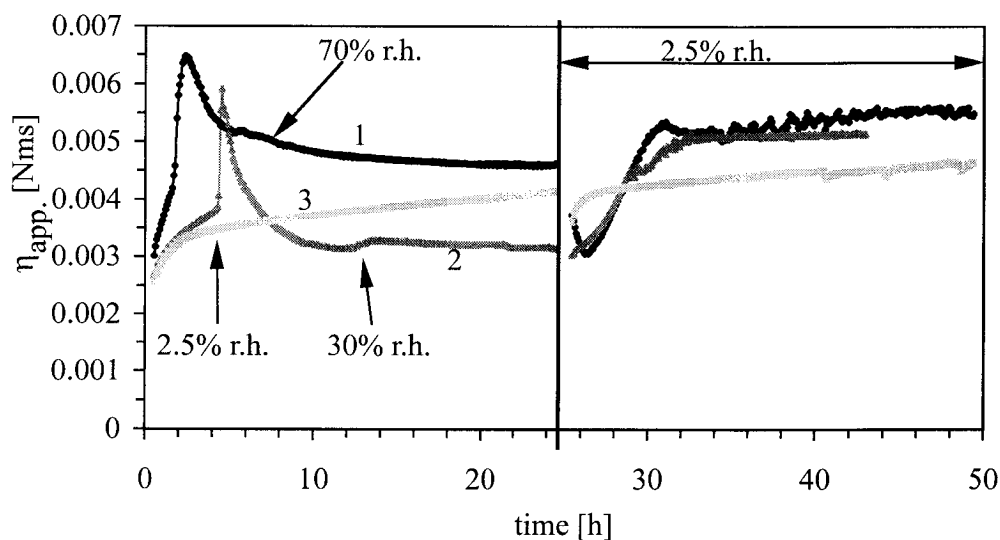
Figure 5-11 Sugar silicon oil, sample 1,2 & 3, change of viscosity versus time whilst applying different levels of relative humidity (thorn type stirrer, Bohlin CVO, constant angular velocity 10 1/s, $c_{v,s}$=33.5% v/v, T=30°C)

The y-axis represents the apparent viscosity. In a first step the sample was exposed to a humid atmosphere, which was for sample 1, 70%r.h., for sample 2, 30%r.h. and for sample 3, 2.5%r.h. After a certain time the atmosphere was then changed from humid to dry (2.5%r.h.) and the reactions of the samples were followed. The temperature was kept constant at 30°C.

For sample 1 viscosity increases steeply during the initial 2 h and reaches a maximum. Then a rapid decrease takes place which levels off over time. It has to be noted that the first point measured represents a sample that is amorphous and had equilibrated to an atmosphere of 2%r.h. (mixed, refined and kneaded under dry atmosphere), whereas the last points belong to a sample that is crystalline and has equilibrated to an atmosphere of 70%r.h. which causes a significant difference in viscosity. Looking at the "dry" part of the graph it can be seen that for sample 1 viscosity first decreases, passes a minimum and then increases to a value higher than it reached at 70%r.h., whereas sample 2 shows a steady increase at first and finally levels off. The reason for this behavior will be discussed at a later stage. First the effects taking place in the humidification step will be assessed. Sample 3 shows a steady increase in viscosity but no maximum is observed.

In order to assess the mechanisms behind, a new sample was prepared. It was exposed to a rel. humidity of 70% and a temperature of 30°C was applied during rheological analysis.

Before and during rheological measurement subsamples were taken at distinct times and analyzed for presence of amorphous phases and for agglomerates. The positions of sampling are illustrated in Figure 5-12.
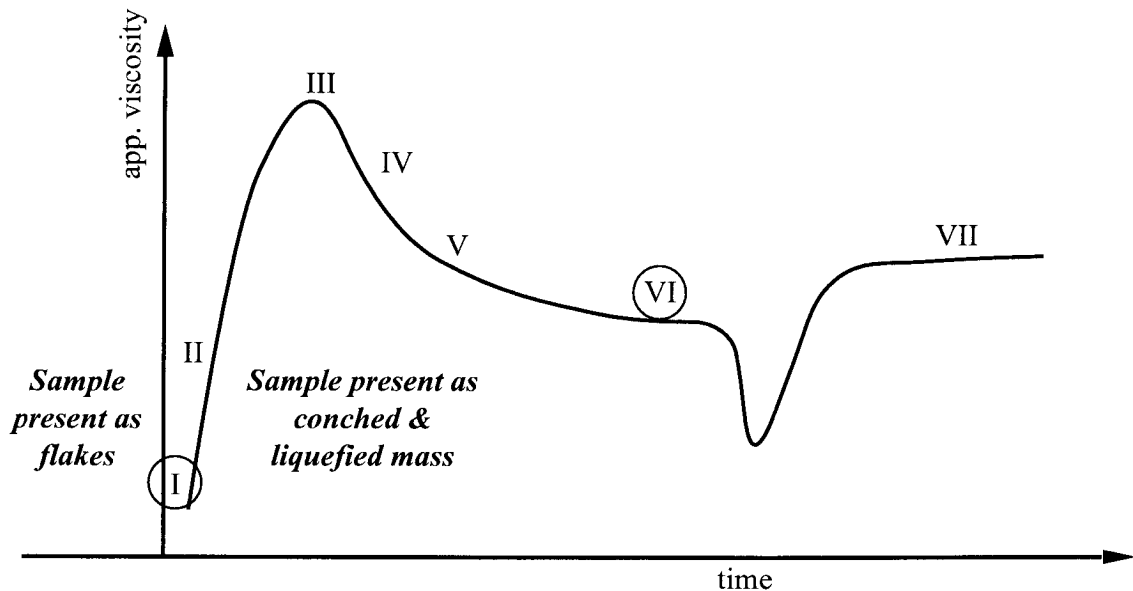
Figure 5-12 *Positions of sampling, before and during rheological measurement, schematic drawing of the obtained app. viscosity - time function*

Employing the sorption balance for analysis allows to analyze for the presence of amorphous phases. Amorphous phases are characterized by a peak in the weightsignal (water uptake & release). The analysis revealed that both the refiner flakes and the mass after kneading show
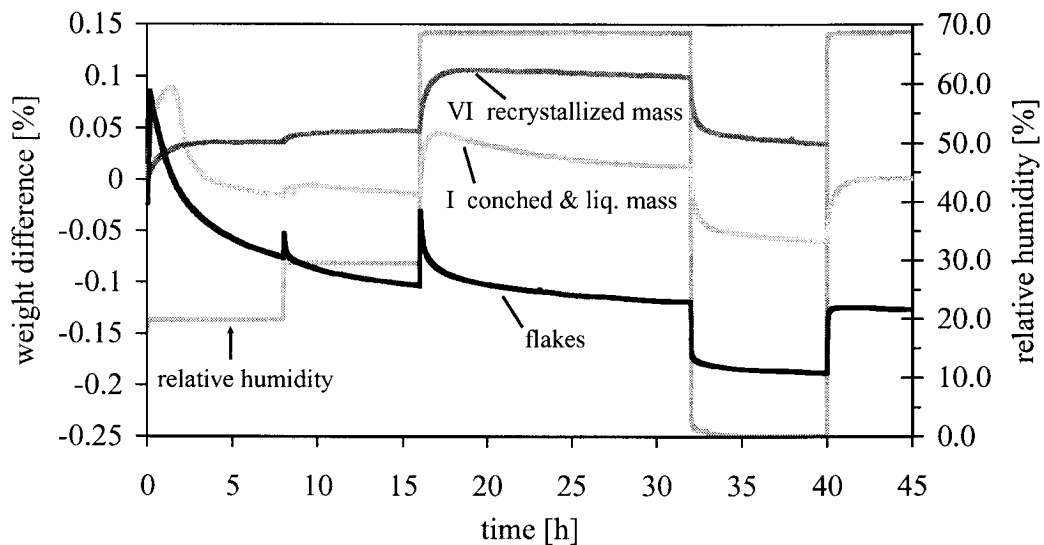
Figure 5-13 *Sorption balance results (weight difference as a function of time for different levels of humidity) for flakes of sugar silicon oil, conched and liquefied mass, and samples taken at end of humidification in rheometer, T=30°C*

-71-

a maximum for the change of weight versus time (Figure 5-13). Whereas the sample taken at the end of the rheological measurement exhibits no maximum. This proves that in the beginning the sugar contains amorphous phases which do recrystallize in course of the experiment.

Recrystallisation is observed as a maximum both in change of viscosity and in weight as a function of time. Thus the rheological method is suitable for detecting amorphous sugar phases and their transition to crystalline.

Looking at the influence of water sorption and recrystallisation on agglomerate formation, agglomerate analysis was performed by laser diffraction (see See "Agglomerate Analysis" on page 39.). Therefore the samples were treated with different energy input which caused a breakdown of the agglomerates, i.e. shows the agglomerate size and stability (Figure 5-14).
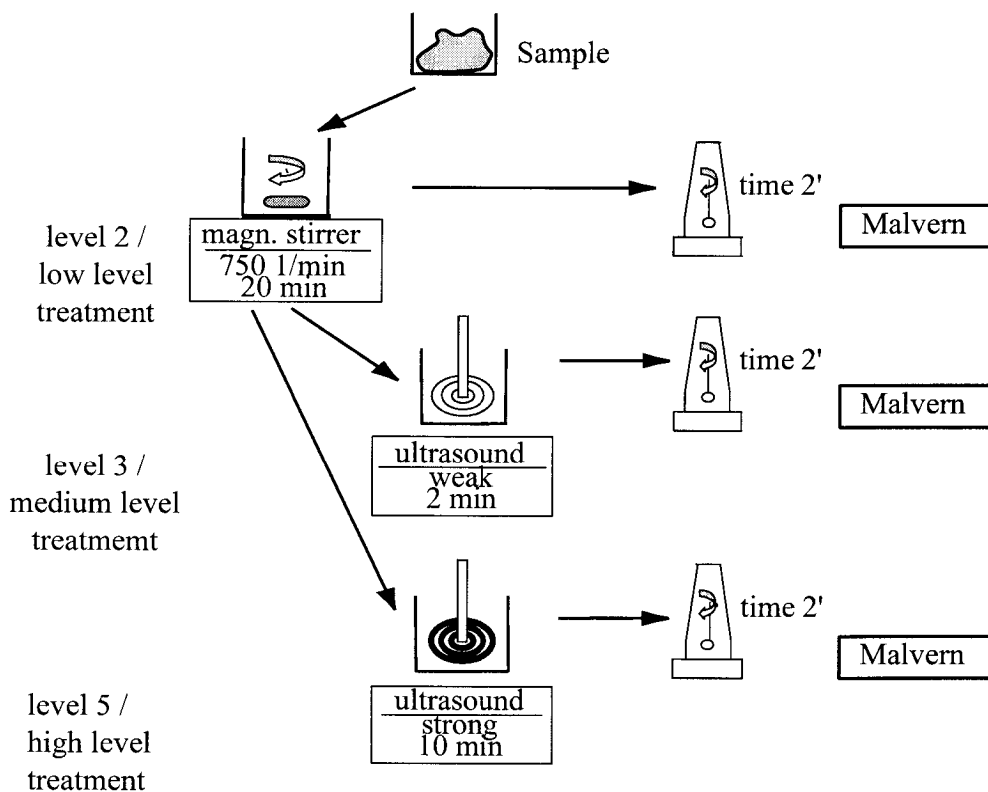
Figure 5-14 Sample preparation and treatment for agglomerate size analysis

For the samples taken at positions described in Figure 5-12 the corresponding size distributions - obtained after low stress levels were applied during agglomerate analysis (level 2 treatment)- are illustrated in Figure 5-15. In order to assess the strength of the agglomerates the sample was also treated at higher stresses (level 3 & 5). The size distributions resulting from level 3 and level 5 (primary particle size distribution) are given in Figure 5-16 and Figure 5-17.

Comparing these graphs it is found that sample I and II exhibit similar size distributions. They were taken at the beginning of the measurement and are expected to be similar. Sizes of sample III, IV, V and VI are also quite similar but different to the sizes of sample I and II. They were taken when recrystallisation has passed the maximum. Comparing now sample I
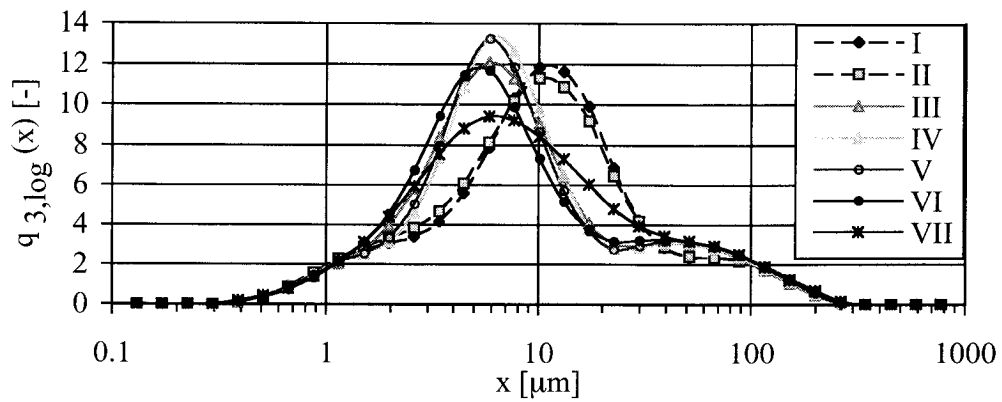
Figure 5-15 *Particle sizes obtained for level 2 treatment, sugar silicon oil*
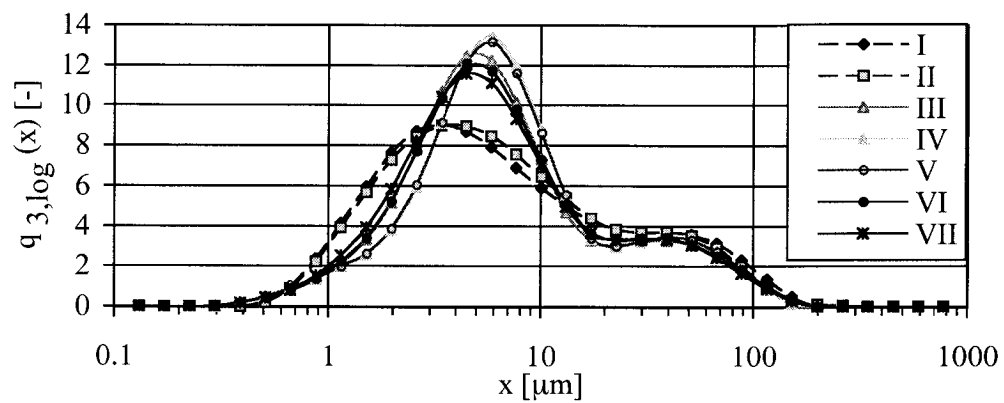
Figure 5-16 *Particle sizes obtained for level 3 treatment, sugar silicon oil*
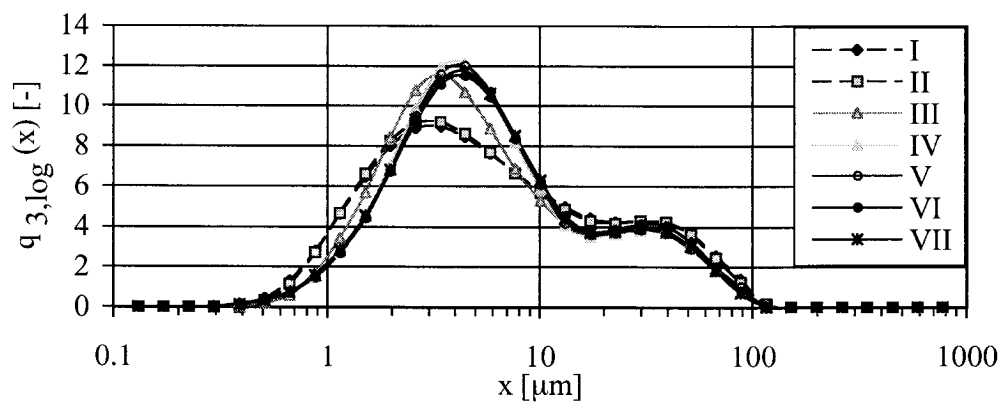
Figure 5-17 *Particle sizes obtained for level 5 treatment, sugar silicon oil*

with sample VI for the low level (level 2) treatment (Figure 5-15) yields that I is coarser and thus contains bigger agglomerates than VI. Going to level 3 treatment the opposite is the case. Sample I is now the finest whereas the size of VI hasn't changed much. This means that

the agglomerates in sample I are bigger than in sample VI but less stable. Level 5 treatment (Figure 5-17) reveals the distribution of the primary particles. Compared to Figure 5-16 not much change is observed for sample I but sample VI shows a decrease in size and is still coarser than I. It can be concluded that sample VI contains relatively hard agglomerates which are formed in the course of recrystallization. The individual particles are bound together by solid bridges which result from liquid bridges that were build during humidification (water sorption) and finally solidified during recrystallization. To better illustrate the processes involved, the mechanisms behind are described in the following section.

5.2.2   Model for Formation and Transition of Amorphous Phases

In the previous chapter it was shown that amorphous sugar surfaces and their transition to the crystalline state significantly effect the structural properties of a sugar oil suspension. This is due to the adsorption of water and the formation of a sticky and liquid layer at the surface. In order to visualize the layer formation, micrographs from amorphous sucrose were taken and the change in appearance during the sorption of water was followed.

Figure 5-18 shows a picture (a) of amorphous sucrose before major water sorption has taken place. Leaving the sample for 30 min. at room conditions it can be seen that the powdery structure has converted into a liquid structure (b). The same is happening to the amorphous layers which are present at the sugar surfaces after refining. With the help of these pictures it can be easily imagined what effect such sticky layers have on the flow properties and thus on the moveability between neighboring particles (see also *Peleg, M. (1983)*, *Peleg, M. (1993)*).

a.) before water sorption   b.) after water sorption
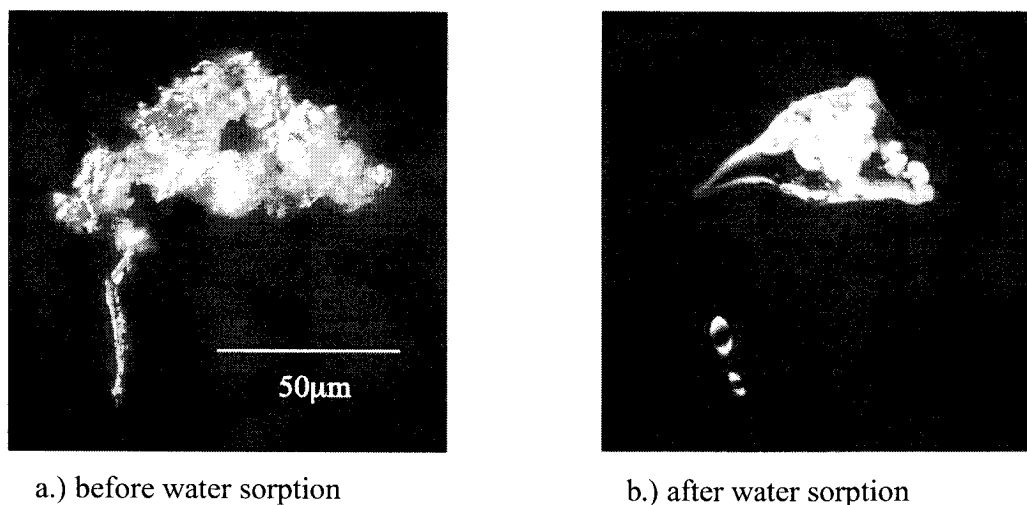
Figure 5-18 Amorphous sucrose, change in structure due to water sorption

In order to link the effects discussed so far together and to illustrate and summarize the underlying mechanisms a model for water sorption, recrystallization and its effect on flow behavior is proposed. This model is given in Figure 5-19. It shows the different processes occurring in the course of mixing, refining, kneading and rheological measurement.

Refining of sugar generates amorphous surfaces and also agglomerates. In the following kneading step these so-called primary agglomerates are destroyed which leads to liquefaction of the mass (A). Performing this under dry atmosphere ensures that the amorphous surfaces do not recrystallize. The surfaces have not been in contact with water so far, i.e. no water or only small amounts of water (resulting from the water dissolved in the silicon oil) are adsorbed to the sugar surface. In this state the sample is placed in the rheometer and exposed to a humid atmosphere. Now water is adsorbed to the sugar surface (B) which increases the difference in polarity of the systems. As the surface is amorphous the sugar is dissolved in the water which forms a sirup like, sticky layer. This layer further increases the adhesion between the particles (*Schuchmann, H. (1994)*) which gives rise to viscosity. Due to the high concentrations and the weak dispersing in the rheometer the particles can adhere to each other and form liquid bridges. Once enough water is adsorbed the sugar starts to recrystallize. Thereby the crystalline structure underneath the amorphous surface acts as a seed for crystallization. When recrystallizing the sucrose builds up the crystal structure in which no space for water is available, i.e. the water is expelled. Liquid bridges now become solid bridges and thus form strong agglomerates. The expelled water de sorbs hence the water content is reduced which reduces the difference in polarity thus reduces viscosity. Also the sirup like layers disappear which further reduces viscosity. Finally crystalline sugar together with some water adsorbed to its surface is present. Owing to kinetics it is also possible that in some volume elements the concentrated sugar solution didn't crystallize but solidified as glass which means, still amorphous but now with water inclusions. This also leads to an increase in difference of polarity hence is a factor that increases viscosity. As these phenomena take place at the surface only small volumes are sufficient to cause a large effect. The downside is that analytical methods require a certain amount of substance to overcome the threshold of the method. As small volumes are involved many analytical methods are at their limit. Rheological behavior is related to particle interactions and they are related to interfacial properties. Therefore this method could provide a tool where even small amounts of amorphous material can be detected.

A   *refining and kneading (deagglomeration)*

fracturing

formation of
press agglomerates
and *amorphous surfaces*

kneading
deagglomeration

B   *humidification and recrystallization*

+H_2O

water sorption
formation of
sirup like layer
increased interactions

agglomeration

formation of
liquid bridges

-H_2O

recrystallization
desorption of water
formation of solid bridges
rigid agglomerates

η

dry atmosphere   **humid atmosphere**

+H_2O

water sorption

increase in difference
in polarity
agglomeration
sticky layers

-H_2O desorption

recrystallization
desorption of water

refining &
kneading

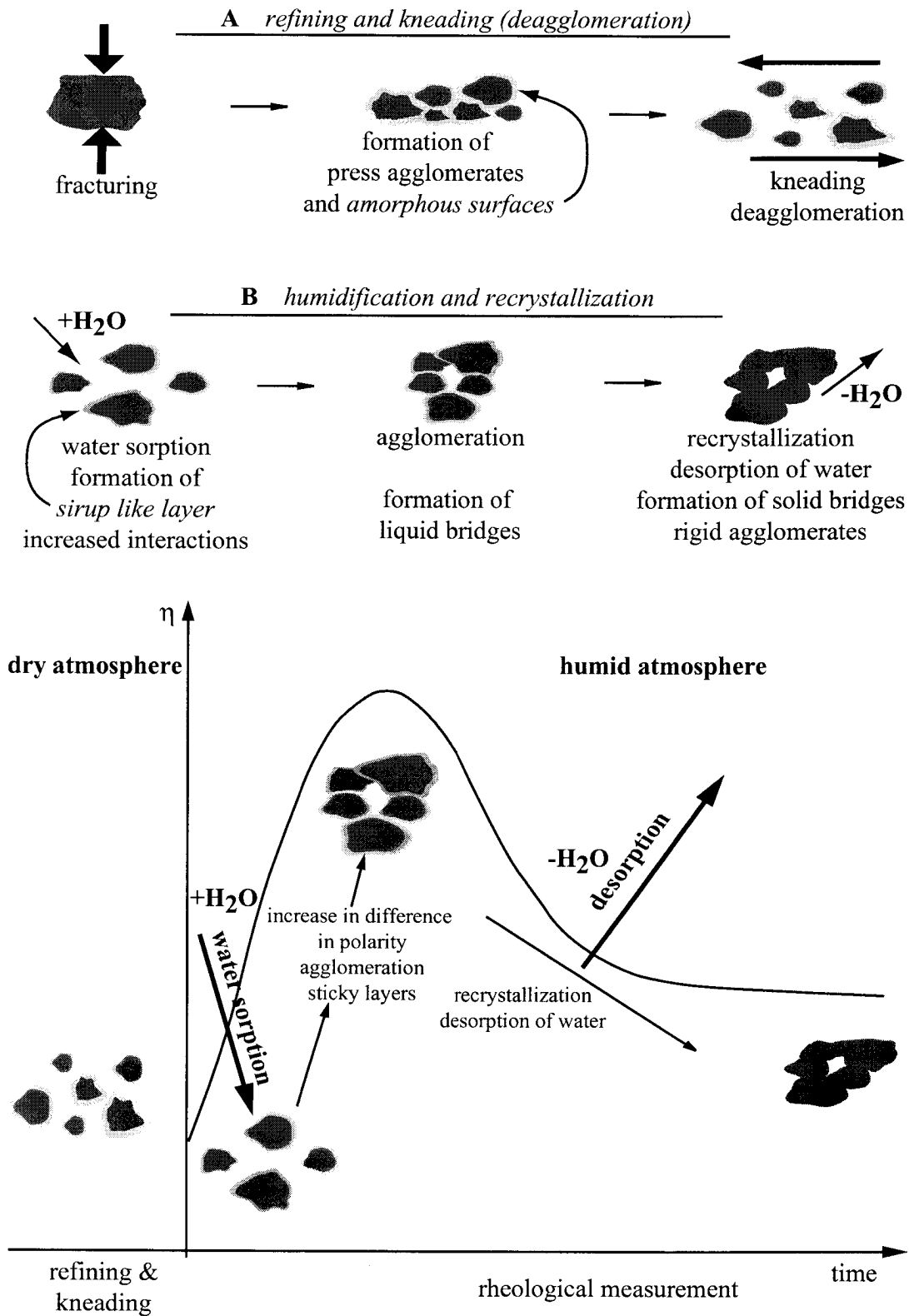rheological measurement

time

Figure 5-19 Model for agglomerate formation, deagglomeration, water sorption, recrystallisation and its relevance to rheology

-76-

5.2.3   Rheology - Influence of Water Sorption

Sugar silicon oil suspensions were found to change their rheological properties depending on the humidity of the ambient air. To further investigate this effect a well deagglomerated sample, that had been recrystallized in the rheometer before, was used for analysis. Also for this sample recrystallization was detected as a maximum in viscosity like it was for the samples discussed before. This clearly confirms the previous results. After recrystallization (humidification step, 70% r.h., 0-27h), the sample was exposed to different head space humidities and the rheological behavior was measured with a thorn type stirrer. In Figure 5-20 the resulting flow curve is shown. Reducing the humidity from initially 70% to 2.5% first leads to a drop in viscosity which passes a minimum, increases and finally levels off. The viscosity reached in the plateau is regarded as an equilibrium value. Increasing now the humidity to 20% r.h. decreases viscosity. Further increase of humidity up to 50% r.h. leads to a further reduction of viscosity. Applying humidity levels of 60% and 70% r.h. gives rise to viscosity.
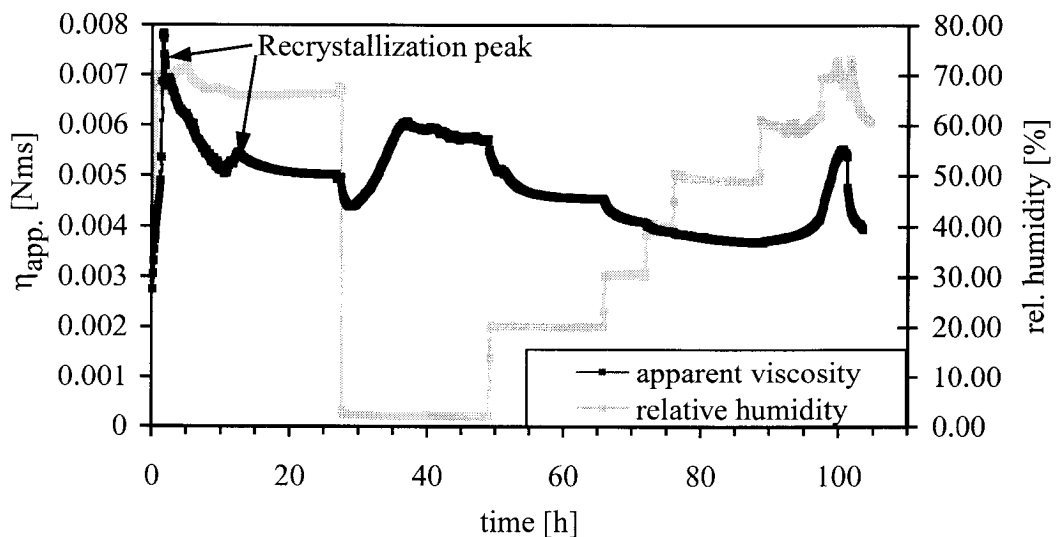
Figure 5-20 Influence of humidity on the flow behavior of a deagglomerated and recrystallized sugar silicon oil suspension, helical ribbon impeller, Bohlin CVO, constant angular velocity 10 1/s, $c_{v,s}=33.5\%$ v/v, $T=30°C$

Compared to limestone - silicon oil this system shows the opposite behavior. Increasing the humidity first leads to a decrease of viscosity. This indicates, that the particle interactions are reduced when water is adsorbed. It is assumed that the adsorbed water forms a deformable layer and thus a deformable, flexible interface. This reduces "friction" between the particles and therefore lead to a decrease in viscosity. The actual mechanism behind is still unknown and the explanation given is only a hypothesis. For higher levels of humidity an increase of viscosity is observed. For increased humidity more water molecules are adsorbed. Sucrose will be soluted and sticky, sirup like layers are formed. Particle contact now leads to adhesion and formation of liquid bridges (lowering of glass transition temperature, contact time sufficient to cause agglomeration, (*Rao, M.A., Hartel, R.W. (1998)*)). Agglomerates are formed that are bound together by liquid bridges. Furthermore these agglomerates immobilize liquid phase which also gives rise to viscosity.
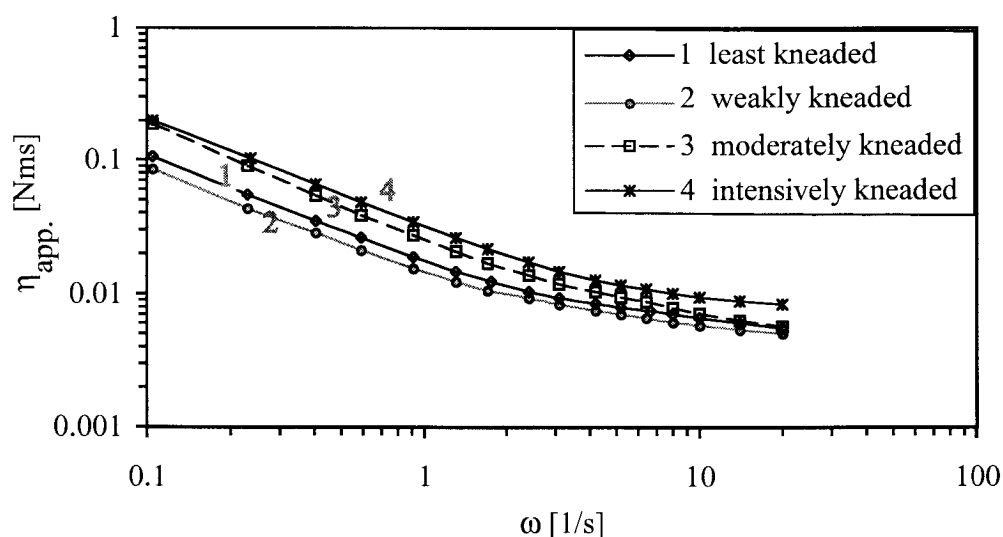
5.2.4   Rheology - Influence of Deagglomeration

In the previous sections it was described how the effects of phase transition and water sorption influence the rheological properties of sugar silicon oil suspensions. These special phenomena need to be taken into account accordingly when the influence of deagglomeration on the rheological properties of sugar oil systems is investigated. In the past the interplay between physical state of the surfaces and its effect on deagglomeration was not known and the results reported left key questions open (*Zielinski, M., Niediek, E.A, Sommer, K. (1974)*). When working with sugar oil systems in which sugar was ground in a previous stage of processing, it is indispensable to have at least control over

- state of the interfaces (crystalline - amorphous)

- the amount of water adsorbed (humidity to which sample is exposed) to the interface.

In order to illustrate the importance of the physical state of the interfaces examples are given where the phase transitions occurred in an uncontrolled and also in a controlled fashion.

Figure 5-21 shows the flow curves of sugar silicon oil samples that have been treated in a lab kneader and deagglomeration progressed with kneading time and intensity. The flow curves were measured with a helical ribbon type of stirrer with a Rheometrics, DSR rheometer. The degree of deagglomeration is increasing from sample 1 to 4. The most deagglomerated sample shows higher viscosities than the least deagglomerated one. In course of deagglomeration (sample 1 to 4) viscosity first decreases and then increases, which is different to what was found for limestone/siliconoil (see 5.1.1 "Rheology - Influence of Deagglomeration" on page 60). The reason for this difference are the more pronounced particle interactions in the sugar silicon oil system. From a certain degree of deagglomeration on the increasing number of free particles (increasing particle interactions) compensate for the release of immobilized liquid phase, i.e. give rise to viscosity, especially in the low shear rate domain, where structural forces are dominant.

Figure 5-21 Sugar silicon oil, influence of deagglomeration and not accounting for phase transition, Rheometrics DSR, helical ribbon impeller, $T=30°C$, $c_{v,s}=33.5\%$ v/v

In another series a sample (sample A) was ground and directly transferred to the lab kneader (room conditions). After deagglomeration (kneading) the sample was stored in a closed beaker for 24 h. The texture of the sample (sample A) directly after kneading was pasty and smooth, like it is shown in Figure 5-22. After storage the texture had changed totally. It can be seen (Figure 5-23) that fluid has separated and that big agglomerates were formed. Due to recrystallization of the sugar, the particles are now bound together and 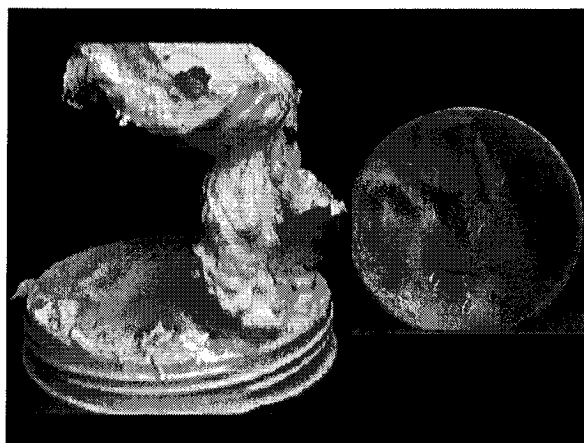the liquid phase is expelled (depletion flocculation) which leads to a densification of the sample and thus to phase separation.
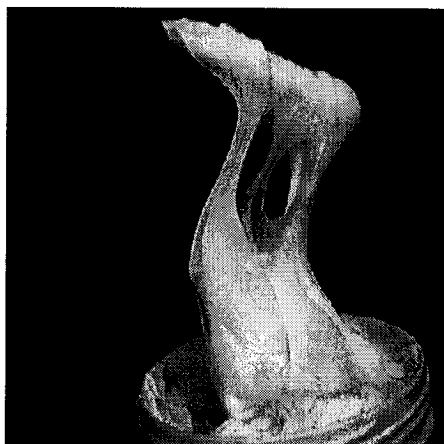
Figure 5-22 Sample A, Sugar silicon oil, deagglomerated/ kneaded directly after refining, no storage of the sample, $c_{v,s}=33.5\%$ v/v, room conditions

Figure 5-23 Sample A, Sugar silicon oil, deagglomerated/kneaded directly after refining, sample was stored for 24h at room conditions in a closed plastic container, $c_{v,s}=33.5\%$ v/v, room conditions

In order to check the influence of storage a sample (sample B) was prepared where the refiner flakes obtained from refining had been stored at room atmosphere (25°C, 25%-35% r.h.) for 3 days prior to usage for kneading. The so prepared sample (stored, kneaded and deagglomerated, liquefied) does not show any phase separation or agglomeration after a storage time of 48h which is seen in Figure 5-24.

To get a better understanding of the underlying effects, subsamples of sample A and B were taken and assessed by microscopy. Therefore the samples were diluted with silicon oil, gently mixed and poured on a glass petri dish. The microscopical observation reveals two different behaviors which are given in Figure 5-25 and Figure 5-26.

Sample A,1 (Figure 5-25) is the subsample of sample A, which was prepared from fresh refiner flakes. Sample A,1 was assessed by light microscopy directly after the kneading step was finished and the surfaces were still in the amorphous state. Sample B,1 (Figure 5-26) is the subsample of sample B which was prepared from stored refiner flakes and hadn't shown any agglomeration after a storage time of 48h.

Looking at Figure 5-25 it is seen that sample A,1 shows the presence of agglomerates. These agglomerates are weakly bound together. Applying shear forces, i.e. shaking of the petri dish, leads to a break down of the agglomerates, but as soon as these forces decline, spontaneous reagglomeration occurs again. This illustrates the attractive forces acting between the particles and the difference in polarity between the liquid and disperse phase that causes
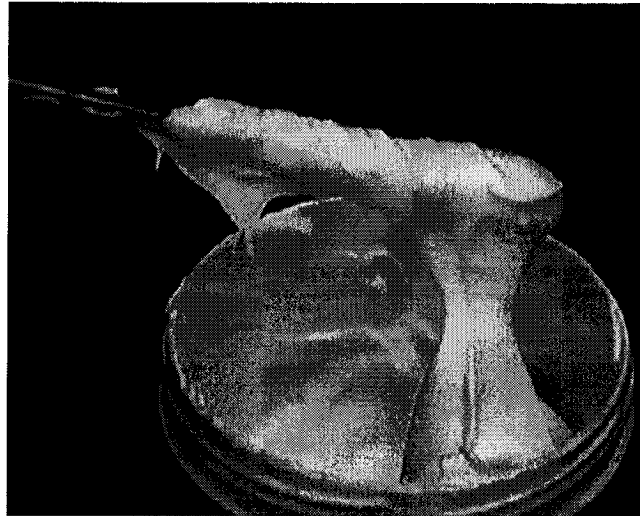
Figure 5-24 Sample B, Sugar silicon oil sample prepared from refiner flakes that had been stored for 3 days prior to usage; sample had been stored for 48h after kneading step was performed

agglomeration. Different to sample A,1 sample B,1 (Figure 5-26) does not show any agglomerates but well dispersed particles. The interfaces had the chance to change from amorphous to crystalline which changes the difference in polarity and thus does not lead to agglomeration.
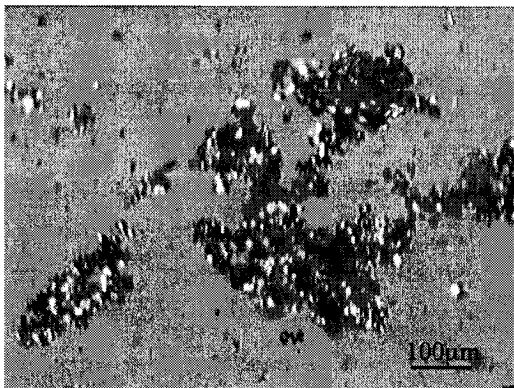
Figure 5-25 Sample A,1; prepared from suspension produced with fresh refiner flakes (still amorphous), sample A prior to storage
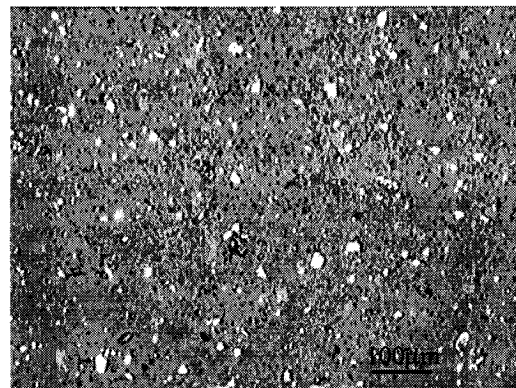
Figure 5-26 Sample B,1; prepared from suspension produced with stored (3d) refiner flakes (recrystallized), sample B

In order to check the influence of storage of the refiner flakes and thus the influence of recrystallized surfaces on the relationship between deagglomeration and flow properties a trial was performed where the refiner flakes had been stored for 3 days prior to kneading. During kneading and rheological analysis the ambient atmosphere was not controlled but relatively constant (25°C, 25%-35% r.h.). The samples were measured with the same setup used for Figure 5-21. In case of working with "aged" (stored) refiner flakes it was found that for

progressing deagglomeration viscosity decreases but approaches a plateau for high levels of deagglomeration (see Figure 5-27). This is illustrated even better when looking at a distinct viscosity for a stirrer speed of 5 1/s for example. It seems that deagglomeration is only of importance for samples showing significant differences in the degree of deagglomeration (highly agglomerated, i.e. least treated sample compared to a well deagglomerated, i.e. intensively treated sample), hence for extreme changes.
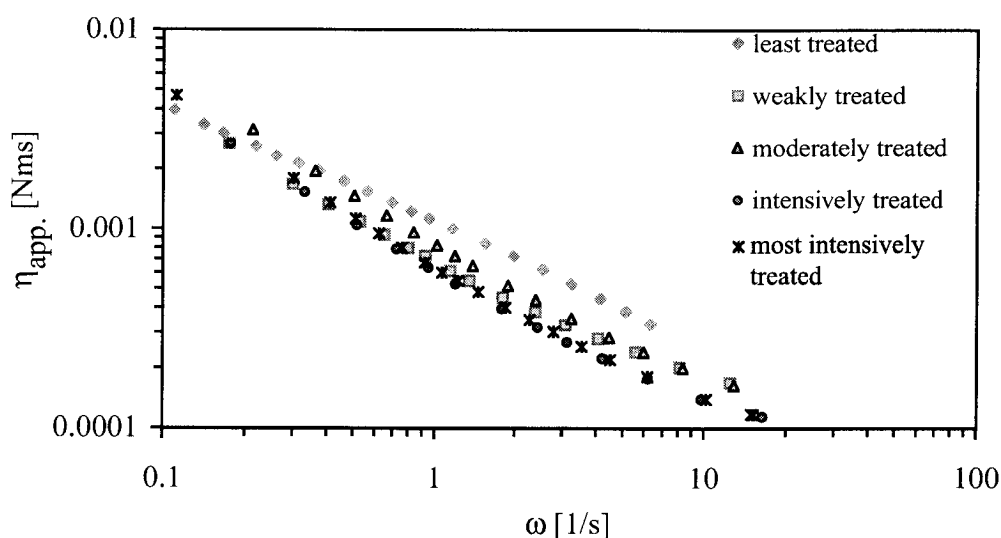
Figure 5-27 *Influence of deagglomeration on flow properties of sugar silicon oil suspensions, non controlled atmosphere, helical ribbon impeller, $c_{v,s}=33\%$ v/v, $T=30°C$, Rheometrics DSR*

In Figure 5-28 the results of that sample (prepared from stored refiner flakes) are compared qualitatively with the results shown in Figure 5-21 (prepared from fresh refiner flakes). Therefore the change of a distinct viscosity (for example at 5 1/s) is plotted qualitatively as a function of deagglomeration. The difference between the two results is obvious and can be explained as follows.

Like described in Figure 5-19 the presence of amorphous phases, the adsorption of water and the formation of agglomerates have a significant effect on the resulting flow properties. It is thought, that in case of curve 1 (corresponds to the sample prepared from fresh refiner flakes) amorphous phases were present to which water is adsorbed. During kneading the primary agglomerates were destroyed and entrapped liquid was released. The degree of deagglomeration thereby defines the amount of primary agglomerates destroyed. For low degrees of deagglomeration few primary agglomerates are destroyed and some liquid is released. In parallel the number of "free" particles has increased and thus interactions are increased. The increased interactions were compensated by the released fluid phase (reduced effective solid volume concentration) and viscosity decreased. For progressing deagglomeration the fluid released could no longer compensate for the increased interactions and viscosity increases. This is due to the fact, that recrystallization was not finished. In course of deagglomeration, agglomerates are broken up and interior surfaces are exposed to the surrounding media. If amorphous phases are present, water sorption will take place and viscosity will be increased during "deagglomeration". This is what was observed for the sample prepared from fresh

refiner flakes (curve 1). There high amounts of amorphous phases must have been present. Different to that, curve 2 corresponds to the sample that was prepared from stored refiner flakes which were most likely recrystallized when the measurements were performed. But also there a "bump" is visible, indicating that some of the particles still contained amorphous phases, but to a much smaller extent than in case of curve 1. For the sample prepared from stored refiner flakes, deagglomeration has a decreasing effect on viscosity.

Structural development with time
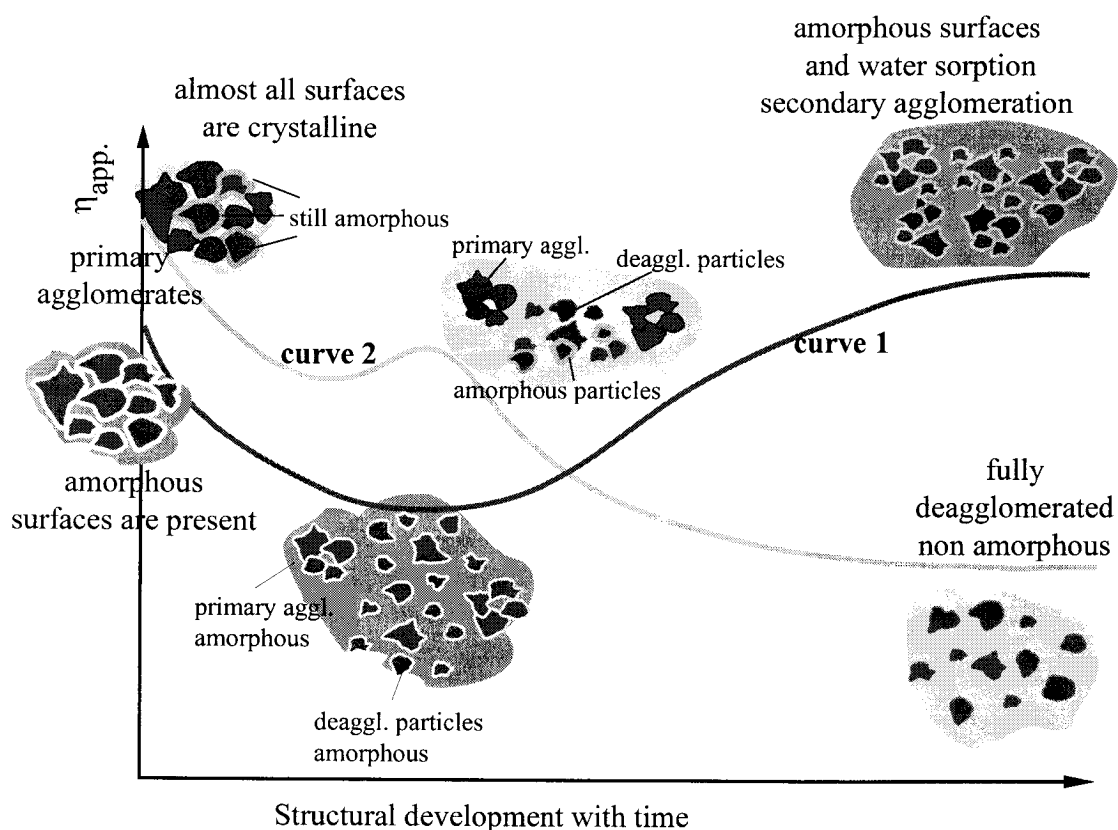
Figure 5-28 Influence of deagglomeration and structural development on viscosity

curve 1: sample prepared from fresh refiner flakes, amorphous surfaces present

curve 2: sample prepared from stored refiner flakes, almost fully recrystallized

In a last trial series all effects were taken into account in order to see the pure influence of deagglomeration on the flow behavior of sugar silicon oil suspensions. The suspensions used were prepared with a higher solid volume concentration (46%) than the ones discussed before (33%). Furthermore the rheological measurements were performed in an other rheometer using different geometries (other cup and stirrer dimensions). Consequently the flow curves can not be directly compared to the ones discussed before. In order to ensure complete recrystallization, the samples were exposed for 24h to a humid atmosphere (35°C, 70% r.h.). Prior to the rheological measurement the samples equilibrated for 24h to the atmosphere which was applied during analysis (30°C, 40% r.h.). During equilibration the samples were stirred at a constant angular velocity using a helical ribbon type of impeller (good mixing, no sedimentation). The rheological measurements were performed with a helical ribbon type

stirrer at a head space humidity of 40% r.h. and 30°C with a Bohlin rheometer. The focus here was to study the influence of small changes in agglomerate content on rheology. Therefore the agglomerate size distributions didn't deviate much from the primary particle size distribution. In Figure 5-29 the size distributions for sample A and B obtained for weak (level 2) sample treatment are shown.
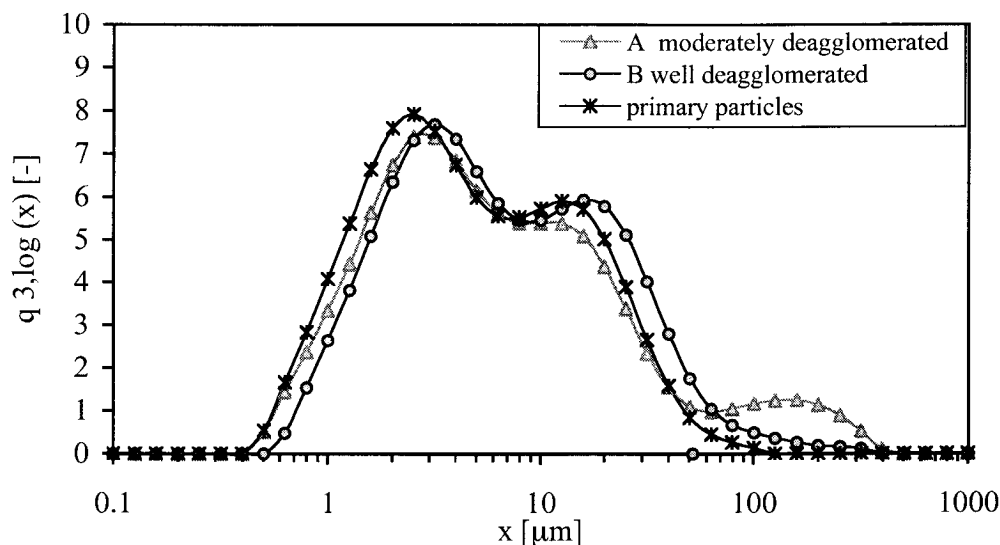
Figure 5-29 *Particle size distributions for sugar silicon oil suspensions, weak sample treatment (level 2)*
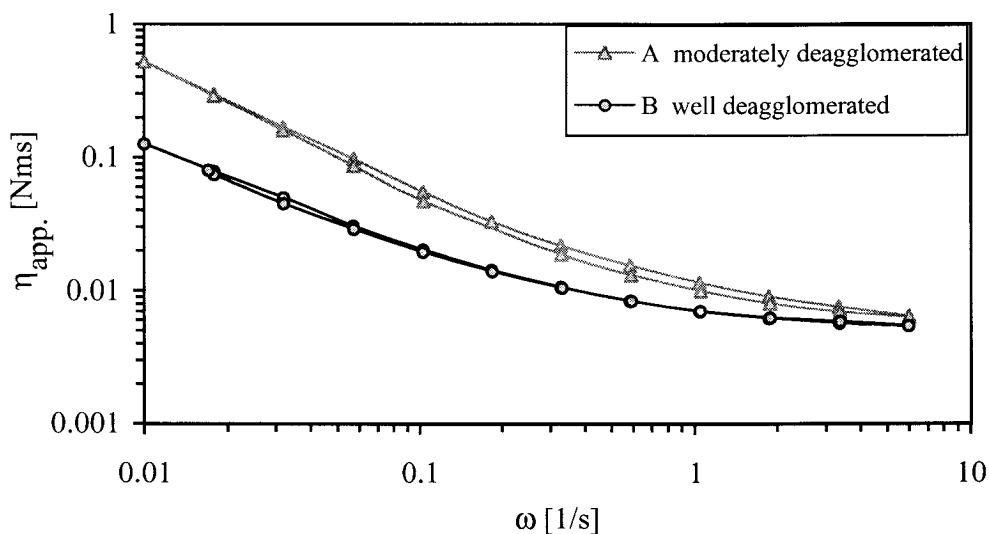
Figure 5-30 *Influence of deagglomeration on rheology of sugar silicon oil samples, Bohlin CVO, helical ribbon impeller, $c_{v,s}$=46% v/v, controlled atmosphere, 40% r.h., T=30°C*

In Figure 5-30 the corresponding flow curves are plotted. The well deagglomerated sample B shows lower viscosities than the sample A, which contains larger agglomerates. This indi-

cates that the more deagglomerated the better viscosity. This means that particle interactions are compensated by the release of fluid phase and thus viscosity is decreased. This is also expressed in the models given in Figure 5-19 and Figure 5-28.

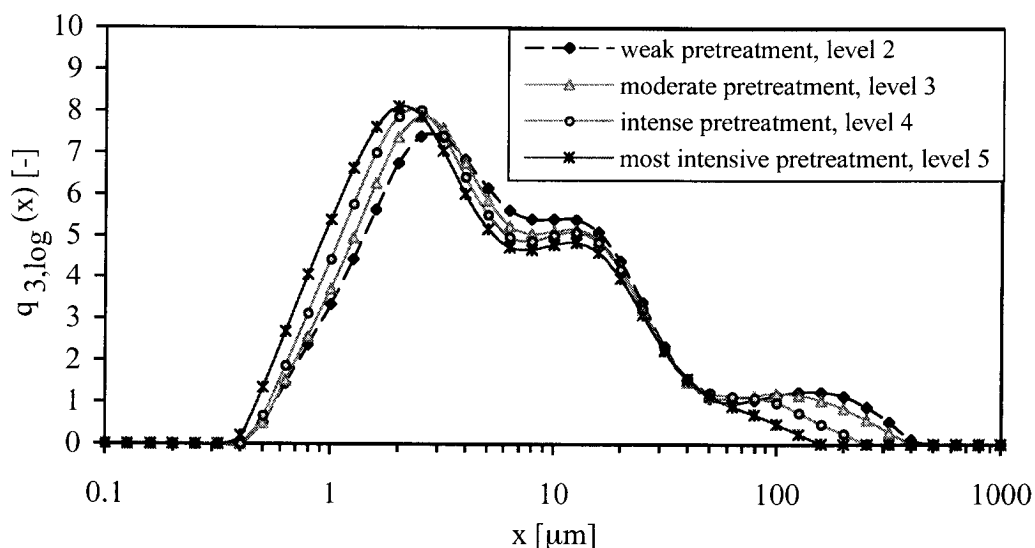To assess the stability of the agglomerates which are present in case of sample A, agglomerate stability test were performed according to the method described earlier (see See "Agglomerate Analysis" on page 39.). Figure 5-31 shows the size distributions obtained after different treatments.

Figure 5-31 Stability of agglomerates, size distributions obtained after different pre treatments

Although the intensity of the treatment was increased it was not possible to achieve complete deagglomeration. This can be seen when comparing the curves for primary particles given in Figure 5-29 and Figure 5-31. It can be concluded that the agglomerates being formed are relatively stable. This further confirms the formation of stable agglomerates based on recrystallization.

5.2.5 Summary

During refining so-called primary agglomerates, resulting from compression are formed. Furthermore the surfaces of the fractured sugar particles are present in the amorphous state. In the kneading step, deagglomeration and recrystallization has to be performed. Thereby the kinetics of deagglomeration and recrystallization are of importance. Recrystallization of insufficiently deagglomerated samples cause the formation of stable agglomerates that are bound together by solid bridges. Consequently recrystallization has to be separated from the deagglomeration step. Therefore particles have to be dispersed first and be kept in the well dispersed state whilst recrystallizing. Incomplete recrystallization increases particle interactions through water sorption. The effect of fluid release due to deagglomeration could thereby be overcompensated by the increased particle interactions and thus increases viscosity. Recrystallization of amorphous sucrose suspended in silicon oil could be monitored by controlled head space rheometry. There it was found that during humidification viscosity

first increases, reaches a maximum, decreases and finally levels off. Due to its hygroscopic nature amorphous sucrose picks up water from the ambient air which leads to an increase of difference in polarity of that system, hence increased particle interactions which gives rise to viscosity. When studying the flow behavior of sugar oil systems the effect of water sorption and amorphous-crystalline state transitions have to be taken into account.

5.3   Sugar - Cocoa butter - Lecithin - System

In the previous section a model system composed of sugar and silicon oil had been used. Moving now closer to the chocolate system, silicon oil needs to be replaced by cocoa butter and the solid volume concentration has to be increased from previously 46% to 61.3%. To obtain suspensions that still can be handled practically, it is necessary to add an emulsifier (here non standardized liquid soy lecithin). Otherwise rheological measurements could not be performed. This is due to the high viscosity of the mass and its formation of slip layers which cause inhomogenous flow or even disruption of flow.

A solid volume concentration $c_{v,s}$ of 61.3% equals a solid mass concentration $c_{m,s}$ of 72% and thus a fat content of 28% w/w which is in some cases desirable for chocolate. Compared to the sugar-silicon oil system, complexity has increased now. The continuous phase became more hydrophobic, an emulsifier was added and the solid volume concentration was increased. All these factors influence the particle interactions significantly, and thus additionally affect the flow behavior.

Similar to the preparation steps used before, the sugar was mixed with a defined quantity of cocoa butter and refined under controlled atmosphere (cold and dry, 18°C, r.h.<10%r.h) using a 3 roll lab refiner. The refiner flakes were kept under controlled atmosphere (cold and desiccator). For preparation of the suspension (deagglomeration, addition of emulsifier and cocoa butter) they were transferred to the lab kneader where kneading, liquefaction and recrystallization took place whilst a controlled head space atmosphere was applied. If not reported differently, the lecithin content of all samples used here is about 0.7% w/w. The concentration figure refers to the total quantity of lecithin used and not to the quantity of the active components, which are the phospholipids. As non standardized soy lecithin was used, the amount of acetone insoluble components is about 60% w/w.

In a first step the influence of humidity on a recrystallized and deagglomerated sample was measured.

5.3.1   Rheology - Influence of Water Sorption

In order to assess the influence of humidity on the flow behavior a sample was prepared such as recrystallization was performed during kneading. Analyzing the sample with the sorption balance revealed the crystallinity of the sample. Figure 5-32 shows the water sorption for different humidity levels applied versus time. The curve does not show any maximum, which indicates the absence of amorphous phases.

This sample was now used for determining the influence of water sorption on the rheological properties of the sugar-cocoa butter-lecithin suspension. Therefore the sample was placed in the rheometer (Bohlin CVO) and a controlled head space atmosphere was applied. The measurement was performed at a constant angular velocity of 3 1/s using a helical ribbon type geometry which ensured good mixing and prevented sedimentation.

Figure 5-33 shows the influence of different levels of humidity on the flow properties of this type of sample. In the beginning a dry atmosphere was applied and a decrease in viscosity is observed. To explain this behavior it has to be noted that prior to rheological measurement sample preparation had taken place. There the sample was kneaded in a lab kneader and exposed to a high humidity in order to allow for recrystallization. Consequently the sample has adsorbed water during this step. When placing this sample in the rheometer and exposing it to a dry atmosphere, the surrounding conditions for the sample were changed. The water
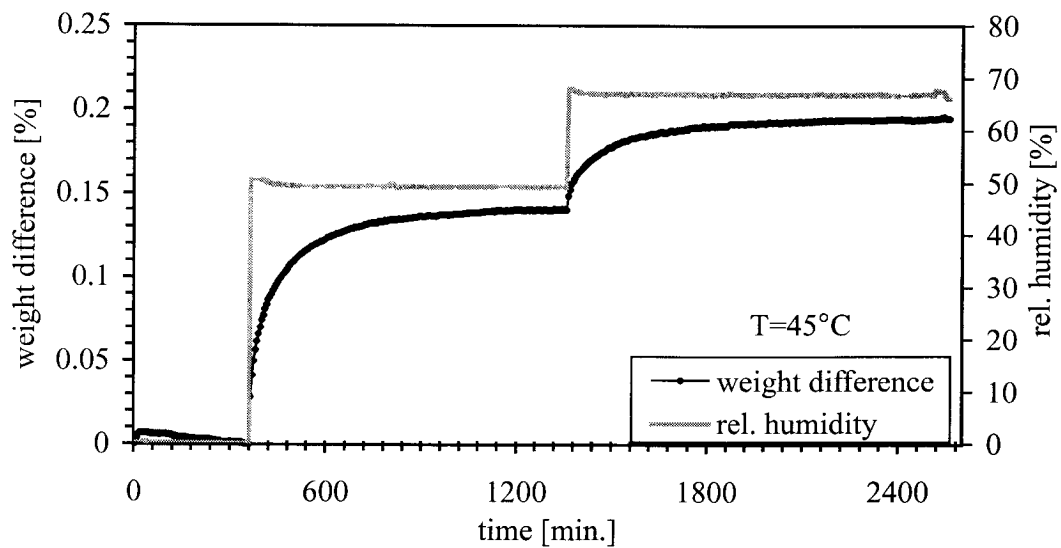
Figure 5-32 Sorption balance measurement of sugar cocoa butter lecithin sample, after kneading, T=45°C
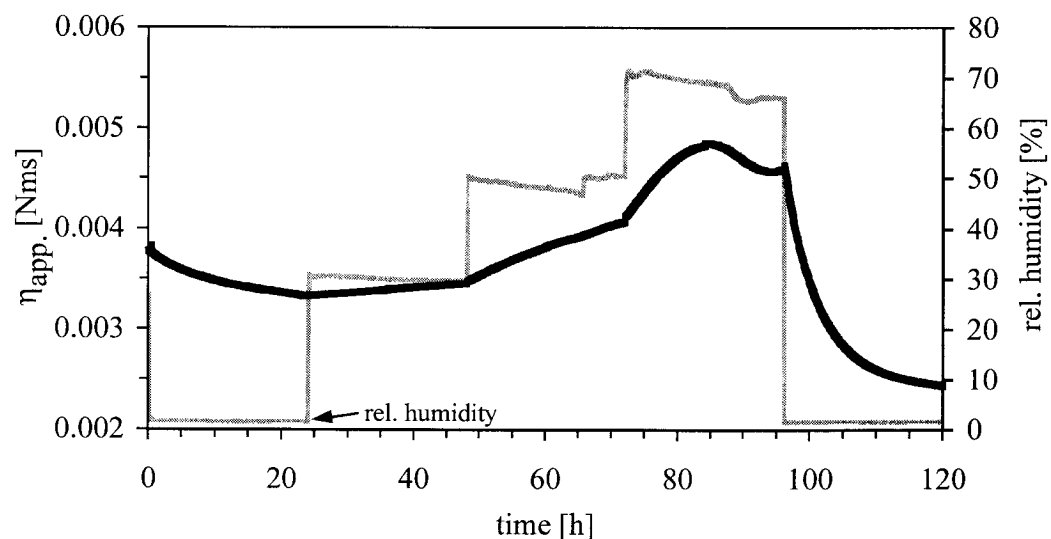
Figure 5-33 Influence of humidity on rheology of a sugar cocoa butter lecithin suspension, helical ribbon impeller, Bohlin CVO, T=40°C, constant angular velocity 3 1/s, $c_{v,s}$=61% v/v

adsorbed to the sample (during the preparation step) is released and as a consequence viscosity decreases. In course of the rheological measurement humidity is increased further up to levels of 70% r.h. It can be seen that viscosity is always increasing. For humidity levels of 70% a steep increase in viscosity is observed. Furthermore it is seen that at this humidity level (70%r.h.) humidity varies with time and as a consequence also viscosity shows some variations. When finally humidity is decreased to 2% r.h. (dry atmosphere) viscosity decreases as well but now to a level, lower than it had in the beginning. It is assumed that the sample was not fully recrystallized at the beginning. This could also explain the maximum

that is found at 70%r.h. It has to be noted that rheology is affected by the properties of the interface. Although the volume or mass of the amorphous material is rather low, the presence of a thin layer at the surface is sufficient to influence flow properties. As the amount of amorphous material involved is rather small, it is hardly detected by the sorption balance (gravimetric method).

Another way to illustrate the effect of humidity and water sorption on the structure of a sugar cocoa butter suspension is by visual observation of the sample during kneading and humidification.

In Figure 5-34 pictures of the sample taken at different levels of humidity are shown. The sample had been recrystallized prior to these series. The sample was placed in the lab kneader and different levels of humidity were applied during kneading. Figure 5-34-a shows the structure of the sample after it had been exposed to a humidity of 3% r.h. for 30min. The sample appears smooth in texture and exhibits a thin paste like structure. Figure 5-34-b and Figure 5-34-c show the sample after it was exposed for 15min. to a humidity of 50% and 62%. It can be seen that structure has changed completely. The sample appears now more sticky and disruption of flow is observed. When increasing the humidity to 70% (Figure 5-34-d) the sample becomes crumbly and is no longer pulled between the kneading arms. It builds up a bridge above the kneading elements. Increasing humidity up to 90% (Figure 5-34-e) reveals a texture that is pulled in again. It is still crumbly but has softened compared to the sample that was exposed to 70%. Decreasing humidity down to 3% the soft, thin paste like structure is obtained again. This cycle was continued several times and always the same results were found.

These structural changes as a function of water sorption can be explained by the formation of liquid bridges and the build up of agglomerates. The stability of these agglomerates thereby depend upon the degree of saturation which was shown by Schubert and Rumpf (*Schubert, H. (1973), Rumpf, H. (1974)*). For dry conditions no water is adsorbed and no liquid bridges are formed. Consequently no agglomerates are present which would disturb continuity of flow. Applying humid conditions water is adsorbed which is not miscible with the oil phase and thereby forms a third phase. The water is adsorbed to the sugar particles. In contact zones between the particles capillary condensation occurs and liquid bridges are formed. Increasing levels of humidity gives rise to further adsorption and condensation. Finally all particles are surrounded by water and can easily move in their water capsulate. At these high levels of saturation (>0.8) the strength of the agglomerates decreases and the texture becomes softer again.

a; 3%r.h. 40°C

b; 50%r.h. 40°C

c; 62%r.h. 40°C

d; 70%r.h. 40°C

e; 90%r.h. 40°C
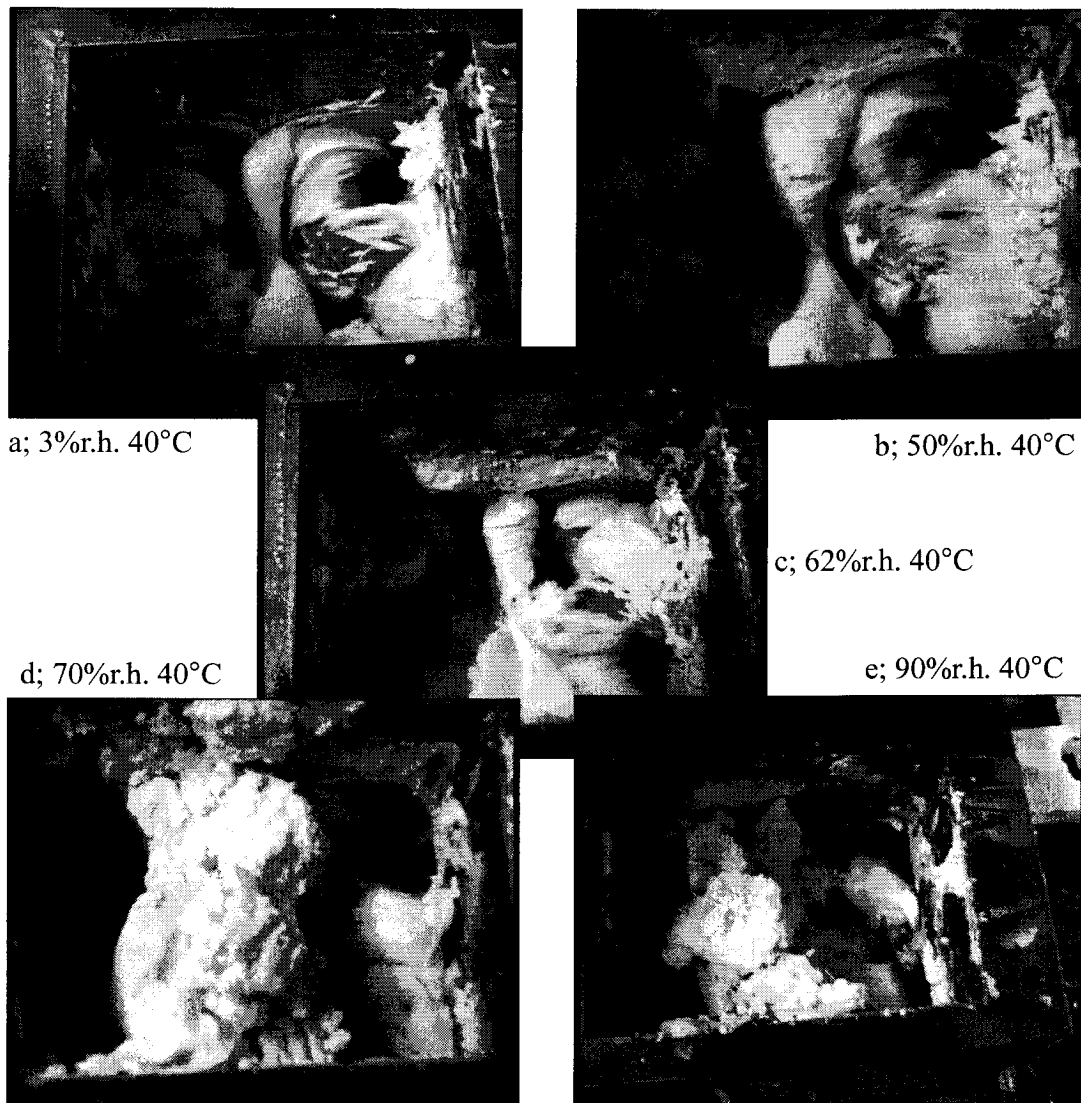
Figure 5-34 Structural changes during kneading and humidification, relative humidity varied between 3% and 90%, mixture of sugar and cocoa butter, $c_{v,s}=62\%$, without addition of emulsifier.

5.3.2   Rheology - Influence of Deagglomeration

Like in the previous sections also for this system the influence of deagglomeration is of interest especially as it represents a model system for chocolate. Furthermore in this system the solid volume concentration is rather high and thus small changes in free liquid phase or in the effective solid volume concentration have a significant effect on the flow behavior (*Farris, R.J. (1968), Chong, J.S., Christiansen, E.B., Baer, A.D. (1971), Chang, C., Powell, R.L. (1994)*).

In order to minimize the influence of water sorption when performing rheological measurements a dry atmosphere (2.5%r.h.) was applied during measurement. Prior to all rheological measurements the samples had to equilibrate first. Therefore they were exposed for a time of 24h to a head space humidity of 2.5%. During this time the sample was stirred at a constant angular velocity and the change in viscosity was recorded over time and thus revealed whether or not an equilibrium had been reached. In all cases measurements were only performed after such an equilibrium was reached.

In a first trial series the flakes obtained from refining had been exposed to an atmosphere of 70% r.h. and 40 °C for 5 days to ensure recrystallization. As recrystallization occurred in the state of rest, fairly hard and big agglomerates were present in the refiner flakes. The so prepared flakes were then kneaded in a lab kneader. Different levels of mechanical energy/power were applied to the sample in order to achieve different degrees of deagglomeration.

Figure 5-35 shows the particle size distributions of samples that have been treated with different mechanical power/energy input. The size distribution were measured after the weakest pretreatment was applied (level 2). For reasons of comparison the size distribution of the primary particles is given as well (obtained after level 5 treatment, most intense pretreatment). Between the samples there is only little difference in terms of agglomerates' size and quantity.
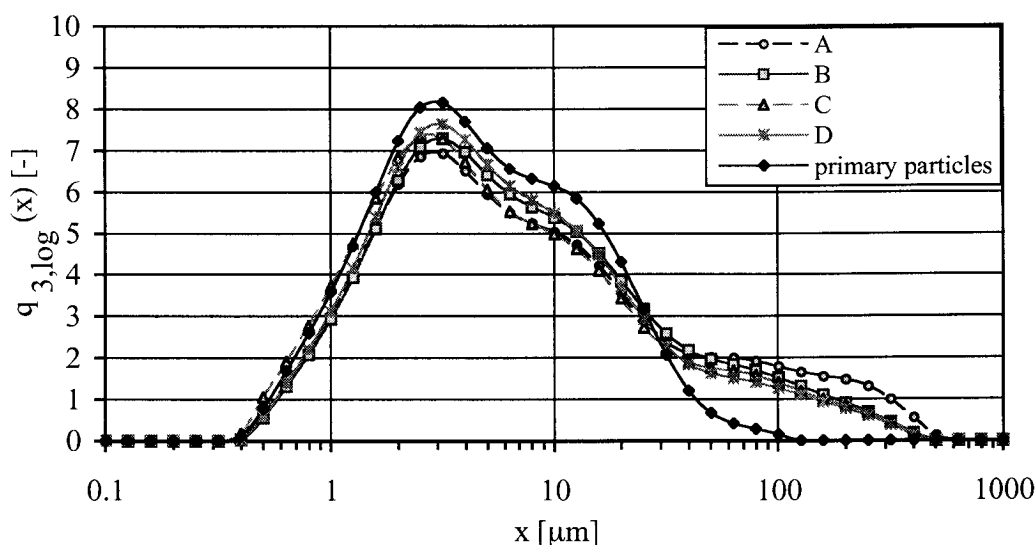
Figure 5-35 Agglomerate size of differently kneaded samples, sugar cocoa butter lecithin, measured by laser diffraction, obtained after lowest level pretreatment (level 2)

In order to discuss this, the power and energy input applied to the samples during kneading are given in Figure 5-36. It can be seen that the samples have experienced low power and high power input. Also energy input was varied through the time of processing. Although the samples had experienced different power and energy input only negligible difference in agglomerate size and content was found. This indicates that the stresses which acted during kneading were not sufficient to destroy the agglomerates. Taking into account that recrystallization took place in the flake like state and thus in the state of rest it can be concluded that the particles formed agglomerates that are bound together through solidified bridges. Such strong agglomerates can be hardly destroyed in a kneading process like it was used here.
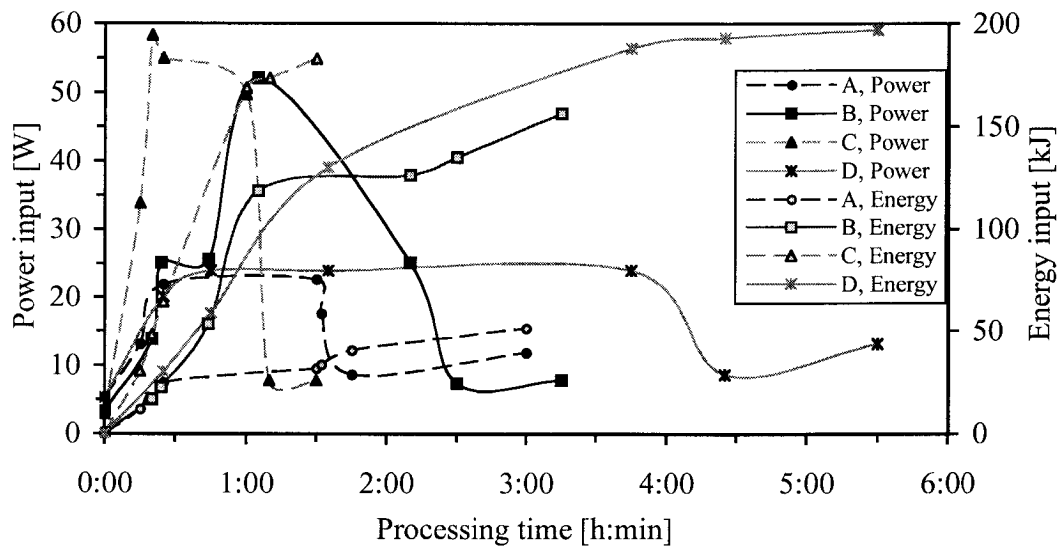
Figure 5-36 *Energy and power input during the kneading step, refiner flakes had been recrystallized in the flaky state prior to kneading, sugar cocoa butter lecithin, $c_{v,s}$=61%*

Looking at the flow curves of these samples, see Figure 5-37, only the sample that was least kneaded and consequently had bigger and more agglomerates (sample A) than the others also shows the highest viscosity. All other samples can be considered equal. This demonstrates that no other factors than agglomerate content and size are involved. As all samples had been prepared from the same batch of refiner flakes, it illustrates also the repeatability of the suspension preparation step (kneading, dosing), and of the measuring step.
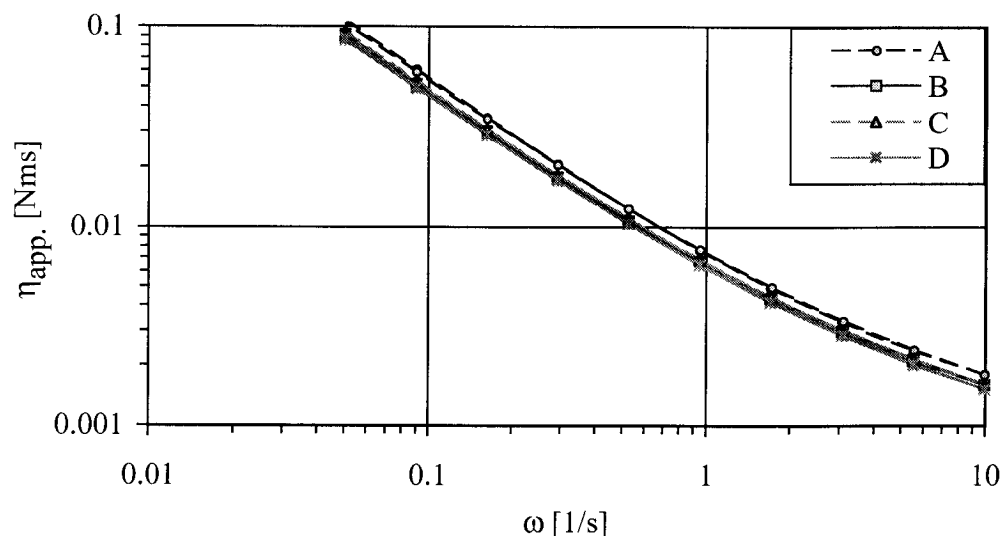
Figure 5-37 *Flow curves of samples prepared with recrystallized refiner flakes, sugar cocoa butter lecithin, Bohlin rheometer, T= 40°C, helical ribbon impeller*

In a second trial series samples were deagglomerated more differently to see the effect of deagglomeration better. Therefore amorphous refiner flakes were used for kneading. Through varying the kneading conditions (kneading time, kneading intensity and time when humid atmosphere is applied) different degrees of deagglomeration as well as complete recrystallization could be achieved. Also all sample were checked for crystallinity in the sorption balance. Analysis of the size distribution, see Figure 5-38, revealed that the samples were significantly different in agglomerate size and content (measuring size distribution after level 2 pretreatment, see Section 4.1.2.1).
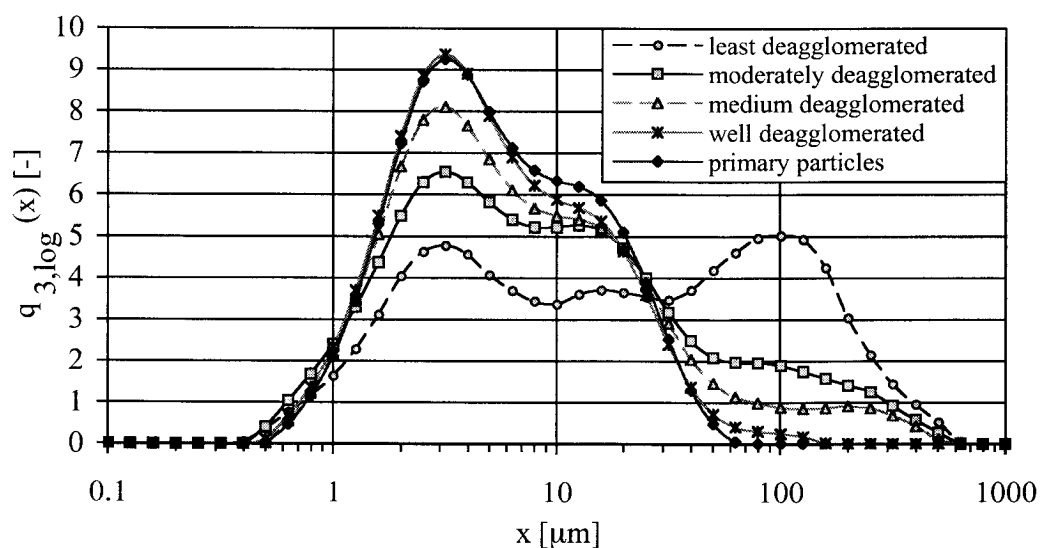
Figure 5-38 *Agglomerate size distribution, level 2 pretreatment, sugar cocoa butter lecithin*

The resulting flow properties are illustrated in Figure 5-39. It can be seen that the better the deagglomeration, the lower viscosity. Deagglomeration effects rheology now in the same way like for the limestone silicon oil system. Its viscosity decreasing effect is attributed to the release of immobilized liquid phase and is no longer compensated by increased particle interactions (compare to Figure 5-21 on page 78).
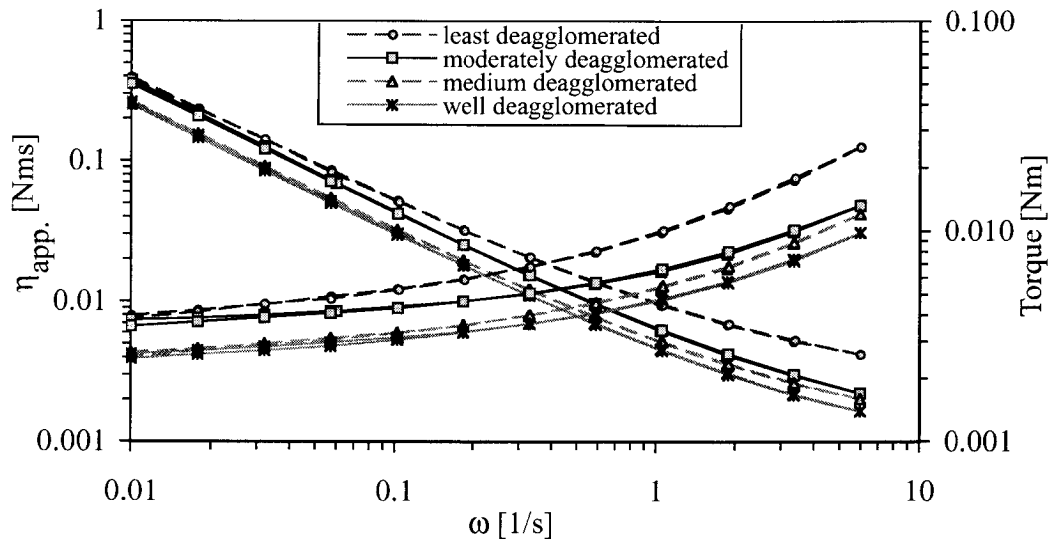
Figure 5-39 *Influence of deagglomeration on flow properties, sugar was recrystallized during kneading in lab kneader, measured with helical ribbon impeller, rate controlled mode, Bohlin rheometer, T=40°C*

Looking at the differently deagglomerated samples, it appears that for big reductions in agglomerate size also the viscosity is reduced significantly. Going more towards a fully deagglomerated sample, relative reduction of viscosity decreases. In the "structural" domain (low angular velocity) viscosity reduction is less pronounced than in the "hydrodynamic" domain. In the hydrodynamic domain the flow behavior is mainly determined by the effective volume concentration which explains why the influence of deagglomeration is higher there.

In addition to the release of fluid phase also the effect of changing the free interfacial area needs to be discussed. In case of deagglomeration, the contact points between the particles become accessible to emulsifier molecules. This can have an effect on the amount of emulsifier adsorbed to the interfaces. Therefore the effect of emulsifier concentration on the flow behavior was investigated.

5.3.3 Rheology - Influence of Lecithin Concentration

The amount of emulsifier added is key for the rheological properties of this type of suspennions. In the past sugar - cocoa butter suspension had been subject of investigations, where different factors and their influence on flow properties of lower concentrated suspension were analyzed (*Finke, A. (1991)*, *Tscheuschner, H.D. (1993b)*).

When working with higher solid volume concentrations emulsifiers need to be added to obtain a flowable texture. This requires to determine the influence of emulsifier concentration. Therefore a well deagglomerated and recrystallized sample was used. The agglomerate and primary size distribution of the sample used is given in Figure 5-40.
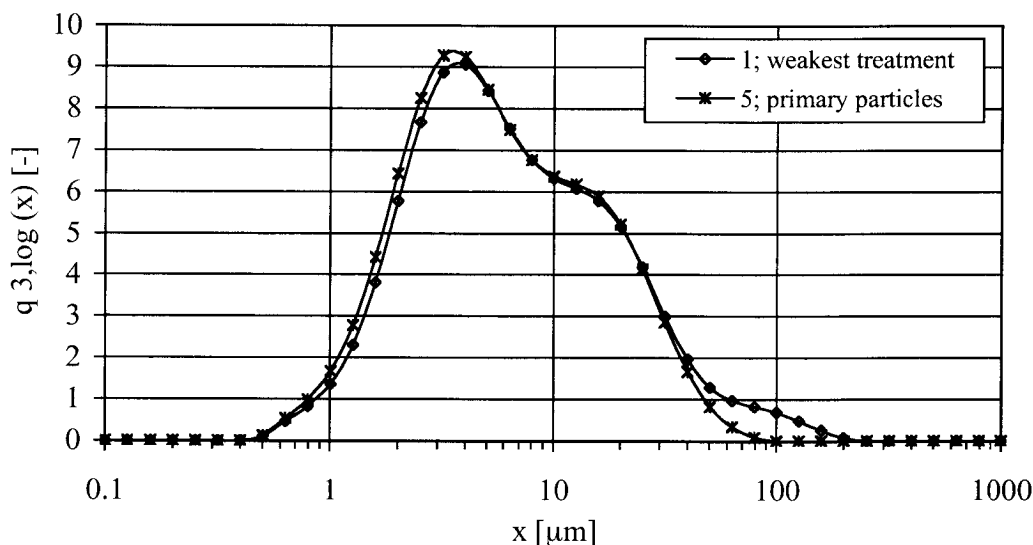
Figure 5-40 Agglomerate and primary size distribution of the sample used for assessing the influence of emulsifier concentration on flow properties, sugar cocoa butter lecithin

The sample was placed in the rheometer and measurements were performed using a helical ribbon type impeller. In the course of rheological measurement different amounts of lecithin were added to the sample, and due to the good mixing properties of the stirrer geometry, effect on rheology could be observed online. In Figure 5-41 the evolution of viscosity over time is plotted. The starting sample used here did already contain 0.5% lecithin and further lecithin was added step wise till a final content of 1.5% w/w was reached. The rapid increase of viscosity is thereby governed by two kinetics:

• the kinetic of mixing and homogenizing

• the kinetic of emulsifier adsorption/desorption

Looking at the evolution of viscosity it can be concluded that the system reaches a new equilibrium within a time of 30 min. Having reached the new equilibrium, flow curves were measured which are plotted in Figure 5-42.

Starting off with a sample containing 0.3% and adding lecithin step wise up to a concentration of 1.5% causes an increase of viscosity. For concentrations higher than 0.3% the desired effect of viscosity reduction is not observed. The reason for increasing viscosity is that lecithin is obviously available in excess and thus forms micelles in the continuos phase which gives rise to viscosity. To finally prove this, emulsifier sorption measurements need to be performed which would deliver the sorption isotherm for this type of lecithin.

These findings will now be related to the effect of deagglomeration. Deagglomeration increases the free surface area. Lecithin would be able to adsorb to those newly formed "free
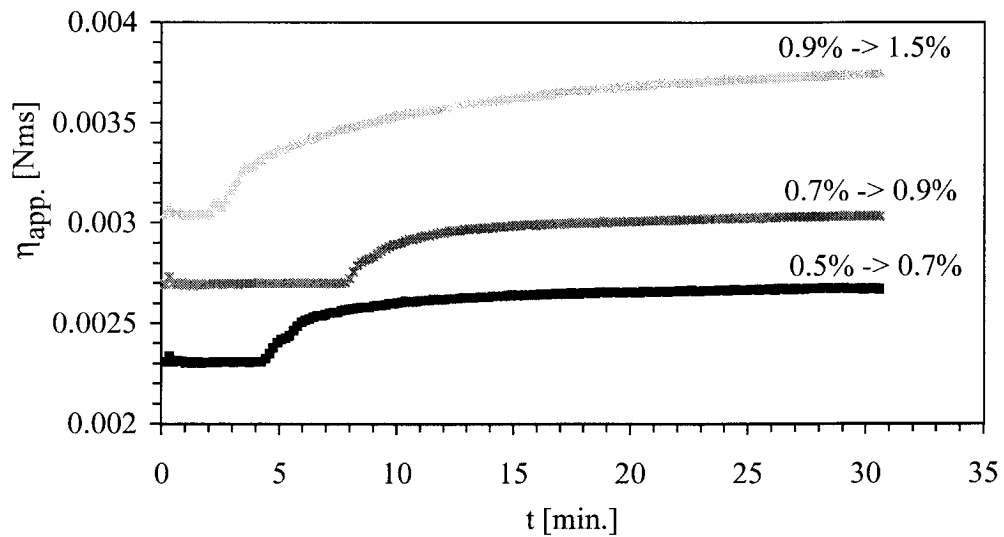
Figure 5-41 *Effect of lecithin addition on viscosity, observation versus time, sugar cocoa utter lecithin, Bohlin rheometer, T=40°C, helical ribbon impeller, $c_{v,s}$=61%, 2.5%r.h.*
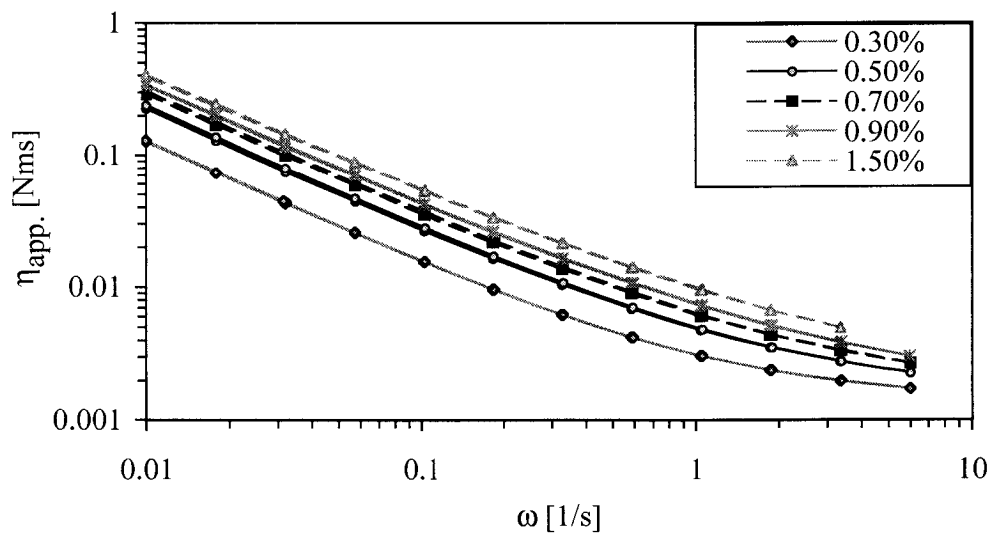
Figure 5-42 *Effect of lecithin addition on flow behavior of a well deagglomerated sample, sugar cocoa butter lecithin, Bohlin rheometer, T=40°C, helical ribbon impeller, $c_{v,s}$=61%, 2.5%r.h.*

surfaces". Consequently the excess lecithin concentration would decrease hence viscosity would decrease. This is illustrated schematically in Figure 5-43.

At first the principle relationship between viscosity and lecithin concentration is discussed. For small quantities (<0.2% w/w) viscosity decreases considerably. For increasing lecithin concentration, a minimum in viscosity is reached. For higher lecithin concentrations, viscosity increases. This is due to the fact that at higher concentrations, emulsifier is available in excess. Looking at the relationship between surface area and degree of deagglomeration, it
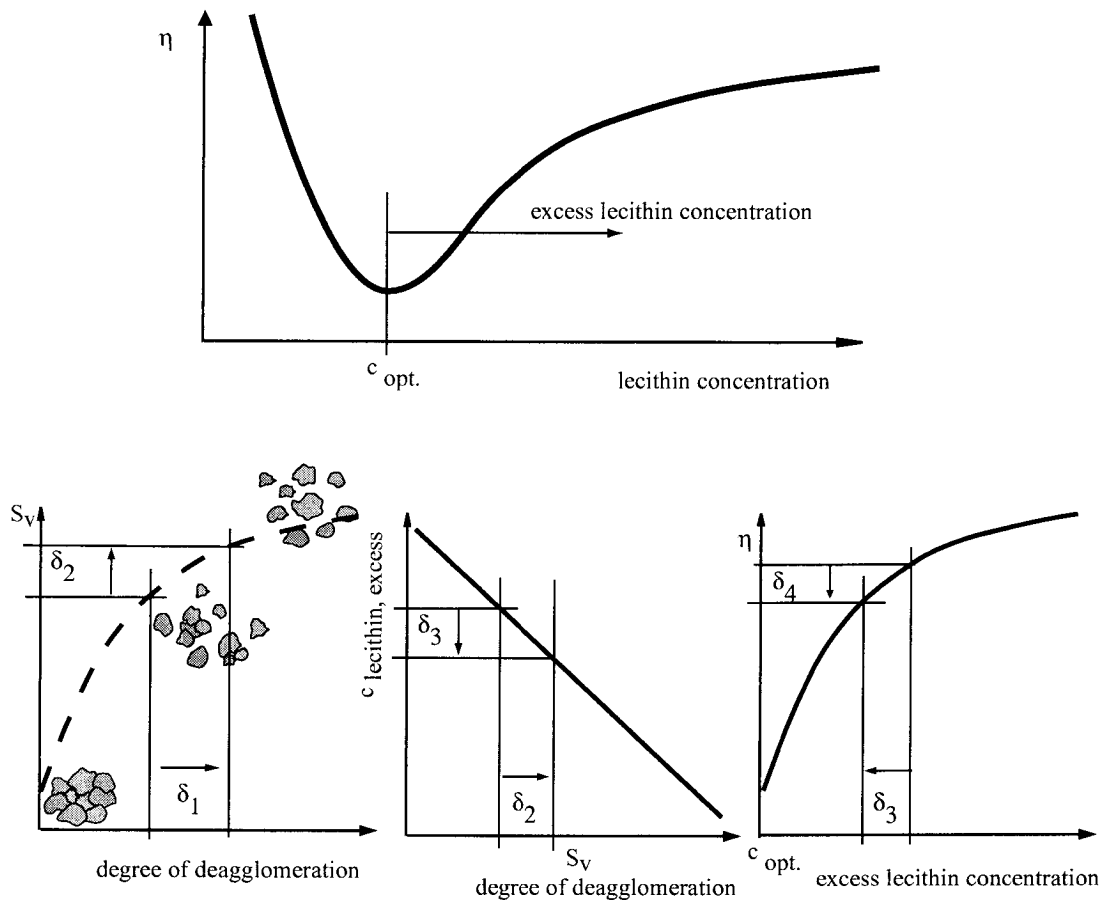
Figure 5-43 *Interactions between lecithin concentration and rheology, influence of change in free surface during deagglomeration and its impact on excess lecithin concentration and rheology*

it obvious that for increasing deagglomeration, surface is increasing as well. A change in degree of deagglomeration of δ_1 will thereby increase surface by δ_2.

Considering the relationship between excess concentration of lecithin and surface area, it is seen that for a given total lecithin concentration the excess concentration will decrease proportionally to the increase of surface area. If surface area is increased by δ_2 the excess concentration is reduced by δ_3.

In the last graph viscosity as a function of excess concentration is shown. If the excess concentration is reduced by δ_3, viscosity is reduced by δ_4. This shows that better deagglomeration (increase by δ_1) can also reduce viscosity which is due to the decrease of excess lecithin concentration. To be able to judge on the influence a reduction of excess concentration has on rheology, some calculations were made. Therefore the different values for δ_1 to δ_4 were calculated.

In order to estimate the amount of free surfaces generated during deagglomeration, the specific surface area as calculated by the laser diffraction device (Malvern 2000) is considered. It is known that this gives not the exact surface area, but is regarded as sufficient for an estimative calculation. Table 5-1 gives the specific surface area of the differently deagglomer-

ated samples. The specific surface area was calculated for the samples after they had been exposed to the lowest level pretreatment (level 2). This state is considered to be the one, which most likely corresponds to the size distribution that is present in course of rheological measurement hence "is seen by the rheometer".

Table 5-1 *Specific surface area as obtained by laser diffraction measurement for differently deagglomerated samples, level 2 pretreatment*

Degree of deagglomeration	specific surface area m²/g as given by Malvern
least	1.5
moderately	1.71
medium	1.75
well	1.94
primary particles	1.95

Like shown in Figure 5-39 deagglomeration yields a decrease of viscosity. In order to correlate degree of deagglomeration and viscosity, a measure for the degree of deagglomeration is required. Deagglomeration changes the size distribution of the particles. The width of the distribution expresses the amount of coarse particles and thus of the agglomerates. Relating the width of an agglomerate containing distribution to the width of the primary particles' size distribution will give an integral measure for the degree of deagglomeration (ψ). The width of the distribution is thereby expressed by the difference between the $X_{95,3}$ and $X_{5,3}$ value.

$$\psi = \frac{(X_{95,3} - X_{5,3})_{\text{primary particles}}}{(X_{95,3} - X_{95,3})_{\text{agglomerate containing}}} \qquad (\psi \le 1) \qquad (5.3)$$

Along with agglomerate size and content the specific surface area changes. Also for this value a relative number (S_{rel}) can be calculated as follows.

$$S_{rel} = \frac{(S_{sample} - S_{least})}{S_{least}} \qquad (5.4)$$

S_{least} is the surface are of the least deagglomerated sample whereas S_{sample} is the surface area of the sample looked at. Therefore this gives a measure of how surface area is increasing during deagglomeration.

In order to assess the rheological changes, a relative viscosity (η_{rel}) for the differently deagglomerated samples is calculated. Therefore the apparent viscosity of the sample looked at (η_{sample}) is taken at an angular velocity of 1 1/s (could be any other velocity as well) and related to the apparent viscosity (at 1 1/s) of the least deagglomerated sample (η_{least}).

$$\eta_{rel} = \frac{\eta_{sample}}{\eta_{least}} \qquad (5.5)$$

Figure 5-44 gives the correlation between degree of deagglomeration, relative viscosity and relative changes of specific surface area. It can be seen that in course of deagglomeration viscosity is reduced by half although specific surface area is increased by 30%. The data are based on the sample shown in Figure 5-39.
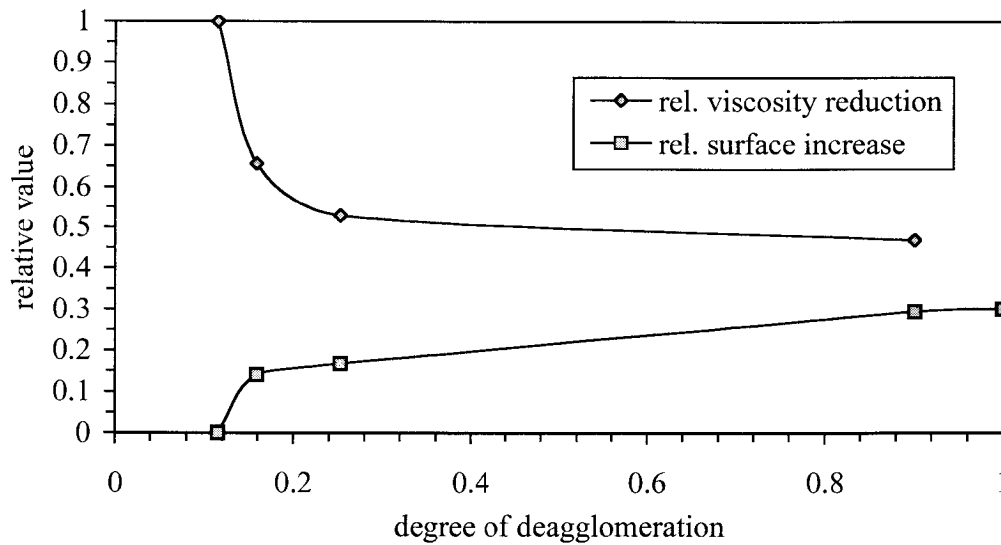
Figure 5-44 *Correlation between degree of deagglomeration, relative viscosity and relative changes of specific surface area*

In order to link deagglomeration and its effect on viscosity to the changes in excess emulsifier concentration, the influence of emulsifier concentration needs to be taken into account. The increased surface area will decrease the excess emulsifier concentration. The relationship between emulsifier concentration and relative viscosity is given in Figure 5-45.
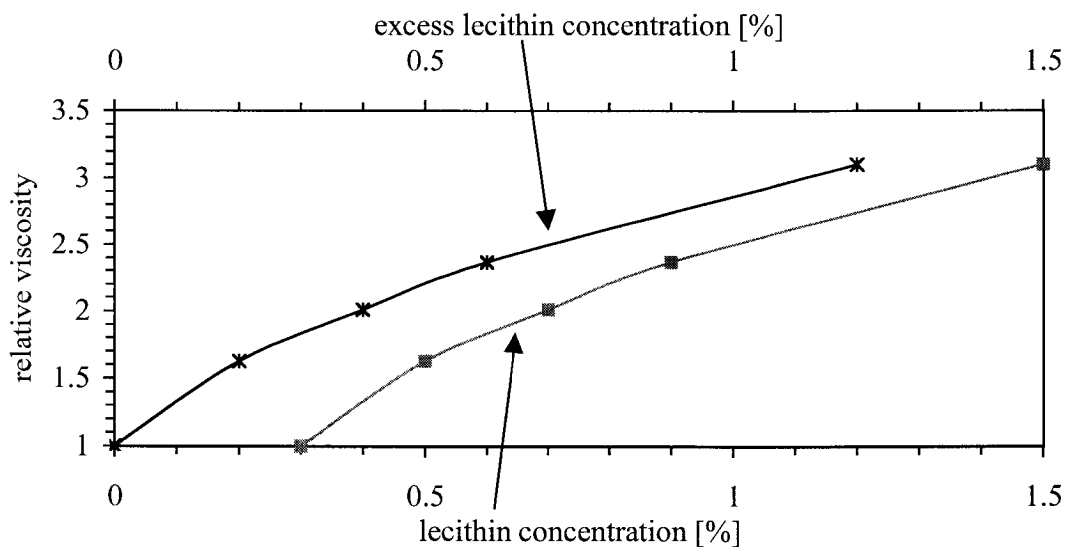
Figure 5-45 *Relative viscosity in relation to emulsifier concentration and excess emulsifier concentration*

Here relative viscosity is calculated as the ratio between the apparent viscosity at 1 l/s to the apparent viscosity of the sample with the optimum (here: lowest) lecithin concentration. These data were derived from the measurement shown in Figure 5-42.

$$\eta_{rel} = \frac{\eta_{app. \ (1 \ 1/s)}}{\eta_{app. \ (1 \ 1/s, \ optimum)}} \tag{5.6}$$

The excess lecithin concentration was calculated as the difference between the actual lecithin concentration and the optimum lecithin concentration. In a preliminary approach and in absence of other data the optimum lecithin concentration was here set to the lowest lecithin concentration used. The optimum lecithin concentration is expected to be between 0.2% and 0.3%, which is also confirmed by literature (*Finke, A. (1991)*). From the optimum lecithin concentration and the corresponding surface area, an specific surface coverage can be calculated. Therefore it is necessary to know the amount of surface active components that are present in the lecithin. In a first approach the amount of acetone insoluble components is taken as the value which correlates with the amount of surfactants that are present in the lecithin. The lecithin used has an approximate surfactants content of 60%w/w (acetone insoluble components). An optimum lecithin concentration of 0.3% would then correspond to a surfactants concentration of 0.3% * 0.6 which equals 0.18% of surfactants. The surface area of the sample used for the lecithin concentration series is about 1.95 m²/g. Hence, the specific surface coverage is calculated as 0.18 g surfactants/100g substance related to an area of 195 m² per 100g solids. As a solid content of 72% w/w was used the surface area in 100g substance is 195m²/100g solids * 72 g solids per100g substance and the coverage θ then is calculated to

$$\theta = \frac{0.18g \cdot 100g}{195m^2 \cdot 100g \cdot 0.72} = 1.28 \times 10^{-3} \frac{g}{m^2} \tag{5.7}$$

Linking this to the effect of deagglomeration, it is seen that in case of the least deagglomerated sample the specific surface area has decreased compared to the well deagglomerated sample. The corresponding optimum concentrations are thereby calculated as follows.

The least deagglomerated sample has a specific surface area of 1.5m²/g (see Table 5-1). With the above given figures on θ, surfactants concentration, and solids content, an optimum lecithin concentration for the least deagglomerated sample can be calculated. The calculated value is 0.23% w/w.

$$c_{opt} = \theta \cdot 150\frac{m^2}{100g} \cdot 0.72 \cdot \frac{1}{0.6} \tag{5.8}$$

With this value, the excess lecithin concentration can be calculated for the least deagglomerated sample. The excess lecithin concentration in this case would be 0.47%. This is calculated from the lecithin concentration that is used in the test (0.7%) reduced by the optimum concentration (0.23%) which equals 0.47%.

For the well deagglomerated sample the excess lecithin concentration is calculated accordingly and is found to be 0.4% (0.7%-0.3%).

From Figure 5-45 it is seen that a decrease in excess lecithin concentration from 0.47% to 0.4% yields a decrease in relative viscosity from 2.2 to 2 and thus decreases viscosity by 9%.

This shows that the decrease in viscosity observed during deagglomeration can not be solely attributed to the change in excess lecithin concentration but is to a large extent attributed to the release of immobilized liquid phase. It can also be concluded that once some deagglomeration is achieved, further changes in deagglomeration do not greatly influence viscosity

(see Figure 5-44). Whereas small quantities of emulsifier significantly affect viscosity (see Figure 5-45). This again proves that this system is mainly dominated by particle interactions.

5.3.4   Summary

Sugar as the disperse phase in a highly concentrated suspension of sugar cocoa butter and lecithin is the hydrophilic component in this lipophilic - hydrophilic system. The sorption of water increases the difference in polarity and gives rise to particle interactions which causes an increase of viscosity. Deagglomeration first decreases viscosity which then levels off for higher degrees of deagglomeration. Lecithin as a surface active component has its optimum concentration below 0.3%. In other studies performed with lower concentrated suspensions (*Finke, A. (1991)*) an optimum value of 0.2% was reported. Working at a lecithin concentration of 0.7%, means working under conditions where viscosity is increased compared to the optimum case, hence emulsifier is available in excess. Deagglomeration goes together with an increase of surface, hence reduces the excess lecithin concentration which leads to a decrease of viscosity. At the same time, a plateau for the relationship between viscosity and deagglomeration is approached. This indicates that both changes, reduction of excess lecithin concentration and release of immobilized liquid phase, are too minor in effect to have a great influence on rheology. Furthermore this shows that a limit is reached which can only be exceeded, if the particle interactions are reduced (emulsifier concentration, type of emulsifier). Other influencing factors such as sterical or mechanical factors like particle size, -shape, -morphology seem to play a less important role.

5.4 Comparison of Agglomerate Stability and Factors of Influence

In this section the various systems looked at so far will be compared to each other and differences will be discussed.

The systems that had been investigated, are composed of particles that are smaller than 100μm. Particle of such size can be either obtained from size reduction processes (grinding) or size building steps (e.g. crystallization). The process looked at here is grinding. It represents the process that is used within this part of the food industry. Grinding can be performed in many ways. Depending on the type of grinding machine and the characteristics of the product, different effects can be observed (*Rumpf, H. (1962)*). Roll refiners are commonly used in chocolate production. In that type of machine, size reduction takes place due to large compression forces and shear forces (*Niediek, E.A. (1972)*, *Niediek, E.A. (1975)*).

When fracturing the fractured pieces of the particle are in contact with other particles. They are pressed together (compressive forces) which causes agglomeration (*Schütz, W., Schubert, H. (1976)*, *Dahneke, B. (1972)*, *Rumpf, H. (1974)*, *Rumpf, H. et al. (1976)*). The agglomerates formed here are called primary agglomerates and result from press agglomeration.

Size reduction performed with this type of machinery is automatically linked to agglomeration (*Niediek, E.A. (1972)*, *Von der Ohe, W. (1967)*). Therefore in a second step deagglomeration needs to take place. Deagglomeration in this sense now refers to deagglomeration of the primary agglomerates, but as effects like recrystallization take place, primary agglomerates can change to secondary agglomerates which are obtained from recrystallization. Those are much more stable and harder to destroy. Having managed to deagglomerate completely, the primary particles need to be stabilized to avoid tertiary agglomeration, resulting from reduction of free surface energy. This can be achieved through reducing the difference in polarity of the system, hence influencing the attractive interactions by changing the properties of the interfaces through addition of surfactants.

To deagglomerate effectively, the stability of the agglomerates needs to be known. To obtain data about the stability of the agglomerates a method was developed and applied as described in 4.1 "Agglomerate Analysis" on page 39. There different stress levels were applied to the sample in course of sample preparation. The lowest stress level is thereby represented by the so called level 2 pretreatment; the highest stress level, which is supposed to reveal the size distribution of the primary particles is called level 5 pretreatment.

Starting off with a refined limestone silicon oil system it can be assumed that agglomerates being present are purely of primary nature, i.e. result from the refining process. For a sample (was shown in Figure 5-6 on page 64 in a different context) that had been weakly deagglomerated during kneading, the following size distributions were obtained. The sample was treated at different stress levels (see Figure 5-46). Curves 1 to 3 correspond to purely mechanical stresses applied to the sample. Curve 1 represents level 2 treatment whereas curve 2 and 3 were obtained, after the sample was circulating in the dispersing unit of the laser diffraction device for 1 min. and 10 min. with maximum stirrer speed. This leads already to a significant break down of agglomerates. Application of ultrasound with half of its maximum power input, caused complete disruption of the agglomerates (curve 4). Increase of sonication power and time (curve 5) did not lead to any further reduction in size, hence all agglomerates were destroyed.
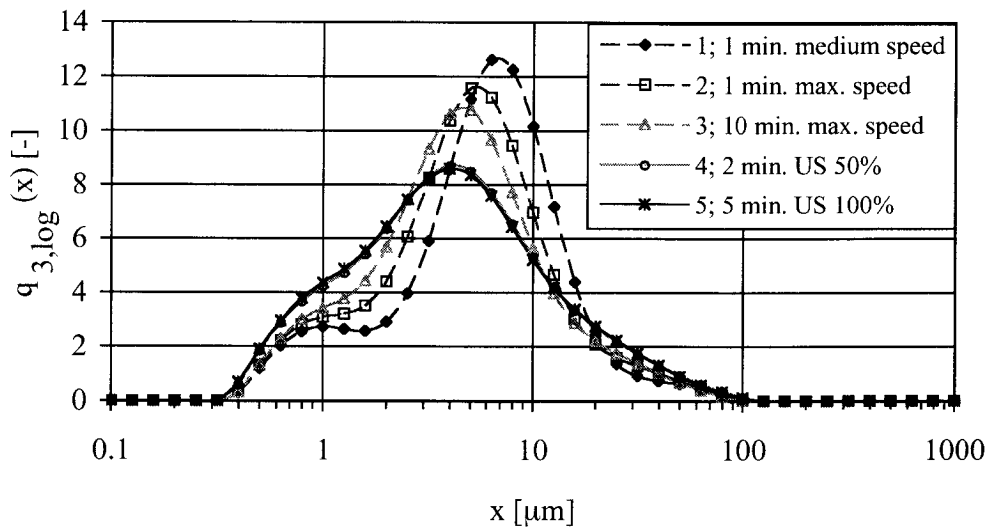
Figure 5-46 *Stability of agglomerates for the limestone silicon oil system*

In the following a sample that is composed of sugar and silicon oil is considered. It had been also refined and kneaded but the size distribution shows significant differences to the before mentioned limestone silicon oil sample (the sugar silicon oil sample corresponds to the sample taken at position I when the effect of state transition was discussed in 5.2.1 "Influence of State Transitions (Amorphous - Crystalline)" on page 69).
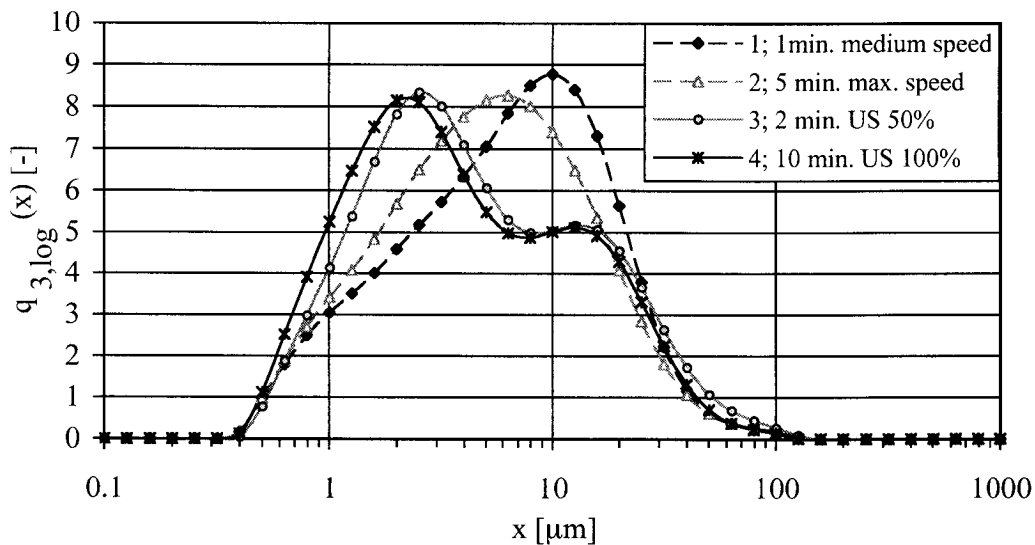
Figure 5-47 *Stability of agglomerates for the sugar silicon oil system, sugar contains amorphous surfaces, i.e. is not recrystallized yet*

In Figure 5-47 the size distributions of the differently treated sugar silicon oil samples are given. In order to see the effect of material characteristics on the grinding behavior, the primary particle size distributions for limestone (curve 5, Figure 5-46) and sugar (curve 4, Figure 5-47) are compared. For this comparison the different shape of the size distribution

curves become evident. This already indicates a difference in the break down behavior. It shows for sugar a bimodal distribution. One part of the distribution covers the fine particles with a mode diameter of 2μm and a second part of the distribution represents the coarse fraction with a mode of 15μm. Also limestone shows this bimodality but only for the weakly treated samples, which are composed of agglomerates and primary particles. The primary particles do not show such a clear bimodal distribution.

Taking the shape of the agglomerates into account, bimodality can be explained as follows. Refining causes compression and consequently yields plate like agglomerates. In combination with the primary particles two different shapes are existing. If all agglomerates are destroyed, the plate like structure should have disappeared, i.e. elimination of the bimodality which is the case for limestone. The sugar system seems to establish a bimodal distribution during deagglomeration. This means that the primary particles are also composed of two types of particles. For the fine particles shape is more regular, i.e. similar dimensions in all directions. Whereas the bigger particles have experienced plastic deformation when passing the roll refiner and thus are now plate like. This is also confirmed by microscopy. [Observing the sample by microscopy and simultaneously inducing a rotating motion of the particles (shaking the sample holder, which most conveniently is a petri dish) allows to assess all dimensions of the particles.] Furthermore it is seen that as soon as stresses are increased to higher levels (ultrasound treatment) complete breakdown of the agglomerates occur. The same is found for limestone silicon oil. It can be concluded that in the beginning weak agglomerates are present (flocks) which can be easily destroyed. The bonds between these flocks are of van der Waals nature. The sample discussed here contains non recrystallized sugar, i.e. the sugar surfaces are amorphous and probably have already taken up some water.

In Figure 5-25 on page 80 a picture of sugar agglomerates is shown, where the sugar still contained amorphous surfaces. The results from laser diffraction measurement confirm that microscopical observation. In case the sugar surfaces had been recrystallized, no agglomerates could be detected by microscopy (Figure 5-26 on page 80). Figure 5-48 gives the
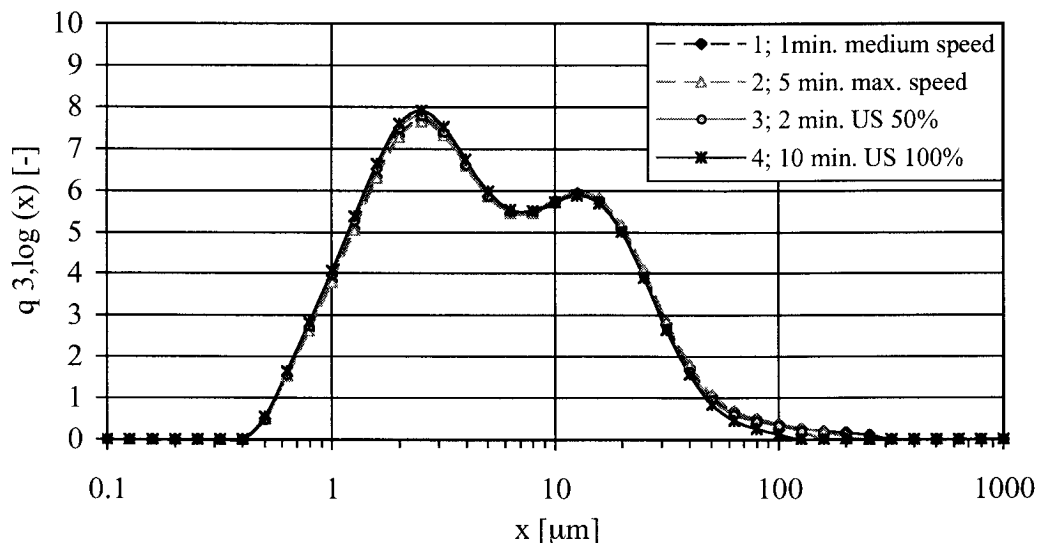
Figure 5-48 Stability of agglomerates for the sugar silicon oil system, sugar had been recrystallized during kneading but was not ideally dispersed

agglomerate stability of a recrystallized and well kneaded sample. Also there no weakly bound agglomerates can be detected. This means that amorphous surfaces cause agglomeration of the sugar particles whereas crystalline surfaces do not show this high affinity to agglomerate in a silicon oil continuous phase.

In a next step samples composed of sugar and cocoa butter and lecithin are considered. There it will be looked at two different samples. Both samples belong to the same batch of grinding and thus are the same directly after refining, but further treatment was carried out in different ways.

The refiner flakes of the first sample were stored for 5 days at ambient air conditions of 70% r.h. and 40°C. During this time the amorphous sugar recrystallized and stable agglomerates were formed. The sample was then kneaded in the Brabender lab kneader. To achieve good deagglomeration the sample was intensively kneaded (pasty structure) for 1 h. After kneading, agglomerate size measurements were performed.

Figure 5-49 gives the size and stability of these agglomerates. Pure mechanical treatment (curve 1 and 2) does not affect the agglomerates. Application of ultrasound at the lowest level leads to a partial break down of the agglomerates. Increase of sonication power and time causes a further breakdown. This illustrates that the agglomerates present here are of a different nature than the agglomerates present in the silicon oil sample. There application of ultrasound caused almost complete deagglomeration.
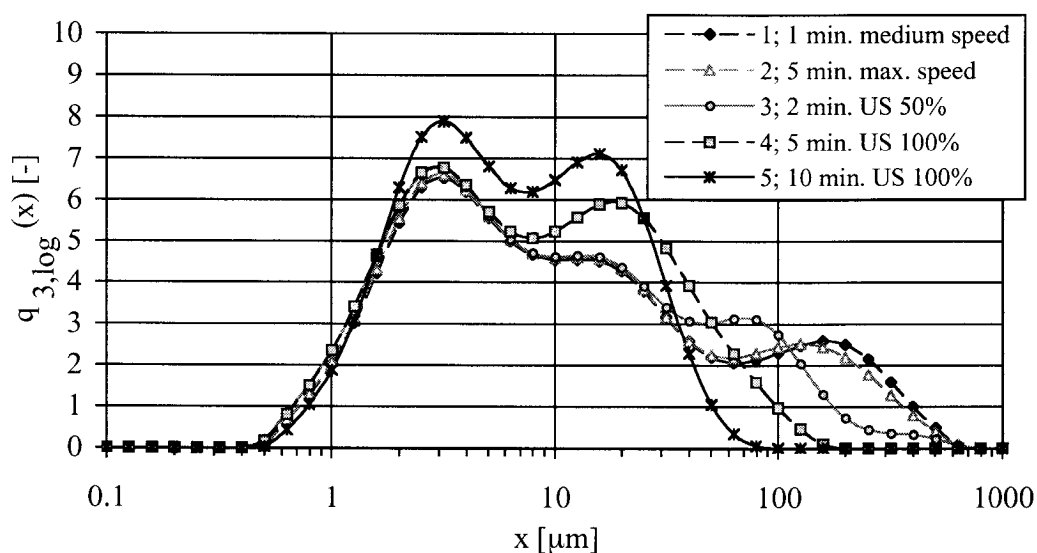
Figure 5-49 Particle size for a sugar cocoa butter suspension, recrystallized before deagglomeration was performed, recrystallized in the flake like state (state of rest)

The second sample was kept under dry and cold atmosphere (sealed containers filled with drying pearls, 0% r.h., 4°C) during storage. Kneading was performed in two stages. In stage 1 the sample was exposed to a dry atmosphere whilst it was intensively kneaded. This was to deagglomerate before water sorption and thus recrystallization can take place. After a smooth texture was obtained the sample was exposed to a humid atmosphere (40°C, 70-80% r.h., 14h) to allow for recrystallization. To avoid agglomeration, the sample was kneaded during the humidification step. Afterwards agglomerate analysis was performed.

Figure 5-50 shows the results of the agglomerate analysis. It can be seen that almost no agglomerates are present. Applying the ultrasound at the lowest level (curve 3) causes already complete deagglomeration. Compared to Figure 5-49 the agglomerates present here
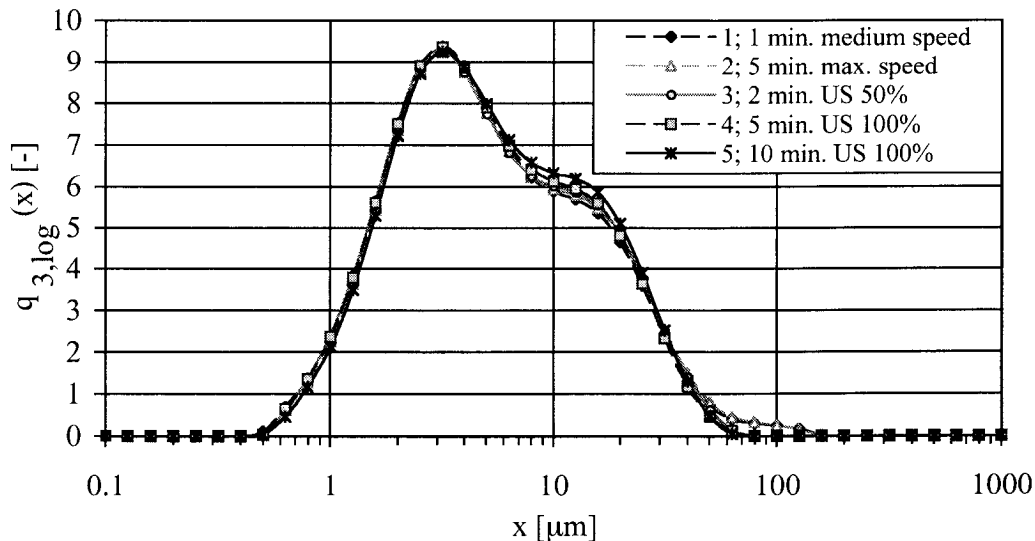
Figure 5-50 Particle size for a sugar cocoa butter suspension, recrystallized after deagglomeration, particles had been well dispersed during recrystallization

are much smaller in size and less stable. When looking at the size distribution obtained for most intense treatment (curve 5) it appears that the first sample has formed stable secondary agglomerates. These agglomerates result from recrystallization that has occurred in the flake like state and thus in the state of rest. The second sample was recrystallized after the primary agglomerates (press agglomerates which result from the refining process) had been destroyed. Kneading of the sample and thus ensuring good dispersing of the particles during humidification and recrystallization avoids the formation of secondary agglomerates.

In order to emphasize the importance of the processing conditions, an example is shown where recrystallization was also performed during kneading. The sample used here is composed of sugar and silicon oil. The sample was refined and deagglomerated whilst a dry atmosphere was applied. Then the final amount of liquid phase was added yielding a liquid consistency. Afterwards a humid atmosphere was applied in order to allow for recrystallization (70%-80% r.h., 40°C). Due to the texture of the sample (thin paste like) kneading was less effective and the particles could not be dispersed well enough. This led to an agglomeration during recrystallization although kneading has taken place. Figure 5-51 shows the corresponding size distribution obtained for strong pre-treatment (level 5, primary particles) in the course of size analysis. It is seen that humidification leads to recrystallization and thus to the formation of agglomerates.

As soon as recrystallization processes take place reagglomeration processes occur simultaneously. Reagglomeration can only be avoided, if during the time required for recrystallization (time determined by kinetics of: water sorption and water transport; dissolving of sugar; formation of sirup like, sticky layer; formation of bridges; recrystallization; hardening of bridges; formation of solid bridges), in every volume element the forces applied are higher
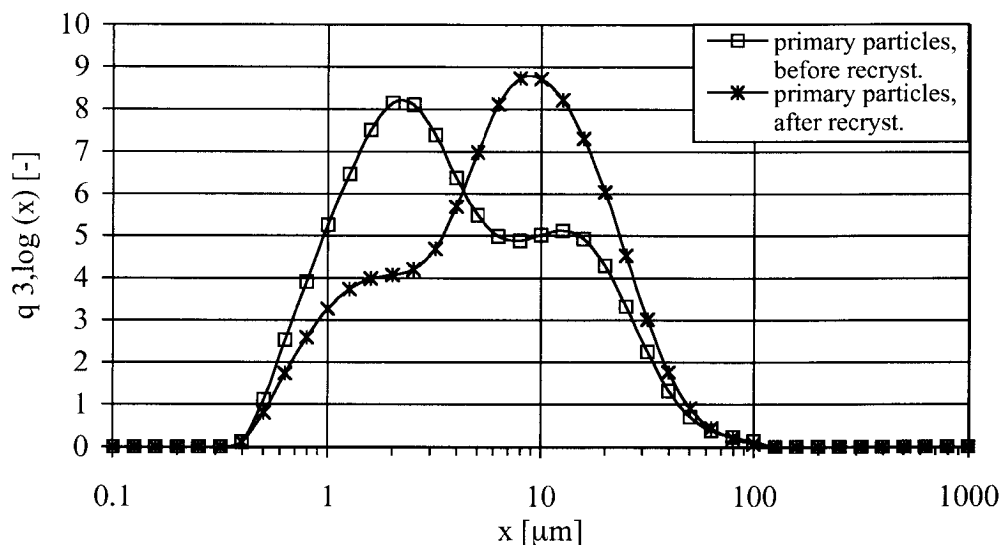
Figure 5-51 *Particle size distribution before (amorphous) and after (recrystallized) humidification, recrystallization took place whilst low stresses had been applied during kneading, sugar silicon oil*

than the forces that act between the particles. It has to be noted that the forces that act between the particles do increase with time.

In technical apparatus the forces acting on the product most often show an intensity distribution and thus the product passes zones of high and low stresses. Therefore the time particles stay in contact before passing a "separation zone" must be shorter, than the time required for recrystallization. The time required for recrystallization depends on the glass transition temperature and on the processing conditions. For the sucrose silicon oil system it was found that exposure times of 6h, a temperature of 40°C and an atmosphere of 70% r.h. were not sufficient to fully recrystallize, whereas processing times of 24h are considered to be sufficient. This strongly depends upon the system used as well as on the temperatures applied. Increase of temperature above glass transition temperature accelerates crystallization, hence reduces the time required for recrystallization (*Kedward, C.J. et al. (1998), Hartel, R.W. (1993), Hartel, R. W., Shastry, A.V. (1991)*).

This clearly shows the importance of water sorption and the conditions chosen for processing in order to recrystallize without formation of secondary agglomerates.

For model systems and for pilot and lab scale work, it is a manageable effort to proceed according to these conditions. When working with a real chocolate system on production scale, these ideal lab conditions can no longer be maintained. Even when working under dry atmosphere chocolate contains components (milk powder and cocoa solids) which act as an internal source for water and thus sugar can start to recrystallize at an early state.

In the previous sections, sample that had been refined and kneaded were discussed. In the following trial series, it was looked at the strength, size and quantity of the agglomerates that are present in refiner flakes prior to any kneading step. Therefore a chocolate mix was prepared and refined whilst applying different conditions. The chocolate used here was a milk chocolate having a composition as described in 3.1.3.5 "Milk Chocolate" on page 34.

In a first run refining was carried out under normal room atmosphere (25°C, 50% r.h.). In a second run refining was performed applying a nitrogen atmosphere free of water. In both cases the refined sample was directly fed into a glass beaker filled up with cocoa butter. The cocoa butter protected the fresh surfaces from water and thus the influence of water sorption during sample preparation was diminished.

These samples were then handled according to the sample preparation procedure, i.e. first stirring it with a magnetic stirrer for 30 min., then transferring a sub sample to the Malvern and circulating it in the small sample presentation unit for different times at different stirrer speed levels (half speed, used during measuring; maximum speed, used for partial deagglomeration) and finally applying ultrasound treatment to further deagglomerate it.

In Figure 5-52 the resulting size distribution for these differently prepared samples are shown. First of all it has to be noted that this trial series was analyzed with a Malvern Mastersizer X, using sun flower oil as dispersing media and a 300mm lens ranging from 1.2 to 600 μm. Therefore these results can not be directly compared to the results reported before, but can be compared within this trial series.
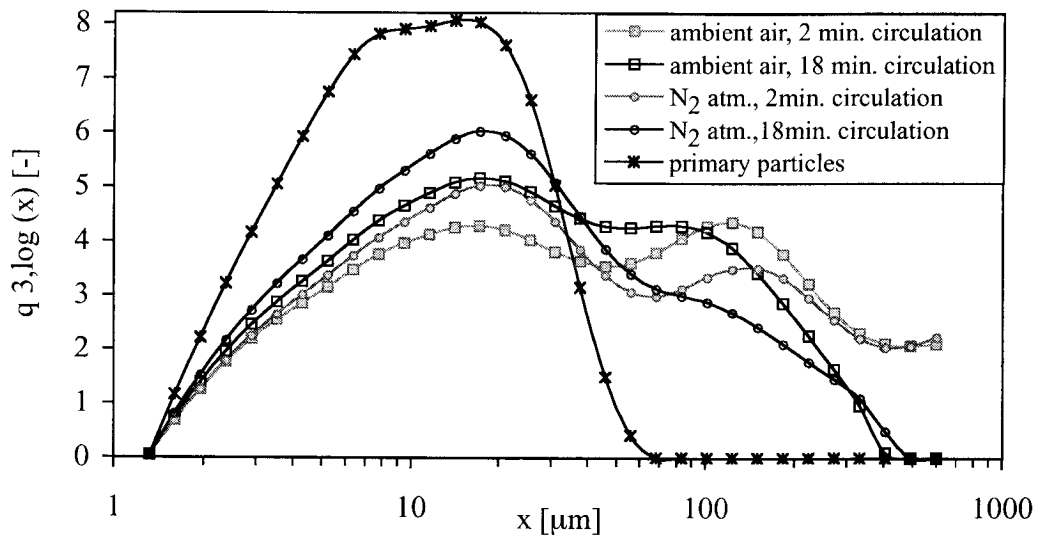
Figure 5-52 Particle size distribution of chocolate refiner flakes refined under normal atmosphere (25°C, 50% r.h.) and nitrogen (N_2) atmosphere

Comparing the two samples, see Figure 5-52, it can be seen, that for the same treatment during preparation, the sample produced under a dry (nitrogen) atmosphere, contains less particles in the size classes bigger than 50 μm. Application of a dry atmosphere during refining yields less agglomerates. This indicates that the time during which the fresh surfaces are exposed to a humid atmosphere, although it is rather short (residence time on rolls < 2s) is sufficient to pick up water from the ambient atmosphere and thus to form bigger and more stable agglomerates. The sample that was exposed to a dry (nitrogen) atmosphere, also contains agglomerates which are of primary nature (press agglomerates). The fresh surfaces of these agglomerates as well could have adsorbed water. In that case the water is not sourced from the surrounding atmosphere but from the neighboring particles (milk powder or cocoa solids), that already contain water. This again emphasizes the importance of water sorption for the characteristics of the systems investigated here.
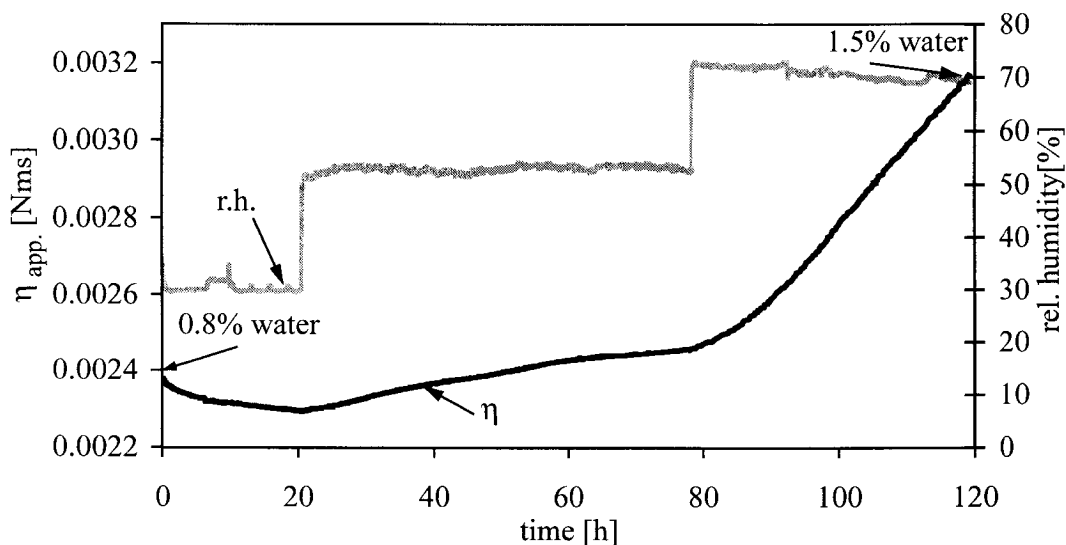
5.5 Chocolate

In the previous chapters model systems were considered. The influence of deagglomeration and water sorption on rheology of chocolate like model systems was discussed. In this section it is looked at the real chocolate system. Therefore commercially available milk chocolate was used in this study.

5.5.1 Rheology - Influence of Water Sorption

Addition of water to chocolate and its influence on flow behavior as well as on the structural changes of the disperse phase are already investigated (*Winkler, T., Tscheuschner, H.-D. (1998)*). In that work water was added as droplets. Addition of water as droplets changes the disperse phase concentration and thus effects the structure of the chocolate. Furthermore the droplets have to be dispersed and transported to the hydrophilic components. The resulting microstructure will depend upon the quality of dispersing, mass transport and dissolving processes (sugar is dissolved in the unprotected water droplets). In order to study the influence of small amounts of water on the rheology of chocolate, here the water is incorporated through water sorption. Water vapor sorption allows to introduce water in the molecular state. Thereby the formation of zones with increased water concentration, like it would be the case by drop-wise addition of water, is totally avoided.

The influence of water sorption on flow properties of chocolate was investigated using head space controlled rheometry. The sample was placed in the rheometer and exposed to different levels of humidity whilst being stirred with a helical ribbon impeller ensuring good mixing.

Figure 5-53 Applying different levels of relative humidity and influence on flow properties of commercial milk chocolate, T=40°C, helical ribbon impeller, const. angular velocity 4/s, Bohlin CVO, 30% w/w fat. Water content of the sample at the beginning and at the end of the measurement was determined by Karl Fischer analysis.

Figure 5-53 shows the influence of water sorption on the flow properties of molten chocolate at a temperature of 40°C. In the beginning viscosity decreases whilst equilibrating to a humidity of 30%. This indicates that the sample had been exposed and equilibrated to a more humid atmosphere prior to measuring. When approaching higher levels of humidity also viscosity increases. It can be concluded that the more humid the atmosphere the higher viscosity. To give an explanation for this behavior the amount of water taken up during water sorption is considered. Measurement of the water content in the beginning and at the end of humidification shows (see Table 5-2) that water content of the chocolate has increased from 0.8% to 1.5% and thus has almost doubled.

Table 5-2 *Water content before and after water sorption process in the rheometer*

Water content before sorption	Water content after sorption
0.8%	1.5%

Introduction of a hydrophilic component into a hydrophilic/lipophilic system like chocolate leads to an increase of the hydrophilic particle interactions and thus to an increase in viscosity. Furthermore it is thought that water adsorbed to the hydrophilic components will lead to a coverage of the solid surface with a liquid product. This results in a smoothening of the surface and thus increases the contact area between the particles which leads to an increased strength of the bonds. As a consequence agglomerates will be formed. These agglomerates immobilize fluid and thus give rise to viscosity.

In order to better understand the interplay between water sorption and rheology, the water sorption characteristic of chocolate were assessed too.

5.5.2   Water Sorption Behavior

To analyze the water sorption behavior of milk chocolate, the same chocolate like used before was assessed in the sorption balance. The sample was kept at 45°C and humidity was increased step-wise in order to give time to the sample to equilibrate. The change in weight was recorded as a function of time. Figure 5-54 gives the water sorption behavior of a commercial milk chocolate.

First it can be seen that chocolate is adsorbing water on a long time scale. Exposure times of 48h are not sufficient to reach an equilibrium at 30% r.h. In the beginning sorption is rather fast and then kinetics slow down. For increased relative humidity the amount of uptaken water rises steeply. This indicates the formation of multilayers and the presence of components with high water binding capacities. Looking at the amount of water adsorbed, the content of water doubles within 25h when increasing relative humidity from 30% to 50%. It is important to note, that the values given do not refer to equilibrium (adsorption not finished within the time of the measurement).

For comparison of rheological measurements with water sorption measurements it is found that changes in viscosity and changes in weight (moisture uptake) occur on similar time scales and follow similar patterns. Although water content significantly increases when changing relative humidity from 30% r.h. to 50% r.h., viscosity only increases by 10%. For a humidity of 70% a steep rise for both, viscosity and water content is observed which is most likely due to capillary condensation. Capillary condensation increases the attraction between particles and thus increases viscosity.
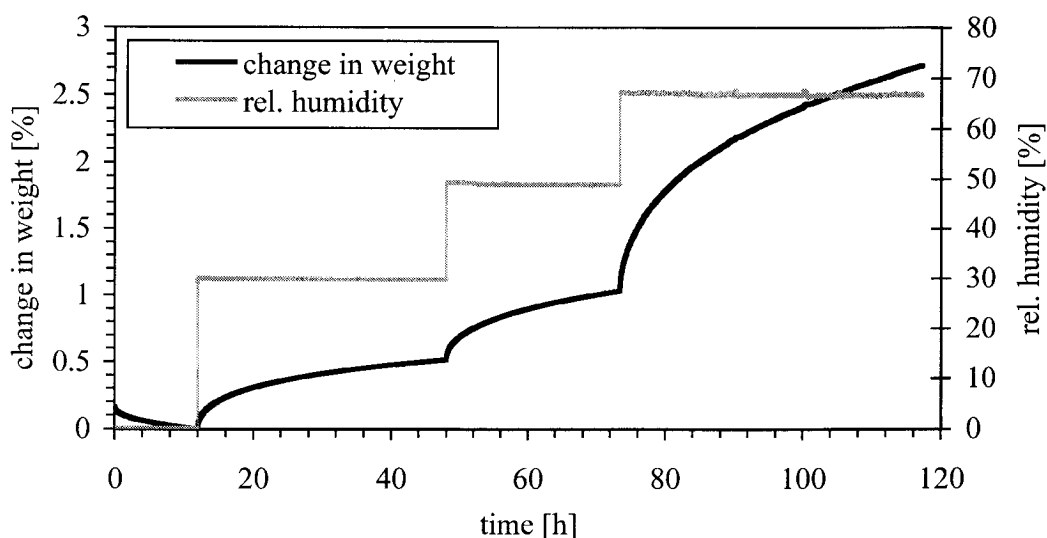
Figure 5-54 *Water sorption behavior of commercial milk chocolate, change in weight as a function of time for different levels of humidity, Sorption balance DVS 1000, T=45°C*

In order to understand the water sorption behavior of chocolate, the sorption behavior of its individual components need to be investigated. The same applies to the model systems, for which water sorption also had a significant impact on rheology.

In the following section, the water sorption behavior of all the materials / ingredients used is described.

5.5.3 Summary

The flow behavior of chocolate is influenced by the amount of water adsorbed to the components. Water sorption is taking place on long time scales (48h and more) without reaching an equilibrium hence water sorption continuously increases viscosity on the observed time scales. The difference in polarity and thus the particle interactions rise with the amount of adsorbed water. In particular capillary condensation is expected to occur which causes the steeper increase of viscosity at higher humidity levels.

Owing to the structure of the product (pasty) some product can adhere to the walls/ to the kneading arms in the lab kneader, hence is not stressed during the most powerful phase (transition from crumbly to pasty). Once the mass is liquefied, the stress levels are decreased and deagglomeration now depends on the probability that agglomerates enter the highest stress zones between the kneading arms (relatively small volume of 3-5ml compared to a total volume of 500ml, flow field in the kneader does not force each particle to pass this zone). This explains why, to a minor extent, agglomerates still can be found after an intense kneading process.

6 Water Sorption Behavior of Various Ingredients

In the previous chapter the influence of water sorption on the rheological properties of chocolate and chocolate like systems was discussed. In the following chapter the water sorption characteristics of the individual components will be described. First the various continuous phases will be considered followed by the description of the disperse phases. For the continuous phases also the effect of water sorption on rheology will be discussed.

6.1 Continuous Phases - Water Sorption - Rheology

6.1.1 Silicon Oil - Rheology

The continuous phase used was a silicon oil with a viscosity of 2000mPas (25°C) obtained from Wacker Chemie, Germany (type AK2000). Viscosity was measured using a cone and plate geometry (4°, 40mm in diameter) whilst applying different levels of humidity. The silicon oil was predryed prior to measurement. Therefore it was stored in a desiccator (filled with drying silica pearls) for 7 days at room temperature.

Figure 6-1 gives viscosity as a function of time for different levels of humidity measured at a temperature of 30°C. Viscosity marginally increases for increased humidity.
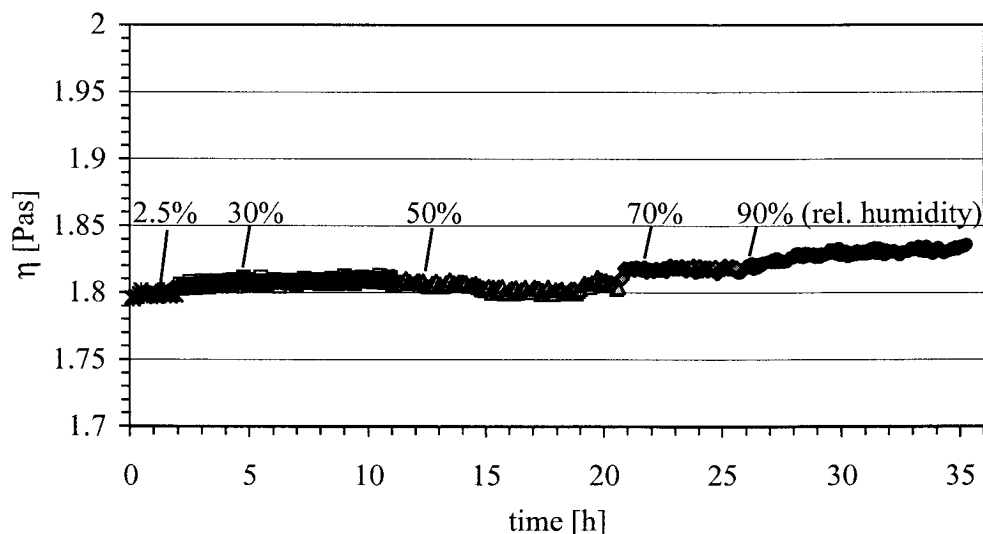
Figure 6-1 *Viscosity of silicon oil, AK 2000, as a function of time for different levels of humidity, cone and plate geometry, 4°/ 40mm, T=30°C, stress controlled, Bohlin CVO 120*

Figure 6-2 gives the viscosity as a function of shear rate for the different levels of humidity. Like shown before no significant difference between the individual curves can be detected. For values approaching shear rates of 0.1 1/s and lower the resolution limit of the set up is reached and the "noise" of the measurement increases.
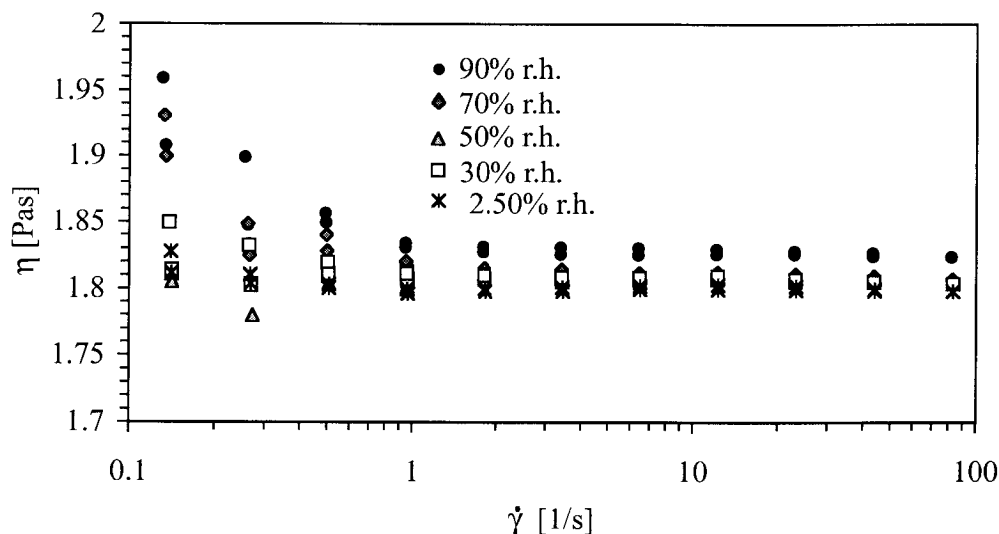

Figure 6-2 *Viscosity function of silicon oil, AK 2000, for different levels of humidity, cone and plate geometry, 4°/ 40mm, T=30°C, stress controlled, Bohlin CVO 120*

It can be concluded that viscosity of this type of silicon oil is only marginally influenced by water sorption.

6.1.2 Silicon Oil - Water Sorption Behavior

Although viscosity of silicon oil is only slightly affected by water sorption, it is important to know the quantities of water being absorbed by silicon oil. Consequently water sorption behavior of silicon oil was determined. Therefore silicon oil was exposed to different levels of relative humidity and sample weight was recorded as a function of time. Figure 6-3 gives the water sorption behavior of silicon oil at 30°C.

During the initial drying step weight is decreasing but no equilibrium is reached. Increase of humidity up to 50% leads to an steep uptake in weight which peaks and then decreases. A further increase of humidity reveals the same pattern like before. The sample first takes up weight resulting from the absorption process and then looses weight due to desorption. It may be concluded that components dissolved in silicon oil are desorbed whilst water is absorbed. Looking at the specification of silicon oil values for solubility of different gases are given.
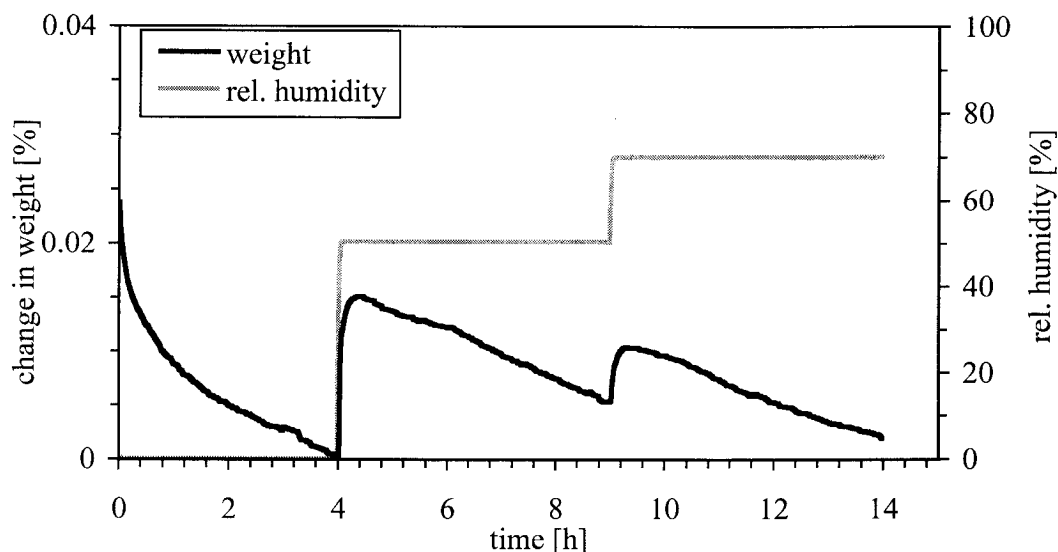
Figure 6-3 *Water sorption behavior of silicon oil, AK 2000, T=30°C, DVS 1000*

Table 6-1gives values for solubility of different gases in siliconoil (taken from *Wacker Chemie (1989)*.

Table 6-1 *Solubility of different gases in silicon oil at room conditions, values depend upon viscosity of silicon oil. A band of values is given as no viscosity is specified*

Component	Solubility cm³/g oil
Air	0.175 - 0.19
Nitrogen	0.163 - 0.172
CO_2	1.00

The solubility of air is about $0.19 cm^3/g$ in maximum. The density of air at 1013mbar and 25°C is $1.18*10^{-3}g/cm^3$.

For silicon oil it is reported that the presence of water dramatically reduces the solubility of these gases (*Wacker Chemie (1989)*). In an extreme approach it is assumed that all gas dissolved in the silicon oil will be expelled as soon as water is absorbed. With the above mentioned values it is found that in 1 g of siliconoil $0.19cm^3$ of air are dissolved. This equals $2.24*10^{-4}g$ of dissolved air per gram silicon oil or 0.0224% w/w.

This shows that the loss of weight observed during water sorption can be explained by the desorption of soluted air. The corresponding values for air soluted in silicon oil and the value for weight reduction are in the same range. With respect to the detection of recrystallization phenomena (see Section 4.4.1 on page 61) it has to be noted that during recrystallization a peak in the weight signal is observed too. The peak observed there, is an order of magnitude higher than the peak obtained for pure silicon oil, i.e. is not only based on release of soluted air but on recrystallization. In case only small quantities of amorphous material have to be detected, silicon oil is not the ideal surrounding media. It already delivers a peak caused by gas release, which could then be of the same order like the peak resulting from recrystallization and thus causes misleading interpretation.

6.1.3   Cocoa Butter & Cocoa Butter - Lecithin

6.1.3.1   Cocoa Butter - Rheology

The influence of water sorption on the rheological properties of cocoa butter was obtained by use of a cone and plate geometry with an angle of 2° and a diameter of 60mm. Figure 6-4 gives the viscosity of cocoa butter as a function of time for different levels of humidity. It can be seen that viscosity is only marginally affected by humidity.
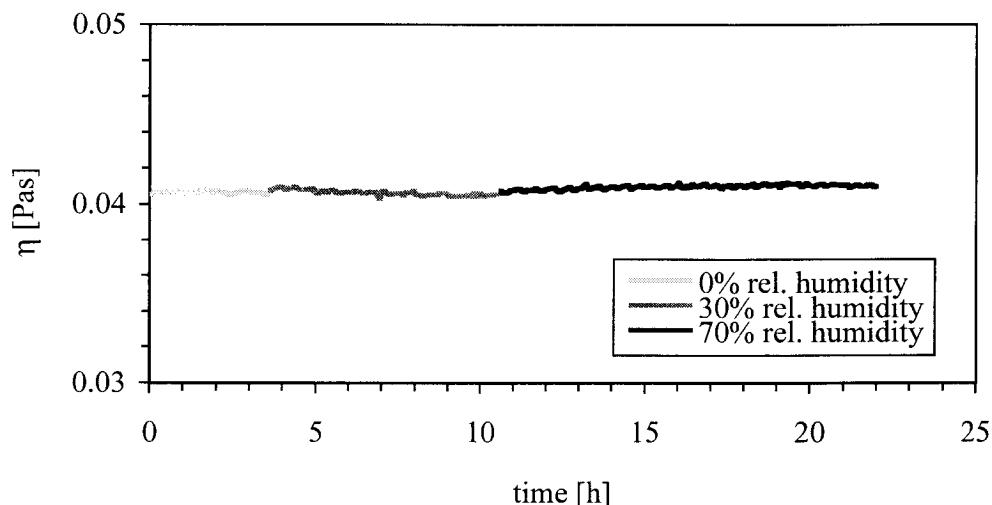
Figure 6-4 Viscosity of cocoa butter as a function of time for different levels of humidity, cone and plate geometry, 2°/ 60mm, T=45°C, stress controlled, Bohlin CVO 120

6.1.3.2   Cocoa Butter - Water Sorption Behavior

Cocoa butter is composed of mono-, di- and triglycerides and also contains phospholipids. The mono- and diglycerides as well as the phospholipids are surfactants. It can be expected that the naturally present surfactants will have an influence on the water sorption behavior of cocoa butter. Figure 6-5 gives the sorption isotherm of commercial, deodorized cocoa butter. It can be seen that equilibration is finished within 2 to 3 hours. The maximum amount absorbed is about 0.18%. During desorption a hysteresis appears and some water (about 0.01%) remains in the sample.

Applying levels of humidity higher than 90% r.h. yields a further uptake of water which always reaches an equilibrium. This indicates that no "condensation" of water is taking place. This is given in Figure 6-6. After desorption the same quantity of water like indicated in Figure 6-5 remains in the sample.

To investigate the influence of naturally present emulsifiers on water sorption cocoa butter was purified. Therefore cocoa butter was cleaned from impurities using a purification method as described in literature (see section 2.1.1.3 "Cocoa butter - purified" on page 14).
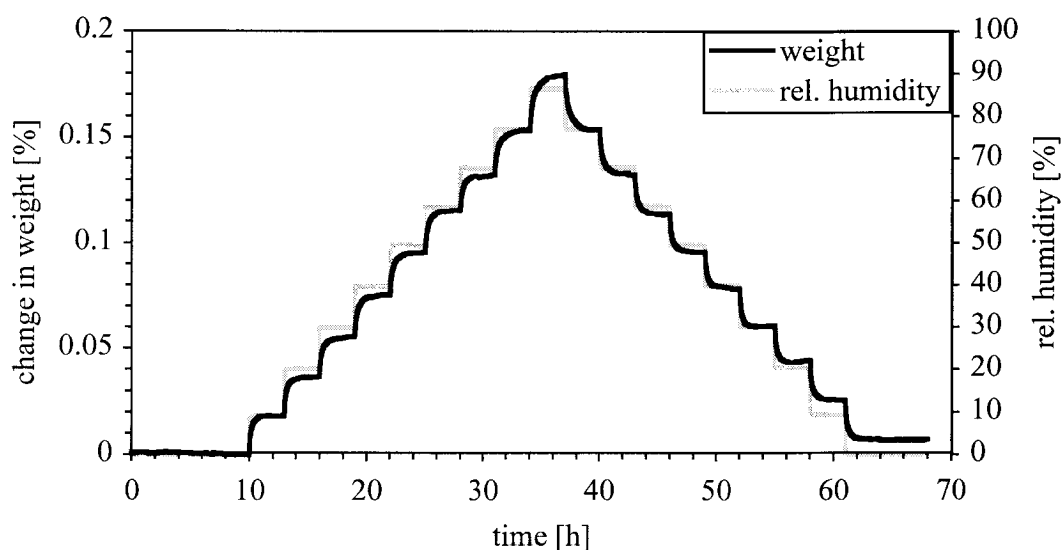
Figure 6-5 *Water sorption isotherm for commercial cocoa butter, deodorized, T=45°C*
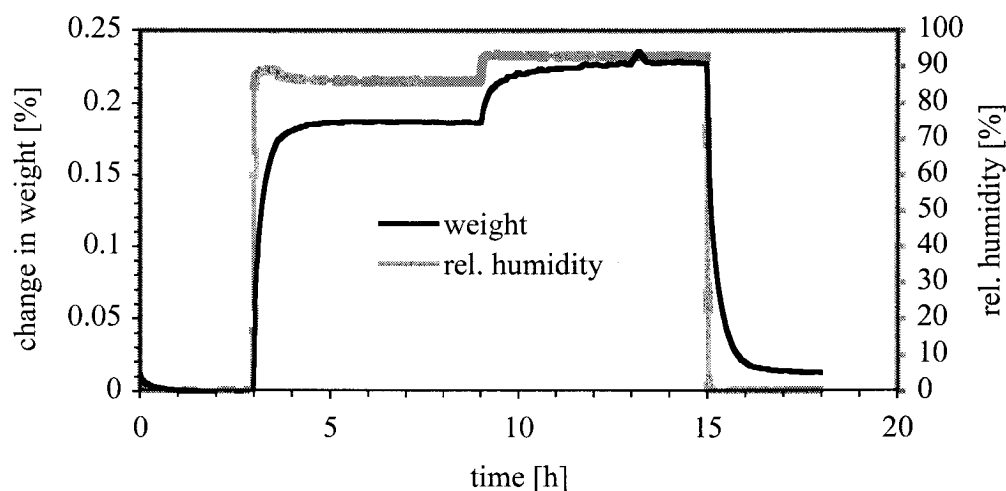
Figure 6-6 *Water sorption behavior of commercial cocoa butter at high levels of humidity, T=45°C*

Figure 6-7 and Figure 6-8 show the sorption isotherm for purified and non purified cocoa butter. It can be seen that the purified cocoa butter absorbs less water than the non purified cocoa butter. Equilibrium is also reached on short time scales.

Like seen before, after desorption still some water remains in the sample. This indicates that the remaining water is not bound to the substances that had been removed during purification.

To assess the influence of emulsifiers like soy lecithin on the water sorption behavior a sample of commercial, non purified cocoa butter with 0.7% w/w of non-standardized soy lecithin (amount of acetone insoluble components > 60%) was prepared. The term soy lecithin
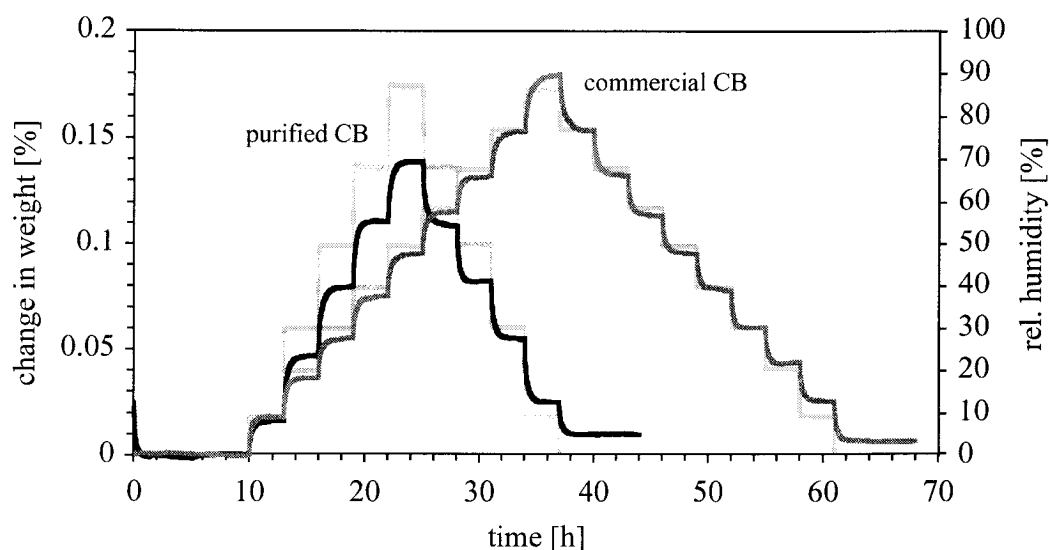
Figure 6-7 Water sorption of commercial, purified and non purified cocoa butter, T=45°C
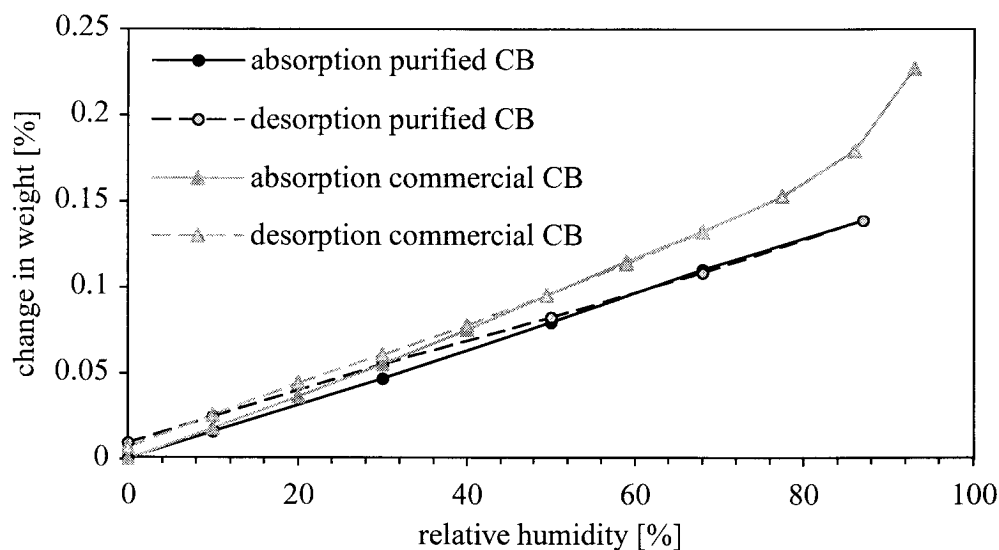
Figure 6-8 Sorption isotherm, comparison between commercial and purified cocoa butter, T=45°C

here refers to the commercial name of the product and not to the chemically precise terminology. Chemically spoken lecithin stands for phosphatidylcholin whereas in confectionery lecithin refers to a phospholipid concentrate obtained from soy bean oil. Comparing the water sorption of a lecithin enriched sample to a commercial, non purified sample of cocoa butter (for two levels of humidity) like illustrated in Figure 6-9, it can be seen that the lecithin containing sample absorbs 20% to 30% more water. Due to the emulsifying properties of lecithin more water can be incorporated into the lipophilic continuous phase. The state in which the water is present in the lecithin cocoa butter mixture was not analyzed.
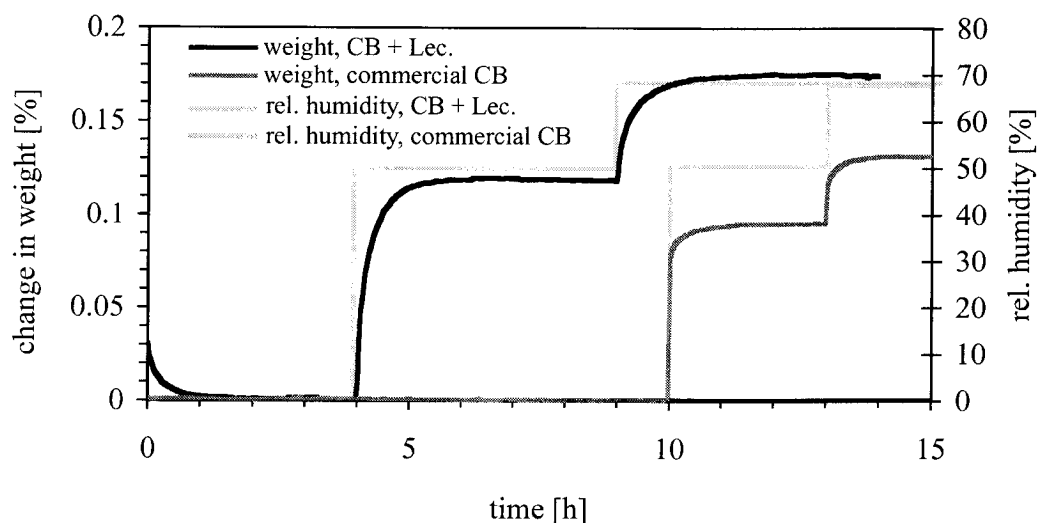
Figure 6-9 Water sorption behavior of cocoa butter with 0.7% of soy lecithin (acetone insoluble components>60%) compared to plain cocoa butter (non purified), T=45°C

6.1.4   Lecithin - Water Sorption Behavior

In the section before the influence of lecithin on the water sorption behavior of oil- lecithin mixtures was discussed. In the following the water sorption behavior of pure lecithin (non-standardized, commercial soy lecithin, acetone insoluble components > 60% w/w) is described. As a commercial, non standardized sample of soy lecithin was used it has to be noted that the sample is composed of various phospholipids (approx. 63%) and soy oil. Therefore this represents a sample composed of phospholipids and oil which is similar to the cocoa butter lecithin mixtures but with higher concentrations of phospholipids (approx. 63% w/w).

Figure 6-10 gives the water sorption behavior of soy lecithin at a temperature of 45°C. Lecithin takes up water without reaching an equilibrium in the given time frame. The water content reached at different levels of humidity is much higher than in any of the systems shown before. This is due to the surface active properties of lecithin. The water absorbed by the lecithin oil system is most probably interacting with the hydrophilic part of the phospholipids and the polar parts of the triglycerides of the oil phase. The state in which the water/phospholipid arrangements are present (formation of micelles or other forms) could not be detected with this method. Analysis of the molecular interactions between phospholipids and water would be a seperate subject which is not covered by the objectives of this work.
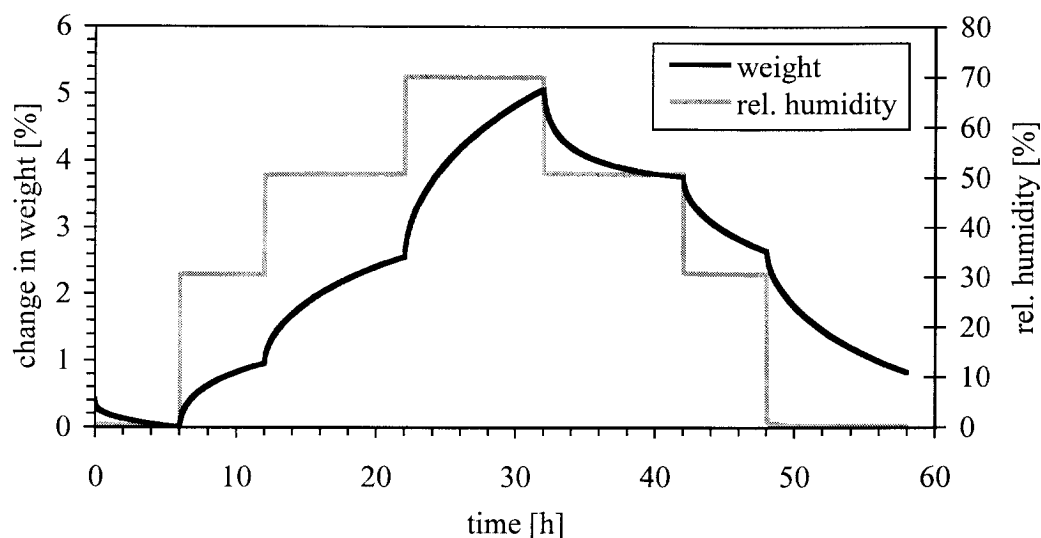
Figure 6-10 *Water sorption behavior of commercial soy lecithin, T=45°C*

6.1.5 Summary

The continuous phases absorb different amounts of water. This is due to their chemical nature and composition. Water sorption only marginally affects the flow properties of silicon oil and cocoa butter. It was found that purified cocoa butter absorbs less water than standard type, non purified cocoa butter. Addition of lecithin increased the amount of water absorbed. Commercial, non standardized soy lecithin which contains more than 60% acetone insoluble components absorbs high amounts of water (more than 5% w/w). This is due to the polar groups present in phospholipids and reflects the amphiphilic character of the phospholipids.

6.2 Disperse Phases - Water Sorption Behavior

6.2.1 Limestone

The lime stone used here was natural limestone with a purity of 99%. It was either used in the dry ground or in the roll refined stage. First the water sorption behavior of the dry ground limestone will be discussed. The particle size distribution of the dry ground limestone is given in section 2.1.2.2 "Limestone - used as a dry ground powder" on page 14.

Figure 6-11 gives the sorption isotherms obtained from multiple, consecutively performed measurements using the same sample. During the first cycle it can be seen that water sorption is showing rapid increase and unsteady conditions. For a relative humidity of 90% capillary condensation can be observed. Desorption is not completed and some water remains in the sample. The second and third cycle of adsorption and desorption show equilibrium conditions for each level of humidity. Due to the incomplete desorption the total uptake of water
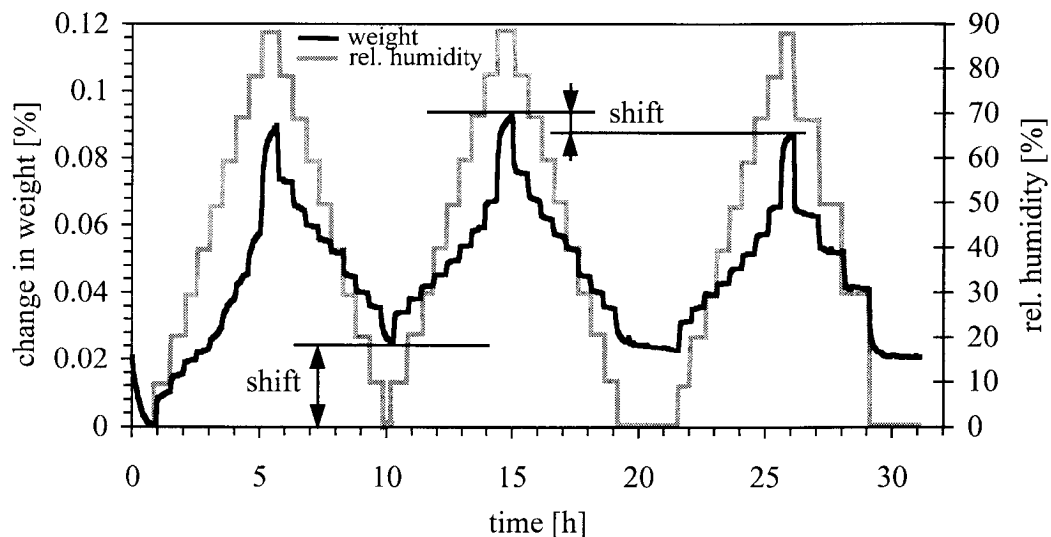
Figure 6-11 Water sorption isotherm of natural and dry ground limestone used for preparation of suspensions, T= 30°C

is less in the second and third cycle. This indicates that the capillary volume has decreased and thus the volume of the pores has been reduced. During the second and third cycle desorption is complete and no water remains in the sample, except for the water incorporated during the first cycle. It is assumed that during the first cycle the impurities have picked up the water which is now bound as crystal water. An indirect proof of this assumption is derived from the water sorption isotherm of pure $CaCO_3$ (obtained from chemical reaction). There water sorption is reaching an equilibrium at each level and water is completely desorbed. This is illustrated in Figure 6-12. The size of the pure $CaCO_3$ is much smaller ($X_{90,3}$= 9µm, $X_{50,3}$=3µm) than of the dry ground limestone ($X_{90,3}$= 26µm, $X_{50,3}$=18µm). Consequently the values for water up take can not be directly compared but the pattern of the adsorption / desorption curve. It has to be noted that the sorption measurement of the pure $CaCO_3$ was performed at an increased temperature of 45°C.
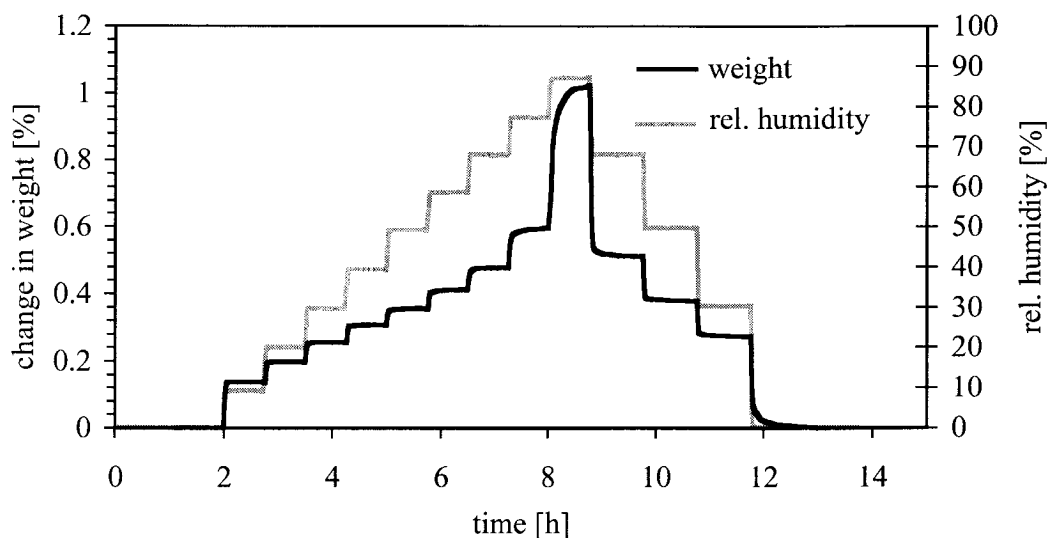
Figure 6-12 *Water sorption isotherm of pure* CaCO₃ *(obtained from chemical reaction),* $T = 45°C$

To study the water sorption behavior of roll refined limestone a mixture of limestone and silicon oil (AK 2000) was prepared and refined. The flakes obtained were also used for the preparation of limestone siliconoil suspensions mentioned earlier (4.3.2 "Influence of water sorption on flow behavior" on page 58). Figure 6-13 gives the water sorption isotherm of the flakes obtained from multiple, consecutively performed measurements. In the first cycle two levels of humidity were used to check for state transition phenomena. During desorption an equilibrium is reached and a dry sample was obtained. During the second cycle capillary condensation occurs and large quantities of water are adsorbed without reaching an equilibrium. Two things have two be noted here. First the amount of water adsorbed during the second cycle is lower than the amounts of water adsorbed during the first cycle. This irreversibility could be explained by the closure of pores and small cracks during the first adsorption. From surface area measurements (*Schwenk, W. (1971), Schönert, K. (1974)*) of fresh and aged surface it is known that surface area can decreases during ageing. Second during desorption water is not completely desorbed and some water remains in the sample. This is due to the capillary condensation. It is assumed that during capillary condensation same components were dissolved in water and thus forms a new structure that can bind water. Such structures can be formed during recrystallization for example. The water is then incorporated as crystal water. An other possibility is, that solutions formed during capillary condensation have solidified during drying without crystallizing and thus are present in the glass like state. The water is then kinetically fixed (glassy state) and will not be released fast enough during desorption (too low molecular mobility in the glassy state). Figure 6-14 gives an enlarged view of Figure 6-13, which expresses the differences in water sorption between cycle 1 and 2 better. These differences are attributed to limestone and not to the behavior of the silicon oil. Silicon oil as shown in Figure 6-3 on page 113 shows a decrease in weight when absorbing water which is due to the fact that dissolved gas is expelled once water is absorbed. The reduction in weight was found to be in maximum 0.02%. When taking into account that in case of the limestone silicon oil sample only 20% w/w are silicon oil it is seen that silicon oil and the release of gas can only count for a weight reduction of $0.2 * 0.02\% = 0.004\%$.
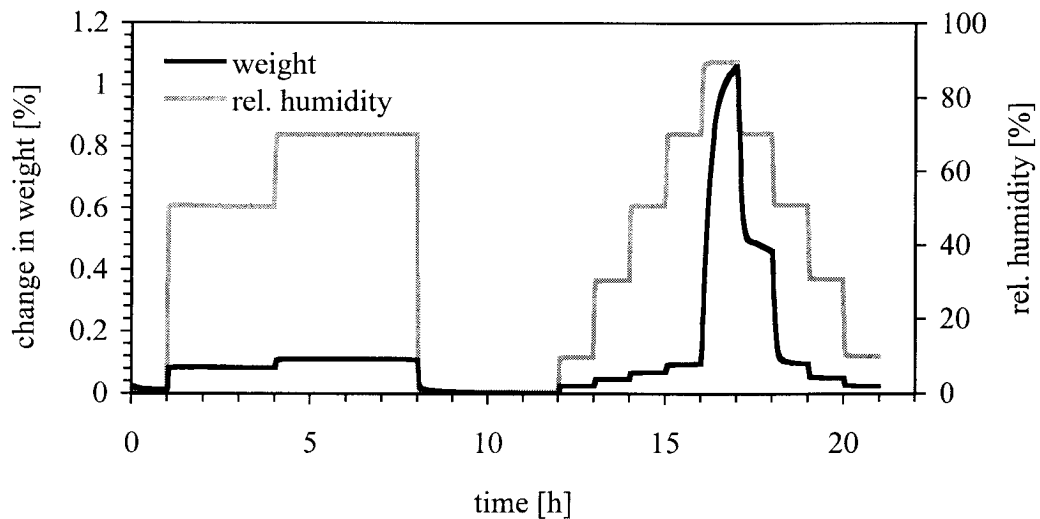
Figure 6-13 *Water sorption isotherm of a refined mixture of limestone (80% w/w) and siliconoil (20% w/w), T= 25°C, measurements performed consecutively*
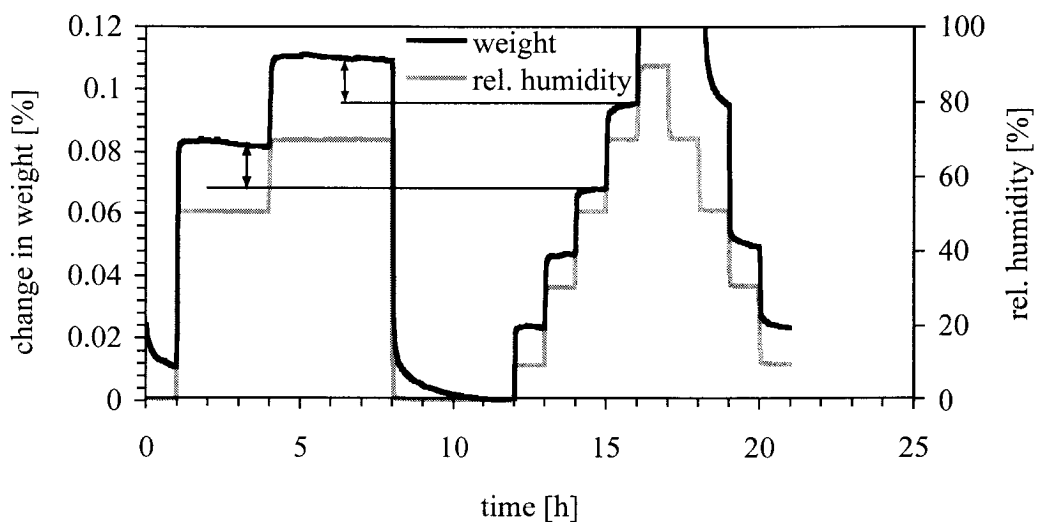
Figure 6-14 *Water sorption isotherm of a refined mixture of limestone (80% w/w) and siliconoil (20% w/w), T= 25°C, measurements performed consecutively, enlarged view of Figure 6-13*

Whereas the difference in weight between 1st and 2nd sorption cycle (see Figure 6-14) were found to be almost 0.02%. This clearly shows that this difference can not be explained by the behavior of the silicon oil but is attributed to ageing effects (closure of pores) of the limestone (see also 5.1.3 "Ageing of Surface" on page 67).

6.2.2   Sugar (Sucrose)

The water sorption behavior of sugar (sucrose) has been widely investigated ranging from purely crystalline to totally amorphous sugar. Often sorption isotherms are reported which are derived for equilibrium conditions and thus do not show the effects that take place with time. The focus here was to obtain data about the sorption behavior as a function of time.

For chocolate manufacture commercial crystalline sugar is used. The water sorption behavior for that raw material (commercial sugar, non ground, Nordzucker) is given in Figure 6-15 and Figure 6-16.
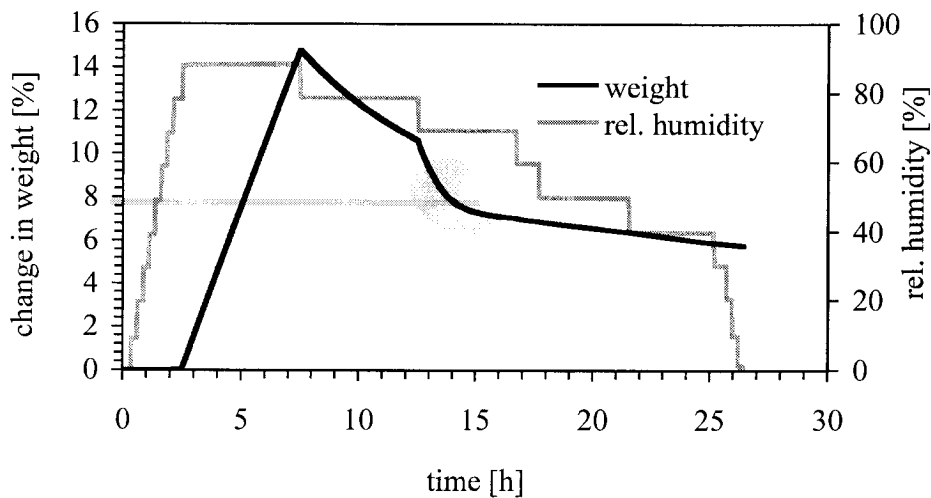
Figure 6-15 *Water sorption behavior of commercial sugar, T=30°C*
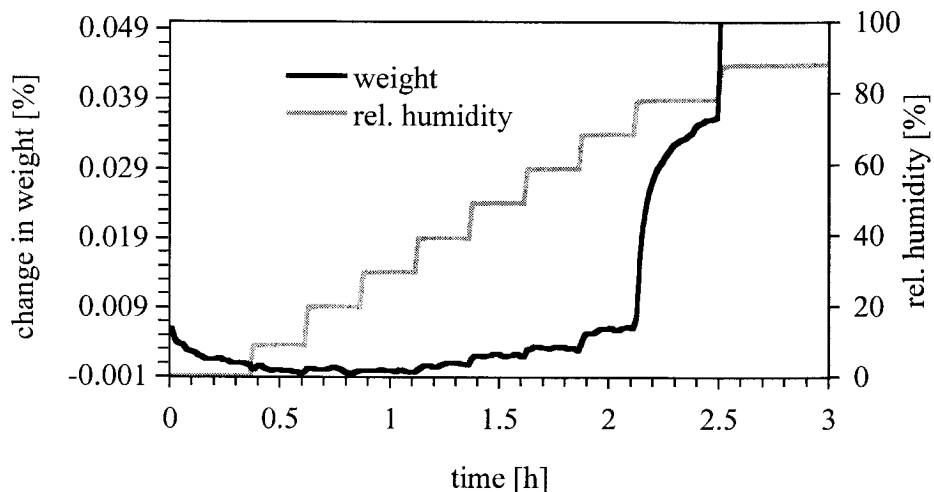
Figure 6-16 *Water sorption behavior of commercial sugar, T=30°C, enlarged view*

For high levels of humidity the effect of capillary condensation can be seen in Figure 6-15. The sugar is dissolved in the water and thus more and more water can be adsorbed giving rise to a steep increase of uptaken water. During desorption of water the sugar water solution

increases its viscosity and the rate of evaporation is slowed down. Further evaporation leads to the formation of a highly viscous, rubber like state and would finally yield a glass like state where almost no evaporation is taking place. Glass transition temperature of water sucrose solution with 5% w/w of water is about 30°C. The temperature during measurement was 30°C and from Figure 6-15 it can be seen that the rate of evaporation is slowed down as soon as a water content of about 7% is reached.

Figure 6-16 gives an enlarged view of the adsorption process for humidity levels below 80% (before capillary condensation occures). The sugar takes up water to quantities of about 0.008% in maximum and no indication for presence of amorphous phases were found (are not expected to be found in a sample originated from crystallization).

Besides the water sorption behavior of purely crystalline sucrose the sorption behavior of amorphous sucrose is of interest also. Therefore a sample of amorphous sucrose obtained from freeze drying was exposed to a low humidity of 10% r.h. at a temperature of 20°C. The uptake of water for such a low level of humidity is illustrated in Figure 6-17. The conditions for this test were chosen in accordance to the conditions present during refining of the sugar oil mixtures.
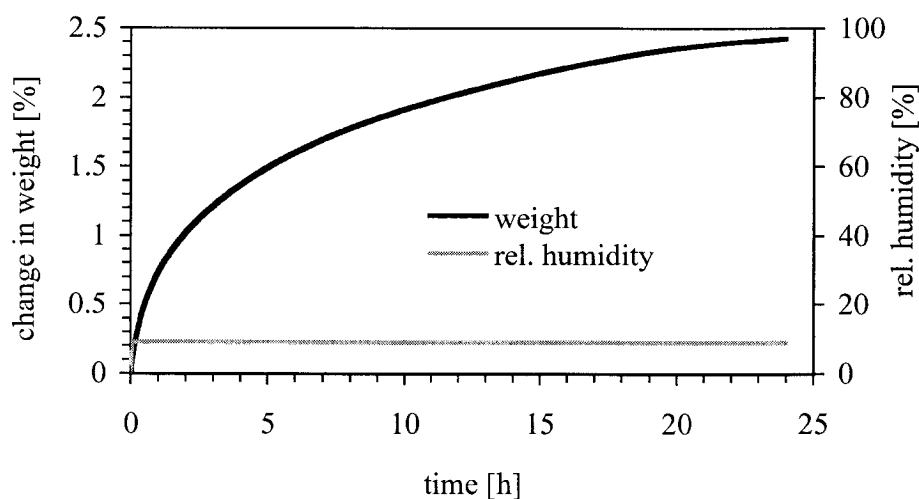
Figure 6-17 Water sorption behavior of amorphous sucrose obtained from freeze drying, T=20°C, 10% r.h.

The amorphous sugar takes up considerable amounts of water without recrystallizing. This shows the highly hygroscopic properties of amorphous sucrose, which has to be taken into account when working with sucrose containing fractions of amorphous material.

In course of chocolate production sugar experiences two major changes.

Starting off with the crystalline and relatively coarse raw material a size reduction is performed first. Thereby the sugar is refined to a particle size below 40μm. Second the sugar surfaces undergo a transition from crystalline to amorphous, which is due to local temperature increase during breakage. Based on the change of particles size and because of the formation of amorphous surfaces, it is expected that the sorption characteristics have changed compared to the sorption characteristic of the raw material. In the following the sorption characteristics of refined sugar will be discussed. Furthermore it will be distinguished

between refined sugar containing amorphous surfaces and refined sugar which had been recrystallized and thus represents a crystalline sugar but with a smaller size than the raw material shown in Figure 6-15.

In order to study the water sorption behavior of pure sugar exhibiting similar particle size like sugar obtained from roll refining, dry ground sugar of different size and state was used. For sorption measurements 3 different samples (A, B, C) were used. Sample A and B (Figure 6-18) exhibit different particle sizes and contain amorphous surfaces. Sample C (Figure 6-19) has a particles size that is between the size of A and B but was recrystallized. Sample C therefore shows the effect of particle's size on water sorption behavior and thus can be compared in this context to the coarse and crystalline raw material (Figure 6-15 and Figure 6-16).

First samples (A and B) are considered which were dry ground in an impact mill to different sizes. During grinding and storage they were kept under a cool and dry atmosphere in order to avoid recrystallization in an early stage of processing. A complete cycle of adsorption, desorption and again adsorption is given in Figure 6-18.
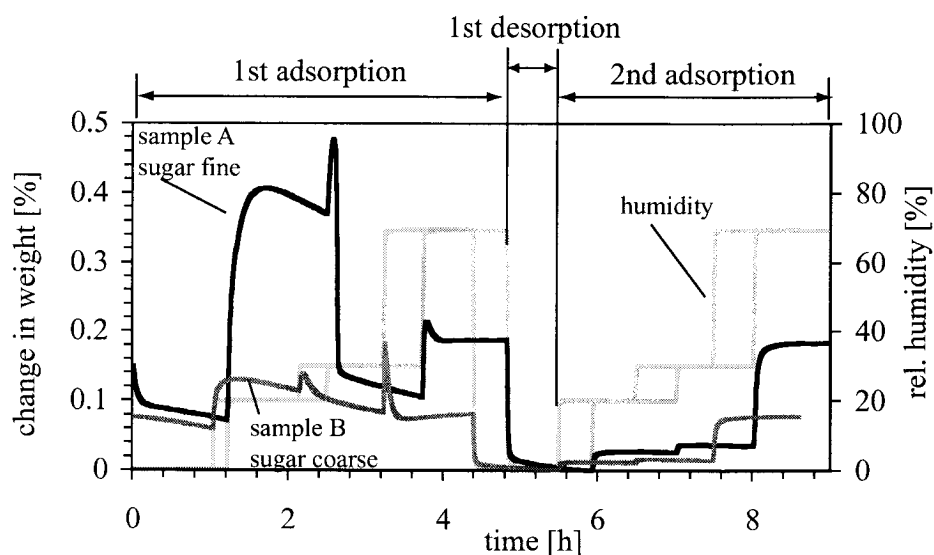
Figure 6-18 Water sorption behavior of dry ground sugar of different size, sample A $(X_{90}=5\mu m)$ and sample B $(X_{90}=37\mu m)$, ground in a dry atmosphere $(20°C, 5\% r.h.)$ and stored at $10°C$ for 8 weeks in sealed containers filled with drying pearls, measurement temperature $T=30°C$

Looking first at sample A, which is a fine ground sample $(X_{90}=5\mu m)$ it can be seen that this sample shows maxima in the water uptake during the 1st adsorption cycle. This proofs the presence of amorphous phases. Comparing the amount of water adsorbed by sample A with sample B it is seen that A adsorbs more water than B. This can be attributed to the different size and the resulting amount of amorphous phases. Sample A was ground to a smaller size and thus more amorphous phase was generated. This is reflected in the first peak which is much higher than for sample B. Looking at the second adsorption cycle the different size and surface area between sample A and B become evident. B is much coarser in size $(X_{90}=37\mu m)$

and thus has a smaller surface area and therefore adsorbs less water at 70% r.h. than sample A. Furthermore it is seen that in the second adsorption cycle no maximum for the weight signal appears which proofs that recrystallization was completed in the first adsorption cycle.

The next sample discussed is sample C. It is dry ground sugar (particle size $X_{90}=16\mu m$) which had been stored for 4 months at room conditions (25°C, 30 to 50% r.h.) in order to achieve recrystallization. Although conditions chosen for recrystallization were in accordance to literature it was not possible to achieve complete recrystallization. The parameters reported in literature also differ significantly. Values about time required for recrystallization are hardly available which makes it rather difficult to choose parameters in a way such as recrystallization is completed and the powdery structure of the product is still maintained.

Figure 6-19 and Figure 6-20 give the water sorption behavior of sample C. First it has to be
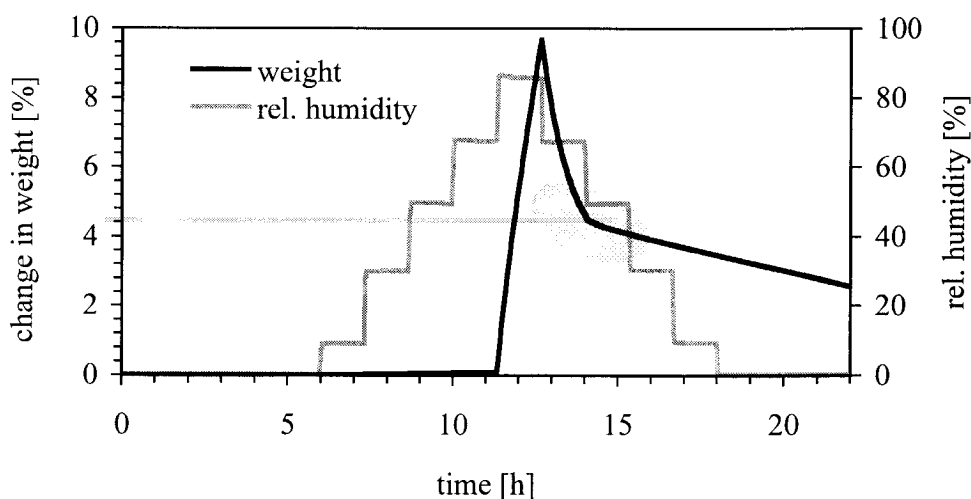
Figure 6-19 Sample C - Water sorption behavior of dry ground and recrystallized sucrose, measurement temperature T=45°C

noted that the measurement was performed at a elevated temperature of 45°C which is 15°C higher than for the ones discussed before. Looking at Figure 6-19 it is seen that for high levels of humidity capillary condensation occurs. In accordance to Figure 6-15 also here desorption follows a different kinetic than adsorption. As the measurement was performed at a higher temperature, the significant change in drying kinetics occur (approaching the glass transition regime) at a lower water content than for the sample shown in Figure 6-15.

An enlarged view of the adsorption process, especially for levels of humidity below 80% r.h. (capillary condensation occurs at 80% r.h.) is given in Figure 6-20. The long lasting initial drying step is required to ensure temperature equilibration. When looking at the amount of water adsorbed by sample C, it is seen that the weight signal exhibits a maximum at a humidity of 70% r.h. and thus still contains amorphous material. The amounts of amorphous phases present is found to be very low. But such small amounts already could have an impact on particle interactions in sugar oil suspensions and thus affect rheological properties and structure. This needs to be taken into account when working with dry ground sugar.
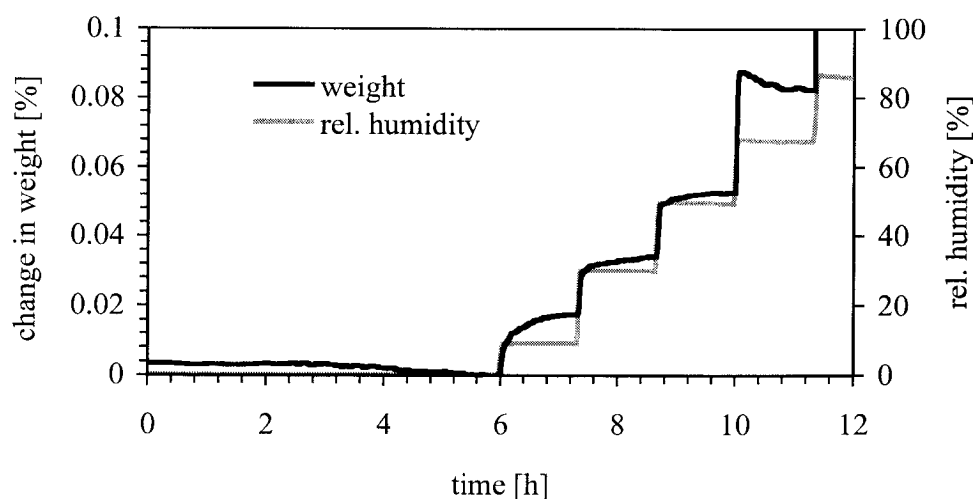
Figure 6-20 *Sample C - Water sorption behavior of dry ground and stored sucrose, measurement temperature T=45°C, enlarged view of Figure 6-19*

Like samples A and B, sample C also has a smaller particle size than the raw material (Figure 6-15).

For a humidity level of 70%, the raw material (see Figure 6-16) adsorbs 0.008% of water, whereas sample B (for the 2nd adsorption cycle) and C adsorb about 0.08% of water. Comparing the amount of water adsorbed by sample B and C to the raw material it is found, that samples B and C adsorb almost 10 times more water than the coarse raw material. The very fine ground sample A adsorbs almost 0.2% of water. This shows how particle size affects the sorption of water.

Both effects, particle size and presence of amorphous phases will influence the amount of water adsorbed and thus become relevant for the rheological properties of sugar (hydorphilic) - oil (hydrophobic) suspensions.

6.2.3   Sugar -Cocoa Butter - Lecithin Mixtures

In course of this work mixtures of sugar cocoa butter and lecithin were used as chocolate like model systems. In chapter 4.5 "Suspensions of sugar - cocoa butter - lecithin" on page 76, it has been seen that the flow properties of these model systems are influenced by the adsorption of water. Therefore it is of interest to study the water sorption behavior of a mixture of sugar - cocoa butter and lecithin. This is the objective of this section.

In chapter 4.5.3 "Influence of lecithin concentration" on page 83, the effect of lecithin concentration on the rheological properties was discussed. Two of the samples used in that trial series were used also for water sorption measurements.

Figure 6-21 gives the water sorption behavior of two sugar cocoa butter lecithin suspensions containing 0.3% and 1.5% of lecithin. It is seen that for increased lecithin concentration the amount of adsorbed water increases. Furthermore it can be seen that the kinetics of adsorption change. The higher the lecithin concentration the longer the time to reach an equilibrium. Looking at the amount of water adsorbed by the sample containing 0.3% of lecithin (0.17%

of water at 70% r.h.) and comparing it to the amount of water adsorbed by a cocoa butter-lecithin mixture (see 6.1.3 "Cocoa Butter & Cocoa Butter - Lecithin" on page 114) it is seen that similar amounts are adsorbed under these conditions. Taking into account that in the sugar - cocoa butter - lecithin mixture only 28% are liquid phase, the liquid phase would only contribute with 28% to the total amount of water adsorbed. From Figure 6-9 on page 117 it is found that a cocoa butter lecithin mixture (0.7% of lecithin) adsorbs about 0.18% of water at 70% r.h. In case of the sugar cocoa butter lecithin mixture, cocoa butter and lecithin would approximately introduce 0.28w/w * 0.18% = 0.05% of water (lecithin concentration is not the same!). The remaining 0.12% (0.17%-0.05%) would have to come fromsugar. The particle size of sugar used here, is in the same range as the sample of dry ground sugar (sample C) discussed in Figure 6-20. The amount of water introduced by sugar would therefore be: 0.08% * 0.72w/w = 0.06%. The calculated amount of water introduced by the components would then be: 0.05% from cocoa butter - lecithin plus 0.06% from the sugar which equals 0.11%. Compared to the actual amount adsorbed (0.17%) 35% of the water are still missing. These estimative calculations indicate that the sorption of water for the mixture is non linear and can not be derived from superimposing the sorption values of the individual components. In which state the water is present (entrapped in micelles, multilayer adsorption, interactions sugar-water-emulsifier) and what sort of phases are formed can not be identified with this method.
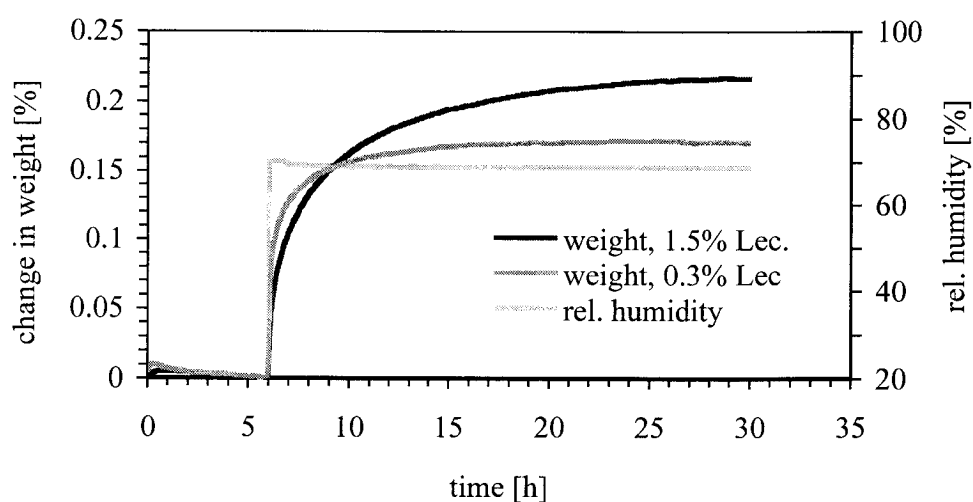
Figure 6-21 *Water sorption behavior of sugar - cocoa butter - lecithin mixtures with different lecithin content, suspension obtained from roll refining and kneading, T=45°C*

6.2.4 Milk Powder

Milk powder is a complex material composed of proteins, lactose, fat and emulsifiers (fat membrane components). From its structure milk powder can be described as a sponge like material exhibiting a large specific surface area. The proteins are capable of binding high amounts of water and lactose can be present in the amorphous state. These physical and chemical attributes give the milk powder its high water sorption capacity. In chocolate, milk powder acts as an internal source for water exhibiting a retarded water release behavior.

In order to study the water sorption behavior of milk powder different types of commercial milk powder were assessed. In a first step the raw materials like obtained from the supplier were used (no grinding has taken place).

Figure 6-22 gives the water sorption behavior of 2 different commercial skim milk powders (A, B). It can be seen that powder A shows a recrystallization peak proofing the existence of amorphous material. Powder B does not develop any recrystallization peak within the time of the experiment and thus it can be concluded that it contains less amorphous material. Both powders adsorb similar amounts of water at the different levels of humidity.
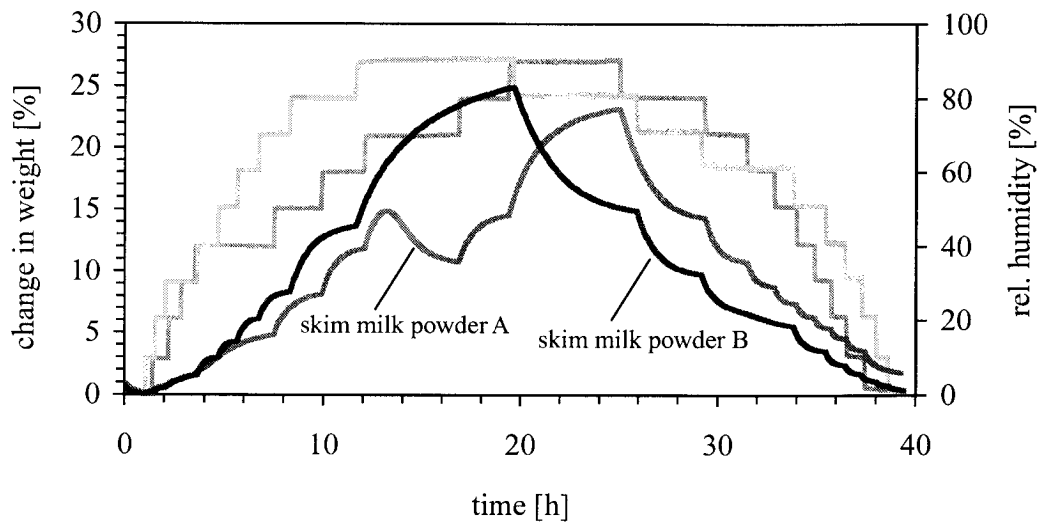
Figure 6-22 *Water sorption behavior of 2 different commercial skim milk powders, T=25°C*

Beside skim milk powder also whey powder is used in chocolate. Whey powder contains more lactose and less protein than skim milk powder.
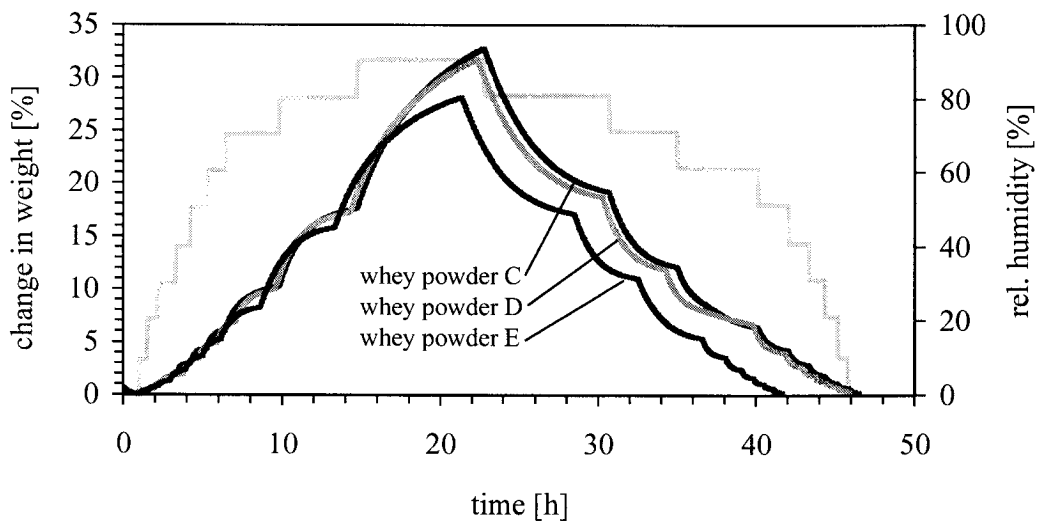
Figure 6-23 *Water sorption behavior of 3 different commercial whey powders, T=25°C*

Figure 6-23 gives the water sorption behavior of 3 different commercial whey powders (C,D,E). It can be seen that none of the powders shows a recrystallization peak within the time frame of the experiment. According to literature (*Saltmarch, M., Labuza, T. (1980), Linko, P. et al (1982)*) recrystallization would be expected and might be observed when exposing the sample to higher temperatures and humidities. Therefore the conclusion that the sample does not contain any amorphous material can hardly be drawn at this stage. Compared to skim milk powders, whey powder adsorbs more water at comparable levels of humidity.

The sorption isotherms looked at so far were measured for the raw material. For processing often mixtures of skim milk and whey powder are used. To see the influence of grinding on the water sorption behavior a mixture of skim milk and whey powder was prepared and ground in a dry milling device (jet mill) applying a dry atmosphere. The particle size of the powder ($X_{90}=35\mu m$) was similar to the particle size of milk powder present in roll refined chocolate flakes.

Figure 6-24 gives the water sorption characteristics of a dry ground milk powder mixture.
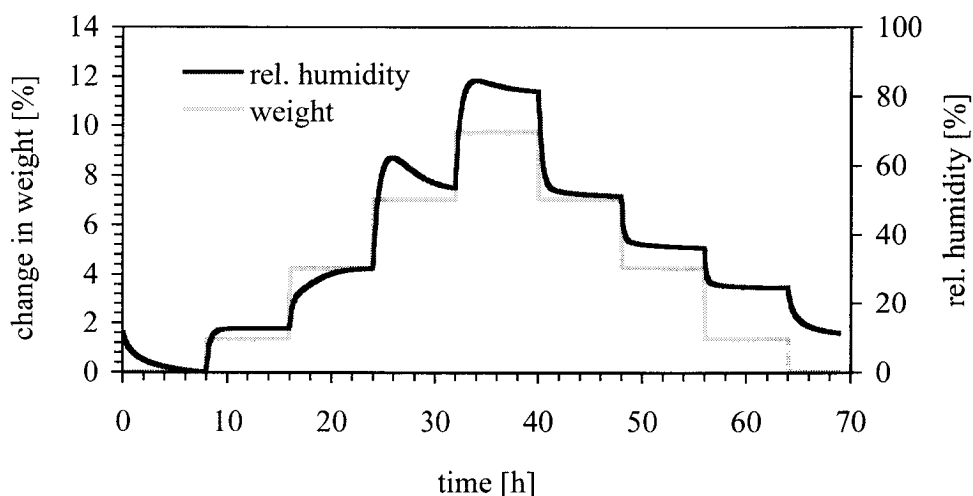
Figure 6-24 *Water sorption behavior of a milk powder mixture (75% w/w skim milk and 25% w/w whey powder), ground in a jet mill applying dry conditions and stored in a cool and dry atmosphere, measurement temperature T=30°C*

During adsorption two maxima can be detected showing the presence of amorphous lactose which was either generated during grinding or had been partially present in the raw material. Recrystallization takes place at levels of water content that are 100 times higher than for sucrose. Furthermore desorption is not complete and water remains in the sample. Depending on the conditions, amorphous lactose can recrystallize as α-lactose mono hydrates and thus contains 1 mol of water bound as crystal water. It is also reported (*Saito, Z. (1988), Bouzas, J., Brown, B.D. (1995), Drapier-Beche, N. et al. (1997), Jouppila, K. et al (1997), Kedward, C.J. et al (1998)*) that lactose can recrystallize as α-lactose or as β-lactose or as a mixture of α-lactose mono hydrate and β-lactose. If measurement conditions could be defined such that only α-lactose mono hydrate is formed, the amount of amorphous lactose could be calculated. The calculation is then based on the difference in weight resulting from

the crystalline water. The difference in weight between initial drying step and final drying step yields the amount of water and thus the amount of newly formed α-lactose mono hydrate which is equivalent to the amount of formerly present amorphous lactose (on a molar basis).

6.2.5   Cocoa Liquor

Cocoa liquor is obtained from grinding of deshelled and roasted cocoa beans. It is composed of cocoa butter and cocoa solids. Chemically it is a mixture of mono-, di,-, triglycerides, proteins, cellulose, starch, water, minerals, polyphenols, phospholipids and other organic compounds present in minor quantities. From its composition it is even more complex than milk powder and contains several compounds that can adsorb large amounts of water.

Figure 6-25 gives the water sorption characteristics of cocoa liquor. The cocoa liquor used here was obtained from deshelled, roasted and fine ground cocoa beans (Ivory coast), exhibiting a particle size of $X_{90,3} < 25 \mu m$, a water content of 1% w/w (Karl Fischer) and a fat content of 54.5% w/w.
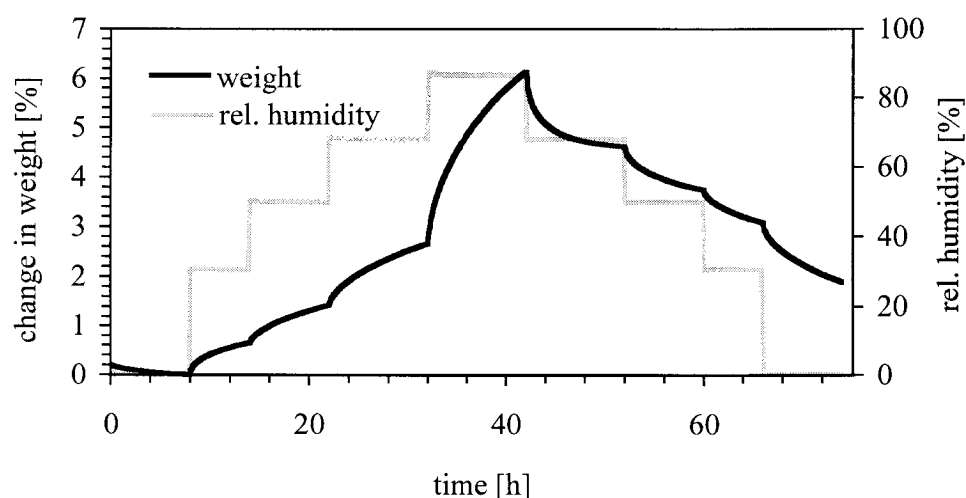
Figure 6-25 *Water sorption behavior of cocoa liquor, Ivory coast, $X_{90,3} < 25 \mu m$, $T = 45°C$*

Adsorption and desorption of water is taking place on a long time scale without reaching an equilibrium. For a high level of humidity water uptake increases steeply which is expected to be caused by capillary condensation. The amount of water absorbed is higher than for chocolate but lower than for milk powder. It has to be taken into account that the amount of fat free and dry solids in skim milk powder is twice the amount of fat free and dry solids in cocoa liquor. Recalculating the amount of adsorbed water on the basis of fat free dry matter shows that for humidity levels below 70% r.h. cocoa liquor adsorbs similar amounts of water as skim milk and whey powder (for this approximate comparison the contribution of cocoa butter can be neglected).

The comparison based on fat free dry matter (derived from calculation) between milk powder and cocoa liquor is given in Figure 6-26. Like milk powder, cocoa liquor acts as an internal source for water in chocolate which has to be taken into account when assessing amorphous crystalline state transitions as well as glass transitions.
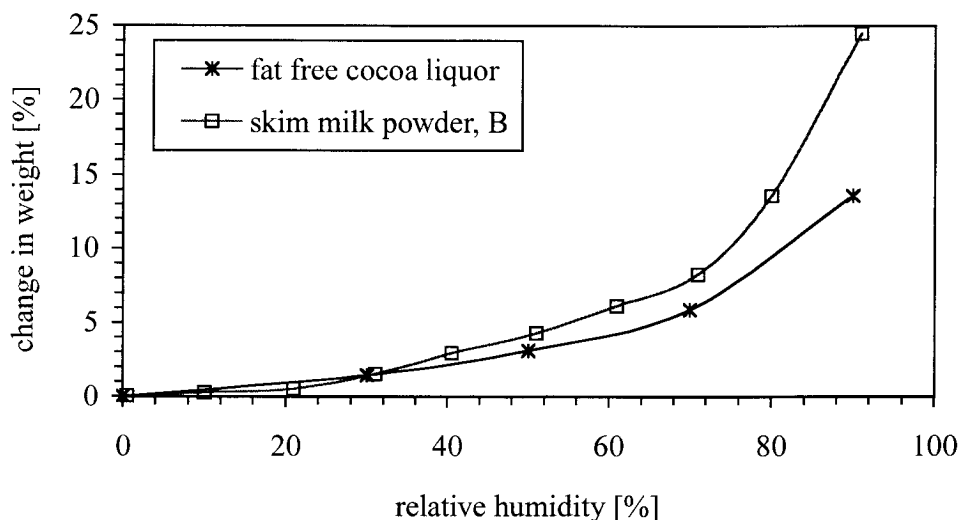
Figure 6-26 Sorption isotherm- comparison between skim milk powder and cocoa liquor based on fat free and dry matter (calculated), T=30°C for milk powder and 45°C for cocoa liquor. Note-points shown here correspond to the endpoints of the sorption measurements (Figure 6-23, Figure 6-25) and do not necessarily represent equilibrium values!

6.2.6 Summary

The disperse phases sugar and limestone adsorb water in quantities below 0.1% w/w. For high levels of humidity (70% r.h. and higher) capillary condensation occurs which irreversibly alters the structure of the product. This is seen in the difference between the sorption isotherms for the first, second and third sorption/desorption cycle. In case of sugar, sucrose is dissolved in the water and a concentrated solution is obtained that solidifies in the glassy state when desorbing the water. For low relative humidity (10% r.h.) amorphous sucrose adsorbs high amounts of water without recrystallizing. For higher levels of humidity recrystallization is observed.

In ground sucrose amorphous phases are present. Being exposed to a warm and humid atmosphere (30°C, 20% r.h. up to 70% r.h.) these amorphous phases recrystallize within 30 to 60 minutes. Mixtures of sucrose-cocoa butter and lecithin show a retarded sorption kinetic. This is due to the reduced diffusibility of water in the cocoa butter matrix. An increase of the lecithin concentration causes an increased adsorption of water which was already found for the continuous phases. The water sorption behavior of the suspensions is thereby dominated by the sorption characteristics of cocoa butter and lecithin, rather than by sucrose.

The disperse phases milk powder and cocoa liquor are composed of several components which can adsorb large quantities of water (proteins, cellulose, starch). For milk powder amorphous phases are found which are attributed to the presence of amorphous lactose. For whey powder it was found that it adsorbs more water than skim milk powder which is most probably related to the specific protein compositions.

Cocoa liquor is a suspension of solids dispersed in cocoa butter. Water sorption in this system therefore takes longer than for milk powder. In respect to the total amount of water adsorbed it was found that on the basis of fat free systems both, milk powder and cocoa liquor adsorb similar quantities of water.

7 Microstructure - Glass & Phase Transition

7.1 Conditions for Recrystallization

In the previous chapters the importance of recrystallization and thus the transition from amorphous to crystalline was shown. In this section conditions under which such transitions can occur are discussed. To model the behavior of amorphous sucrose present after refining amorphous sucrose obtained from freeze drying was used. Employing the sorption balance the amorphous sucrose was then exposed to various conditions causing recrystallization. These conditions were chosen in accordance to conditions present during chocolate production.

Amorphous sucrose was obtained form freeze drying. Therefore a sucrose water solution was prepared (12%w/w sucrose) and added drop wise into liquid nitrogen where the solution was instantaneously frozen. During freeze and post drying most of the water was removed. Samples with different amounts of water (from below 0.2% up to 6% w/w) were obtained and used for further testing. Detailed methods on how to prepare amorphous sucrose by freeze drying are described elsewhere (*Van Scoik, K.G., Carstensen, J.T. (1990), Saleki-Gerhardt, A., Zografi, G. (1994)*).

In a first trial series a sample of well dried amorphous sucrose (water content <0.5% w/w) was exposed to different levels of humidity at different temperatures (30°C and 50°C). Figure 7-1 gives the weight of the sample as a function of time. It can be seen that elevated
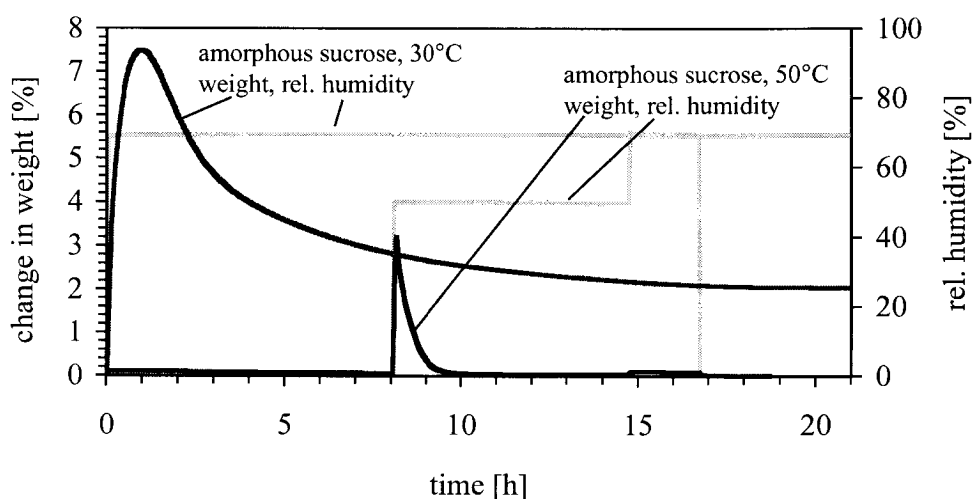
Figure 7-1 *Recrystallization of amorphous sucrose at 30°C and 50°C, powder obtained from freeze drying*

temperatures increase the kinetics of the amorphous - crystalline transition. For 30°C and a humidity of 70% r.h. take up of water and release is taking place on longer time scales than at 50°C and 50% r.h. This is expressed by the broader peak shown by the sample exposed to 30°C and 70% r.h. It can be concluded that although humidity was higher the process takes longer due to lower temperature. Furthermore it is seen that once the sample is exposed to a humid atmosphere rapid water adsorption is taking place. The weight reaches a maximum and drops again. Adsorption is thereby occurring with a different kinetic than the release of water. This is because in the beginning no water was adsorbed to the sample and the gradient of concentration was high. During recrystallization the water is already present at the surface of the sucrose and the gradient to the surrounding, humid media is lower which yields a lower rate of mass transfer.

In a next step the amorphous sucrose was mixed with 50% w/w seasand to avoid caking and related encapsulation of amorphous sugar. To this mixture cocoa butter and lecithin were added. Mixing was performed in dry atmosphere (glove box) yielding a mixture of 35% sucrose, 35% seasand, 29.7% cocoa butter and 0.3% lecithin. This mixture was then exposed to different levels of humidity at a temperature of 50°C. Different to the sample used before, the sample considered now is of paste like structure and thus accessibility of the amorphous sugar by free water has been reduced.

Figure 7-2 gives the water uptake/release as a function of time. In the beginning drying takes place. During this step water from the ingredients is released. As soon as water is provided in the surrounding atmosphere the sample picks it up. Different to Figure 7-1 adsorption takes longer and the peak is much broader. This is due to the decreased mass transfer coefficient owing to the paste like structure whereas before the sample exhibited a powder like structure. Recrystallization is now limited by the transport of water from the ambient air through the liquid matrix to the amorphous sucrose. Before no such barrier existed. This tendency is even more pronounced during the release of water.
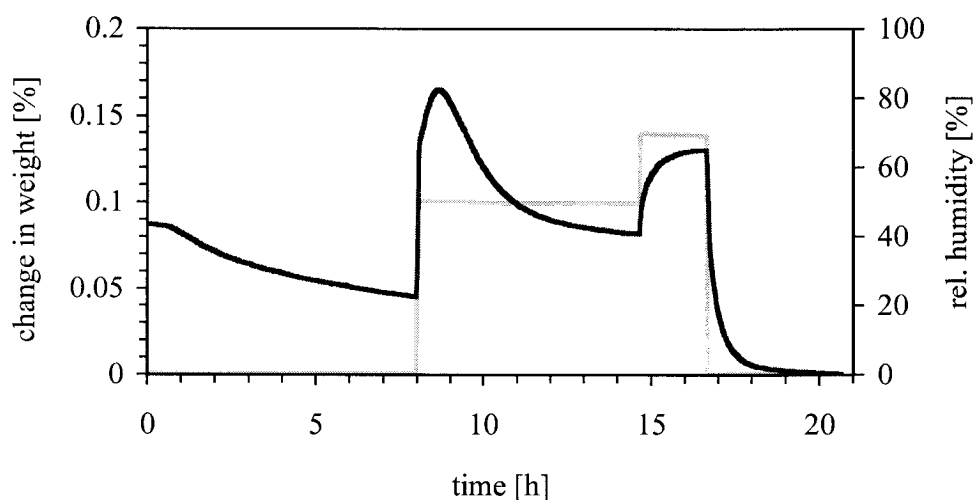
Figure 7-2 Recrystallization of a mixture of amorphous sucrose, seasand, cocoa butter and lecithin at T=50°C, suspension prepared with freeze dried amorphous sucrose powder

The water sorption behavior of both type of samples, i.e. the sample with the powder like structure and the sample with the paste like structure, is given in Figure 7-3.
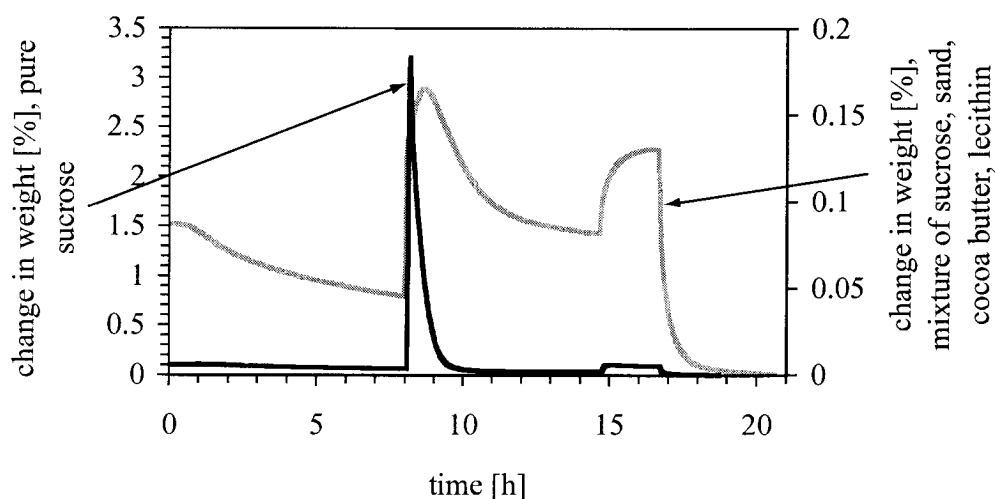
Figure 7-3 *Recrystallization of a mixture (suspension) of amorphous sucrose, seasand, cocoa butter and lecithin at T=50°C compared to pure amorphous sucrose (powder), humidity profile see Figure 7-1 and Figure 7-2. Note: different scales are used!*

The direct comparison illustrates the importance of structure for the kinetics of recrystallization. In the powder like state (gas - solid) the "reaction" of recrystallization is controlled by the inner transport rate (diffusion of water in the amorphous matrix) and takes place on a shorter time scale (narrow peak). In the suspended state (pastes, liquid, solid-liquid) the reaction of recrystallization is controlled by the mass transport rate through the liquid phase to the amorphous surfaces and thus takes much longer (broad peak).

7.1.1   Heat Induced Recrystallization

Recrystallization observed so far, always took place in the presence of water. It is also possible that purely heat induced recrystallization can occur. There mobility of the molecules is increased because of increased temperatures. Recrystallization depends upon the temperature of the product, its glass transition temperature, and melting temperature (*Kedward, C.J. et al (1998), Saleki-Gerhardt, A., Zografi, G. (1994), Roos, Y., Karel, M. (1992)*). In order to check if heat induced recrystallization occurs under certain conditions, amorphous sucrose was mixed with seasand (50% w/w) and exposed to different temperatures. The conditions (time and temperature) applied in this experiment thereby reflect the conditions applied during manufacturing of chocolate. The sample of amorphous sucrose used here was not well dried and did contain water. The water was removed in course of the experiment.

Figure 7-4 gives the change in weight as a function of time. In the beginning a temperature of 25°C and a dry atmosphere of 0% r.h. were applied to the sample. At such conditions amorphous sucrose is in the glass like state and the rate of evaporation is very low. It is seen that the sample slowly releases the water at these conditions. After 48h the temperature was increased from 25°C to 80°C within 4h and the dry atmosphere was maintained. As a consequence the rate of evaporation increased steeply. This can be explained by the fact that at these conditions amorphous sugar transforms into the rubbery state (high molecular mobility) which accelerates mass transport processes. This has not only an impact on evaporation
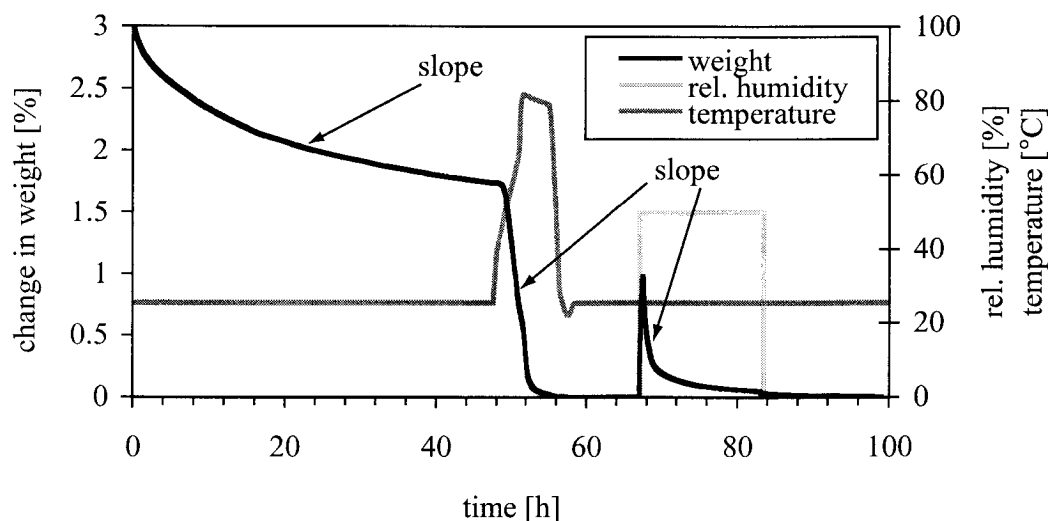
Figure 7-4 *Heat induced recrystallization of an amorphous sucrose/seasand mixture*

but also on recrystallization which can take place in parallel to evaporation. Both will be recorded as a loss of weight and can hardly be separated at this stage. In order to allow for purely heat induced recrystallization, the sample was then kept at 80°C for 4h. At 80°C amorphous sucrose (100% sucrose, no water present) is in the rubbery state and recrystallization is driven by the ratio of temperature difference between sample temperature and glass transition temperature to the difference between melting temperature and glass transition temperature. Heat induced recrystallization will not be expressed by a change in weight and consequently can not be directly detected in the sorption balance. Therefore sorption tests have to be performed at conditions such that changes in weight can be detected.

In case of sucrose it was found that 25°C and 50% r.h. are conditions at which recrystallization kinetics are not too fast and recrystallization can be easily proven. In order to check whether recrystallization was completed during heating and holding of the sample at 80°C, water sorption tests were performed at 25°C and 50% r.h. After temperature had equilibrated, the water sorption measurement was performed. It can be seen that although high temperatures had been applied still amorphous phase fractions are present. This shows that for pure sucrose, the conditions applied were not sufficient to cause complete recrystallization. Temperatures at levels of 80°C are commonly applied in the conching process. Application of such temperatures (20°C above glass transition temperature of pure sucrose) are not sufficient to ensure complete recrystallization of sucrose. This shows that in such a case water is required in order to increase molecular mobility and thus to enable recrystallization.

To demonstrate what effect internally available water has on recrystallization and recrystallization kinetics, further trials with amorphous sucrose were performed and are discussed in the following.

Two samples (A, B) of amorphous sucrose were prepared containing different amounts of water. Both sample were sourced from the same batch of freeze dried material, but sample B was dried further in a post drying process and sample A not. Both samples were analysed in the sorption balance. There first a drying phase took place which was followed by humidification in order to allow for recrystallization. The result of the sorption measurement is given

in Figure 7-5. The conditions applied in the beginning of the measurement (50°C and 0%r.h.) first lead to a further drying of the samples. Looking at sample A it is seen that sample A has a higher water content than sample B.
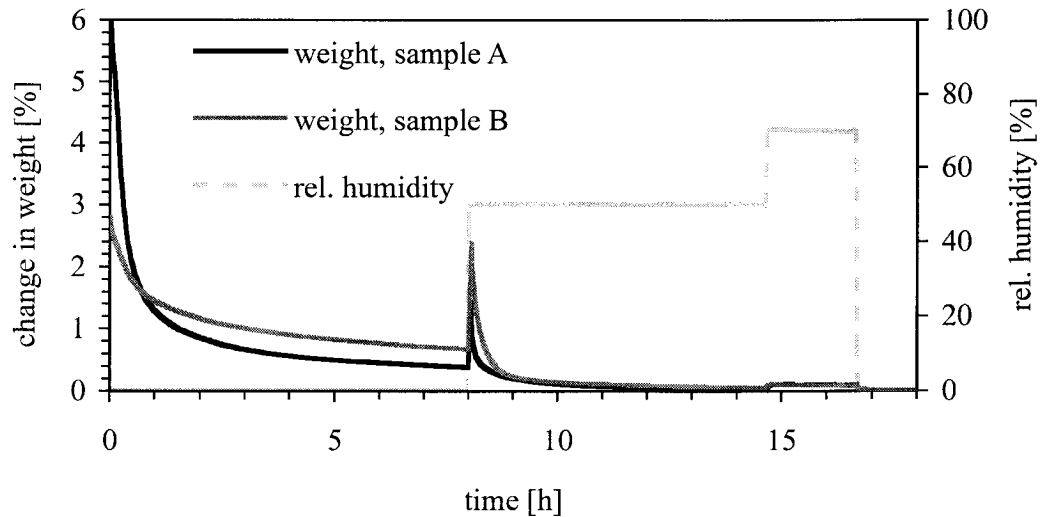
Figure 7-5 Drying kinetics and recrystallization in relation to the presence of "inner" water, amorphous sucrose powder, measured at a temperature of 50°C

During the first hour sample A exhibits a steep decrease in weight which appears to be almost linear, indicating a constant rate of evaporation. Then the curve starts to level off, hence drying is slowed down. In course of the measurement the sample was then exposed to different levels of humidity. The sample takes up water, weight increases, passes a maximum and rapidly releases the water when recrystallizing. It seems that the loss of weight during recrystallization exhibits a similar pattern like for the initial drying step. This indicates similar drying rates and thereby similar mechanisms behind. This will be considered more detailed later in this section.

Looking at sample B, which is of the same origin as sample A but was post dried following to freeze drying, it is seen that in the initial desorption step, drying follows a different kinetic than for sample A. Applying a humid atmosphere of 50% r.h. results in a fast water uptake followed by recrystallization. Thereby sample B adsorbs significantly more water than sample A. This indicates that sample B contained more amorphous material than A although they are of the same batch of production.

In order to discuss the different behavior of sample A and B and to understand the related mechanisms, the rate of evaporation for the different samples will be considered.

Figure 7-6 gives the change in weight and the derived values for the rate of evaporation for sample A during the initial drying step in the sorption balance. It can be seen that in the beginning the rate of evaporation (slope of the "weight vs. time" curve) shows some scattering around a constant value. The data points reflecting the change in weight can be fitted in this region by a straight line which corresponds to a constant rate of evaporation. A constant rate of evaporation is given, when the evaporation is not limited by inner mass transport, i.e.

there is enough fluid available at the surface or interface. It is assumed that this can only be fulfilled if water is provided by some internal release and feeding mechanisms. Such a mechanism is recrystallization. When sucrose recrystallizes there is no space for the water in the sugar crystal and as a consequence the water is expelled. The water is then available as free water which can easily evaporate. Therefore it is concluded that sample A starts to recrystallize during this initial phase of drying, and consequently constant rates of evaporation are found.
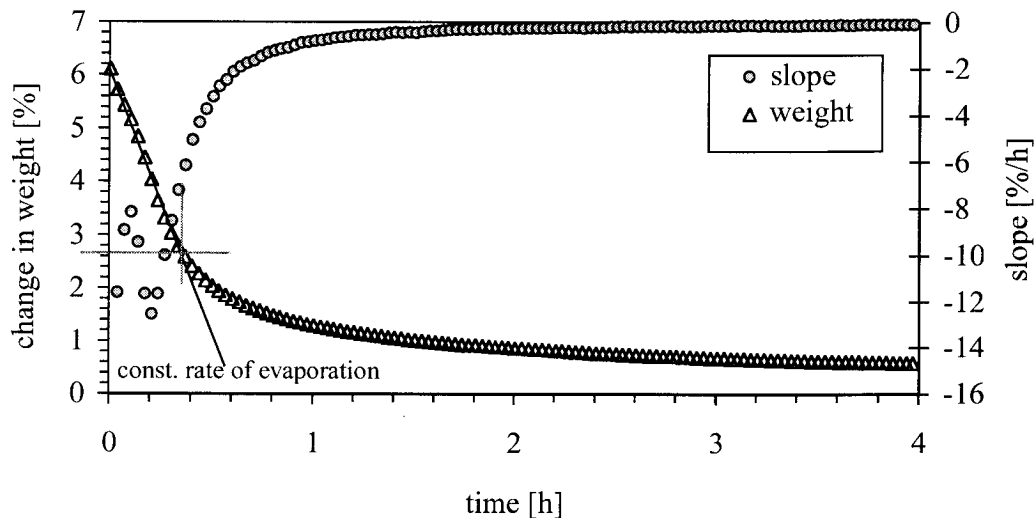
Figure 7-6 Rate of evaporation for sample A at a temperature of 50°C

From a certain point on the weight does no longer change in a linear manner but follows more an exponential like relationship. This is also expressed in the data points giving the slope or the rate of evaporation. The slope/rate of evaporation exponentially approaches zero. The reason for this significant and abrupt change in evaporation rates can be attributed to the effect of glass transition and its impact on molecular mobility, i.e. a slow down of mass transport processes. To better explain this the water content of the sample has to be considered. As illustrated in Figure 7-6 the rate of evaporation is reduced as soon as a water content of 2.5% to 3% and lower is reached. The temperature of the sample thereby is 50°C. Comparing these parameters to the glass transition temperature of sucrose solutions it is found that at a glass transition temperature of 50°C corresponds to a water content of 1.7% whereas a water content of 2.5% corresponds to a glass transition temperature of 40°C. This means that at the point where drying is slowed down, the sample has a glass transition temperature of 40°C which is 10°C below the sample's temperature. From literature and practise it is well known that drying of glass like substances is most effective as long as the product temperature is approx. 10°C above the sample's glass transition temperature. For bigger temperature differences, effects like collapse of the structure occur and for smaller differences mass transport is significantly reduced (*Hartel, R. W., Shastry, A.V. (1991), Witschi, F. (1999)*). When approaching water contents lower than 2.5%, the difference between product temperature and glass transition temperature is getting smaller, i.e. mass transport and thus rate of evaporation is significantly reduced.

7.1.2   Recrystallization Phenomena in Milk Chocolate

In the previous section it was shown that amorphous sucrose can only be fully recrystallized if both water and thermal energy are provided in a sufficient manner. In case of amorphous sucrose it was found that application of elevated temperatures (which had been similar to temperatures that are applied during conching, T=80°C) without providing a humid atmosphere is not sufficient to achieve complete recrystallization (see Figure 7-4). The presence of water was found to be crucial for recrystallization. In contrast to sucrose, milk chocolate is a multi component system in which ingredients are present that act as an internal source for water (milk powder, cocoa liquor). Therefore the effect of internally available water, provided by the ingredients, on the thermally induced recrystallization of chocolate was assessed. For this trial, chocolate flakes were prepared (mixing and refining) under dry conditions. The so prepared chocolate flakes did contain amorphous phases which was proven through water sorption measurements, see Figure 7-7. The amorphous phases that are found
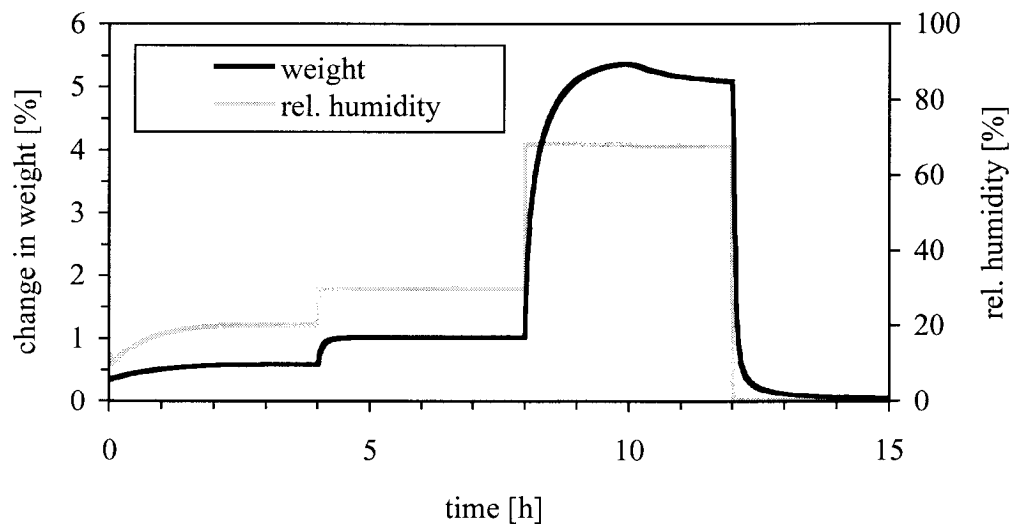
Figure 7-7 *Water sorption measurements of milk chocolate flakes, amorphous phases present, T=45°C*

in milk chocolate do result from sucrose and lactose (milk powder).

The chocolate flakes that contained amorphous phases were placed in the sorption balance and a temperature profile was applied similar to the conditions present during conching. Therefore the sample was heated up to 80°C (measurement chamber had been preheated) and was kept at that temperature for 2h whilst dry atmosphere had been applied. Afterwards the sample was cooled down to 45°C and exposed to different levels of humidity to check for the presence of amorphous phases. The whole cycle is given in Figure 7-8.

It can be seen that no amorphous phases could be detected after temperature treatment. It can be concluded that the amorphous phases have already transformed into the crystalline state during the high temperature treatment. In the previous section, a similar treatment was carried out with a sugar oil mixture. There amorphous phases could still be found although high temperatures had been applied. The difference in behavior, is due to the presence of ingredients that act as an internal source of water. The ingredients present in milk chocolate (milk powder and cocoa) provide the water which is required by the sugar in order to recrystallize.
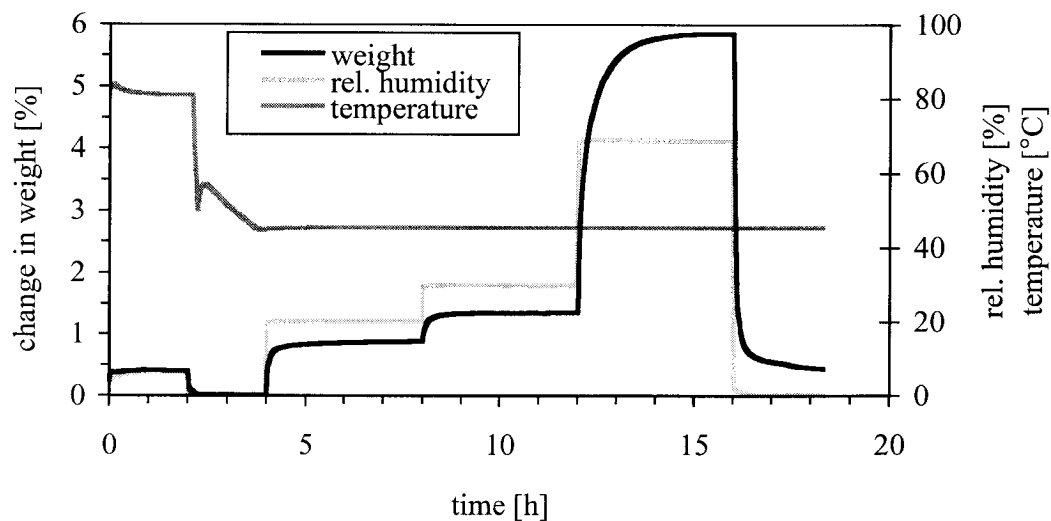
Figure 7-8 Water sorption measurement of milk chocolate flakes and heat treatment

As particle packing density is rather high, the length of diffusion is short and water is delivered on short time scales in sufficient quantities to the amorphous material. In case of milk chocolate, enough water is internally available that is provided from the ingredients. Therefore transport of water to the amorphous material can hardly be controlled and application of a dry atmosphere would not help in that case. Consequently the amorphous material recrystallizes during the time it is exposed to high temperatures (80°C). This shows that if enough water is provided (water content of milk chocolate flakes is on average 1.2% w/w), recrystallization takes place on short time scales (2h) at elevated temperatures. The relationship between water content, and temperature, and time is of special importance for recrystallization.

Along with water uptake of the amorphous material, a change in the structure of the material is observed. This is due to lowering of the glass transition temperature, i.e. softening of the structure. This is of special relevance to milk powder and its structural changes during manufacturing of chocolate which is subject of the next chapter.

7.1.3 Milk Powder

Milk powder for usage in chocolate is commonly obtained from spray or roller drying. These processes were designed to transfer milk into a shelf stable product that can be reconstituted back to milk through addition of water. Milk powder as produced for the time being is designed for optimum usage in water based systems but not for fat based systems. Consequently the properties of milk powder can be further optimized for usage in fat based systems like chocolate. Some aspects that need to be taken into account when using milk powder in chocolate manufacturing are mentioned below. The most obvious factor is the microstructure (*Buma, T.J., Henstra, S. (1971), Roetman, K. (1979)*).

Depending on the drying (roller drying, spray drying) process used for milk powder manufacturing, different structures are obtained (*Kalab, M. (1979), Caric, M. , Kalab, M. (1987).* Often people have tried to link that structure to the structural and rheological properties of chocolate but the reported results do not give a clear picture (*Dewettinck, K. et al. (1996), Attaie, H., Braun, P., Breitschuh, B. (1998), Tscheuschner, H.D. et al. (2000)*). One reason for this is that microstructure of the raw material and thus the structure present before refining, was tried to be linked to properties obtained after processing, i.e. refining. To really determine the influence of microstructure of the individual components on the structural and rheological properties of the processed product, the micro structural changes occurring during processing (refining) need to be considered.

7.1.3.1 Microstructure and Grinding

The process which significantly alters the structure of all components is grinding. To grind solids or solid liquid mixtures different processes can be used. In case only solids are ground dry grinding can be used (impact mills or jet mills). If solid-liquid mixtures are ground it depends upon the fluidity whether roll refining or ball milling is used. In the food area, ball milling is applied if the sample is rather liquid and viscosity does not change too much during grinding.

Roll refining is a process suitable for paste like material. Of all the grinding processes mentioned here, in roll refining the largest deformation and compression occur. It is therefore expected to change the structure to a greater extent than for example impact or jet milling. Furthermore the volume concentration of solids in the grinding zone is high in case of roll refining. This means that during breakage particles are closely surrounded by other particles which causes the formation of press agglomerates. That is not the case for dry grinding in impact and jet mills.

In the following the microstructure of different milk powders is considered. The milk powders were assessed before grinding and some examples are shown after different grinding processes had taken place. For the unrefined powder, microstructure was assessed by cryo SEM (scanning electron microscopy). In some cases the product was also defatted with super critical CO_2 and then assessed with conventional SEM.

All milk powders used are commercially available powders and the following types were analyzed.

Whole milk powder, spray dried, high free fat - Type A

Whole milk powder, roller dried, high free fat- Type B

Whole milk powder, spray dried, low free fat- Type C

Skim milk powder, spray dried- Type D

Skim milk powder, spray dried- Type E

The powders differ in the way they were produced and consequently in their microstructure.

Figure 7-9 shows the microstructure of a high free fat whole milk powder. The powder has a highly porous structure. Lumps of fat are sticking to the outside of the powder particles. This explains the high free fat content of 90% (value reported by supplier). The surrounding matrix results from the frozen glycerol which was used for fixation.

380μm

189μm

94μm
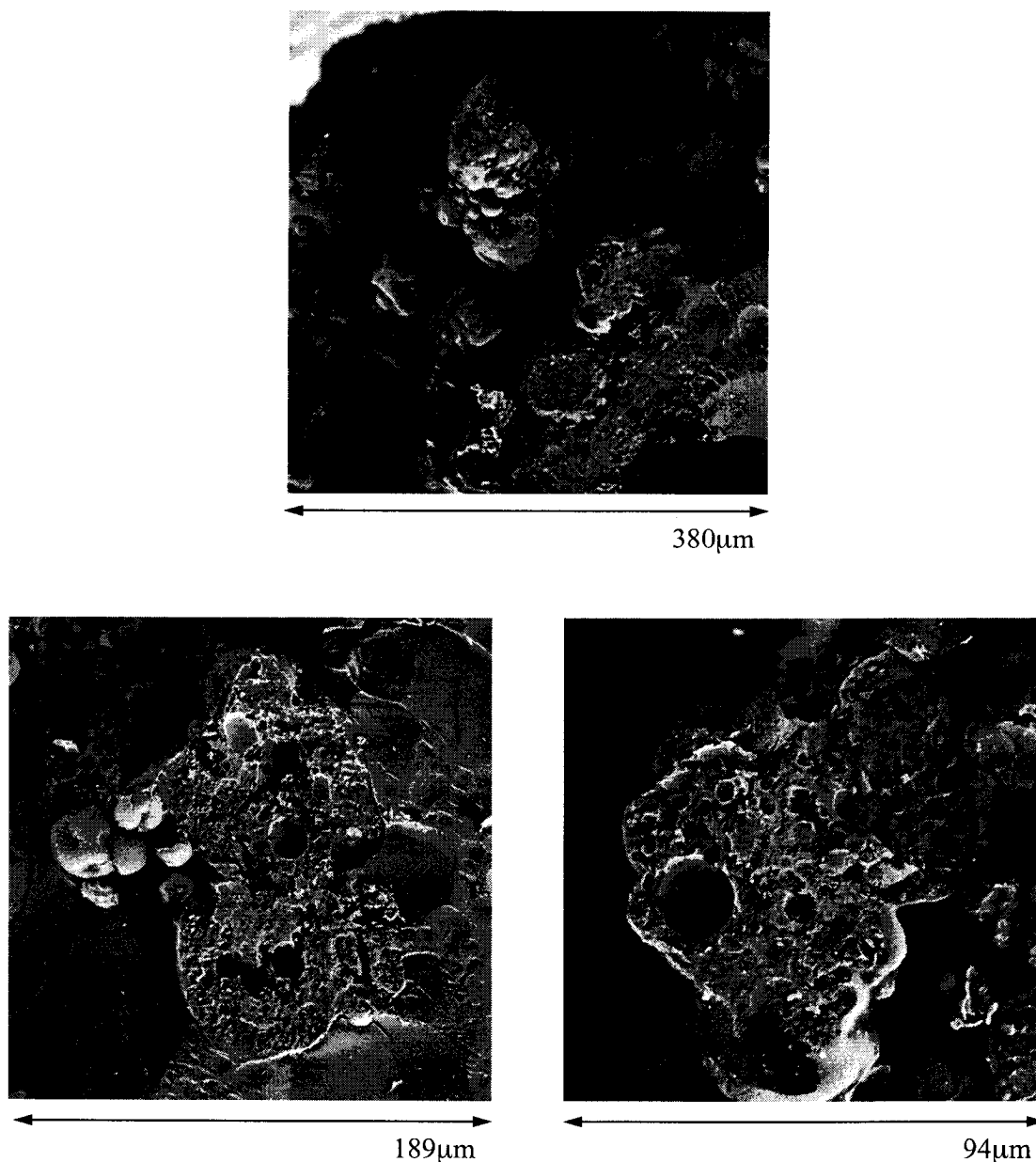
Figure 7-9 Whole milk powder A, spray dried, high free fat, cryo SEM

Figure 7-10 gives the microstructure of a roller dried whole milk powder (B). The typical flake like shape is seen. The inner structure appears to be dense and less porous.

380μm   105μm
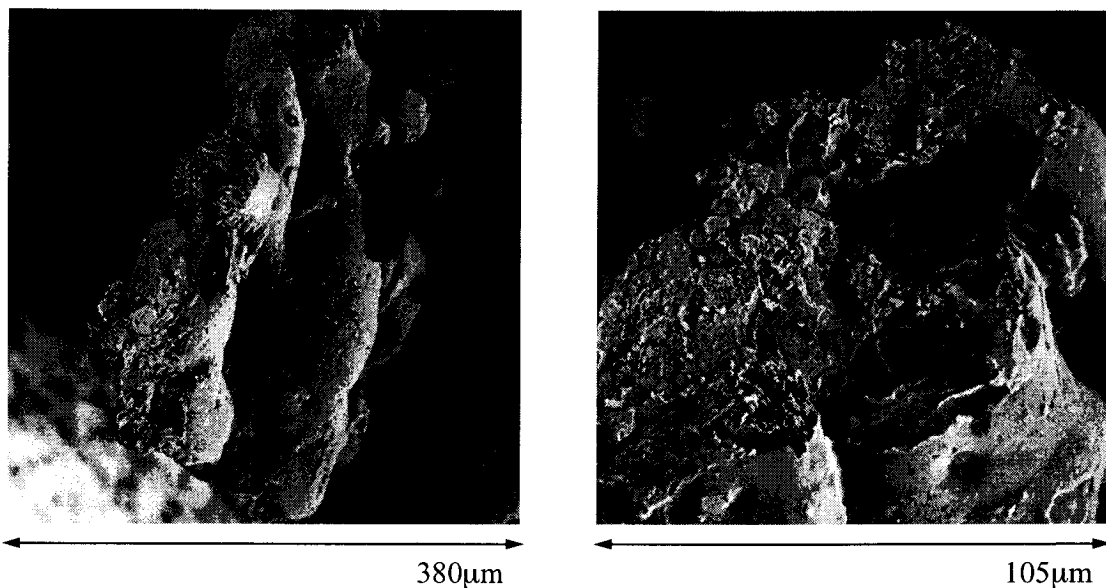
Figure 7-10 Whole milk powder B, roller dried, cryo SEM

Figure 7-11 shows the microstructure of a spray dried whole milk powder (C) that exhibits a low free fat content. In contrary to Figure 7-9 no "lumps" of fat sticking to the outside of the particle were found. Fat droplets are found to be present in the powder matrix. In general the powder shows a highly porous structure.

Figure 7-12 gives the structure of a skim milk powder (D) analyzed by non-cryo SEM. Pictures a to b show the outer structure of the powder. When crushing the powder manually, the interior structure becomes visible (c, d). The powder is also highly porous but different to the whole milk powders the matrix itself is not porous but dense.

380μm

118μm

19μm

37μm
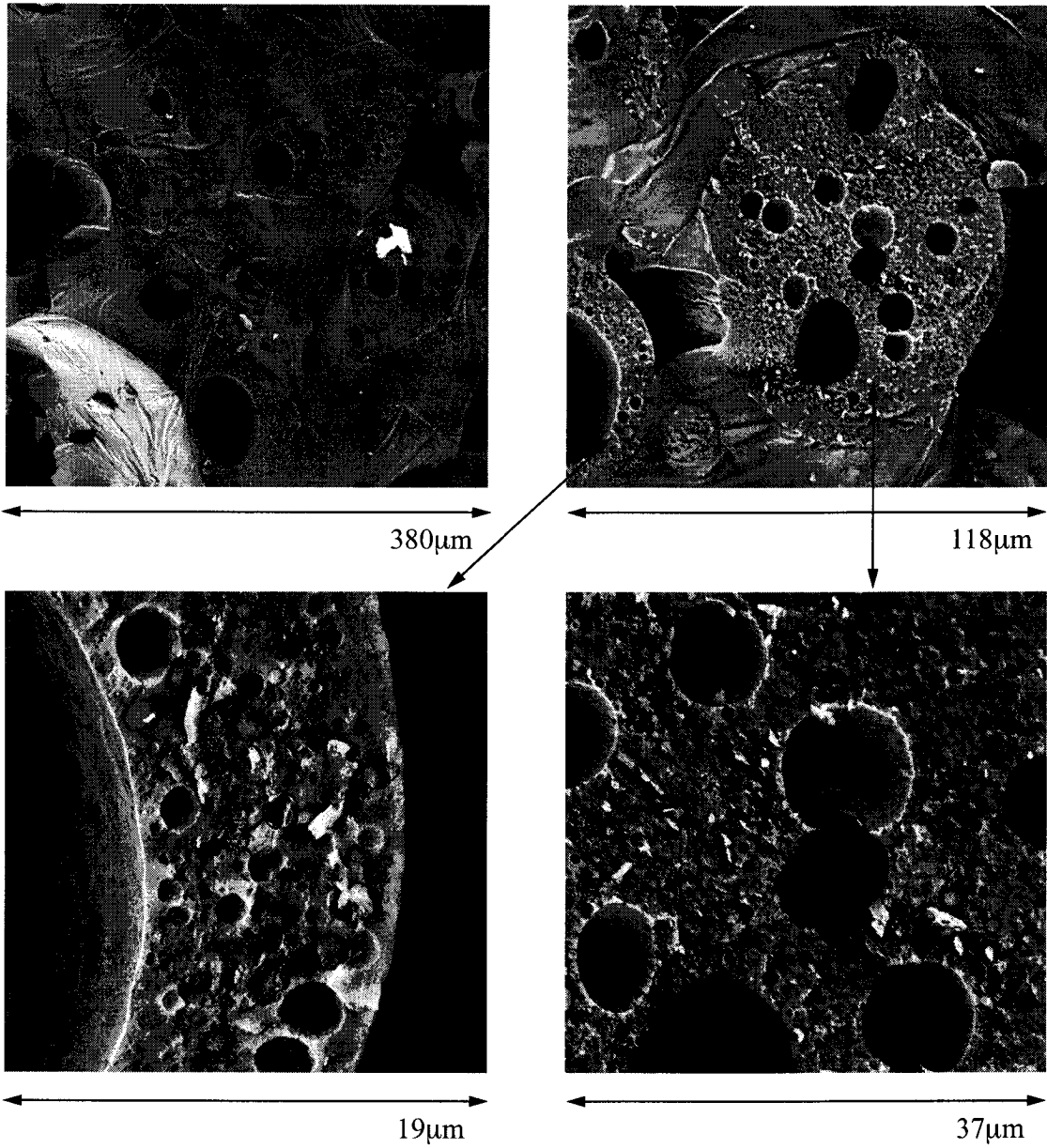
Figure 7-11 Whole milk powder C, spray dried, low free fat, cryo SEM

a   350μm

b   69μm

c   69μm

d   46μm
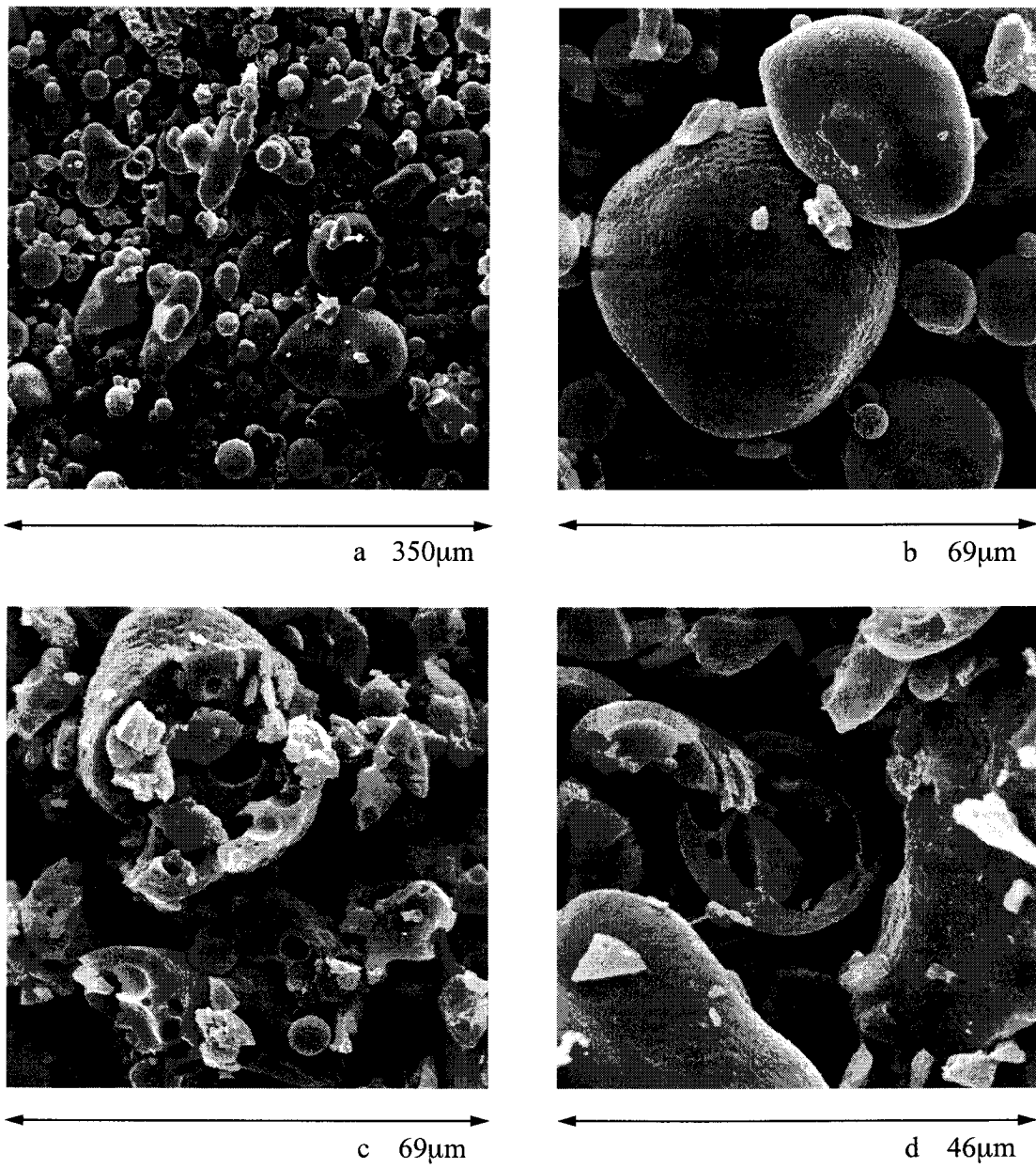
Figure 7-12 Skim milk powder D, spray dried; a, b intact powder; c, d manually crushed

Influence of Grinding

In order to assess the influence of different grinding processes on the structural changes of the different milk powders, the powders were ground in different machineries and their microstructure was analyzed by non-cryo SEM.

The whole milk powder type A was mixed with 25% of vegetable fat and ground in a laboratory 3 roll refiner. The temperature of the rolls was set to 30°C. Sample preparation and refining were done at room conditions (25°C, 40% r.h.). After grinding the powder was defatted using supercritical CO_2 extraction, mounted with double sided tape on the sample holder and observed by conventional SEM. Figure 7-13 gives the structure of whole milk powder type A like it is present after roll refining.

174μm

69μm

35μm

17μm
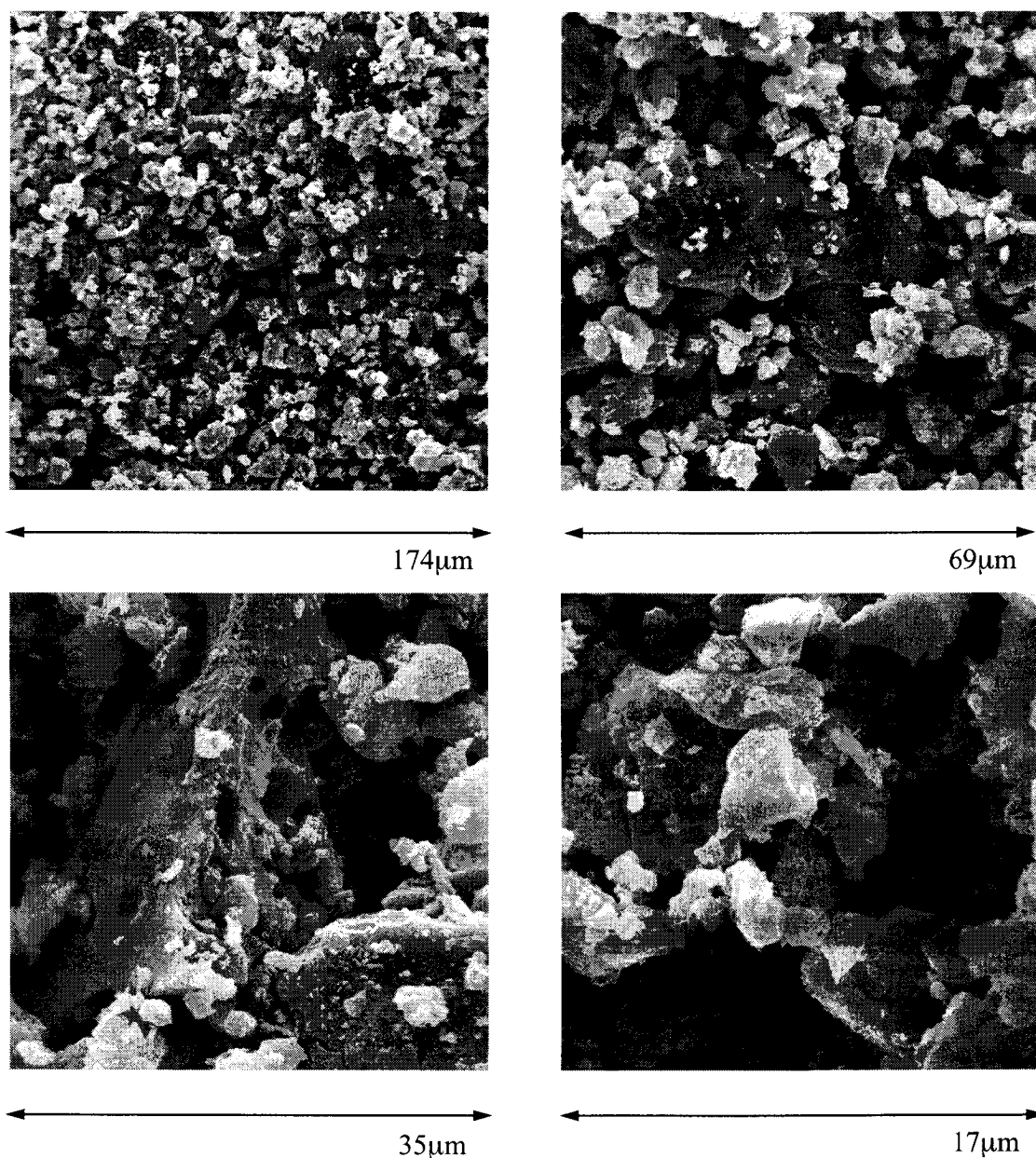
Figure 7-13 Structure of whole milk powder type A, after roll refining

Comparing the structure present after roll refining to the structure of the raw material, see Figure 7-9, it can be seen, that small and dense particles were formed. The coarse porous structure of the raw material was transferred into a size reduced, less porous structure. The sample has experienced large plastic deformation resulting in a compacted structure.

In a next step skim milk powder type D was used. This powder was ground employing two different processes. Process 1 was a dry grinding unit (jet mill). The powder was ground in normal air at a temperature of 15°C. The second grinding process used was roll refining. There the same procedure was used like for the whole milk powder. All samples were defatted using super critical CO_2 extraction mounted with double sided tape on the sample holder and observed by conventional SEM. Figure 7-14 gives the microstructure of the skim milk powder like it is present after dry grinding.

When looking at the dry ground material it can be seen that the porous structure is still present and that particles were ground without showing large plastic deformations. The interior structure was opened during dry grinding.

Considering the roll refined material, see Figure 7-15, structure appears different compared to the dry ground material. Plate like particles were formed. They are composed of individual particles that are pressed together. This illustrates also the generation of press agglomerates which are formed during refining. Those agglomerates need to be separated in the conching step. Beside the plate like and compressed particles some particles are seen were the original porous structure is still present. But for the majority of particles, structure is totally different to the dry ground product.

This is due to the material's properties (deformation behavior) and the conditions applied during grinding (high impact vs. high compression). To exploit the interactions between structural changes during grinding and the physical state of the matrix is subject of the next section.

350μm

174μm

46μm

46μm
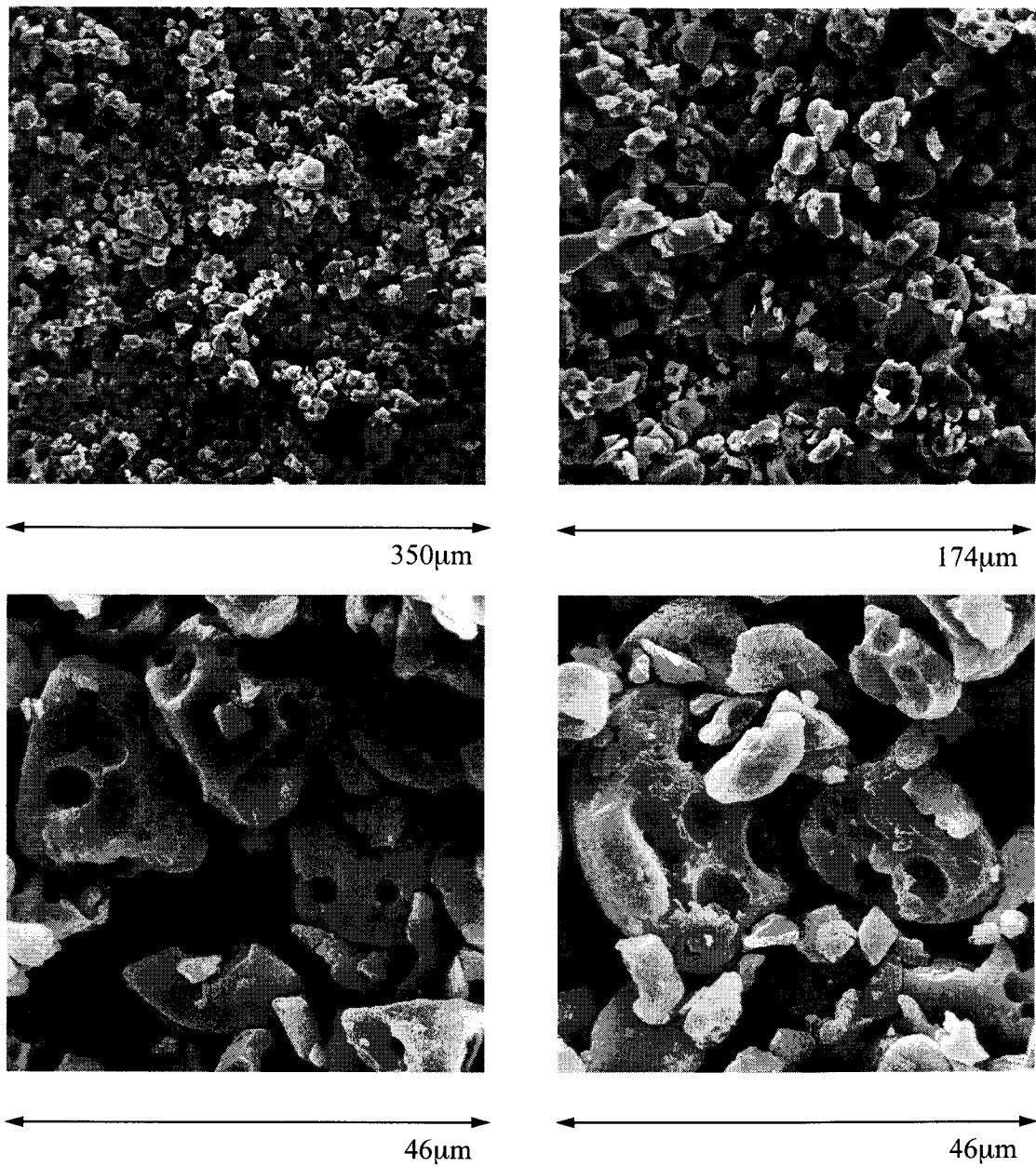
Figure 7-14 Structure of skim milk powder type D, after dry grinding
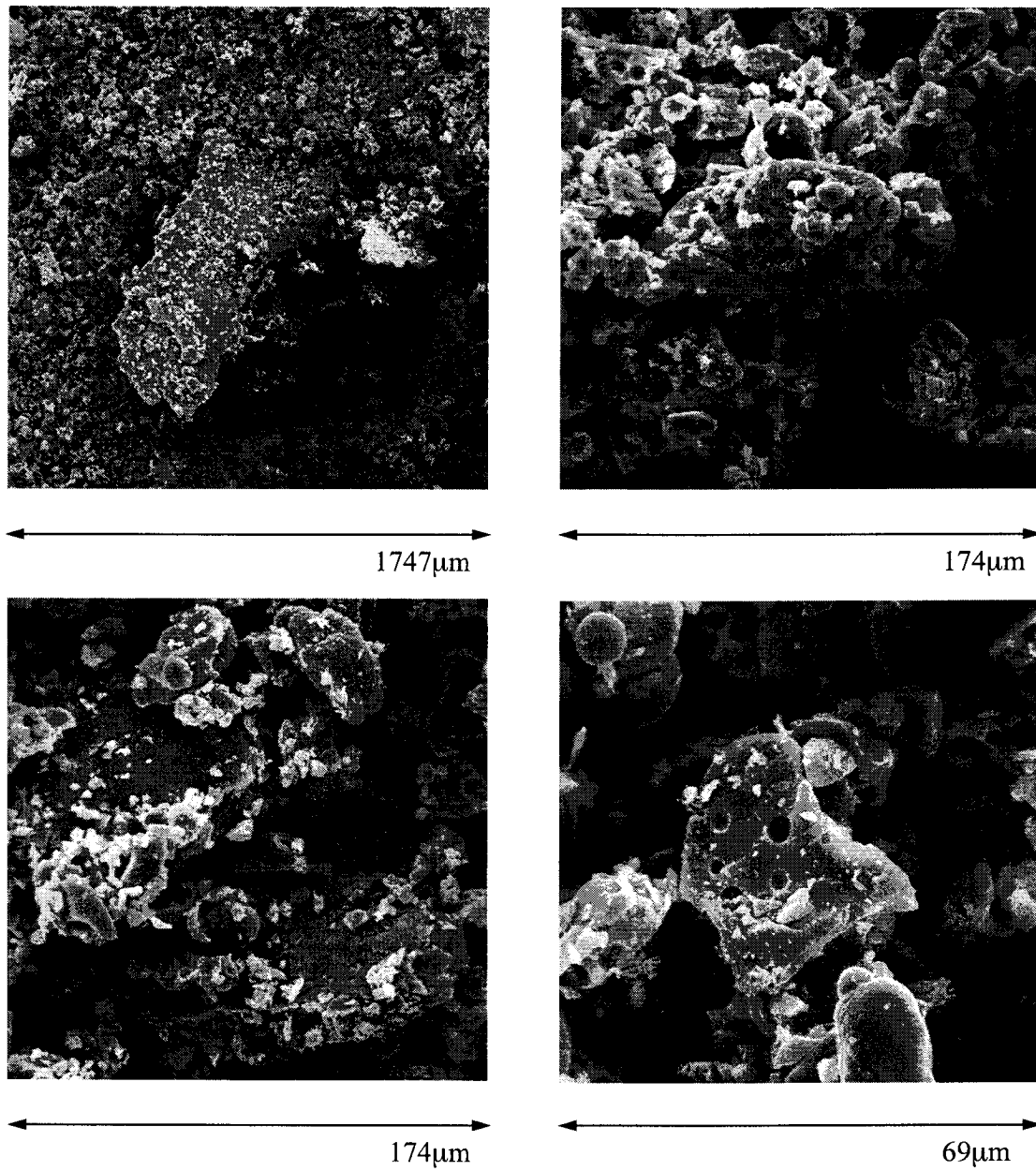
Figure 7-15 *Structure of skim milk powder type D, after roll refining*

7.1.3.2   Grinding and Glass Transition - Hypothesis and Model

Milk powder is a material with a complex structure and composition. It mainly consists of proteins, lactose and in case of whole milk powder also fat. Furthermore milk powder is composed of material that is in the crystalline state and material that is in the amorphous state (*Jouppila, K., Roos, Y.H. (1994)*). In the amorphous state the molecules do not show any regular order like for crystals but an irregular, isotropic structure. This is similar to polymers. The mechanical properties of an amorphous material (*Rao, M.A., Hartel, R.W. (1998)*) strongly depends upon the physical state which could be glass - or rubber like (*Roos, Y.H. (1995-1), Witschi, F. (1999)*). The transition from glassy to rubbery is governed by the temperature. To illustrate the physical properties of such amorphous systems (*Chuy, L.E., Labuza, T.P. (1994), Lloyd, R.J. et al. (1996)*) different aspects will be discussed using a non-milk based amorphous food system as a model example. A suitable model food system which is also build up by an amorphous matrix are hard boiled candies. Hard boiled candies are composed of sugars (sucrose, fructose, glucose) some proteins and a low amount of water. In the following a hard boiled candy will be used to demonstrate the mechanical properties and their dependency on temperature. The hard boiled candy used here had a glass transition temperature of 21.6°C. This was measured by Differential Scanning Calorimetry, DSC (heating rate: 10°C / minute). The DSC result is shown in Figure 7-16.
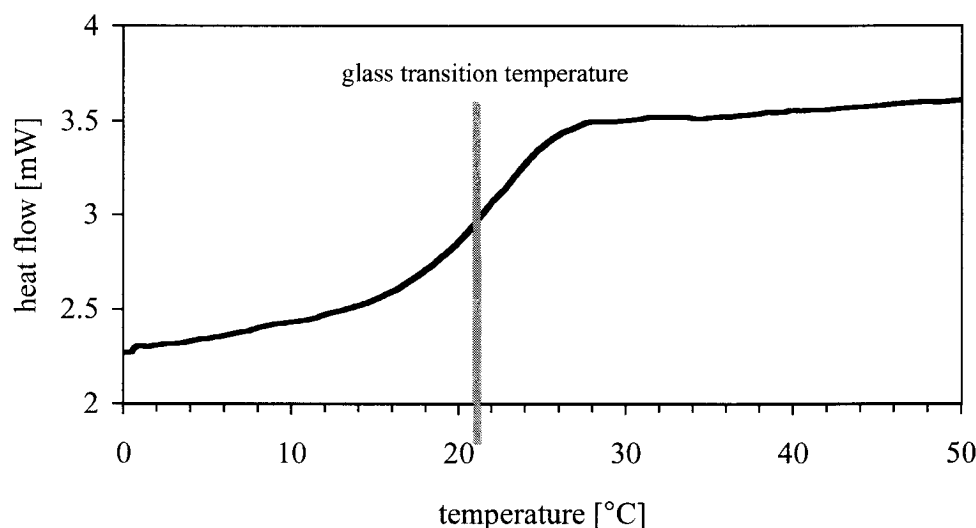
Figure 7-16 *Glass transition temperature of a hard boiled candy, DSC, 10°C/minute heating rate*

To assess the mechanical properties of such a system compression tests were performed at different temperatures. Therefore the sample was compressed between two parallel plates and the relationship between normal force and deformation was analyzed (Rheometrics, RSA). A totally elastic body (spring) shows a linear relationship between force and displacement, whereas a fluid like body performs an infinite displacement at constant force. Bodies exhibiting both elastic and viscous attributes are expected to generate a non linear, viscoelastic behavior.

Figure 7-17 gives the relationship between normal force (here expressed as the load in grams that is applied to the sample) and displacement as a function of temperature for a hard boiled candy. For low temperature the material shows highly elastic properties, the force follows the displacement and almost no hysteresis appears. Increase of temperature leads to viscous deformation and thus a hysteresis appears. Application of mechanical stresses at temperatures above glass transition temperature cause significant viscous deformation. This shows that depending on the product temperature for a given glass transition temperature the mechanical properties change most significantly around the glass transition temperature.
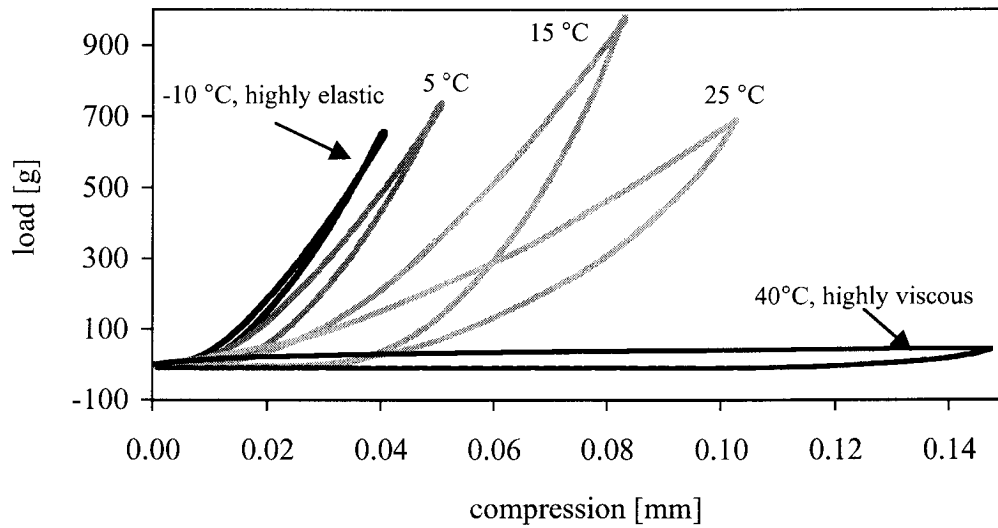
Figure 7-17 Compression test with a hard boiled candy, variable temperature

Knowing about the physical properties of amorphous materials the structural changes occurring during processing can be interpreted and linked to the materials characteristics.

Relating this to the different microstructures found for the milk powders the following is proposed. In case of roll refining the product experiences a rapid temperature increase due to high energy dissipation. This short time temperature increase leads to a transition from glassy state to the rubbery state. The mechanical stresses acting on the sample then cause the densification of the structure. In dry grinding the conditions are different compared to roll refining. There lower compression forces are applied and product temperatures are expected to be lower too (most likely below the glass transition temperature). In that case grinding temperature and most importantly product temperature is below glass transition temperature, which allows to fracture the milk powder particles without significant plastic deformation.

The grinding behavior of milk powder grinding is therefore subject of further investigations. Identification of the interactions between glass transition temperature, grinding conditions (temperature, humidity, type of mill) and resulting microstructure an area of interest. The preliminary results reported here may help to guide the work that is done in future in this area.

7.1.4 Summary

Amorphous sugar is a highly hygroscopic product. Due to that hygroscopic behavior water is adsorbed from the surrounding media. The water can be sourced either from the ambient air or from neighboring particles that carry some water. Milk powder and cocoa solids are particles which act also as an interior source for water. If temperatures are high enough the internally available water is sufficient to cause recrystallization which is the case for chocolate. In the contrary sugar oil systems do not contain any interior water and thus do not recrystallize when applying the same thermal conditions like for chocolate.

The physical properties of amorphous systems strongly depend upon the temperature of the product. Below glass transition temperature the product is in the glass like state. Mechanically the product is brittle and does not show large deformations during compression. In the rubbery state the product undergoes large deformation under compression. The material characteristics thereby determine the structure of the material like it is present after grinding. For milk powder it was shown that depending on the type of grinding (dry grinding or roll refining) different structures are obtained. Relating processing temperatures to product's property specific transition temperatures, allows to operate in a range where the structural changes can be positively influenced and controlled during processing.

7.2 Kinetics of State Transition and Water Sorption

In the previous chapters the water sorption behavior as well as conditions for recystallization of amorphous sucrose was discussed. In this chapter the kinetics of water sorption and state transition will be summarized and comparisons between the different systems are made.

In order to focus on the time scale on which water sorption and state transition takes place, the same graphs like shown before will be used but now with special emphasis on the area where recrystallization starts.

For the various sucrose systems it was found, that depending on the presence of an oil phase, kinetics are slowed down.

In case of dry ground sucrose powder (shown in Figure 6-18 on page 124) it is found that water sorption takes place on time scales of about 10 to 30 min. This is given in Figure 7-18. To better illustrate the kinetics, only the part of the sorption curve is shown where a peak for the weight signal is found.
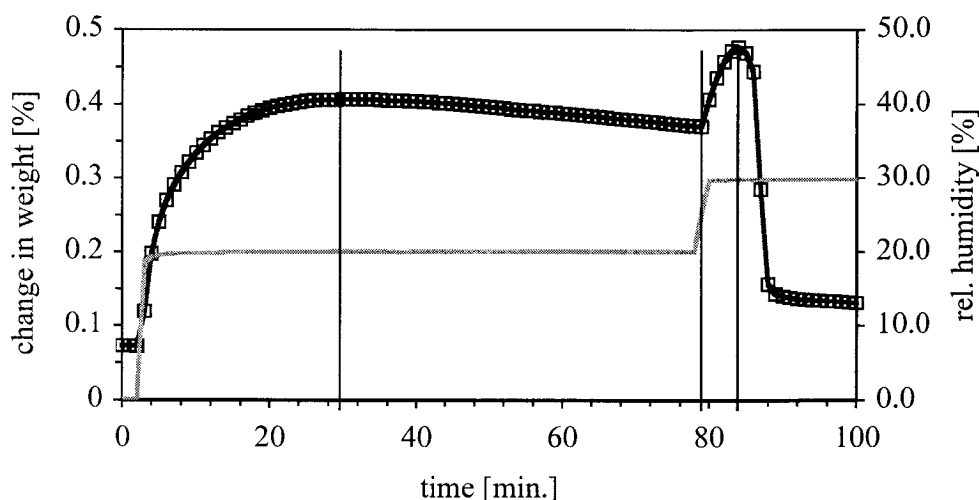
Figure 7-18 *Water sorption behavior of dry ground sucrose powder, fine ground powder, sample A, T=30°C*

In the dry ground powder, the amorphous phases are most probably located at the surface of the particles and thus are well accessible by water.

In case of freeze dried sucrose (Figure 7-1 on page 133) the amount as well as the location of the amorphous material is different to dry ground sucrose. The freeze dried material is composed of spherical and highly porous particles, with a diameter of approx. 1mm. The amorphous phases are present on the surface as well as in the volume. From this point of view, it is expected that water sorption and recrystallization will take longer than for the dry ground sucrose. The water sorption of the freeze dried sucrose is shown for two different temperature in Figure 7-19. In order to get a better view on the time scale, only the period till the maximum is passed is given. If water sorption is carried out at elevated temperatures (50°C) but at reduced humidity (50% r.h. instead of 70% r.h.), water uptake and recrystalli-
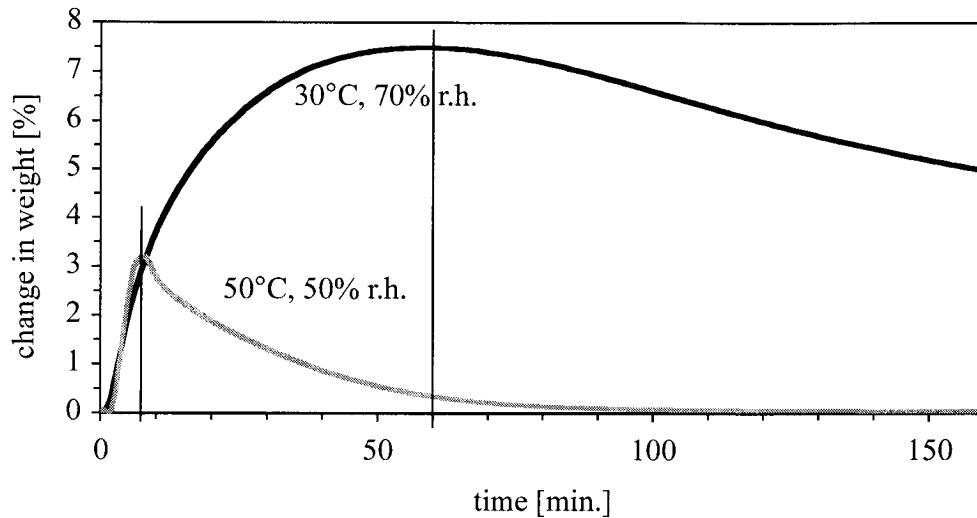
Figure 7-19 Water sorption of freeze dried sucrose, T= 30°C and 50°C

zation takes place much faster than at 30°C. The time to reach the maximum is found to be 60 min. at 30°C and 8 min. at 50°C.

Beside pure sucrose also systems that contain an oil phase were studied. In Figure 7-20 the
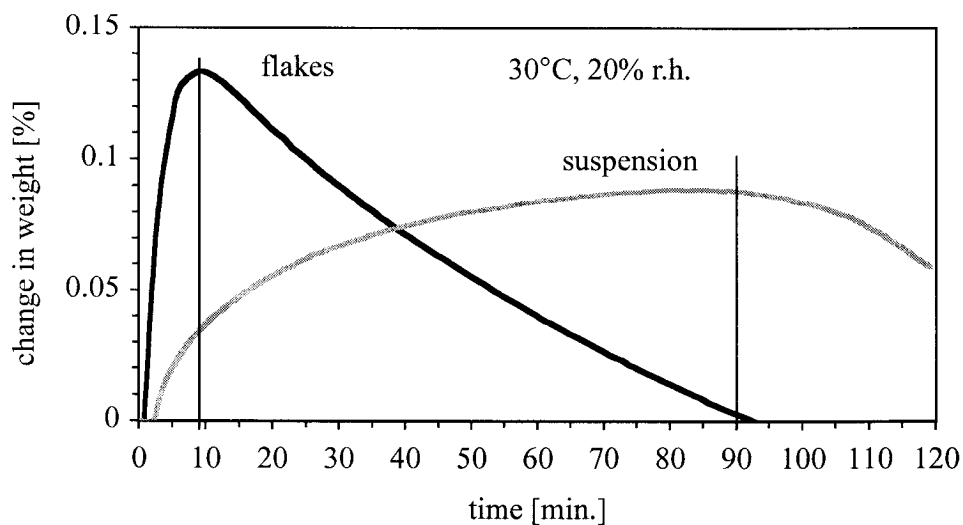
Figure 7-20 Water sorption of flakes and suspension, sucrose-silicon oil, T=30°C

sorption behavior of flakes that were obtained from roll refining and which are composed of silicon oil and sucrose, is shown. Apart from flakes also measurements for the paste like state (suspension, obtained after kneading) are given. Like for the graphs shown before, also here

only that period is shown in which the first maximum is passed. The original graph is given in Figure 5-13 on page 71.

Depending on the structure of the sample (flakes are powder like, kneaded sample is paste like), the time to reach the maximum is different. For the flakes the maximum is reached within 10 min. whereas for the paste like sample the maximum is reached after 90 min.

Beside sucrose, lactose is the other chocolate component that is present in the amorphous state. Also lactose recrystallizes and thus act as a "gluing agent" which can form agglomerates in the chocolate. Recrystallization behavior of amorphous lactose has been widely investigated (Aguilar, C., Ziegler, G. (1993), Roos, Y., Karel, M. (1992), Ziegler, G., Aguilar, C. (1994a)). It was found that under similar conditions, lactose recrystallizes on longer time scales than sucrose and thus act as a "gluing agent" at a later stage of chocolate processing.

Within this work only the sorption behavior of milk powders and dry ground milk powder mixtures was studied. In Figure 7-21 the water sorption of a dry ground mixture of skim and whey powder is given (original curve see Figure 6-24 on page 129).
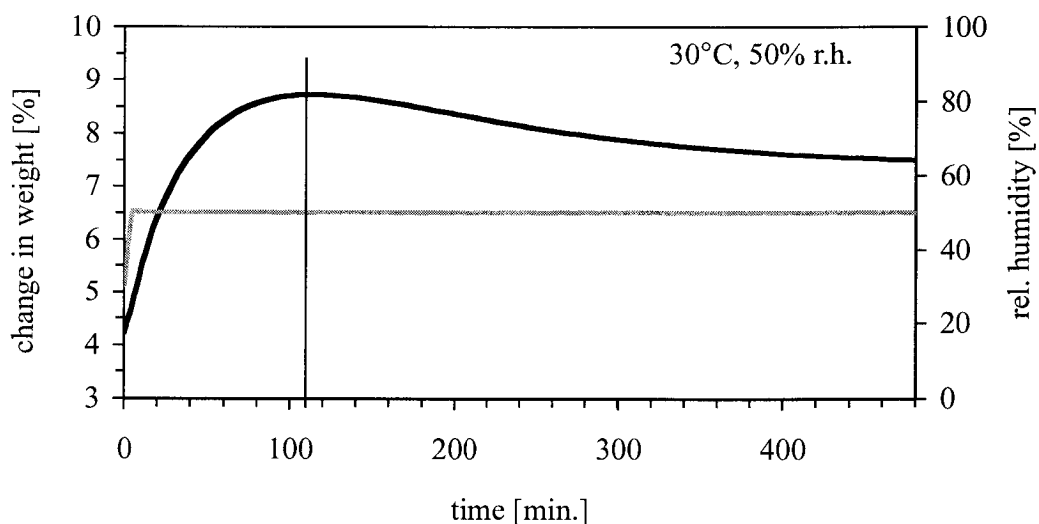
Figure 7-21 Water sorption of a dry ground mixture of whey (25% w/w) and skim milk (75% w/w) powder, T= 30°C, only that part of the sorption curve shown where the maximum appears

The time to reach the maximum is about 110min. for the dry ground mixture. This means that the time scale for recrystallization is 10 times longer than for dry ground sucrose powder. Increase of temperatures allows to shorten that time but still two different time scales for recrystallization (sucrose and lactose) will be present. The process has to account for these differences and needs to be designed accordingly.

It has to be noted that all measurements were carried out at moderate temperatures. During conching temperatures are higher and thus recrystallization is expected to be much faster.

7.3 Model for Interactions

In the previous chapters it was shown that water sorption, glass transition, amorphous-crystalline transition, agglomeration and deagglomeration have a significant impact on the rheological and structural properties of suspensions. In this sections the different interactions will be summarized and a qualitative model is proposed.

In case amorphous, disordered structures are present the two factors temperature and accessible water (or plasticizer in general) determine the structural changes taking place in such a system. Recrystallization is a process that considerably alters the structure (*Saltmarch, M., Labuza, T. (1980a), Van Scoik, K.G., Carstensen, J.T. (1990), Van den Berg, C. et al. (1993), Aguilar, C., Ziegler, G. (1993), Ziegler, G. (1998)*). Recrystallization depends upon temperature and presence of water (plasticizer) which both give rise to molecular mobility and thus allow the molecules to arrange themselves into the energetically preferred state (*Roos, Y., Karel, M. (1992), Kedward, C.J. et al. (1998)*). The processes involved and the mechanisms behind can be explained using a state diagram (*Ahlnek, C., Zografi, G. (1990), Roos, Y.H. (1995-2)*. In the following the state diagram of amorphous sucrose will be used and the conditions under which transitions can take place will be discussed for sugar-oil model systems and for chocolate.
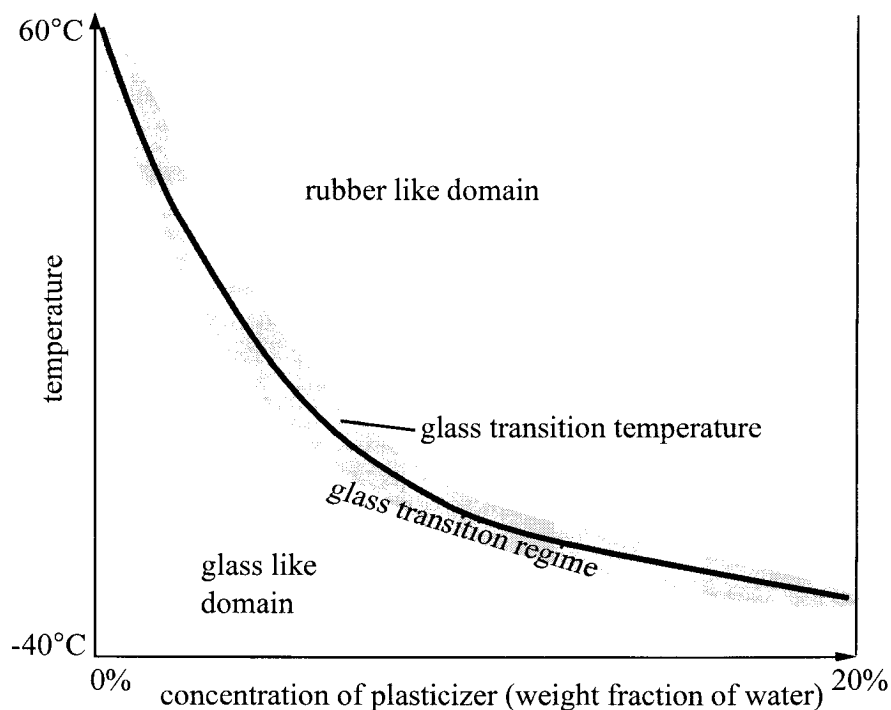
Figure 7-22 Schematic state diagram, glass transition temperature as a function of plasticizer content

The state diagram generally gives the relationship between the amount of solute (here sucrose) and the resulting glass transition temperature. For discussion of low moisture systems it is of primary interest to see the effect of plasticizer (here water) on the glass transition temperature in the relevant range of water concentration. Consequently Figure 7-22 gives a

schematic state diagram for sucrose water solutions where the relationship between glass transition temperature and the amount of plasticizer is illustrated (*Roos, Y. Karel, M. (1991)*).

From Figure 7-22 it is obvious that for low quantities of water small variations in water content have a strong effect on glass transition temperature.

The domain underneath the line denotes the glassy state where the product shows glassy, solid like behavior. The regime above the line represents the rubbery state where the product shows viscous, fluid like behavior. It has to be noted that there is not a "sharp" transition between these two states but a transition regime in which properties of the product significantly change. The line separating these two regimes gives the temperature at which "glass transition" occurs (see also *Roos, Y.H. et al. (1996), Rao, M.A., Hartel, R.W. (1998)*).

It has to be noted that the state diagram does not include information on the kinetics of transition, e.g. crystallization or structure collapse (*Roos, Y.H. (1995-2)*); it just denotes whether a transition can take place or not.

To obtain information about the time scale on which a transition can be observed a Deborah number can be defined. In the field of rheology the Deborah number (De) compares the material's characteristic time required for deformation (t_d) to the process or observation time (t_o) (*Barnes, H.A., Hutton, J.F. (1989), Steffe, J.F. (1992)*).

$$De = \frac{t_D}{t_O} = \frac{\text{time required to deform}}{\text{time of observation}} \qquad (7.1)$$

If a material deforms under stress during the observation time, then the time scale of deformation, i.e. the time required to deform is shorter than the time of observation and flow (deformation or change) is observed.

In this case De < 1 which denotes a fluid like behavior. Consequently De >> 1 describes solid like behavior. A classical example is the flow of glaciers or of glass used for windows. For short observation times, no flow (deformation or change) is observed and the material would be called a solid, whereas when observing the same material over years flow is detected.

Interpreting a modified Deborah number De* as a number that compares the time during which product characteristics change to the time of processing or observation then the following, more general view can be applied:

De* < 1 means that product characteristics change during the time of processing, or time of observation, or time of exposure to specific conditions.

De* > 1 means that during the time of observation, or the time of exposure to specific conditions product characteristics do not change

$$De^* = \frac{\text{time required for product to change its characteristics}}{\text{time of processing or time of exposure}} = \frac{t_C}{t_P} \qquad (7.2)$$

Taking De* and the state diagram into consideration, new processes can be designed in a way such as specific product properties and the related kinetics of transition are taken into account.

To summarize qualitatively the relationship between temperature, concentration of accessible plasticizer and the specific properties, an illustration is given in Figure 7-23. The objective of the diagram is to illustrate the wide range of the properties of amorphous products and how they are related to temperature and the amount of plasticizer. It has to be noted that the

concentration of plasticizer is an effective concentration. It refers to the amount of accessible plasticizer, i.e. that amount of plasticizer that is mobile and free to act as diluting agent (*Slade, L., Levine, H. (1993)*) which usually is different to the total amount of plasticizer.

In this "map" 3 zones can be identified

- the metastable zone where the product is in the glassy state

- the transition zone, determined by the glass transition temperature (T_g) and the glass transition water content (W_g)

- the "reactive" zone where the product is in the rubbery state

The names of the different zones reflect their dynamic character as the product is thermodynamically not in equilibrium (*Slade, L., Levine, H. (1993)*).
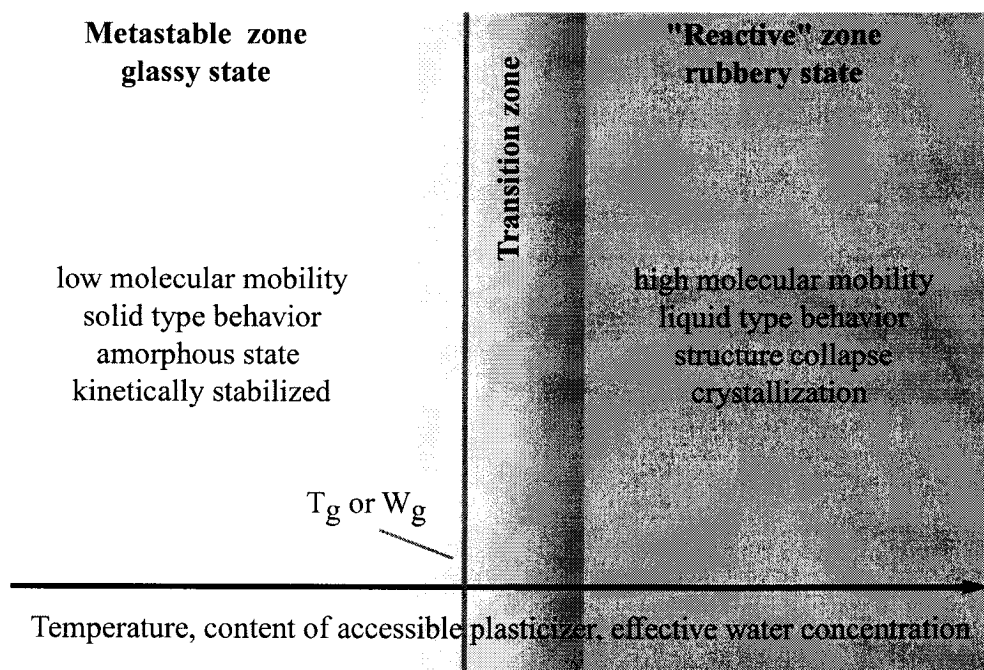
Figure 7-23 Qualitative model for interactions and effects

In the metastable, glass like domain the product has some distinct physical properties which are of major importance for processing. From a mechanical point of view the product is brittle and deforms elastically. There is no pronounced plastic domain before fracturing. From a mass transfer point of view the glassy product exhibits a high resistance against mass transport, i.e. low diffusion coefficient. In the glass like structure all molecules are arranged in a disordered way with a low molecular mobility. The product exhibits a high viscosity ($>10^{12}$ Pas). Due to the low molecular mobility, the molecules can not rearrange themselves in an ordered structure. Consequently the disordered, amorphous structure is stabilized and maintained in the glass like regime. From a textural and structural point of view a glassy powder is non-adhesive and free flowing. In this state the product is only forming weak agglomerates.

For increase of temperature or amount of accessible plasticizer (water), the product will pass through the transition regime and enters the reactive zone.

Thereby the specific properties dramatically change which is based on the increased molecular mobility (*Ahlnek, C., Zografi, G. (1990)*). In case of glassy powders (for example freeze dried sucrose) the surfaces are highly sensitive to water uptake. Due to the amorphous structure the functional groups of the molecules are not perfectly saturated by surrounding molecules and thus can interact with molecules of the surrounding media. In case of sugar, water can interact via hydrogen bonds with the sugar molecules and form sirup-like layers. Further increase of water content finally leads to a collapse of the powder structure (*Rao, M.A., Hartel, R.W. (1998), Blanshard, J.M.V., Lillford, P.J. (1993)*). The mechanical properties change from a solid type of behavior to a viscous behavior and due to increased molecular mobility the amorphous material can crystallize and transfer into the energetically preferred state (*Roos, Y.H. (1995-2)*).

In order to relate the different properties to kinetics, so called "stability maps" (*Roos, Y.H. et al. (1996), Rao, M.A., Hartel, R.W. (1998)*) or "dynamics maps" (*Slade, L., Levine, H. (1993)*) are used. These maps give a qualitative and also a quantitative description of the time scale or rate on which the transition take place if temperature or content of accessible plasticizer is changed (*Roos, Y.H. (1995-1), Roos, Y.H. (1995-2), Rao, M.A., Hartel, R.W. (1998)*).

Figure 7-24 gives a general food stability map. The x-axis represents the temperature or the
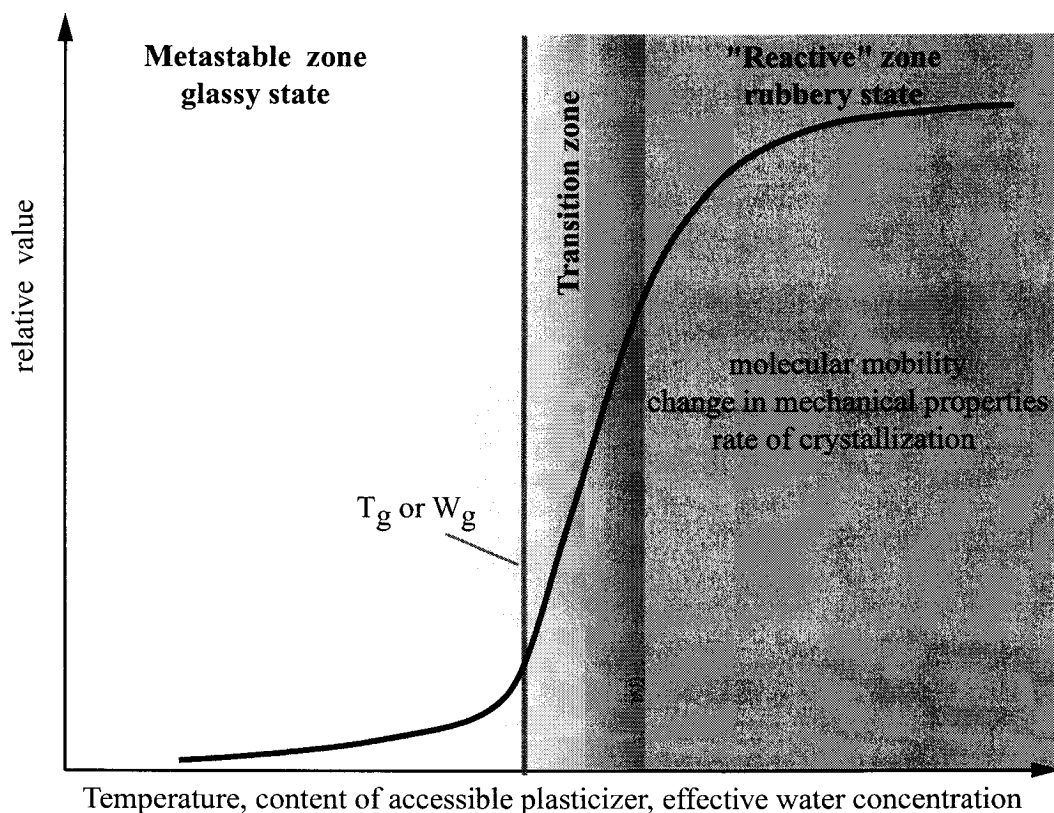
Figure 7-24 Stability map, showing effects of temperature, and accessible plasticizer content on molecular mobility, change in mechanical properties, and rate of crystallization.

amount of accessible plasticizer and the y-axis shows the relative rate at which product properties change. This relationship is characterized by a sigmosoidal curve. Molecular mobility

is almost "zero" in the metastable (glassy) zone. As soon as temperature is increased or the water content is increased above the water content of the glass like state (W_g), molecular mobility rises steeply. The same applies to the changes in mechanical properties. If the product is in the glassy state, small variations in temperature do not significantly change the mechanical properties. As soon as the transition regime is reached, the mechanical properties change till the product is fully viscous. In case of crystallization, the rate of crystallization increases as soon as the product is in the transition or the reactive zone. If water content is increased too much, the product solutes and crystallization rate decreases again. That is of course beyond the range which is of interest here.

Based on the stability map a link to the De*-number can be established which is shown in Figure 7-25. The De*-number gives the ratio between the time scale on which a product
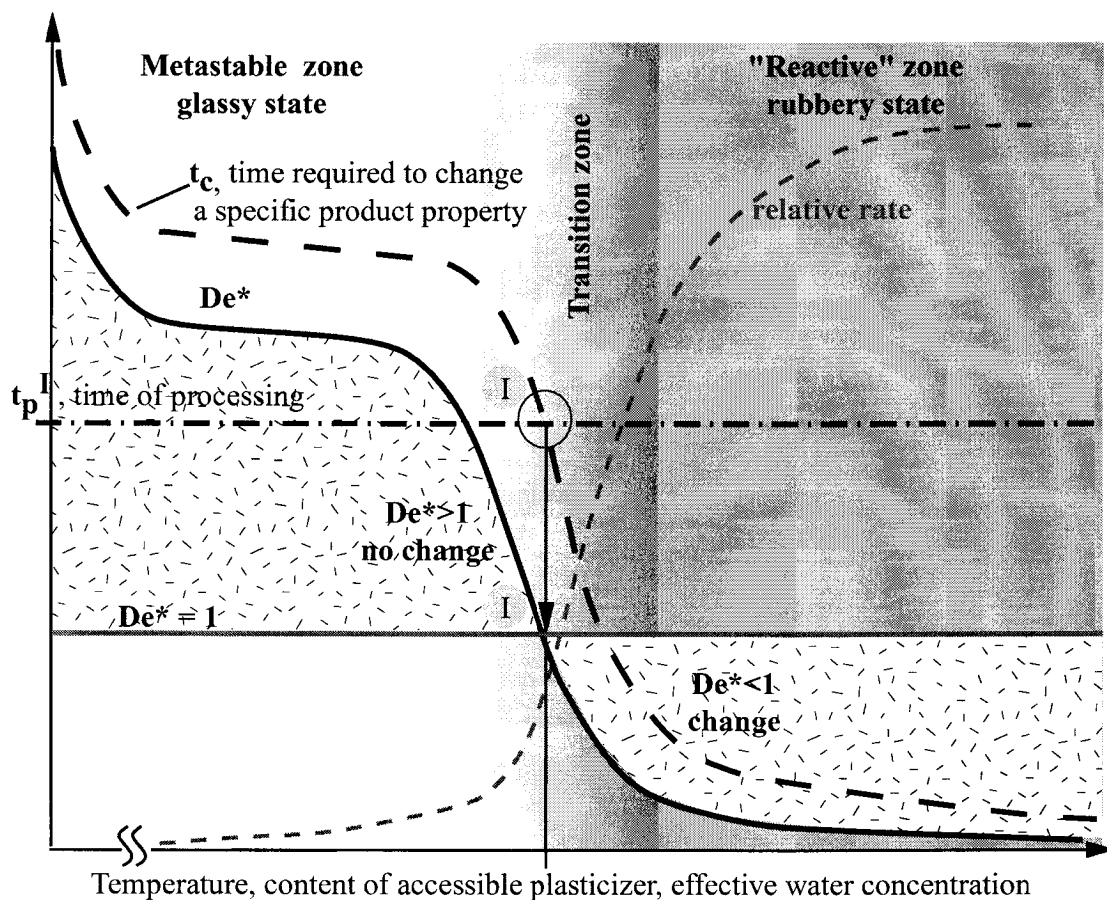
Figure 7-25 *Correlation of the stability map with the concept of modified De*-number*

changes its product characteristics (t_c), to the exposure or processing time (t_p) during which it is exposed to certain conditions. The time scale (t_c) on which product properties change (see Figure 7-24), is inversely related to the relative rate of change. In the "highly" glassy state it will take long times ($t_c \rightarrow \infty$) for the product to change. Whereas in the "highly" rubbery state, the product changes almost instantaneously ($t_c \rightarrow 0$).

Relating this to processing conditions, the corresponding processing times have to be considered. For a given (constant) processing time t_p^I, a De*-number can be derived. With

increase of temperature and (or) water concentration, the value for t_c changes. Consequently De* will follow a similar pattern as the curve for t_c. At the crossing point of t_c and t_p^1, De* equals 1. For conditions (low temperature, low water content) where t_c is higher than t_p, the value of De* will be bigger than 1, i.e. the product will not change under these conditions within the given processing time. At higher temperatures and water content, there are also conditions where t_c is smaller than t_p^1 and consequently De* is below 1. In that case the product will change its properties during processing. Depending on the objectives, the process can be operated in a way that either product properties change (De*<1) or do not change (De*>>1) during processing. This could be achieved by choosing t_c and t_p in the right ratio.

The time of change t_c can thereby be adjusted by the processing conditions (temperature, amount of plasticizer) whereas t_p is given by the processing time.

It is of utmost importance to know the characteristic times at which product properties change. Building on the kinetics and their relation to the interactions between temperature and content of plasticizer, new processes can be proposed. There the different physical properties, i.e. state transitions and characteristic times (De*-numbers), should be accounted for and utilized in an advantageous way in order to achieve the specific and desired product properties. This concept will be applied in the following section and gives the basis for the proposed new processes.

8 Process Proposal

In course of this work the interactions between

- Rheological and structural properties of sugar oil suspensions
- Effect of deagglomeration
- Influence of water sorption
- Physical state transitions (amorphous crystalline)
- Microstructural changes (grinding and microstructure) and its relation to glass transition

had been investigated and qualitative models for interactions were proposed. Based on these results, new ways to process chocolate are going to be presented.

For the conventional process of chocolate manufacturing the following steps are involved:

- Mixing of the different ingredients
- Pre refining of the mixture
- Refining of the pre refined mixture to the final particle size
- Conching of the flake like refined material (heating, kneading and mixing with further liquid)

Building on the results of this work, it is important to

- Deagglomerate sufficiently
- Recrystallize the amorphous surfaces

in order to achieve controllable, stable and optimum rheological properties.

Consequently by an appropriate process the following tasks will be accomplished:

- Provide a homogenous mixture of ingredients
- Disperse primary agglomerates that result from refining
- Avoid reagglomeration - maintain well dispersed state
- Transfer amorphous phases (introduced by raw material, generated during refining) into the crystalline state
- Allow for flavour formation in order to develop the typical aroma

It is known that the flow properties of the product also significantly depend upon the type and concentration of emulsifiers used. Nevertheless the base mixture to which emulsifier is added, should be in an optimum state in respect to its rheological properties. Addition of emulsifier will then allow to achieve the desired, final rheological (structural) properties. The "desired" flow properties thereby depend on the processing requirements (moulding, enroabing, etc.) as well as on sensorial perception (type of mouth feel - sticky, chewy etc.) that needs to be accomplished. These are product specific attributes which depend on the individual application. The flow properties can thereby be adjusted and managed through addition of the appropriate type/mixture and concentration of emulsifiers.

8.1 Aspects Concerning Processing

It was shown before that sucrose forms an amorphous phase during refining. The same applies to lactose present in milk powder. In case of lactose it has to be noted that the raw material "milk powder" already contains a certain amount of amorphous lactose. Amorphous phases are highly hygroscopic and pick up water from the surrounding media.

Ingredients present in (milk) chocolate, like milk powder and cocoa particles contain water which act as an internal source for water (*Tscheuschner, H.D. et al. (1992), Tscheuschner, H.D. et al. (1993), Tscheuschner, H.D. (1993a), Winkler, T., Tscheuschner, H.-D. (1998b)*). In addition, during and after refining water is also picked up from the surrounding atmosphere.

Directly after refining a "highly reactive" mixture is present. It was shown that deagglomeration is achieved most efficiently when the agglomerates are destroyed before the "chain reaction" water uptake and recrystallization starts. If this reaction takes place after deagglomeration was accomplished, the particles have to be kept in the dispersed state in order to avoid reagglomeration. This can be only performed in a sequential manner, if all sources of water are under control. In case of pure sugar oil mixtures no internal source of water is present and water up take is controlled by the ambient atmosphere. For (milk) chocolate, internal sources of water (milk and cocoa particles) are present and the start of the reaction can be hardly controlled. Consequently water uptake, recrystallization and deagglomeration take place almost simultaneously. Therefore it has to be ensured that deagglomeration is achieved on time scales shorter than required for recrystallization. Furthermore, during recrystallization the particles have to be kept separate from another, i.e. have to stay in the dispersed state.

For recrystallization water needs to be available. Predrying and thus reduction of the water content of the ingredients is only desirable to an extent, where still enough water is available to allow for recrystallization. Furthermore it has to be noted that predrying of the ingredients has also an impact on the structural changes that take place during grinding (see also Section 7.1.3.1 on page 141 and Section 7.1.3.2 on page 150).

The flakes resulting from refining have a powder like structure. To change this structure mechanical energy needs to be applied in an effective manner. With the conventional type of reaction chambers (conches) this is not possible. The time required till the structure changes to paste like and thus effective kneading and dispersing can take place, is longer than the time for water uptake and recrystallization. Times for water uptake and start of recrystallization were found to be less than 30 min. for sucrose oil systems. This value is derived from water sorption measurements with amorphous sucrose oil systems (see also Section 7.2 on page 153). Taking into account that in case of chocolate the water is sourced from neighbor-

ing particles and thus diffusion lengths are very short, the time for water uptake is even more reduced. Furthermore increase of temperature additionally accelerates recrystallization. This means that in todays processes, the time for recrystallization is shorter than the time scale on which deagglomeration takes place. Consequently the De*-number for recrystallization is below 1, i.e. the product changes during processing hence recrystallizes. In contrary to that, the De*-number for deagglomeration is above 1. The reason therefore is that during the time the product recrystallizes (critical processing time), only negligible deagglomeration is taking place. In order to deagglomerate effectively, the time for deagglomeration should be shorter than the time required for recrystallization. This means that for new process, the De*-number for deagglomeration has to be smaller than De*-number for recrystallization and both have to be below 1.

Consequently the process must be designed in a way such as the De*-numbers of all individual processes are reflected. Concerning deagglomeration first a structure has to be obtained where mechanical energy can be introduced effectively. In the classical process the time required to build such a structure and thus the time of dispersing is longer than the time required for recrystallization. In consequence insufficient deagglomeration is achieved. Therefore the process needs to be modified to obtain shorter dispersing times.

Short processing times combined with intensive kneading and dispersing can be provided in an adapted extruder type of equipment. There also powder like material can be treated and liquid components can be added at certain times/positions in the process. It is proposed to use an extruder type of equipment to perform the structure forming part of the chocolate making process. The structural changes will then take place within a time frame of 1 - 30 minutes. To further support deagglomeration as well as recrystallization also ultrasound elements or other type of electro magnetic waves can be used.

Once the structural changes are managed, aroma formation needs to be under control. In studies performed together with industry, it was found that formation of aroma compounds correlates with the viscosity (molecular mobility) and temperature of the product. As soon as a liquid like structure was present certain aroma compounds were formed (typically after final addition of cocoa butter and lecithin).

This indicates that a low viscosity and thus good conditions for diffusion accelerate the aroma formation. In order to illustrate this, aroma development was tracked in a trial series over the period of conching. For this purpose samples were taken after different times of conching and aroma compounds were analytically quantified. As an example the formation of lactones was considered. From its physical data the lactone analyzed here can be considered as non volatile (boiling temp. 122°C at 6mm Hg). The lactone is formed by an intramolecular cyclisation reaction and therefore depends upon molecular mobility (*Belitz, H.-D., Grosch, W. (1992)*). Based on that dependency the reaction can be considered as an indicator for molecular mobility.

Figure 8-1 gives the formation of lactone related to the textural changes during processing. The same pattern was found in 4 different conches, ranging from lab scale (4kg) to pilot plant (20kg, 200kg) to plant scale (6000kg). The processing time is given as a dimensionless, relative time that is calculated as the ratio between actual time to total processing time. After a relative time of 0.85 the product was transferred into the fully liquefied, low viscous state. It can be seen that from that point on the concentration of lactone significantly increases which goes along with the increased molecular mobility due to reduced viscosity.

This indicates that the aroma formation part could be separated from the structure formation part to a certain extent.

To allow for aroma generation good mass transfer properties are required that are supported by good mixing. This is achieved best in a high shear device.

To ensure good dehumidification high surface to volume ratios and high surface renewing rates are beneficial (thin films or droplets).

It should be taken into account that aroma formation depends to a great extent on the raw materials and ingredients used. Therefore the conclusions drawn can only indicate the direction for a given recipe. Furthermore the effect of amorphous phases and their potential to act as an carrier of flavour compounds as well as their relevance to aroma formation is not fully understood yet. To obtain information on the process of aroma formation (aroma reactions, internal flavor release or redistribution) further research is required.
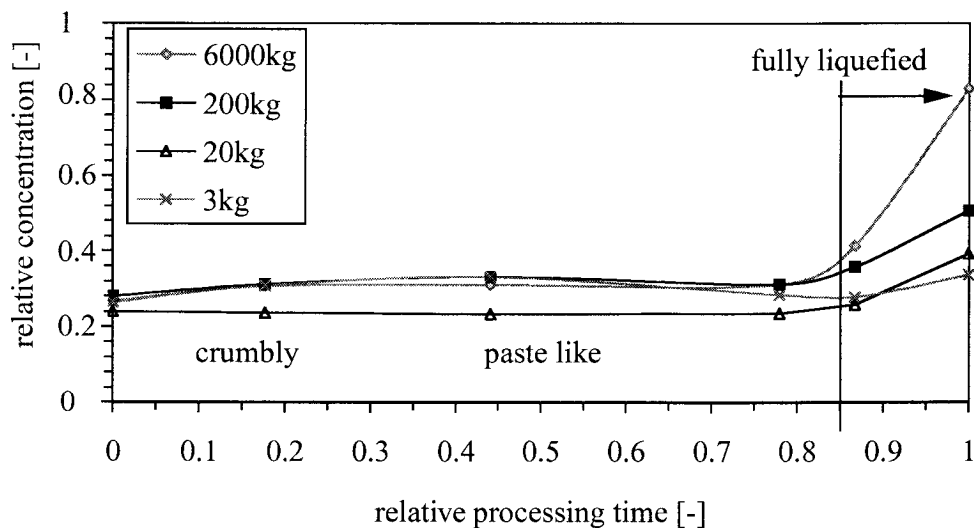
Figure 8-1 *Formation of lactone during conching and related to texture of product*

Consequently the process proposals given here mostly focus on the structure formation part. Their effect on aroma formation need to be further investigated.

A possible process could be composed of a unit, where the dispersed structure is formed first followed by a unit where the aroma generation can take place and the suspension is kept in a well dispersed state. Finally evaporation will take place. Depending on the desired flavour profile, dehumidification might also be done before or during aroma formation.

A schematic drawing of such a process is given in Figure 8-2.

Based on the principle unit operation steps that need to be carried out different types of processes can be designed. Three possible process designs will be described in the following. The starting material for all suggested processes is a mixture of typical chocolate ingredients that had been refined/ground in any type of milling processes.
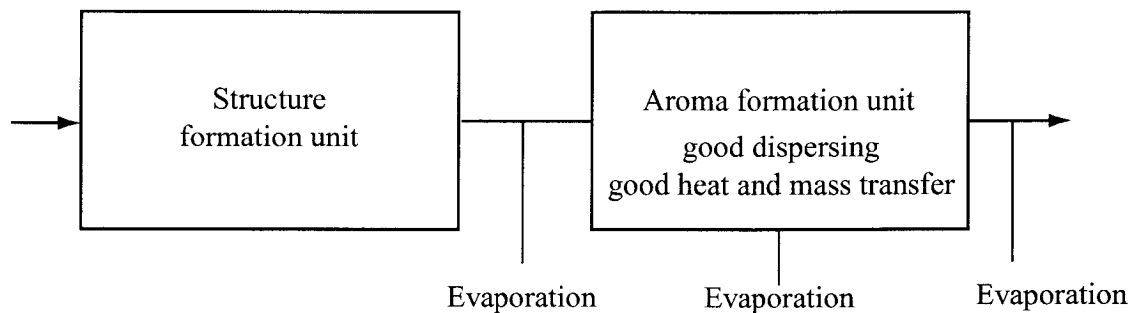
Figure 8-2 General process proposal

First process proposal

In the first process proposal, given in Figure 8-3, the refined material is fed into an extruder type of equipment where intensive kneading takes place. Addition of further liquid and surfactant leads to liquefaction of the mass. The liquid like mass is then transferred into the aroma reaction and evaporation unit. This unit is designed as a continuous process. If recrystallization was completed before entering the second process step also a low shear unit can be used. In case of a continuous process the fluid like material could be transported through a static mixing unit where good mixing and heat transfer is ensured. In case recrystallization was not completed and therefore further dispersion is required a combination of dynamic and static mixer is used. The dynamic mixer could be for example a high shear rotor stator device. The mixing unit is then followed by a thin film evaporator or a spraying unit, where the final water content of the product is achieved. During thin film evaporation further additional shearing can take place, ensuring that any agglomerates that might have formed are reduced in their size.
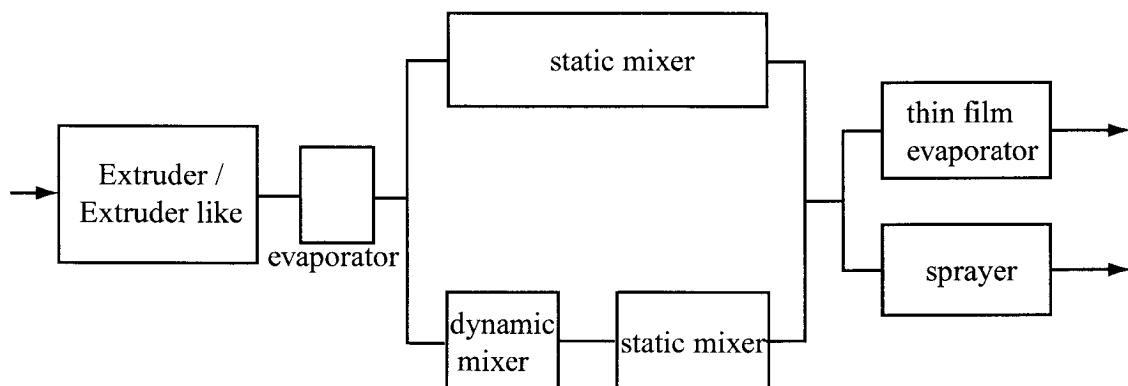
Figure 8-3 First process proposal - fully continuous

Second process proposal

This second proposal (Figure 8-4) is related to a semi-continuous process. The first mechanical step is again executed in an extruder type of equipment. Following to that, the aroma reactions, dispersing, mixing and evaporation are performed in a batch-wise operating apparatus, offering the possibility to combine aroma reactions and dehumidification. It is also possible to work with material that has not been fully recrystallized. This might have an
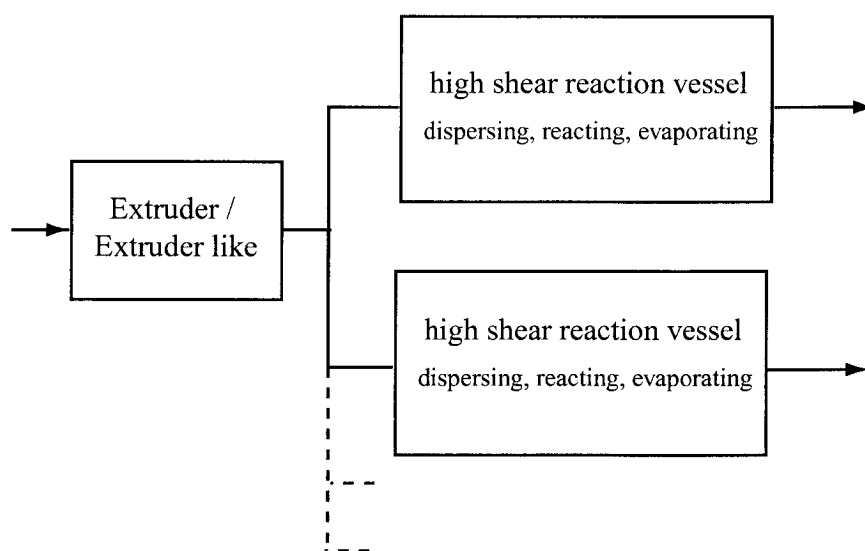
Figure 8-4 *Second process proposal - semi continuous*

impact on aroma generation. Therefore high shear elements are part of the apparatus. They could be implemented in a circulation loop or mounted directly in a vessel. Deagglomeration and also recrystallization can also be further supported by application of ultrasound. Sonication devices can be installed at positions similar to high shear units. Different to the first proposal this process offers the possibility to adjust the residence time in the reaction unit independent from the flow rate, which becomes of interest for long aroma generation times.

Third process proposal

A third possibility is to perform all steps in a high shear, stirred tank reactor.

Opposite to the conventional processes it will now be worked from the liquid state (pure cocoa butter and lecithin) to the viscous state. This would require to add the flakes step-wise or continuously to the liquid phase. This allows to apply high shear by rotor stator devices and to work in the "low viscous range" right from the beginning. Due to the low viscosity the amorphous-crystalline transition, dispersing and aroma reactions can start at the same time, which might have an impact on aroma formation. Deagglomeration and also recrystallization can also be further supported by application of ultrasound. Sonication devices can be installed in a circulation loop or directly in the vessel.
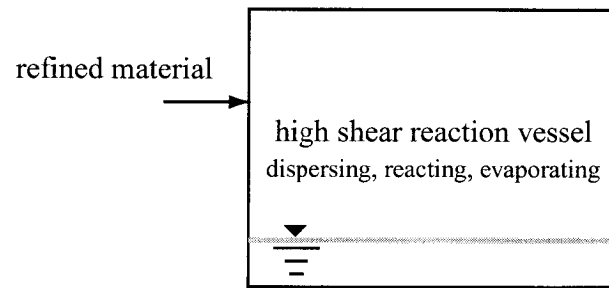
Figure 8-5 *Third process proposal - batch wise*

Independent from the type of process chosen, it is of utmost importance to perform the deagglomeration, recrystallization and dispersing step directly after refining. The three processes proposed give an example for how the individual De* numbers can be reflected. Based on the principle designs given here, the process can then be tailored (time, temperature, time of evaporation, etc.) towards the product specific needs (sensorial perception, process requirements, e.g. moulding step).

8.2 Aspects Concerning Raw Materials

In order to design the complete process and not just the "conching step", also the specific product properties of the individual ingredients need to be considered and have to be related to processing.

When looking at the raw materials, the influence of water content on the structural properties of milk powder with respect to structural changes during refining has to be taken into account. Milk powder with a low glass transition temperature or a soft matrix deforms plastically during refining and thus leads to coarse particles (*Aguilar, C., Ziegler, G. (1993)*, *Ziegler, G., Aguilar, C. (1994b)*). It is also possible that through compression the interior fat is fully encapsulated in the matrix. From a structural point of view a milk powder with a less porous structure (after refining) and a high content of free fat (after refining, free in the sense of free for flow processes which is not the same like free in terms of solvent extraction) is desired (*Dewettinck, K. et al. (1996)*, *Ziegler, G., Aguilar, C. (1994a)*, *Aguilar, C., Ziegler, G. (1995)*, *Tscheuschner, H.D. et al. (2000)*). Beside these pure physical-mechanical attributes (*Verhey, J. (1986)*) other milk powder related factors which affect the physical-chemical and thereby the interfacial properties of the chocolate need to be investigated and understood in the future. Such factors are for example related to protein (degree of denaturation, type of protein, location of protein), milk fat composition (triglycerides, surfactants) and fat membrane components (*Heathcock, J. (1985)*, *Fäldt, P. Bergenstahl, B. (1996)*, *Fäldt, P. Bergenstahl, B. (1996)*, *Pepper, T., Holgate, H. (1985)*, *Boyd, L.C. et al. (1999)*).

For cocoa liquor (*Hoskin, J., Dimick, P., Daniels, R. (1980)* it was shown by other authors (*Niediek, E.A. (1968)*, *Tscheuschner, H.D. (1993b)*) that an optimum particle size exists. Grinding cocoa liquor too fine, leads to an increase of the cocoa liquor's yield value.

For the fats used (cocoa butter and milk fat) their chemical composition has to be taken into account especially with respect to the presence of surfactants (*Gaonkar, A.G. (1989)*, *Oehl-*

mann, S. et al. (1994)). Controlling the fatty acid composition, thereby is a tool that helps to design textural appearance of the final product (softness, snap) (*Full, N.A. et al. (1996), Yella Reddy, S. et al. (1996), Kaylegian, K. (1997))*.

The combined approach of assessing product properties, understanding micro structural and physical and chemical changes that occur under certain conditions, allows to design a process where the individual product characteristics are reflected. In such a process the specific time scales would be adjusted towards another in an effective manner.

In order to study the interactions between structure formation and aroma generation in more detail, an apparatus was designed and built in course of this work that allows to

- Apply defined mechanical stresses to the sample

- Apply defined thermal stresses to the sample

- Measure the mechanical and thermal stresses

- Trace structural and compositional changes

- Apply defined atmospheric conditions to the sample

- Sample the product as well as the head space

- Produce product in quantities sufficient for sensorial testing

The description of the apparatus and the type of investigations that can be performed, are subject of the next chapter.

9 Test Stand for Controlled Stress Experiments

Conching is the process where the powdery product obtained from refining is intensely kneaded, heated and thus undergoes a structural transition from powdery to pasty to liquid. Looking at the general structure of this material it can be described as a wet bulk material which is exposed to mechanical stresses and through release of inner liquid changes its structure to a paste like material. After addition of further liquid and emulsifier it transforms into a concentrated suspension. In order to apply mechanical energy effectively to such a material its special characteristics in each phase of transition need to be taken into account.

9.1 Basic Aspects

Wet bulk material with low content of liquid phase

Dry bulk solids show for slow deformation Coulomb-type of behavior. The shear stresses depend upon the normal stresses applied and increases with these. Furthermore shear stress does not depend upon the rate of deformation. This general behavior is illustrated qualitatively in Figure 9-1. Small addition of liquid will not change this behavior very much but cohesion will be increased due to capillary effects (*Buggisch, H. (1993)*).
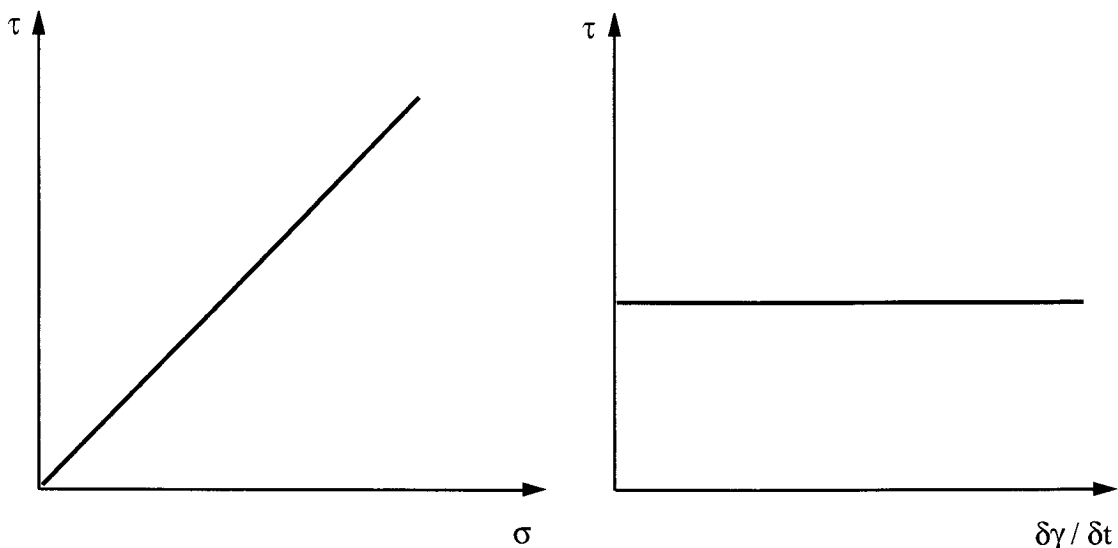
Figure 9-1 *Relationship between shear stress - normal stress and rate of deformation for dry bulk solids*

Suspensions

Suspensions can be considered as wet bulk solids exhibiting a degree of saturation "S" of liquid phase of 1. For moderate concentrated suspensions, all voids are filled with liquid phase and the solids are separated from another by liquid phase. Therefore from a model point of view (solid volume concentration and resulting average distance between particles, *Windhab, E.J. (1995)*) direct particle-particle contacts are not given. In such a system shear stresses depend upon the rate of deformation but not on the pressure or normal stresses acting on the sample. These characteristics are summarized in Figure 9-2.
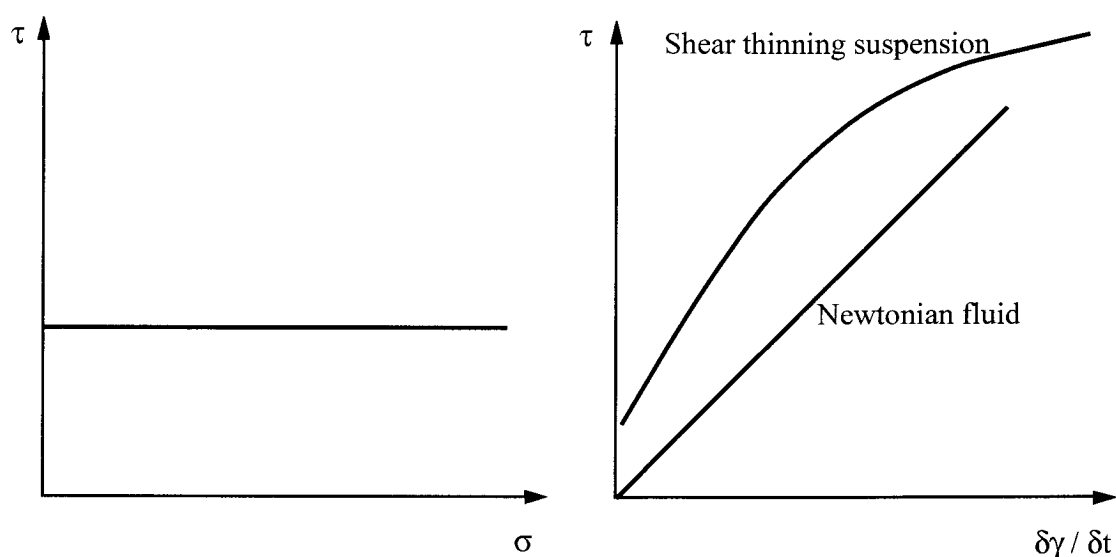
Figure 9-2 Relationship between shear stress (τ)- normal stress (σ) and rate of deformation for suspensions ($\delta\gamma/\delta t$)

The transition state: Pastes

Starting off with a dry bulk solid and adding more and more liquid phase to it, the degree of saturation S will approach 1 and thus a suspension is obtained. If the degree of saturation is getting close to 1 a sudden change in the behavior of the material is expected. An applied external force does no longer act on the system of particles alone but also on the liquid phase. Increase of normal force leads to compression, both of the particle system (reduction of porosity) and of the entrapped air. Consequently liquid will be released, which gives rise to the degree of saturation. If through compression a saturation degree of 1 is reached, the external forces are now carried by the incompressible liquid and the material exhibits a fluid like behavior, i.e. shear stresses depend upon rate of deformation but not on pressure (*Raschka, K. (1990), Raschka, K., Buggisch, H. (1992)*).

The characteristics of the paste like system are illustrated in Figure 9-3

Ceramic like systems which show all 3 types of characteristics were investigated by Raschka (*Raschka, K. (1990)*). There a ring shear apparatus was used that allowed for application of normal forces to the sample whilst the responding shear stresses required to deform the material were recorded. Such a device has to be adopted to the special needs of the system that
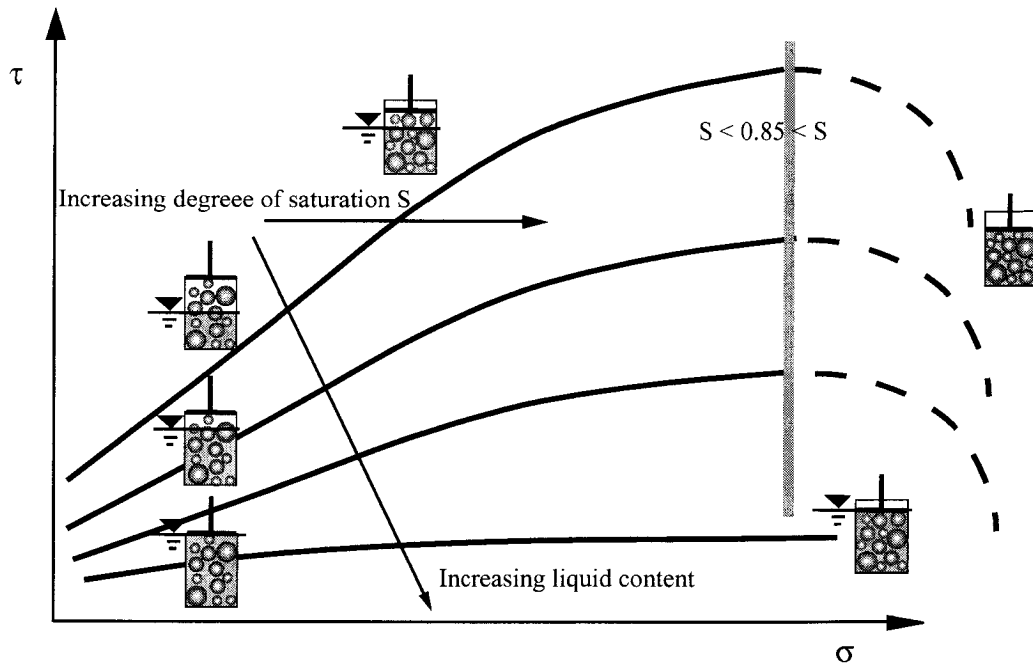
Figure 9-3 *Characteristics of pastes: Influence of increased pressure on shear stress and on degree of saturation for systems with different liquid phase concentration*

should be investigated. Therefore a new ring shear apparatus was designed and built in course of this work.

9.2 Design of Ring Shear Apparatus

9.2.1 Working Principle

In the field of powder mechanics different devices are known to analyze the flow properties of dry bulk solids. Besides the well known Jenike tester, ring shear tester are used as well. The advantage of a ring shear tester is to have infinite deformation, hence the material can be stressed over a long time. Furthermore stresses can be altered and the material's response can be studied using the same sample. In Figure 9-4 the general setup is illustrated schematically.

The sample is placed in the ring type channel and covered with a lid. Applying normal forces to the lid causes compression of the sample. Measuring of the filling height reveals the degree of compression. Turning either the cup or the lid yields deformation of the sample and thus require a certain shear stress which is reflected in the torque necessary to turn. The principle of this system remains unchanged although when working with wet bulk solids. There some modifications towards tightening of the system need to be made. To have such an apparatus available, both for measuring and for processing of chocolate, severe modifications are required.

Ring for measuring Shear-stress and Normal-stress
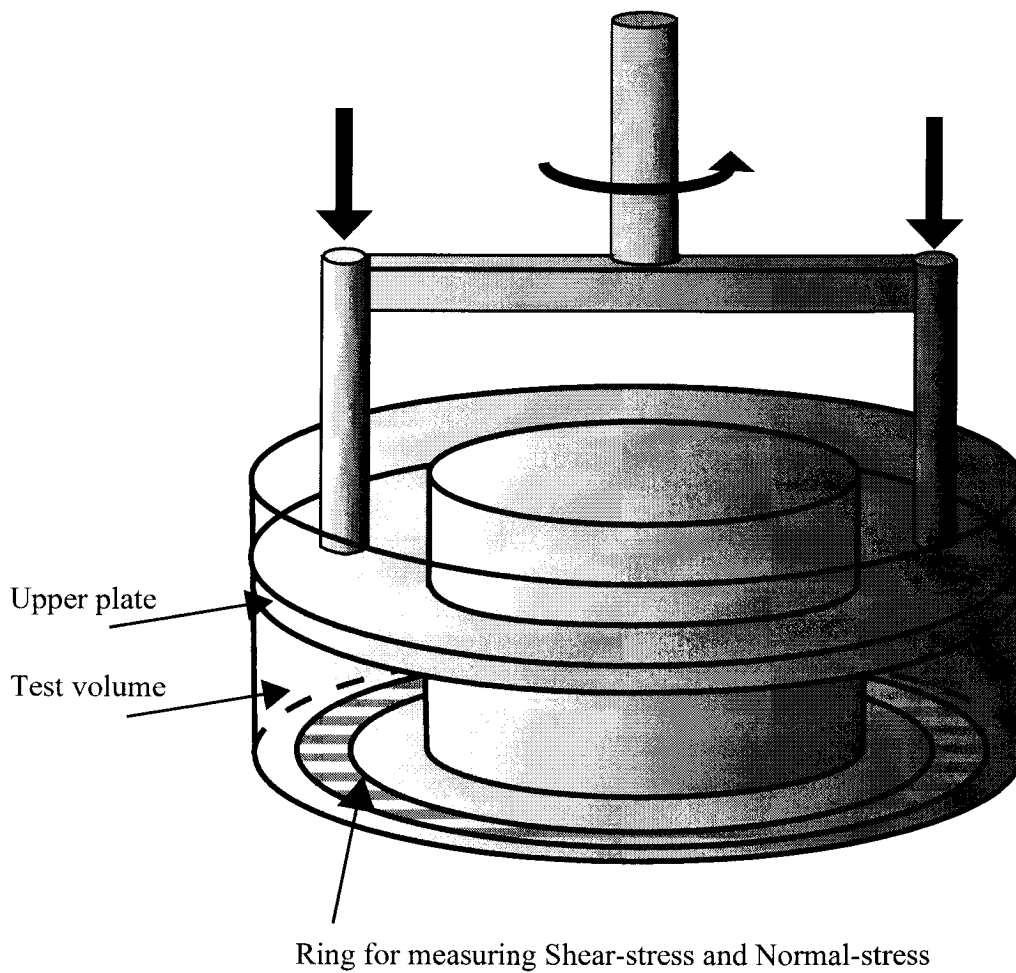
Figure 9-4 Principle design of a ring shear tester used for dry materials

9.2.2 Working with Chocolate - Requirements

The intention is to use a ring shear apparatus for production of chocolate and simultaneously measuring the structural changes occurring during processing. Furthermore production could be performed under well defined conditions, offering the opportunity to understand the interactions between the mechanical, thermal and chemical processes and their influence on the quality of the product. In order to achieve these objectives, the design of the ring shear apparatus needs to reflect the given requirements.

In respect to the conventional type of chocolate production, such an apparatus must have the following attributes:

- Temperature controlled

- Heatable up to 90°C

- Narrow temperature profile within the sample

- Good cooling properties (high mechanical energy input)

- Application of conditioned atmosphere

- Good mixing properties

- Sampling of head space

- Openings for on line sensors (flow field, structure)

- Inlets for addition of liquid

- Inlets for sampling of product

- Fluid tight sealing

- Volume sufficient to provide sensory samples (4 kg max.)

- Speed adjustable

- High sensitivity of transducers to assess different stages (powder, paste, liquid)

- On line recording of data like stress, deformation rate, degree of compression, temperature

- Good cleaning properties

- Good accessibility

- Food grade design - stainless steel

Based on these requirements an apparatus was designed meeting all these demands. Its technical data are given in the next section.

9.2.3   Technical Data and Design

The Ring Shear Conche designed on the basis of a ring shear tester has the following technical specifications.

Table 9-1 Technical data of Ring Shear Conche

Normal stress (max.)	500 kPa
Shear stress (max.)	500 kPa
Volume (max.)	4 l
Outer diameter	377 mm
Inner diameter	200 mm
Minimum speed	0.03 1/min.
Maximum speed	77 1/min.
Height of filling	1 to 50 mm
Temperature (max.)	90°C

In Figure 9-5 the technical options are illustrated which account for the special properties of the product in each phase of processing
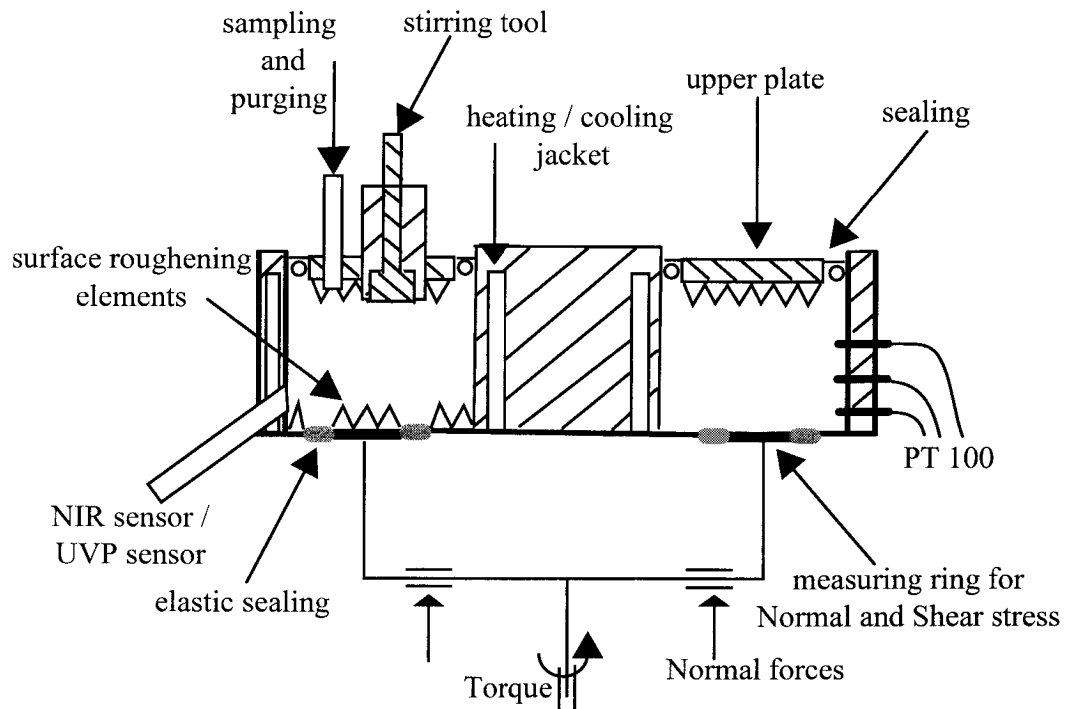
Figure 9-5 *Technical options of the Ring Shear Conche*

9.2.4   Sample Preparation - Preconditions

To be able to assess the structural changes occurring during the transition from a powder like to a paste like material mechanical power and energy have to be applied under controlled conditions. Therefore the Ring Shear Conche will be used. There normal and shear forces can be applied in a well defined manner. In plain laminar shear flow no mixing is taking place, hence potential mixing tasks necessary during processing can not be handled in this type of flow. In order to study the influence of different liquid phase contents on the transitions from powder to paste, a homogenous mixture has to be available prior to any measurements carried out with the Ring Shear Conche.

As stated earlier, the powder like product is composed of agglomerated solid particles that have liquid phase entrapped. Application of mechanical stresses leads to break up of the agglomerates and thus to release of liquid phase which alters the structure. The amount of liquid phase thereby influences the consistency as well as collapse of the structure.

To be able to work with different liquid phase contents two approaches are possible:

1. Refining of ingredient mixtures with different content of liquid phase

2. Working with a standardized ingredient mixture for refining and add liquid phase to the refined flakes during conching

Solution 1 will yield homogenously distributed (not on a micro scale) liquid phase which is immobilized within agglomerates. Controlling the refining process when working with different liquid content is rather difficult. Furthermore it is questionable, if similar results for

agglomerate size, strength and size of primary particles can be obtained for different content of liquid phase.

Solution 2 requires application of mechanical power to the sample (mixing) prior to usage in the Ring Shear Conche. Furthermore homogenous mixing of liquid phase and a powder will already lead to a structural transition.

The liquid phase in this system is cocoa butter which starts to solidify for temperatures below 36°C, i.e. at room temperature most of the liquid phase is in the solid state. Transforming cocoa butter into the solid and powdered state would allow to perform powder/powder mixing rather then powder / liquid mixing. In addition the "liquid phase" is yet available in two states - free and immobilized. Furthermore the properties of the liquid phases can be changed independently from each other. Special fatty acid compositions could be used, which influences the melting and liquefaction behavior of the system. It would be possible to melt and thus to liquefy immobilized fluid first. In a second step, increase of temperature would then melt and liquefy the "free" fluid or vice versa.

In a specially designed premixing process the chocolate flakes or other refined ingredient mixtures are mixed with solidified "liquid phase". Solidification of cocoa butter was performed using a spray chilling process. There liquid droplets of atomized cocoa butter are sprayed into a cold atmosphere where they solidify in the polymorphic state. Post treatment of solidified cocoa butter leads to transition into the high melting crystalline state (*Wagner, T. (1997)*).

The size of the obtained solidified cocoa butter particles can be adjusted in the atomizing and spraying step and be further classified in any mechanical size separation step.

In order to obtain a homogenous distribution of cocoa butter particles it has to be taken into account, that melting of the cocoa butter leads to a liquefaction of the whole mass. Therefore the cocoa butter should be well dispersed and each chocolate flake particle should be homogeneously surrounded by cocoa butter. The following simple calculation provides some data on the number and size of cocoa butter particles required in order to provide a basis for obtaining a homogenous mixture.

For a given number based ratio between flake particles and cocoa butter particles the amount (mass) of cocoa butter (m_{CB}) added to the chocolate flakes (m_{CF}) and the average size of the chocolate flakes (x_{CF}) yields the maximum size of the cocoa butter particles (x_{CB}).

The number (n) of cocoa butter particles surrounding a chocolate flake particle determines the micro-homogeneity,

$$n = \frac{N_{CB}}{N_{CF}} \qquad\qquad (9.1)$$

with N_{CB} being the number of cocoa butter particles and N_{CF} the number of chocolate flakes.

The amount (mass) of cocoa butter particles m_{CB} with the density ρ_{CB} and the quantity of chocolate flakes m_{CF} determine the mass based ratio c_m.

$$c_m = \frac{m_{CB}}{m_{CF}} \qquad\qquad (9.2)$$

The chocolate flake particles have an average size of x_{CF} (volume based diameter of a sphere with similar volume) and a density ρ_{CF}, then c_m is given as

$$c_m = \frac{N_{CB} \cdot x_{CB}^3 \cdot \rho_{CB}}{N_{CF} \cdot x_{CF}^3 \cdot \rho_{CF}} = n \cdot \frac{x_{CB}^3 \cdot \rho_{CB}}{x_{CF}^3 \cdot \rho_{CF}} \qquad (9.3)$$

and the size of the spherical cocoa butter particles, x_{CB} is calculated as

$$x_{CB} = x_{CF} \cdot \sqrt[3]{\frac{c_m \cdot \rho_{CF}}{n \cdot \rho_{CB}}} \qquad (9.4)$$

Chocolate most often has a fat content of 31% w/w. Depending on the raw materials used, the chocolate flakes obtained after refining exhibit fat contents between 23% w/w and 29% w/w. In case of refiner flakes with 23% fat, 11.6g of fat per 100g flakes are added in the course of conching, whereas in case of 29% of fat only 2.9g fat per 100g of flakes are added. For an addition of 11.6g fat c_m equals 0.116 and in case of 2.9g fat, c_m is about 0.029.

Taking chocolate flakes with an average size of 500µm and a density of 1.2 g/ml being surrounded by n cocoa butter particles with a density of 0.95 g/ml yields a size x_{CB} for the cocoa butter particles. The number of cocoa butter particles thereby determines the ideal arrangement. Preferably each flake particle should be homogenously surrounded by many small cocoa butter particles

In Table 9-2 values for the number and the corresponding size of cocoa butter particles are given that were calculated for different, theoretical arrangements. It can be seen, that working with cocoa butter particles having a size of about 100µm supports achieving homogeneity.

Table 9-2 *Number of surrounding cocoa butter particles per chocolate particle (average size 500µm) and corresponding size of cocoa butter particles*

c_m	n	x_{CB} / µm
0.116	4 (Tetrahedra)	167
0.116	6 (Octahedra)	146
0.029	4 (Tetrahedra)	105
0.029	6 (Octahedra)	92

In an experimental approach mixing tests and analysis of homogeneity were performed.

9.2.5   Mixing of Chocolate Flakes and Cocoa Butter Powder

To verify the theoretical considerations mixing experiments were carried out using a Brabender lab kneader for mixing of chocolate flakes and cocoa butter powder. The cocoa butter powder was obtained from spray chilling. The powder had been stored to alter the crystalline modification and is free flowable at room temperature. The desired size class of 100µm to 150µm was obtained from dry powder sieving.

To check mixing homogeneity an on-line Near Infrared (NIRVIS, Bühler, Switzerland) device was employed. Measuring the reflectance over a range of wavelength, from 1000nm to 2400nm revealed a components specific spectra. As on-line sensor a probe was used where

the "analyzing window" had a diameter of 8mm. Hence small volumes can be assessed in respect to their composition. Preparing a mixture of the two ingredients and performing measurements after various mixing times at different positions in the kneading chamber yields the quality of mixing. This was evaluated through comparison and overlaying of the corresponding spectra measured (see Figure 9-6 to Figure 9-9).

In Figure 9-6 the spectra of absorbance for pure cocoa butter powder, chocolate flakes and finished chocolate is given. It can be seen that the spectra of cocoa butter is significantly different from chocolate flakes. The spectra of the chocolate flakes represents 5 individual mea-
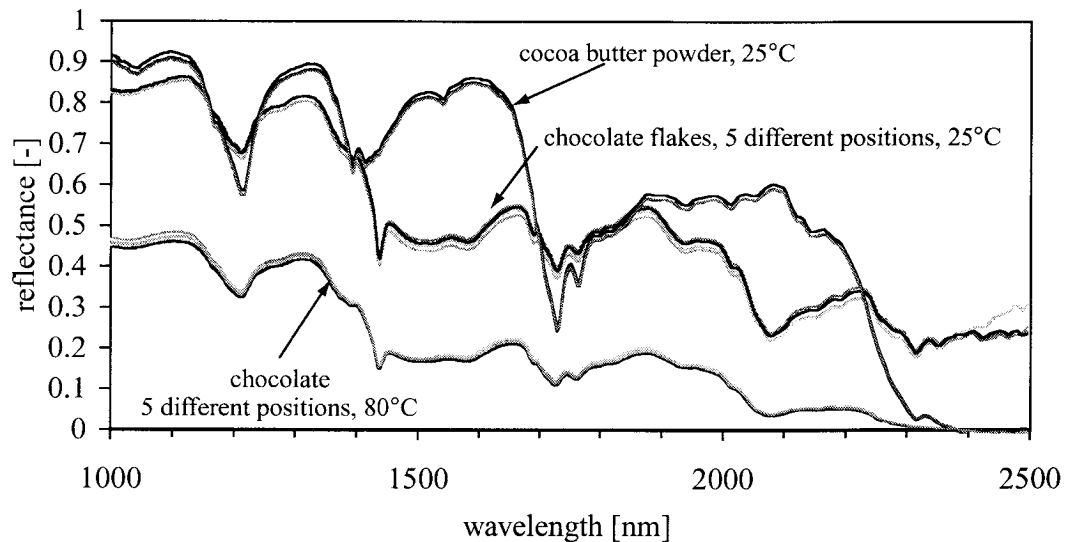

Figure 9-6 *Spectra of absorbance of pure cocoa butter powder, chocolate flakes and liquid chocolate, measured at different positions in the kneading chamber*

surements performed at various positions within the product. This gives the basic variation within the chocolate flakes. Looking at chocolate, 3 spectra at different positions were recorded. The variation is much less than for chocolate flakes and demonstrates the homogeneity of this system. The spectra follows the same pattern like flakes but at a lower level, which is probably due to different scattering behavior of powder compared to fluid chocolate which also is considered to be the reason for the difference seen at wavelengths above 2200nm.

Figure 9-7 to Figure 9-9 show the development of the mixing homogeneity as a function of time. In the beginning, areas of almost pure cocoa butter powder can be identified. After a mixing time of 3 min. the different spectra measured at different positions already approach each other. Mixing for 11 min. yields spectra which have come close to each other and thus demonstrate good homogeneity. Only a marginal difference to the spectra of chocolate flakes can be detected.
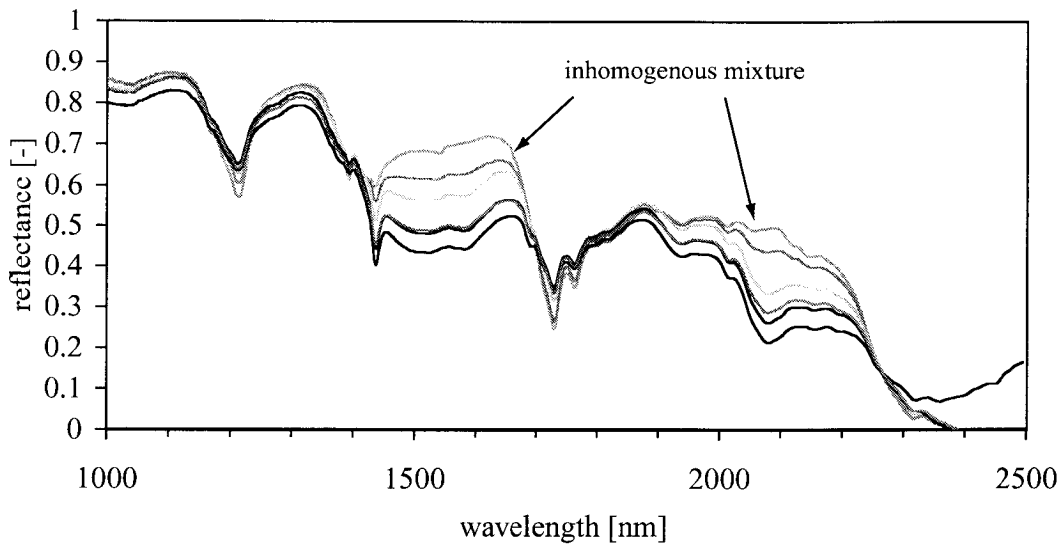
Figure 9-7 *Spectra of absorbance of an extreme inhomogenous mixture, measured at 6 different positions in the kneading chamber, before mixing*
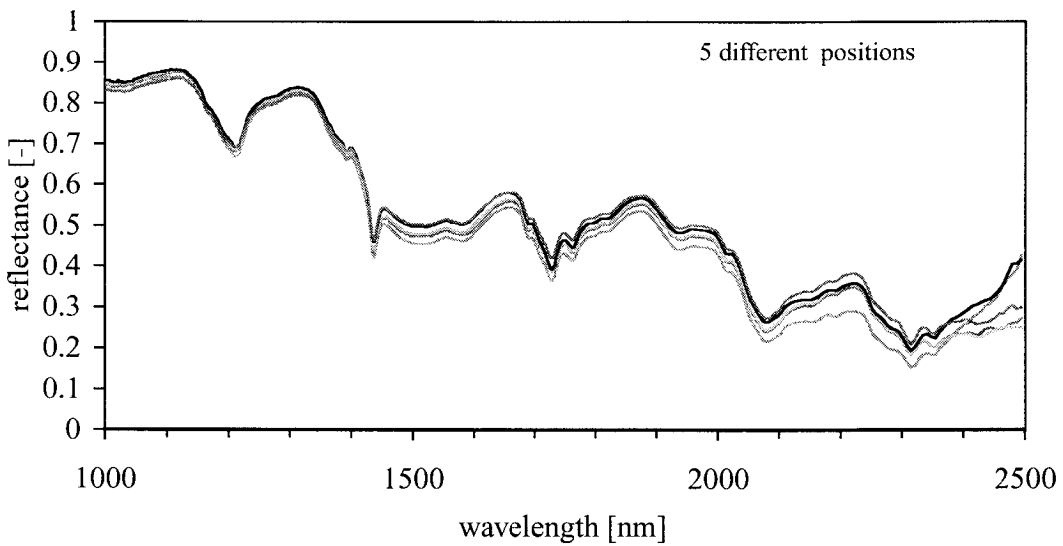
Figure 9-8 *Spectra of absorbance after 3min. of mixing time, measured at 5 different positions in the kneading chamber*
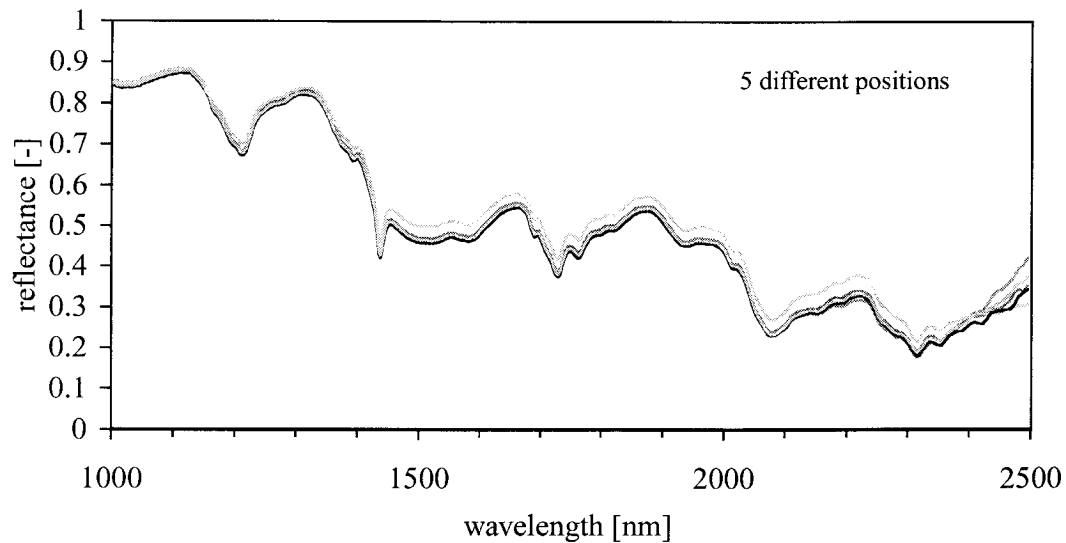
Figure 9-9 *Spectra of absorbance after 11 min. mixing time, measured at 5 different positions in the kneading chamber*

With these measurements it is shown that mixing of chocolate flakes and cocoa butter powder in a Brabender lab kneader allows to obtain homogenous mixtures. With this powder mixing step, it is possible to homogenously introduce different amounts of fat phase. This provides the basis for varying the fat content in the trial series.

Within this work the Ring Shear Conche had been designed and was put into operation. Experimental work to be carried out with this apparatus, is subject of future research activities.

10 References

Ahlnek, C., Zografi, G. (1990)
The molecular basis of moisture effects of the physical and chemical stability of drugs in the solid state, Internat. Journal of pharmaceutics, 62, p. 87-95

Aguilar, C., Ziegler, G. (1993)
Lactose in spray dried whole milk powders and the processing of milk chocolate, 47th P.M.C.A. production conference, Hershey, Pennsylvania

Aguilar, C., Ziegler, G. (1995)
Viscosity of molten milk chocolate with lactose from spray dried whole milk powders, Journal of food science, Vol. 60, No.1

Attaie, H., Braun, P., Breitschuh, B. (1998)
Influence of fractionated milk fat and free fat content on physical properties of milk chocolate, ETH-Zurich, Laboratory of Food process engineering, Internal research report

Barnes, H.A., Hutton, J.F. (1989)
An Introduction to Rheology, Elsevier, Amsterdam

Becker, U. (1984)
Physikochemische Grenzflächeneinflüsse auf das Fliessverhalten von Suspensionen, Thesis, Universität Dortmund, Germany

Beckett, S.T. (1994a)
Control of Particle size reduction during chocolate grinding, The Manufacturing Confectioner, May, p. 90-97

Beckett, S.T. (1994b)
Industrial chocolate manufacture and use, 2nd edition, Blackie Academic & Professional, London

Belitz, H.-D., Grosch, W. (1992)
Lehrbuch der Lebensmittelchemie, 4. Auflage, Springer-Verlag, Berlin

Blanshard, J.M.V., Lillford, P.J. (1993)
The Glassy State in Foods, Nottingham University Press

Bouzas, J., Brown, B.D. (1995)
Interactions affecting microstructure, texture and rheology of chocolate confectionery products, Chapter 16 in Ingredient Interactions, Gaonkar, A., Marcel Dekker, New York

Boyd, L.C. et al. (1999)
Isolation and characterization of whey phospholipids, Journal of Dairy science, No.82

Braun, P., Windhab, E.J. (1995)
Zum Einfluss der Desagglomeration und interpartikulärer Wechselwirkungen auf das Fliessverhalten konzentrierter Suspensionen, Vortrag auf dem VDI Fachausschuss Lebensmittelverfahrenstechnik, Baden-Baden

Braun, P., Windhab, E.J., Attaie, H. (1997)
Deagglomeration and its influence on rheological properties of concentrated suspensions: Investigations on a sucrose/silicon oil system, 1st internat. symposium on food rheology and structure, Zurich, Switzerland

Brito-De La Fuente, E. et al. (1996)
On the use of helical ribbon based viscosimetry for the determination of flow curves, Proceeding of the XIIth International Congress on Rheology, Quebec, Canada, p. 672, 673

Buggisch, H. (1993)
Characterization of wet solids, Symposium prints, Reliable flow of particulate solids, 23.-25. August 1993, Norway

Buma, T.J., Henstra, S. (1971)
Particle structure of spray dried milk products as observed by scanning electron microscope, Netherland milk dairy journal, No. 25

Caric, M. , Kalab, M. (1987)
Effects of drying techniques on milk powders quality and microstructure: a review, Food microstructure, Vol. 6

Chang, C., Powell, R.L. (1994)
Effect of particle size distribution on the rheology of concentrated bimodal suspensions, Journal of Rheology, 38 (1)

Cheng, D. et al. (1990)
The effect of particle size distribution on the rheology of an industrial suspension, Journal of materials science, 25

Chong, J.S., Christiansen, E.B., Baer, A.D. (1971)
Rheology of concentrated suspensions, Journal of applied polymer science, Vol. 15

Chuy, L.E., Labuza, T.P. (1994)
Caking and stickiness of dairy based food powders as related to glass transition, Journal of Food Science , Vol. 59, No.1, p. 43-46

Dahneke, B. (1972)
The influence of flattening on the adhesion of particles, Journal of colloid and interface science, Vol. 40, No.1

Dewettinck, K. et al. (1996)
The free fat content of dried milk products and flow properties of milk chocolate, Milchwissenschaft, 51, (1)

Drapier-Beche, N. et al. (1997)
Evaluation of lactose crystalline forms by nondestructive analysis, Journal of dairy science, 80, p. 457-463

Eischen, J.C. (1999)
Bildanalytische und rheologische Untersuchung zum Orientierungs- und Strukturierungs-
verhalten von faserförmigen Partikeln in laminaren Scherströmungen, Thesis, ETH Zurich

Farris, R.J. (1968)
Prediction of the viscosity of multimodal suspensions from unimodal viscosity data, Trans-
actions of the society of rheology, 12:2

Fäldt, P. Bergenstahl, B. (1996)
Spray dried whey protein/lactose/soybean oil emulsions, 1. Surface composition and parti-
cle structure, 2. Redispersability, wettability, particle structure, Food Hydrocolloids, Vol.
10, No. 4

Fäldt, P. Bergenstahl, B. (1996)
Changes in surface composition of spray dried food powders due to lactose crystallization,
Lebensmittel Wissenschaft und Technologie, Vol. 29, Nos. 5&6

Finke, A. (1991)
Rheologische Eigenschaften von Kakaobutterdispersionen mit Schokoladeninhaltskompo-
nenten, Thesis, Technische Universität Dresden, Germany

Finke, H. (1965)
Handbuch der Kakaoerzeugnisse, 2. Auflage, Springer Verlag, Berlin

Full, N.A. et al. (1996)
Physical and sensory properties of milk chocolate formulated with anhydrous milkfat frac-
tions, Journal of food science, Vol. 61, No. 4

Gaonkar, A.G. (1989)
Interfacial tensions of vegetable oil/water systems:effect of oil purification, Journal of the
American oil chemists' society, Vol. 66, No. 8

Gleissle, W., Baloch, M.K. (1983)
Flow behaviour of concentrated suspensions at high shear stresses and shear rates in Eighth
International Technical Conference on Slurry Transportation, San Francisco, California,
USA

Gutzow, I., Schmelzer, J. (1995)
The vitreous state, Springer Verlag, Berlin

Hartel, R. W., Shastry, A.V. (1991)
Sugar Crystallization in Food Products, Critical review, Food Science and Nutrition 30(1)

Hartel, R.W. (1993)
Controlling Sugar Crystallization in Food Products, Food Technology, November 1993

Hausmann, A., Tscheuschner, H.-D. (1992)
Veränderung des Strukturzusstandes von Schokoladenmasse beim Conchieren, Zucker-
und Süsswarenwirtschaft 9

Heathcock, J. (1985)
Characterization of milk proteins in confectionery products, Food microstructure, Vol. 4

Hess, W. (1980)
Einfluss der Schubbeanspruchung und des Verformungsverhaltens bei der Druckzer-kleinerung von Kugeln und kleinen Partikeln, Thesis, University of Karlsruhe, Germany

Hiemenz, P.C., Rajagopalan, R. (1997)
Principles of colloid and surface chemistry, 3rd edition, Marcel Dekker, New York

Hoskin, J., Dimick, P. (1980)
Observations of chocolate during conching by scanning electron microscopy and viscosimetry, Journal of food science, Vol. 45

Hoskin, J., Dimick, P., Daniels, R. (1980)
Scanning electron microscopy of the theobroma cacao seed, Journal of food science, Vol. 45

Israelachvili, J.N. (1985)
Intermolecular and surface forces, Academic Press, London, ISBN 0-12-375180-2

Jouppila, K., Roos, Y.H. (1994)
Glass transitions and crystallization in milk powders, Journal of dairy science, 77, p. 2907-2915

Jouppila, K. et al. (1997)
Glass transition, water plasticization, and lactose crystallization in skim milk powders, Journal of dairy science, 80, p. 3152-3160

Kalab, M. (1979)
Scanning electron microscopy of dairy products: an overview, Scanning electron microscopy, Vol. III, p. 261-272

Kamal, M.R., Mutel, A. (1985)
Rheological properties of suspensions in newtonian and non-newtonian fluids, Journal of polymer engineering, Vol. 5, No. 4

Kao, S. et al. (1975)
Rheology of concentrated suspensions of spheres, Part I & II, Journal of colloid and interface science, Vol. 53, No. 3

Karlshamns (1997)
Akomed R, Product specification, Karlshamns, Sweden

Kaylegian, K. (1997)
Milkfat fractions in chocolate, 51st P.M.C.A. Production conference, Hershey, Pennsylvania

Kedward, C.J. et al. (1998)
Crystallization kinetics of Lactose and Sucrose based on isothermal differential scanning calorimetry, Journal of Food Science, Vol. 63, No. 2

Kleinert-Zollinger, J. (1991)
Die Endveredelung der Schokolade, ZSW, 5

Koglin, B. (1974)
Systematik der Dispergiermittel, Chemie Ingenieur Technik, No. 17, p.720-726

Koglin, B. (1978)
Agglomeration and Dispersion in Suspensions, Ger. Chem. Eng., No. 1, p.252-258

Krupp, H. (1967)
Particle Adhesion, Theory and Experiment, Advanced Colloid Interface Science, 1

Lewis, T.B., Nielsen, L.E. (1968)
Viscosity of dispersed and aggregated suspensions of spheres, Transactions of the society of rheology, 12:3

Ley, D. (1983)
Vergleich und Beurteilung von Conchiersystemen, Süsswaren, 10

Linko, P. et al. (1982)
Water sorption porperties and the effect of moisture on the structure of dried milk products, Food industries of South Africa, October, reproduced from: Lebensmittel - Wissenschaft & Technologie Zürich, Switzerland, Vol.15 (1982) No.1

Lloyd, R.J. et al. (1996)
Glass transition and cacking of spray dried lactose, Int. Journal of Food Science and Technology, 31, p. 305-311

Martinez-Padilla, L.P. et al. (1999)
Rheological characterization of model food suspension containing discs using three different geometries, Journal of Food Process Engineering, 22, p. 55-79

McClements, D.J. (1999)
Food Emulsions, CRC Press, Boca Raton

Metzner, A.B., Otto, R.E. (1957)
Agitation of Non Newtonian fluids, A.I.Ch.E. Journal, Vol. 3, No. 1

Metzner, A.B. (1985)
Rheology of suspensions in polymeric liquids, Journal of rheology, 29 (6)

Niediek, E.A. (1968)
Untersuchungen zur Ermittlung optimaler Verfahren für die Herstellung von Schokolademassen, Thesis, University of Karlsruhe, Germany

Niediek, E.A. (1972)
Untersuchungen zu den Zerkleinerungsvorgängen in Feinwalzen am Beispiel Milchschokolademasse, Gordian, No. 4, p. 121-131

Niediek, E.A. (1975)
Untersuchungen zur Bearbeitung fliessfähiger Stoffe mit dem Walzenstuhl, Chemie Ingenieur Technik, No. 17, p. 699-708

Niediek, E.A. (1978)
Optimum refining process for cocoa mass, Review for chocolate, confectionery and bakery, vol.3

Niediek, E.A. (1979)
Aromasorptionseigenschaften von amorpher Saccharose und Lactose, Gordian, No. 2

Niediek, E.A. (1982)
Differences in properties between the crystalline and amorphous forms of sucrose and lactose, Zeitschrift für Lebensmitteltechnologie und Verfahrenstechnik (International Journal of food technology and food process engineering), Vol. 33

Niediek, E.A. (1991a)
Amorphous sugar, its formation and effect on chocolate quality, 45th P.M.C.A. Production conference, Hershey, Pennsylvania

Niediek, E.A. (1991b)
Amorphous Sugar, its formation and effect on chocolate quality, The Manufacturing Confectioner, June

Oehlmann, S. et al. (1994)
Butteroil emulsification with milk derived membrane and protein fractions, Journal of foods science, Vol. 59, No.1

Ouriev, B. (2000)
Ultrasound Doppler Based In-Line Rheometry of Highly Concentrated Suspensions, Thesis, ETH Zurich, No. 13523, ISBN: 3-905609-11-8

Peleg, M. (1983)
Physical properties of food powders, Chpt. 10 in Physical properties of foods, eds. Peleg, M., Bagley, E.B., AVI publishing, Westport, CT

Peleg, M. (1993)
Glass transitions and the physical properties of food powders, in The glassy state of Foods, Blanshard, J., Lillford, P., Nottingham University press

Pepper, T., Holgate, H. (1985)
Role of milk protein in chocolate, Leatherhead Research report, No. 524

Rao, M.A., Hartel, R.W. (1998)
Phase/state transitions in foods, p. 57-86, Marcel Dekker AG, Basel, Switzerland

Raschka, K. (1990)
Bestimmung der Fliesseigenschaften feuchter Schüttgüter mit Anwendungen bei der Schneckenextrusion, Fortschrittsberichte VDI Reihe 3 Nr.227, VDI Verlag, Düsseldorf

Raschka, K., Buggisch, H. (1992)
Bestimmung der Fliesseigenschaften feuchter Schüttgüter und Pasten mit einem Ringschergerät, Aufbereitungs-Technik, 33, Nr.3

Rhône-Poulenc (1995)
Silicones, Properties & Applications, brochure, Rhône -Poulenc Europe, Lyon , France

Roetman, K. (1979)
Crystalline lactose and the structure of spray dried milk products as observed by scanning electron microscopy, Netherland milk dairy journal, No.33

Roos, Y. Karel, M. (1991)
Plasticizing effect of water on thermal behavior and crystallization of amorphous food models, Journal of food science, Vol. 56, No.1

Roos, Y., Karel, M. (1992)
Crystallization of amorphous lactose, Journal of Food Science, Vol. 57, No. 3

Roos, Y.H. (1995-1)
Phase transitions in foods, Academic Press, San Diego, California

Roos, Y.H. (1995-2)
Characterization of food polymers using state diagrams, Journal of Food Engineering, 24, p. 339-360

Roos, Y.H. et al. (1996)
Glass transition in low moisture and frozen foods: effects on shelf life and quality, Food Technology, November 1996

Rostagno, W. (1969)
Chocolate particle size and its organoleptic influence, Manufacturing confectioner, 49, (May)

Roth, D. (1976)
Amorphisierung bei der Zerkleinerung und Rekristallisation als Ursachen der Agglomeration von Puderzucker und Verfahren zur deren Vermeidung, Thesis, University of Karlsruhe, Germany

Rumpf, H. (1962)
Grundlegende physikalische Probleme bei der Zerkleinerung, Chemie Ingenieur Technik, No.11, p.731-741

Rumpf, H. (1974)
Die Wissenschaft des Agglomerierens, Chemie Ingenieur Technik, No.1, p.1-11

Rumpf, H. et al. (1976)
Mechanismen der Haftkraftverstärkung bei der Partikelhaftung durch plastisches Verformen, Sintern und viskoelastisches Fliessen, VDI-Berichte, No. 260

Sadler, L.Y., Kian, G.S. (1991)
Minimize solid-liquid mixture viscosity by optimizing particle size distribution, Chemical engineering progress, (3)

Saito, Z. (1988)
Lactose crystallization in commercial whey powders and in spray dried lactose, Food Microstructure, 7:75

Saleki-Gerhardt, A., Zografi, G. (1994)
Non-isothermal and isothermal crystallization of sucrose from the amorphous state, Pharmaceutical Research 11(8)

Saltmarch, M., Labuza, T. (1980a)
SEM investigations of the effect of lactose crystallization on the storage properties of spray dried whey, Scanning electron microscopy, Vol. III

Saltmarch, M., Labuza, T. (1980b)
Influence of relative humidity on the physicochemical state of lactose in spray dried sweet whey powders, Journal of Food Science, Vol. 45, p. 1231-1242

Schmitt, A., Baumberg, R., Küpers, G. (1997)
Serie Schokolade Herstellung, Mischen - Vorwalzen - Feinwalzen - Conchieren in Korrelation zu wesentlichen Einflussgrössen, Teil 1 - 6b, Süsswaren 1-10

Schönert, K. (1974)
Über die Eigenschaften von Bruchflächen, Chemie Ingenieur Technik, No. 17, p. 711-715

Schubert, H. (1973)
Kapillardruck und Zugfestigkeit von feuchten Haufwerken aus körnigen Stoffen, Chemie Ingenieur Technik, No. 6, p.396-401

Schuchmann, H. (1994)
The role of adhesive bonding and kinetic energy for agglomeration, in Jowitt, R.,Engineering and Food, Int. Congress on Engineering and Food 7, part 1

Schütz, W., Schubert, H. (1976)
Der Einfluss von Anpresskräften auf die Partikelhaftung, Chemie Ingenieur Technik, Vol. 48, 6

Schwenk, W. (1971)
Oberflächenveränderung von Feststoffen nach Zerkleinerung im Hochvakuum durch die Wirkung feuchter Luft, Thesis, University of Karlsruhe, Germany

Slade, L., Levine, H. (1993)
The glassy state phenomenon in food molecules, in "The glassy state in foods", edited by Blanshard, J.M.V., Lillford, P.J., Nottingham University press

Sommer, K. (1974)
Physikalische Vorgänge beim Conchieren, Thesis, University of Karlsruhe, Germany

Sommer, K., Palke, E. (1974)
Conchierforschung, Ergebnisse und Fortschritte bei der Entwicklung neuer Schokoladeherstellungsverfahren, Süsswaren, 7

Steffe, J.F. (1992)
Rheological methods in food process engineering, Freeman Press Michigan

Süsswaren (1994)
Conchen im Ueberblick, Marktübersicht, Süsswaren, 6

Tsai, S., Zammouri, K. (1988)
Role of interparticular Van der Waals force in rheology of comcentrated suspensions, Journal of rheology, 32 (7)

Tscheuschner, H.D., Wünsche, D. (1979)
Rheological properties of chocolate masses and the influence of some factors, in Food Texture and Rheology, ed. Sherman, P., Academic press, London

Tscheuschner, H.D. et al. (1992)
Einfluss von Prozessbedingungen des Conchierens auf die Griessbildung von Schokoladenmassen, Zucker- und Süsswarenwirtschaft, 11

Tscheuschner, H.D. (1993a)
Untersuchungen zur Entstehung und Vermeidung der Griessbildung beim Conchieren von Milchschokoladen, AIF Forschungsbericht, No. 104D

Tscheuschner, H.D. et al. (1993)
Einfluss stofflich bedingter Faktoren auf die Griessbildung von Schokoladenmassen beim Conchieren, Zucker- und Süsswarenwirtschaft, No. 12

Tscheuschner, H.D. (1993b)
Schokolade, Chapter 4 in Rheologie der Lebensmittel, Weipert, D., Tscheuschner, H.D., Windhab, E., Behr's Verlag, Hamburg, Germany

Tscheuschner, H.D. (1995)
Neue Erkenntnisses über physikalische Vorgänge beim Conchieren, Zucker- und Süsswarenwirtschaft, 2

Tscheuschner, H.D. (1997)
Feststoffe modifizieren Fliesseigenschaften, Zucker- und Süsswarenwirtschaft, 10

Tscheuschner, H.D. (2000)
Grundlagen der Schokoladenherstellung, Süsswaren, Vol. 3

Tscheuschner, H.D. et al. (2000)
Einfluss der Milchpulverart auf das Verarbeitungverhalten und die Fliesseigenschaften von Milchschokoladenmassen, Teil 1 u. 2, Zeitschrift für Süsswarenwirtschaft, ZSW, Vol. 4

Van den Berg, C. et al. (1993)
The ultrastructure and stability of amorphous sugars, in The glassy state in Foods, ed. Blanshard, J., Lillford, P., Nottingham University press

Van Scoik, K.G., Carstensen, J.T. (1990)
Nucleation phenomena in amorphous sucrose systems, Internat. Journal of Pharmaceutics, 58, p. 185-196

Verhey, J., Vos, E. (1971)
Air free atomization: a method for producing spray powders without vacuoles, Netherland milk dairy journal, No. 25

Verhey, J. (1986)
Physical properties of dried milk in relation to chocolate manufacture, Netherland milk dairy journal, No. 40

Von der Ohe, W. (1967)
Einzelkorn Druckzerkleinerung in einem Walzenspalt mit und ohne Friktion, Thesis, University of Karlsruhe, Germany

Wacker Chemie (1989)
Siliconöle AK, Merkblatt, Wacker Chemie München

Wagner, T. (1997)
Kaltsprühen ein- und mehrphasiger Flüssigkeiten, Thesis, Eidgenössische Technische Hochschule Zürich, Switzerland

Weichert, R. (1976)
Untersuchungen zur Temperatur an der Bruchspitze, Thesis, University of Karlsruhe, Germany

Weichert, R., K. Schönert (1976)
Temperatur an der Bruchspitze, Chemie Ingenieur Technik, No. 6

Windhab, E.W. (1986)
Untersuchungen zum rheologischen Verhalten konzentrierter Suspensionen. Thesis VDI Verlag Düsseldorf, Germany, 1986

Windhab, E.J. (1995)
Rheology of food processing, Ch. 5 in Physico-chemical aspects of food processing, ed. Beckett, S.T., Chapman & Hall

Windhab, E.J. (1997)
The relationship between process, structure and rheology of food suspensions, emulsions and foams, Engineering & Food, Ed.: R. Jowitt, Sheffield academic press, E 92-96

Windhab, E.J. (2000)
Fluid immobilization - a structure related key mechanism for the viscous flow behavior of concentrated suspension systems, Proceedings of the 2nd international symposium on food rheology and structure, Zurich

Winkler, T., Tscheuschner, H.-D. (1998a)
Agglomeration durch Feuchtigkeit, Zeitschr. f. Süsswarenwirtschaft1-2

Winkler, T., Tscheuschner, H.-D. (1998b)
Feuchte der Kakaofeststoffe fördert Agglomeration, Zeitschr. f. Süsswarenwirtschaft 3

Witschi, F. (1999)
Influence of microstructure on the drying kinetics of a foamed amorphous model food concentrate, Ph.D. Thesis, ETH, Zürich

Yella Reddy, S. et al. (1996)
Temperaing method for chocolate containing milk fat fractions, JAOCS, Vol. 73, No. 6

Ziegleder, G. (1997)
Aromaentwicklung beim Conchieren, Teil 1 & 2, Süsswaren, Vol. 11 & 12

Ziegler, G., Aguilar, C. (1994a)
Physical and microscopic characterization of dry whole milk with altered lactose content, part 1 & 2, Journal of dairy science, Vol. 77, p. 1189-1204

Ziegler, G., Aguilar, C. (1994b)
Controlling the conching process, 48th P.M.C.A. production conference, Hershey, Pennsylvania

Ziegler, G. (1998)
Changes during conching, Congress on chocolate technology, ZDS, Cologne, Germany

Ziegler, G. (1999)
Research spurs new conching processes, Candy industry, June

Zielinski, M., Niediek, E.A, Sommer, K. (1974)
Einfluss des Knetens und Rührens auf das Fliessverhalten von hochkonzentrierten Suspensionen, Teil 1 und 2, Gordian Vol. 4 & 5

Curriculum Vitae

Name:	Peter Braun
Date of birth:	15. 12. 1964, Freiburg i. Brsg., Germany
Nationality:	German

Since 1998	Group leader at Kraft Foods, R&D Inc. Munich, Germany, Responsible for external and basic research within the confectionery category
1995-2000	Ph.D. thesis at the Laboratory of Food Process Engineering (ETH Zurich) and at Kraft Foods R&D Inc., Munich. In parallel Project Engineer at Kraft Foods, R&D Inc., Munich, confectionery category
1993-1995	Project Engineer at Kraft Jacobs Suchard, R&D Inc., Neuchatel, CH
1991-1993	Process Engineer in operations at Kraft Jacobs Suchard Manufacturing, Lörrach, Germany
1985-1991	Study of Chemical Engineering at T.H. Karlsruhe, Germany